

DOT HS-800 527

PB 202 537

# **HSRI TWO-DIMENSIONAL CRASH VICTIM SIMULATOR: ANALYSIS, VERIFICATION, AND USERS' MANUAL**

**Highway Safety Research Institute  
The University of Michigan  
Huron Parkway and Baxter Road  
Ann Arbor, Michigan 48105**

**Contract No. FH-11-6962**

**December 1970**

**Final Report**

Reproduced by  
**NATIONAL TECHNICAL  
INFORMATION SERVICE**  
Springfield, Va. 22151

PREPARED FOR:

U.S. DEPARTMENT OF TRANSPORTATION  
NATIONAL HIGHWAY TRAFFIC SAFETY ADMIN STRATION  
WASHINGTON, D.C. 20590

A

263

The contents of this report reflect the views of the Highway Safety Research Institute of The University of Michigan, which is responsible for the facts and the accuracy of the data presented herein. The contents do not necessarily reflect the official views or policy of the Department of Transportation. This report does not constitute a standard, specification or regulation.

1. Report No. DOT-HS-8φφ-527	2. Government Accession No.	3. Recipient's Catalog No.	
4. Title and Subtitle HSRI Two-Dimensional Crash Victim Simulator: Analysis, Verification, and Users' Manual.		5. Report Date December 31, 1970	6. Performing Organization Code
		8. Performing Organization Report No. Bio M-70-8	
7. Author(s) D.H. Robbins, R.O. Bennett, and V.L. Roberts		10. Work Unit No.	
9. Performing Organization Name and Address Highway Safety Research Institute University of Michigan Huron Parkway and Baxter Road Ann Arbor, Michigan 48105		11. Contract or Grant No. FH-11-6962	
		13. Type of Report and Period Covered Final Report January 1, 1969 - December 31, 1970	
12. Sponsoring Agency Name and Address Department of Transportation National Highway Traffic Safety Administration Washington, D.C. 20590		14. Sponsoring Agency Code	
		15. Supplementary Notes	
16. Abstract  <p>This report deals with the development and use of mathematical models for the simulation of automobile occupant kinematics in the event of a collision. This model was developed as a tool to study advanced concepts and designs of seat-restraint systems from the viewpoint of occupant protection. After a discussion of the state-of-the-art of mathematical modeling of the crash victim, an analytical description of the HSRI Two-Dimensional Crash Victim Simulator is presented. This model consists of a segmented, eight-mass dynamic model of a human interacting with the interior of a vehicle in a symmetric frontal or rear crash. The degree to which predictions of the model agree with experimental impact sled test data is presented and the report concludes with a detailed Users' Manual for those individuals desiring to exercise the HSRI Two-Dimensional Crash Victim Simulator.</p>			
17. Key Words		18. Distribution Statement	
19. Security Classif.(of this report)	20. Security Classif.(of this page)	21. No. of Pages	22. Price

## ACKNOWLEDGMENTS

This research program was carried out by staff of the Biosciences Division of the Highway Safety Research Institute, The University of Michigan. The program was under the direction of Dr. D. H. Robbins, Dr. V. L. Roberts, and Mr. R. O. Bennett.

Mrs. J. M. Becker deserves special mention for her contributions to this work, particularly in the handling of discontinuous forces.

## TABLE OF CONTENTS

	Page
TABLES	iv
FIGURES	vi
I. INTRODUCTION	1
A. State of the Art	3
II. ANALYTICAL DESCRIPTION OF THE TWO-DIMENSIONAL CRASH VICTIM SIMULATOR	7
A. Selection of Parameters	7
B. Formulation of the Model	12
C. Body	13
D. Contact Surfaces	22
E. Seat Cushion	35
F. Joints	39
G. Restraint System	46
III. EXPERIMENTAL VERIFICATION OF THE MATHEMATICAL MODEL	52
A. Choice of a Criterion of Verification	52
B. The Experiment	54
C. Preparation of a Data Set for the Computer Simulation	71
D. Comparison of the Sled Test Data with the Predictions of the Model	77
IV. USERS' GUIDE FOR THE TWO-DIMENSIONAL CRASH VICTIM SIMULATOR	81
A. Description of Input Data Cards	81
B. Information Tables	97
C. General Program Output	104
D. Teletype Users' Guide	113
E. Overall Program Description and Flow Diagrams	128
F. Integration of Discontinuous Accelerations	128
G. Subprogram Descriptions and Flow Diagrams	136
H. Symbol Dictionary	197
REFERENCES	249

TABLES

Table	Page
I. Subscripts of Body Joints	16
II. Subscripts of Body Segments	16
III. Subscripts of Contact Arcs	16
IV. Normal Contact Surface Indices	25
V. Occupant Contacts Versus Vehicle Contacts	28
VI. Weights and Moments of Inertia of HSRI 50th Percentile Sierra Dummy	72
VII. Input Data Cards	83
VIII. Subscripts of Body Joints	97
IX. Subscripts of Body Segments	97
X. Subscripts of Contact Arcs	97
XI. LCONTL Values	97
XII. Belt Parameter Index	98
XIII. NBELT Values	98
XIV. Occupant Position Options	98
XV. Normal Contact Surface Indices	98
XVI. Occupant Contacts Versus Vehicle Contacts	99
XVII. Input Table Switches	101
XVIII. IBUG Switches	101
XIX. Indices for the Injury Criteria Quantities	102
XX. Probability Labels	103

TABLES (Concluded)

Table	Page
XXI. Sample V-Card Debug Input Data Set	105
XXII. Intermediate General Printout	107
XXIII. Program Comments	112
XXIV. Input Constants (in numerical order)	118
XXV. Input Constants (in alphabetical order)	120
XXVI. Variables (in numerical order)	122
XXVII. Variables (in alphabetical order)	125

## FIGURES

Figure	Page
1. Schematic of mathematical model showing occupant, possible contact surfaces, seat, and restraint system.	2
2. AMA deceleration profile.	10
3. Complex deceleration trace.	11
4. Body element lengths, centers of gravity, and moments of inertia.	14
5. Body angles.	15
6. Definition of body contact radii.	23
7. Definition of vehicle contact surface (shown for driver).	24
8. Description of seat bottom.	36
9. Form of friction in joints.	40
10. Form of symmetric joint stops for neck and two spinal joints.	41
11. Form of nonsymmetric joint stops of hip, shoulder, elbow, and knee.	42
12. Shoulder belt geometry.	47
13. Lap belt geometry.	48
14. HSRI impact sled.	55
15. Test setup for two-dimensional model validation.	57
16. Vehicle kinematics.	58
17. Excursion of head center-of-gravity and H-point as a function of time.	59
18. Resultant chest linear acceleration in g's.	60
19. Resultant head linear acceleration in g's.	61



## FIGURES (Concluded)

Figure	Page
20. Seat belt loads.	62
21. Shoulder harness loads.	63
22. Forward motion of H-point.	64
23. Forward motion of head center-of-gravity.	65
24. Pitch angle of head.	66
25. Pitch angle of the upper leg.	67
26. Centers-of-gravity and dimensions of forearms, upper arms, and lower spine.	68
27. Centers-of-gravity and dimensions of pelvic area, upper legs, and lower legs.	69
28. Centers-of-gravity and dimensions of head and upper torso.	70
29. Test configuration for seat property tests.	73
30. Seat load-deflection characteristics.	74
31. Seat load-deflection characteristics at seat front.	75
32. Load-deflection characteristics of seat belts.	76
33. Description of time-varying debug table.	106
34. Simplified program flow chart.	129
35. Usage of program subroutines.	130
36. Library routines called by program.	131



## I. INTRODUCTION

This report deals with the development and use of a mathematical model for the simulation of automobile occupant kinematics in two dimensions in event of a collision. The model was developed as a tool to study advanced concepts and designs of seat restraint systems from the viewpoint of occupant protection.

A schematic for the two-dimensional model is shown in Figure 1. The three parts of the model are the occupant, the vehicle, and the deceleration profile. The occupant is represented by eight mass elements located in the head, upper torso, lower torso, upper leg, lower leg, upper arm, and lower arm. Attached to the various body elements are geometric surfaces serving to outline the body in order that contact between the occupant and the interior or exterior of a vehicle can be predicted. The vehicle is represented by a series of planar contact surfaces which can be arranged to represent either a vehicle interior for occupant kinematics studies or the exterior for pedestrian studies. Belt restraints are included in the model if their use is desired. Forces are applied to the body of the occupant whenever interaction is sensed between the occupant and the vehicle. In order to produce occupant motions, a front-end or rear-end deceleration is applied to the vehicle and the resulting occupant motions listed as computer program output.

In addition to the analytical description of the model in Part II, a Users' Guide is included as Part IV of this report. Sections are included describing preparation of input data decks and the options available in studying the output produced by the computer program. The techniques which can be used in operating the model at a teletype terminal remote from The University of Michigan are described in a Teletype Users' Guide. Documentation of the program includes an overall program description, subroutine descriptions and flow diagrams, and a complete symbol dictionary.

The comparison of the predictions of the model with experimental

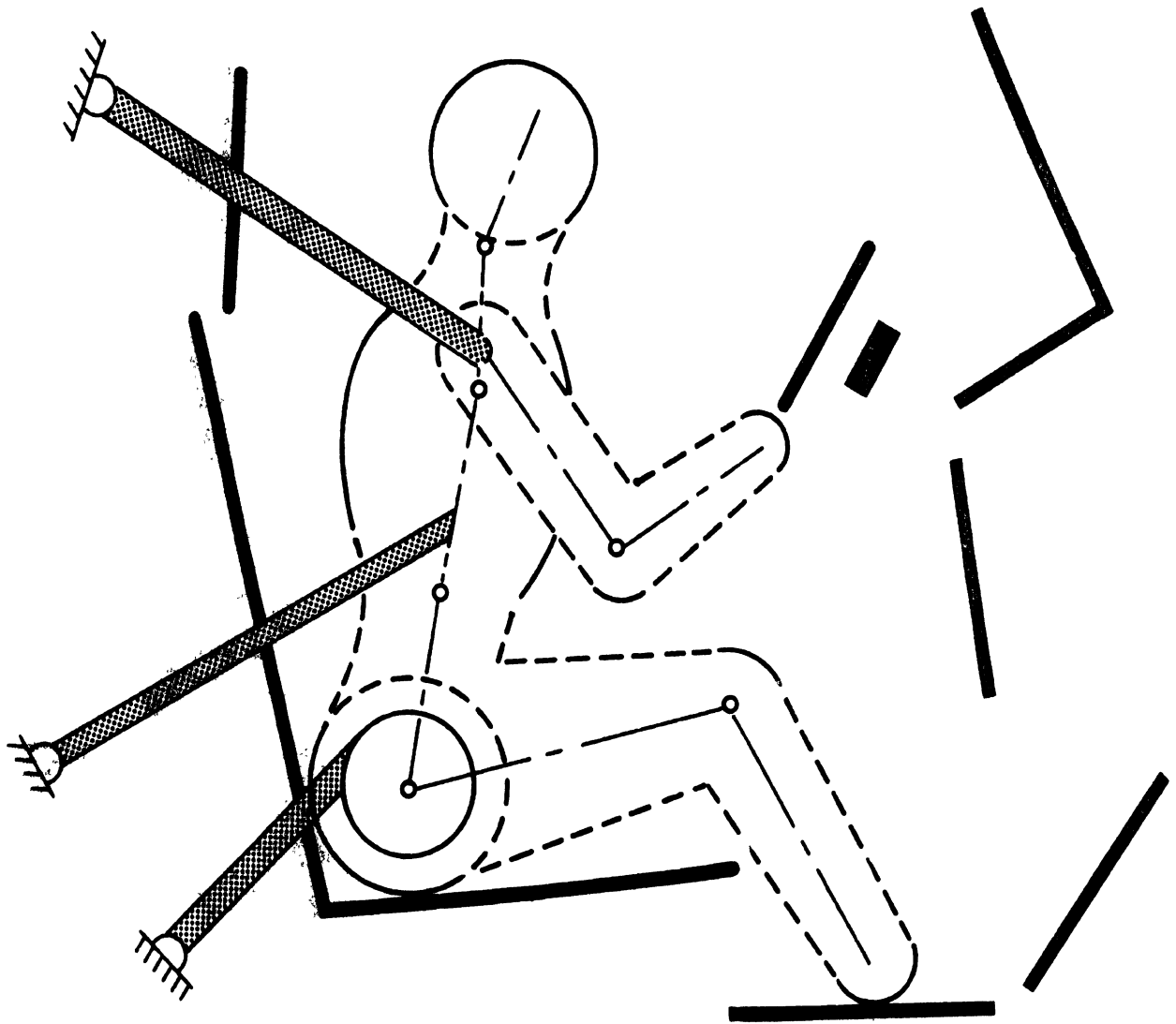


Figure 1. Schematic of mathematical model showing occupant, possible contact surfaces, seat, and restraint system.

impact sled tests is the subject of Part III of the report. The complex problem of gathering a set of input data describing the occupant and the vehicle is discussed and the techniques by which this is carried out are described. The equally difficult task of obtaining appropriate experimental data is also considered. Comparisons between a 30 mph impact sled test involving a belt-restrained 50th percentile male dummy and the predictions of the model conclude Part III.

The model which is described in this report is proposed as a powerful tool for studying and designing advanced integrated seat-restraint systems. It has been exercised several hundred times to study belt restraint systems, various deceleration profiles, headrest and seatback shape, pedestrian kinematics, occupant size and position, etc., and represents the current state of the art in two-dimensional crash victim simulators.

#### A. STATE OF THE ART

Mathematical models have been developed for the motion of the human body in several environments, including auto occupant dynamics,<sup>\*1-8</sup> human gait, and the motions experienced by the legs and arms during walking.<sup>9-11</sup> This work is often applied to the design, development and use of prosthetic devices. In connection with aerospace applications, analytical studies of self-generated motions possible in free-fall<sup>12-14</sup> and 0-gravity environments are being carried out and find application in such activities as sky-diving and space-walking. Also, studies are being made of such work tasks as lifting,<sup>15,16</sup> resulting in the development of work capability amplifiers.

Fundamental theoretical work has been carried out in the field of mathematical models for more than sixty years, as seen in the work of Fischer.<sup>17</sup> However, it is only with the coming-of-age of the high speed computer in the last twenty years that practical solutions of equations as

---

\*Note: Only a small number of representative papers published on this subject are included in this list.

complex as those proposed by Fischer have been realized. Hence, the mathematical simulation of human body motions has become a very active research topic in the last ten years.

Generally, two approaches have been used in analyses simulating auto occupant protection. On one hand, various researchers have adopted relatively simple physical models for studying specific aspects of human kinematics. Weaver<sup>18</sup> has used a two-mass, two-degree-of-freedom model to simulate belt loadings and head impact velocity in the case of a lap-belted occupant. Similar models have been developed by Aldman<sup>19</sup> and Renneker<sup>20</sup> for studying slack in restraint systems and the effect of various input deceleration profiles. Other authors, including Martinez,<sup>21</sup> Mertz,<sup>22</sup> and Roberts,<sup>23</sup> have used somewhat more sophisticated models for studying the phenomenon of whiplash. Roberts has added an additional complicating factor to his model—the motion of the brain mass inside the brain case.

On the other hand, several authors<sup>1-8</sup> have developed more complex models of human kinematics utilizing several masses for simulating body motions. In addition, complex vehicle geometry is introduced in these simulations to provide an intricate array of forces acting on the segmented occupant. Particularly noteworthy in the early development of these models are the efforts of McHenry.<sup>2</sup> All these models are marked by extensive development programs requiring at least two years from project initiation to the production of a functioning computer program.

Most of the modeling work mentioned above has been concerned with simulations of occupant motion in two dimensions. The only known published simulations involving three dimensions are those of Roberts,<sup>1</sup> Thompson,<sup>4</sup> Robbins,<sup>6</sup> and Young.<sup>7</sup> The first of these is a simple-one-mass model capable of simulating belt loads and upper torso motions in three dimensions, while the second is part of a large program involving vehicle crush characteristics. The third model simulates a three-dimensional occupant by three masses and twelve degrees-of-freedom while the recently completed fourth model describes the occupant by twelve masses and thirty-one degrees-

of freedom while possessing a less sophisticated model of occupant-vehicle interactions than that of Robbins.<sup>6</sup>

Even with the advent of the highly complex computer programs described here, there still exist major problem areas such as:

1. Verification of the model by experiment;
2. Lack of highly controlled tests;
3. Lack of anthropometric data and verification of the models using human volunteers;
4. Lack of impact test data reduction techniques specifically oriented towards mathematical model verification.
5. Difficulty in using the models because of the complex input data requirements; and
6. Difficulty in using the model at locations other than the laboratories of the developer.

These problems can be classified into two general types: (a) lack of closely coordinated efforts to insure that the mathematical models predict and anticipate physical reality, and (b) ease of use. The latter problem is somewhat easier to approach than the first one. One needs to identify the user and his capabilities and then write a program which is user-oriented. Computer programs of this nature are in actual use, particularly in styling and design laboratories in the auto industry. The users need not be highly trained computer experts.

In assigning staff to the various subject areas of the current research project, a concerted effort was made to coordinate the sled test program and the analytical program. One group was assigned the task of analysis; another group was responsible for the impact sled test program; and a new key group was formed to bridge the gap which was found to exist between the analytical and experimental groups. The task of the key group was to insure that meaningful data was generated in the tests and to establish techniques for reducing this data into a form which could be compared with the output of a mathematical model.

This discussion is intended to show that the current state of the art is quite advanced from the viewpoint of producing computer programs

which predict vehicle occupant motions in a crash environment. However, considerable research must be carried out to make programs of this nature easily usable. Additionally, it is recommended that experimental work accompany the development of future models to make assessment of their validity more straightforward.



## II. ANALYTICAL DESCRIPTION OF THE TWO-DIMENSIONAL CRASH VICTIM SIMULATOR

This part of the report consists of an analytical description of the two-dimensional crash victim simulator, a schematic of which is shown in Figure 1. The parameters which have been chosen for use in the physical model are discussed, then there is a brief presentation of the equations of motion describing the movements of the crash victim. This is followed by a detailed description of the analytical models used to define the mass and geometry of the body, the contact surface causing force interactions between the occupant and the vehicle, the seat, the joint structures connecting the various segments of the body, and a belt restraint system.

### A. SELECTION OF PARAMETERS

Four major groups of parameters have been considered in the development of this model: the occupant, seat, external restraint environment, and the deceleration profile.

The occupant is difficult to describe both experimentally and analytically. Controversy arises over the use of anthropometric dummies, cadavers, human volunteers, and laboratory animals. The physical properties of dummies are the most easily obtained and controlled but there is a question whether they represent human kinematics. Four sets of parameters are used to model the dynamic behavior of the body. First, the body is modeled by eight rigid mass elements representing the head, upper torso, middle torso, lower torso, upper arm, lower arm, upper leg, and lower leg. Second, these mass elements are connected by joint structures represented as viscoelastic, nonlinear, torsional springs. Resistance is slight over most of the range of motion of each joint. However, stops, located at the end of practical motion of each joint, are modeled by a torsional spring possessing a high degree of stiffness. Third, muscle tone is delineated rather crudely in this model by a constant torque, acting in each joint, resisting whatever relative motion is

experienced by the adjacent rigid body elements. Constant torque is also used to model the friction joints found in present generation anthropometric dummies. Fourth, body geometry is represented by the moments of inertia of the eight rigid masses as well as contact body surfaces. These surfaces, which are rigidly attached to the head, torso, hip, and extremities, allow the user of the model to ascertain if a body part impacts any part of the vehicle or seat.

The seat would seem to be easier to describe for use in a model. However, it is unfortunate that very little research has been carried out to determine dynamic deformation characteristics such as stiffness and damping of seats. Three parts of the seat are included in this model: seat back, seat cushion, and head rest. The seat back may apply a force to the lower part of the occupant's back at the hip and to the upper torso. The seat back is modeled by a plane surface. The head rest is independent of the seat back and can be composed of a number of contact surfaces representing a nonplanar geometry. The seat cushion is again represented by a plane. Vertical forces are applied at the hip and at the front of the seat. A horizontal force is also applied at the front of the seat cushion to prevent the lower leg from rotating back "through the seat cushion." Each of these elements is described by dynamic force-deformation relations, friction coefficients, and geometrical configurations.

The external system restraining an occupant is ordinarily defined in terms of specific devices such as a seat belt or an airbag. One common feature of all these devices is the fact that they can be described in terms of a dynamic force-deformation profile. For example, an acceleration-dependent inertial reel used in conjunction with a shoulder harness will have a different characteristic curve than a controlled permanent deformation device or one of the harnesses used in most current production vehicles. In each case a different formula must be used which computes force as a function of deformation and deformation rate. Therefore, provisions must be made for forces to be applied to the occupant in a rather general manner in order that they can be used in modeling any one of the proposed restraint devices.

Three types of interactions are possible between the occupant and vehicle: (a) the seat, already discussed, (b) a system of belts attached to the occupant as a seat belt and/or shoulder harness, and (c) a collection of geometric surfaces representing the profile of a vehicle interior or exterior. These surfaces, each represented by a different dynamic force-deformation relationship, interact with the contact surfaces fixed to the body of the occupant to generate a complex interaction of forces and occupant motions representing the collision of the occupant with seat, restraint system, or vehicle structural member.

An example of a complex set of force interactions between an occupant and a vehicle interior is represented by simulating the airbag restraint system. The occupant is represented in the usual way and may or may not be restrained by a lap belt. Vehicle components such as the seat back, seat cushion, floor, windshield, and lower dash panel are described in terms of contact surfaces. It is necessary to know the force-motion interrelationship between the head or torso and the bag before the simulation can be carried out as the model itself cannot predict any force-deformation relationships. They must be obtained using experimental procedures and be provided as input data for the operation of the computer simulation.

It should also be noted that this general formulation allows studies of much more than a seated occupant restrained in some manner inside the vehicle. Studies have been carried out of more esoteric concepts such as the airbag, the rear-end collision, and the pedestrian. Also, studies of the dynamics of a child in any one of the large number of seats and restraint devices available on today's market are possible.

The deceleration profile which is used in this model is relatively simple, it can be either a forward or rearward deceleration. However, the shape of the profile is limited to 200 linear segments. Typical examples are shown in Figures 2 and 3.

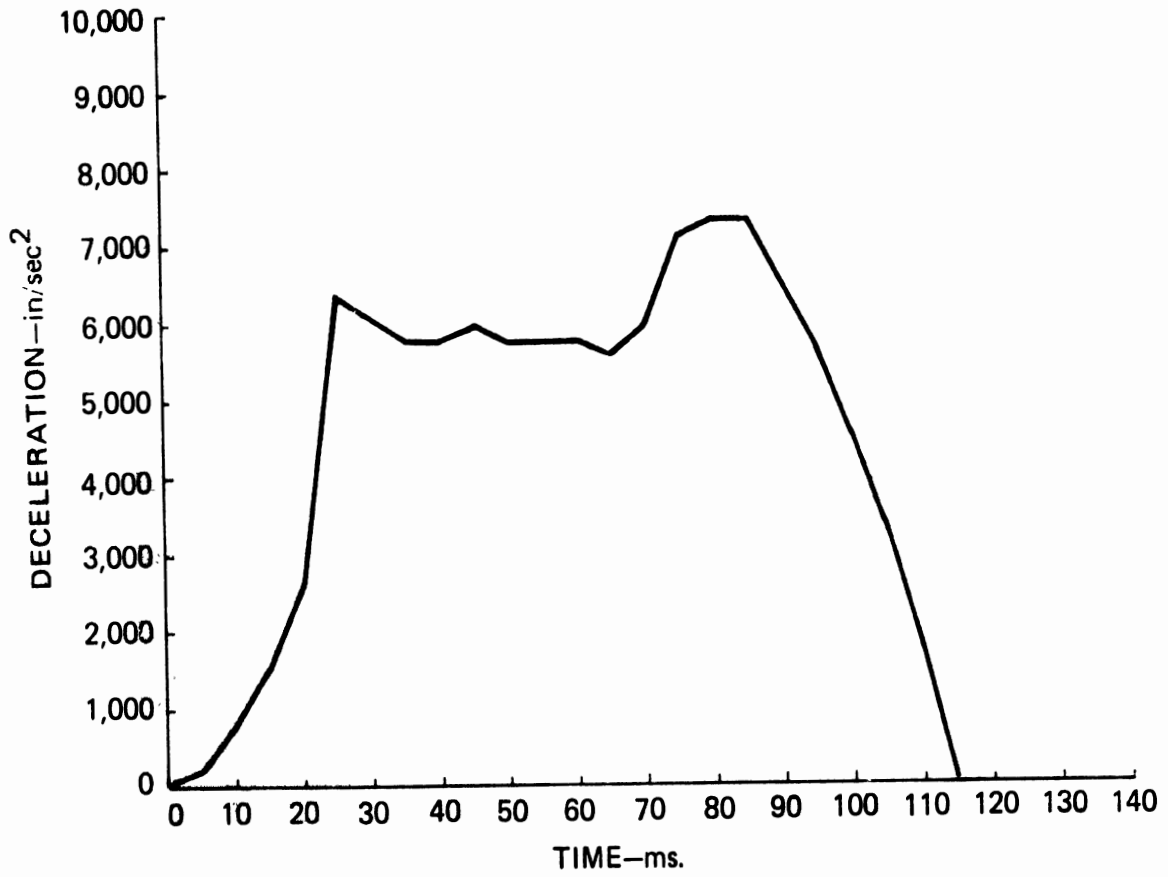


Figure 2. AMA deceleration profile.

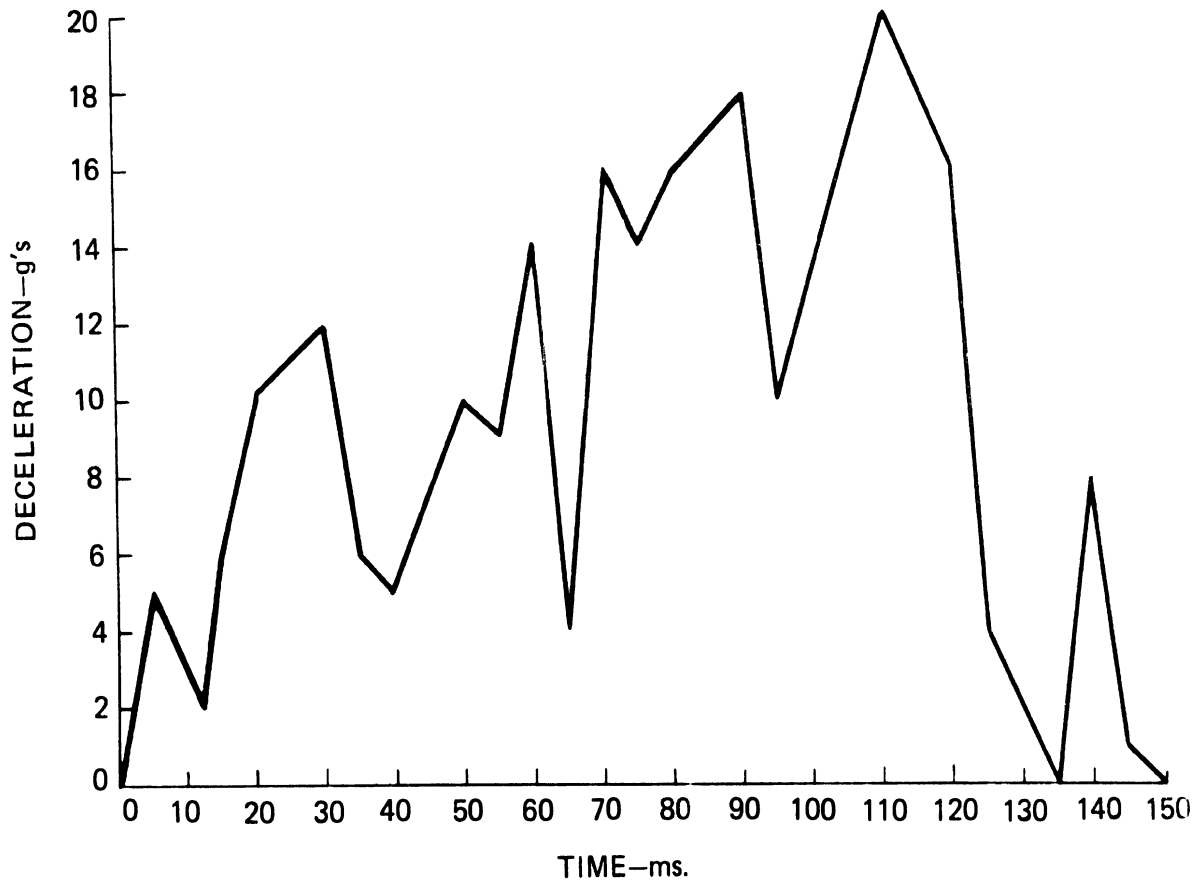


Figure 3. Complex deceleration trace.

## B. FORMULATION OF THE MODEL

The equations of motion are derived by Lagrangian techniques<sup>24</sup>:

$$\frac{d}{dt} \left[ \frac{\partial(\text{KE})}{\partial \dot{Z}_i} \right] - \frac{\partial(\text{KE})}{\partial Z_i} + \frac{\partial(\text{PE})}{\partial Z_i} + \frac{\partial(\text{DE})}{\partial \dot{Z}_i} = F_{Z_i} \quad (\text{II.B.1})$$

where

KE is the system kinetic energy

PE is the system potential energy

DE is the system dissipated energy rate

$F_{Z_i}$  are the classical generalized forces

$Z_i$  are the classical generalized coordinates or degrees of freedom of the model

Since the only driving force is applied to the vehicle and not directly to the body, the  $F_{Z_i}$  terms are all zero. After the energy terms have been written, the resulting equations of motion are rearranged so that all the terms containing generalized accelerations appear on the left-hand side and all others appear on the right-hand side. Thus rearranged, these equations are of the form

$$m \ddot{\vec{Z}} = \vec{b} \quad (\text{II.B.2})$$

where  $m$  is the matrix of generalized acceleration coefficients and  $\ddot{\vec{Z}}$  is the acceleration vector. In this analysis the right-hand side,  $\vec{b}$ , will be called the "generalized force" and contributions to it from the potential and kinetic energy in Eq. (II.B.1) will be referred to as the generalized force from that part of the model. The total generalized force is the vectorial sum of each contributing component (gravity, joints, belts, seat cushion, and contacts). The kinetic energy contributions to the generalized force are centrifugal and Coriolis force terms.

Kinetic energy alone determines the left-hand side of the equations of motion. In the computational procedure, the inverse of the matrix,  $m^{-1}$ ,

multiplied by the generalized force vector,  $\vec{b}$ , yields the solution for the generalized accelerations, i.e.,

$$\ddot{\vec{Z}} = m^{-1} \vec{b} \quad (\text{II.B.3})$$

The generalized force vector may be expanded to show the various contributions

$$\vec{b} = \vec{B} - \vec{G} + \vec{Q} + \vec{D} + \vec{C} + \Delta\vec{b}_Q + \Delta\vec{b}_s + \Delta\vec{b}_J + \vec{D}_b \quad (\text{II.B.4})$$

where

- $\vec{B}$  is due to kinetic energy
- $\vec{G}$  is due to gravity
- $\vec{Q}$  is due to contact forces
- $\vec{D}$  is due to seat cushion
- $\vec{C}$  is due to joint elasticity
- $\Delta\vec{b}_Q$  is due to contact friction
- $\Delta\vec{b}_s$  is due to seat friction
- $\Delta\vec{b}_J$  is due to joint friction
- $\vec{D}_b$  is due to belts

### C. BODY

The crash victim is simulated by eight body segments: three segments in the torso to introduce some flexibility into the spine, one segment for the head, two segments in the arms (right and left combined) representing the forearm and upper arm, and two segments for the legs (right and left combined) representing upper and lower legs. Figure 1 shows a crash victim in a typical seating configuration restrained by a shoulder harness and lap belt. Figure 4 illustrates the body segments and their lengths, centers of gravity, and moments of inertia. Tables I and II contain the subscripting schemes for the body elements and joints which are used in the computer program while Figure 5 shows the angular coordinates defining the orientation in space of

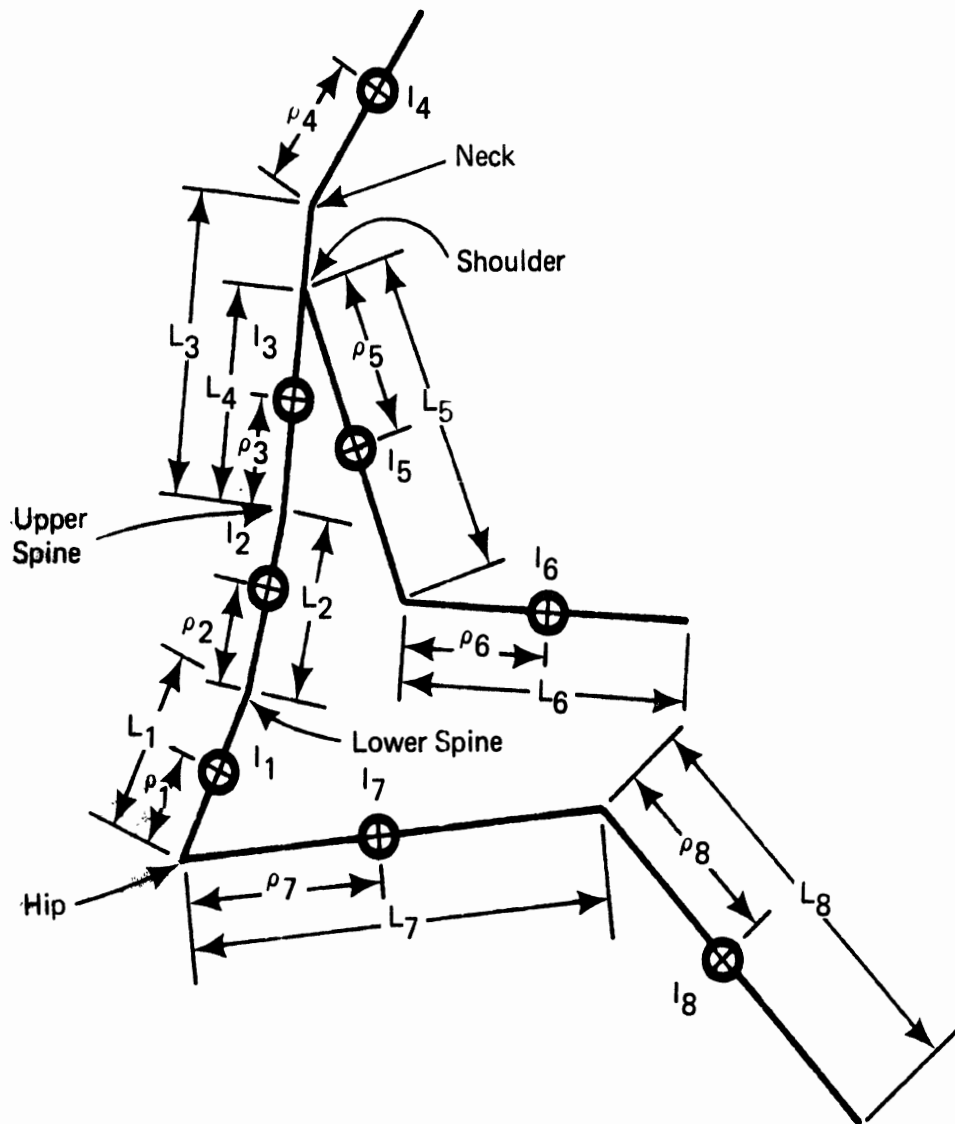
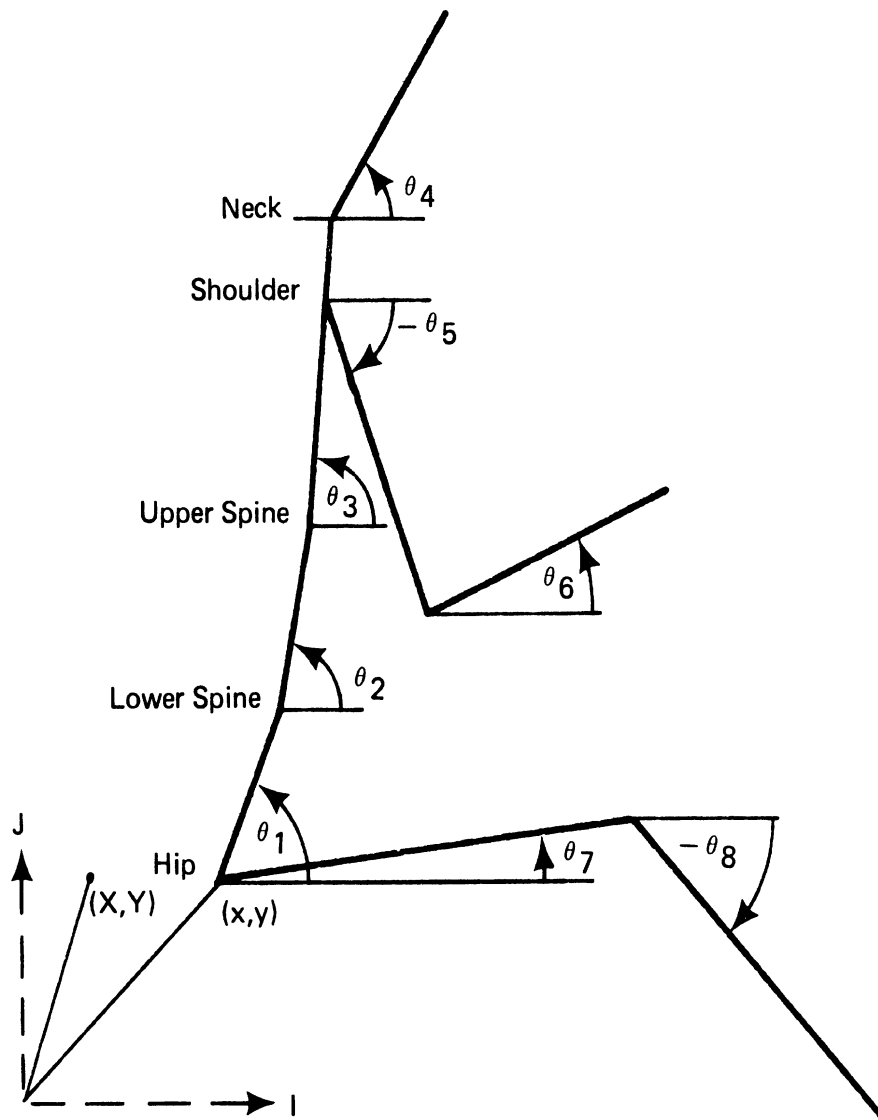


Figure 4. Body element lengths, centers of gravity, and moments of inertia.





$(X,Y)$  = Coordinates for vehicle relative to inertial system. This is the point on the vehicle occupied by the hip at zero time.

$(x,y)$  = coordinates of hip relative to inertial system.

Figure 5. Body angles.

the various body elements and the translational coordinates of the hip. It should be noted that  $x$  and  $y$  plus the eight angles defined in this figure are the generalized coordinates used in the analysis.

TABLE I. SUBSCRIPTS OF BODY JOINTS

Subscript	1	2	3	4	5	6	7
Joint	Hip	Lower Spine	Upper Spine	Neck	Shoulder	Elbow	Knee

TABLE II. SUBSCRIPTS OF BODY SEGMENTS

Subscript	1	2	3	4	5	6	7	8
Body segment	Lower Torso	Middle Torso	Upper Torso	Head	Upper Arm	Lower Arm	Upper Leg	Lower Leg

TABLE III. SUBSCRIPTS OF CONTACT ARCS

Subscript	1	2	3	4	5	6	7	8
Contact arc	Hip	---	Upper Torso	Head	Elbow	Hand	Knee	Foot

The coordinates for the center-of-gravity of each body segment are stated in Eq. (II.C.1) in terms of the generalized coordinates. Based on this the velocities of the eight centers-of-gravity are given in Eq. (II.C.2). Tables I, II, and XIV as well as Figures 4 and 5 should be referred to in reading these equations.

Using Eqs. (II.C.1) and (II.C.2) the kinetic and potential energy associated with the body can be written. After extensive formal manipulation of

the kinetic and potential energies, those portions of the equations of motion which can be stated are terms due to centrifugal and gravitational forces as well as to the matrix. This matrix is shown in Eq. (II.B.2) which forms the bulk of the left-hand side of the equations of motion.

$$\begin{aligned}
 x_1 &= x + \rho_1 \cos \theta_1 \\
 y_1 &= y + \rho_1 \sin \theta_1 \\
 x_2 &= x + L_1 \cos \theta_1 + \rho_2 \cos \theta_2 \\
 y_2 &= y + L_1 \sin \theta_1 + \rho_2 \sin \theta_2 \\
 x_3 &= x + L_1 \cos \theta_1 + L_2 \cos \theta_2 + \rho_3 \cos \theta_3 \\
 y_3 &= y + L_1 \sin \theta_1 + L_2 \sin \theta_2 + \rho_3 \sin \theta_3 \\
 x_4 &= x + L_1 \cos \theta_1 + L_2 \sin \theta_2 + L_3 \cos \theta_3 + \rho_4 \cos \theta_4 \\
 y_4 &= y + L_1 \sin \theta_1 + L_2 \sin \theta_2 + L_3 \sin \theta_3 + \rho_4 \sin \theta_4 \\
 x_5 &= x + L_1 \cos \theta_1 + L_2 \cos \theta_2 + L_4 \cos \theta_3 + \rho_5 \cos \theta_5 \\
 y_5 &= y + L_1 \sin \theta_1 + L_2 \sin \theta_2 + L_4 \sin \theta_3 + \rho_5 \sin \theta_5 \\
 x_6 &= x + L_1 \cos \theta_1 + L_2 \cos \theta_2 + L_4 \cos \theta_3 + L_5 \cos \theta_5 + \rho_6 \cos \theta_6 \\
 y_6 &= y + L_1 \sin \theta_1 + L_2 \sin \theta_2 + L_4 \sin \theta_3 + L_5 \sin \theta_5 + \rho_6 \sin \theta_6 \\
 x_7 &= x + \rho_7 \cos \theta_7 \\
 y_7 &= y + \rho_7 \sin \theta_7 \\
 x_8 &= x + L_7 \cos \theta_7 + \rho_8 \cos \theta_8 \\
 y_8 &= y + L_7 \sin \theta_7 + \rho_8 \sin \theta_8
 \end{aligned}
 \tag{II.C.1}$$

$$\dot{x}_1 = \dot{x} - \rho_1 \dot{\theta}_1 \sin \theta_1$$

$$\dot{y}_1 = \dot{y} + \rho_1 \dot{\theta}_1 \cos \theta_1$$

$$\dot{x}_2 = \dot{x} - L_1 \dot{\theta}_1 \sin \theta_1 - \rho_2 \dot{\theta}_2 \sin \theta_2$$

$$\dot{y}_2 = \dot{y} + L_1 \dot{\theta}_1 \cos \theta_1 + \rho_2 \dot{\theta}_2 \cos \theta_2$$

$$\dot{x}_3 = \dot{x} - L_1 \dot{\theta}_1 \sin \theta_1 - L_2 \dot{\theta}_2 \sin \theta_2 - \rho_3 \dot{\theta}_3 \sin \theta_3$$

$$\dot{y}_3 = \dot{y} + L_1 \dot{\theta}_1 \cos \theta_1 + L_2 \dot{\theta}_2 \cos \theta_2 + \rho_3 \dot{\theta}_3 \cos \theta_3$$

$$\dot{x}_4 = \dot{x} - L_1 \dot{\theta}_1 \sin \theta_1 - L_2 \dot{\theta}_2 \sin \theta_2 - L_3 \dot{\theta}_3 \sin \theta_3 - \rho_4 \dot{\theta}_4 \sin \theta_4$$

$$\dot{y}_4 = \dot{y} + L_1 \dot{\theta}_1 \cos \theta_1 + L_2 \dot{\theta}_2 \cos \theta_2 + L_3 \dot{\theta}_3 \cos \theta_3 + \rho_4 \dot{\theta}_4 \cos \theta_4$$

$$\dot{x}_5 = \dot{x} - L_1 \dot{\theta}_1 \sin \theta_1 - L_2 \dot{\theta}_2 \sin \theta_2 - L_4 \dot{\theta}_3 \sin \theta_3 - \rho_5 \dot{\theta}_5 \sin \theta_5$$

$$\dot{y}_5 = \dot{y} + L_1 \dot{\theta}_1 \cos \theta_1 + L_2 \dot{\theta}_2 \cos \theta_2 + L_4 \dot{\theta}_3 \cos \theta_3 + \rho_5 \dot{\theta}_5 \cos \theta_5$$

$$\dot{x}_6 = \dot{x} - L_1 \dot{\theta}_1 \sin \theta_1 - L_2 \dot{\theta}_2 \sin \theta_2 - L_4 \dot{\theta}_3 \sin \theta_3 - L_5 \dot{\theta}_5 \sin \theta_5 - \rho_6 \dot{\theta}_6 \sin \theta_6$$

$$\dot{y}_6 = \dot{y} + L_1 \dot{\theta}_1 \cos \theta_1 + L_2 \dot{\theta}_2 \cos \theta_2 + L_4 \dot{\theta}_3 \cos \theta_3 + L_5 \dot{\theta}_5 \cos \theta_5 + \rho_6 \dot{\theta}_6 \cos \theta_6$$

$$\dot{x}_7 = \dot{x} - \rho_7 \dot{\theta}_7 \sin \theta_7$$

$$\dot{y}_7 = \dot{y} + \rho_7 \dot{\theta}_7 \cos \theta_7$$

$$\dot{x}_8 = \dot{x} - L_7 \dot{\theta}_7 \sin \theta_7 - \rho_8 \dot{\theta}_8 \sin \theta_8$$

$$\dot{y}_8 = \dot{y} + L_7 \dot{\theta}_7 \cos \theta_7 + \rho_8 \dot{\theta}_8 \cos \theta_8 \quad (\text{II.C.2})$$

The components of the equations of motion due to centrifugal force form  $\vec{B}$  and can be written

$$\begin{aligned}
 B_1 &= L_1 \sum_{j=2}^6 a_j \dot{\theta}_j^2 \sin [\theta_j - \theta_1] \\
 B_2 &= L_2 a_2 \dot{\theta}_1^2 \sin (\theta_1 - \theta_2) + L_2 \sum_{j=3}^6 a_j \dot{\theta}_j^2 \sin (\theta_j - \theta_2) \\
 B_3 &= a_3 \sum_{j=1}^2 L_j \dot{\theta}_j^2 \sin (\theta_j - \theta_3) + L_3 a_4 \dot{\theta}_4^2 \sin (\theta_4 - \theta_3) \\
 &\quad + L_4 \sum_{j=5}^6 a_j \dot{\theta}_j^2 \sin (\theta_j - \theta_3) \\
 B_4 &= a_4 \sum_{j=1}^3 L_j \dot{\theta}_j^2 \sin (\theta_j - \theta_4) \\
 B_5 &= a_5 \sum_{j=1}^3 L_j \dot{\theta}_j^2 \sin (\theta_j - \theta_5) + L_4 a_5 \dot{\theta}_3^2 \sin (\theta_3 - \theta_5) \\
 &\quad + a_6 L_5 \dot{\theta}_6^2 \sin (\theta_6 - \theta_5) \\
 B_6 &= a_6 \sum_{j=1}^{3,5} L_j \dot{\theta}_j^2 \sin (\theta_j - \theta_6) \\
 B_7 &= L_7 a_8 \dot{\theta}_8^2 \sin (\theta_8 - \theta_7) \\
 B_8 &= L_7 a_8 \dot{\theta}_7^2 \sin (\theta_7 - \theta_8) \\
 B_9 &= \sum_{j=1}^8 a_j \dot{\theta}_j^2 \cos \theta_j \\
 B_{10} &= \sum_{j=1}^8 a_j \dot{\theta}_j^2 \sin \theta_j
 \end{aligned} \tag{II.C.3}$$

Due to gravity the contribution to the right-hand side of the equations of motion forms  $\vec{G}$  and can be written

$$\begin{aligned}
 G_1 &= g a_1 \cos \theta_1 \\
 G_2 &= g a_2 \cos \theta_2 \\
 G_3 &= g a_3 \cos \theta_3 \\
 G_4 &= g a_4 \cos \theta_4 \\
 G_5 &= g a_5 \cos \theta_5 \\
 G_6 &= g a_6 \cos \theta_6 \\
 G_7 &= g a_7 \cos \theta_7 \\
 G_8 &= g a_8 \cos \theta_8 \\
 G_9 &= 0 \\
 G_{10} &= g a_9
 \end{aligned} \tag{II.C.4}$$

where

$$\begin{aligned}
 a_i &= m_i \rho_i + L_i \sum_{j=i+1}^6 m_j & i = 1, 2 \\
 a_3 &= m_3 \rho_3 + m_4 L_3 + (m_5 + m_6) L_4 \\
 a_i &= m_i \rho_i & i = 4, 6, 8 \\
 a_i &= m_i \rho_i + m_{i+1} L_i & i = 5, 7 \\
 a_9 &= \sum_{i=1}^8 m_i
 \end{aligned} \tag{II.C.5}$$



The matrix  $m$  in Eq. (II.B.2) formed from the kinetic energy terms is shown as Eqs. (II.C.6) and (II.C.7).

$$\begin{aligned}
 a_i &= I_j + m_j \rho_j^2 + L_j^2 \sum_{k=j+1}^6 m_k && \text{for } i = 10, 11 \\
 &&& \text{and } j = i-9 \\
 a_{12} &= I_3 + m_3 \rho_3^2 + m_4 L_3^2 + (m_5 + m_6) L_4^2 \\
 a_i &= I_j + m_j \rho_j^2 && \text{for } i = 13, 15, 17 \\
 &&& \text{and } j = i-9 \\
 a_i &= I_j + m_j \rho_j^2 + m_{j+1} L_j^2 && \text{for } i = 14, 16 \\
 &&& \text{and } j = i-9 \quad (II.C.7)
 \end{aligned}$$

#### D. CONTACT SURFACES

The nine distinct surfaces simulating the interior of the vehicle and capable of applying forces on the body of the occupant are represented by straight line segments as shown in Figure 7. After the computer program user chooses whether the occupant is a driver, front-seat passenger, or rear-seat passenger, a table is generated showing which body segments are allowed to contact which surfaces.

This computer generated table is equivalent to the corresponding column in Table V. The user may choose to model any special contact surface with one of the standard contact surfaces. The choice of which standard contact to use must include matching the expected interactions of this contact with the table of permissible interactions (the appropriate column of Table V). Each contact surface has a unique name shown in Table IV which will be used in the program output. The user has the option of changing these names to represent, for example, an airbag.



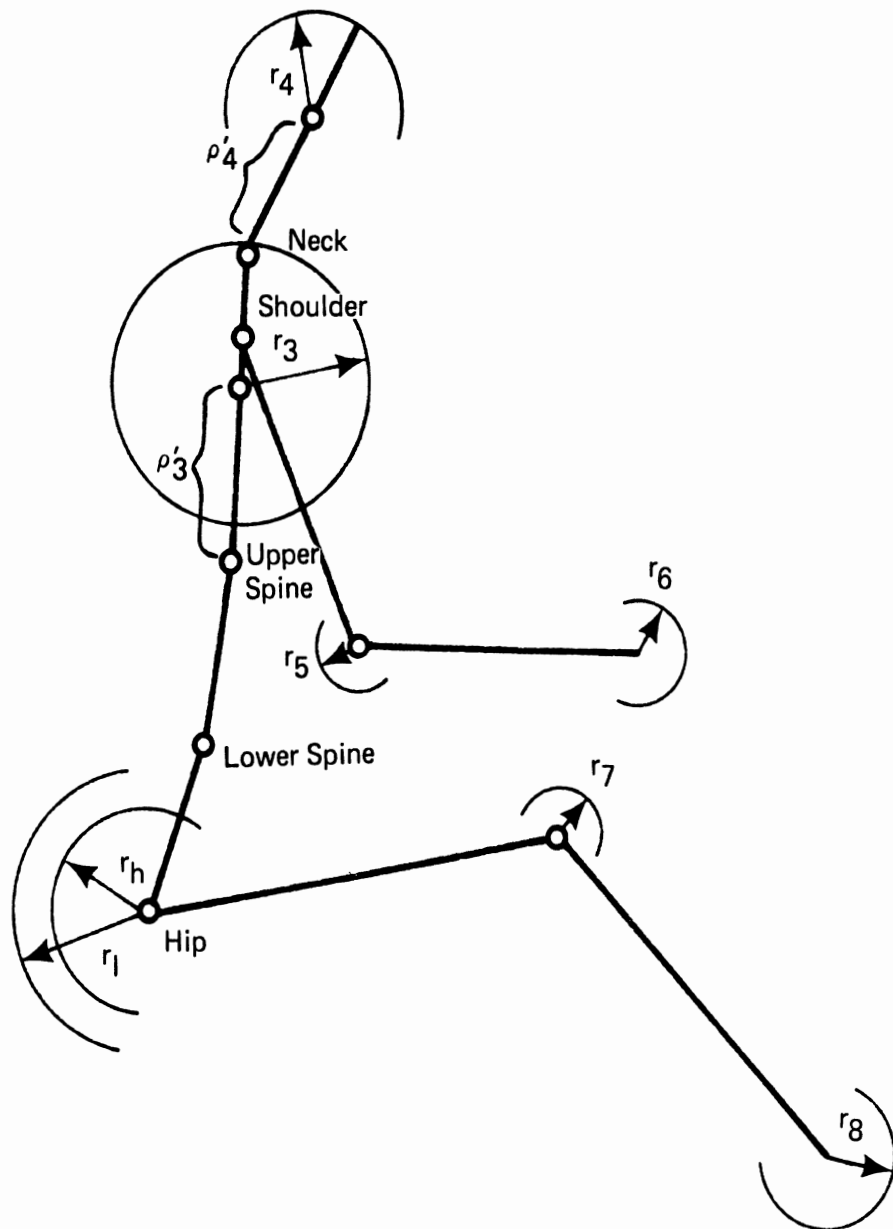


Figure 6. Definition of body contact radii.

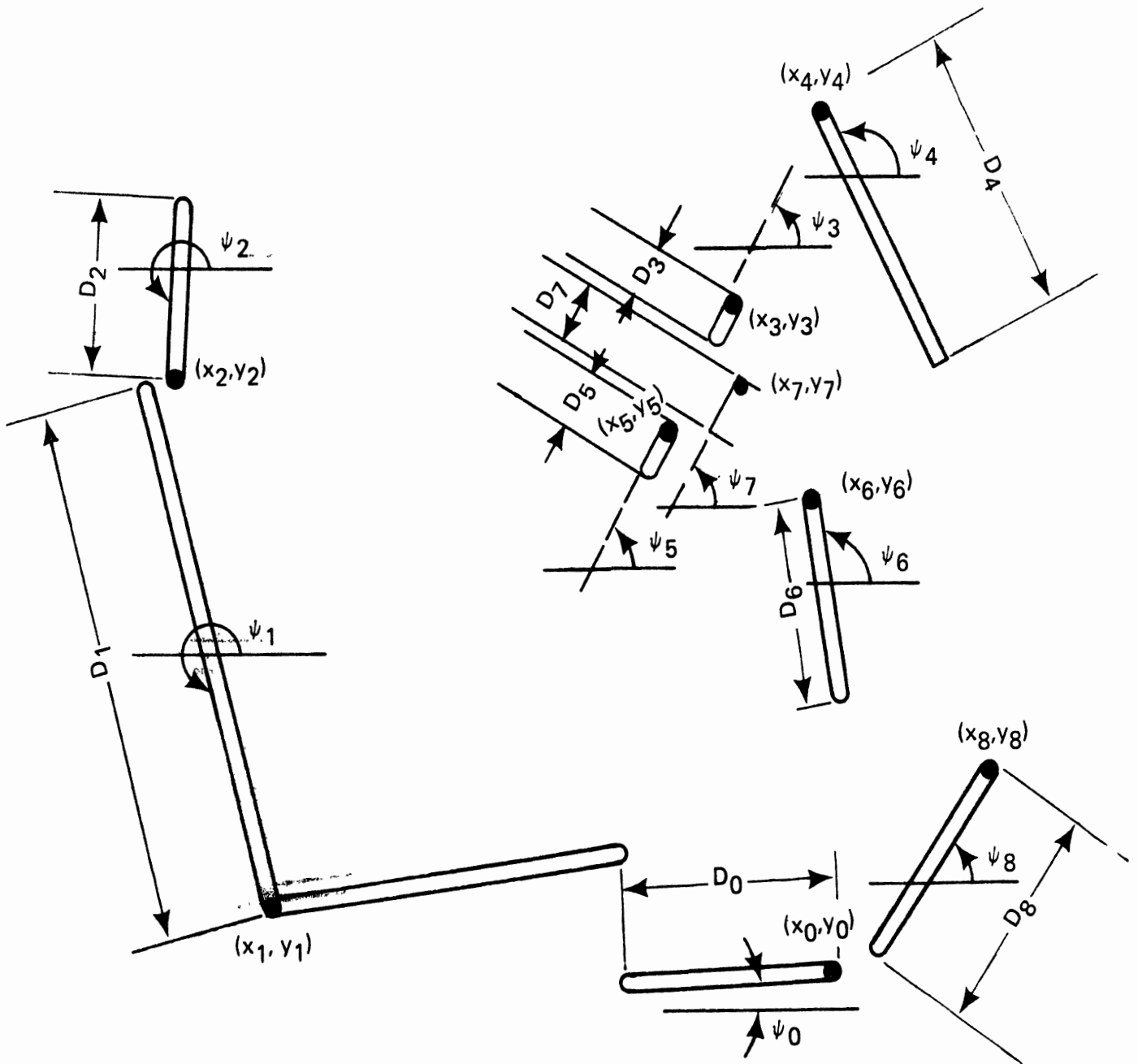


Figure 7. Definitions of vehicle contact surface (shown for driver).

TABLE IV. NORMAL CONTACT SURFACE INDICES

Index*	Normal Contact Surface
0	Floor
1	Seat back
2	Roof or head rest
3	Upper steering wheel, upper dash, back of front seat
4	Windshield
5	Lower steering wheel
6	Lower panel
7	Steering column
8	Toeboard
9	Steering wheel

\*It is permissible to use any index for any other contact surface as long as it is compatible with the table of possible contacts in Table V. For example, an airbag could be simulated by using the various segments of the steering wheel.

Each contact surface is defined by four quantities: the x and y coordinates of its reference point, its length, and its angular orientation. This reference point is at the end of the surface line which is most counter-clockwise relative to the origin. The angle is found by drawing a horizontal line through the other end point and measuring the angle from the forward part of this line to the surface.

Each contact surface produces two forces. The first force acts perpendicularly to the surface through the center of curvature of the contacting body segments and the second force is frictional in nature and has the form:

$$P' = \begin{cases} -\mu_a P \operatorname{sgn} v_T & \text{for } |v_T| \geq \xi_a \\ 0 & |v_T| < \xi_a \end{cases} \quad (\text{II.D.1})$$

where

$v_T$  is the tangential velocity of the body segment along the surface

$P$  is the force applied normal to the contact surface

$\mu_a$  is the friction coefficient

$\xi_a$  is the velocity limit

When the velocity limit (a small quantity such as 0.1 in./sec) is exceeded the friction force is applied; otherwise, it is set to zero representing sliding or Coulomb friction.

The material properties of the contact surfaces are given by a load-deflection polynomial which may be up to the fifth order in both deflection and deflection rate representing a nonlinear, viscoelastic material. This applies while a load is being applied to a surface.

The force developed at any contact interface is given by

$$P_k = \sigma_{0,k} + \sum_{m=1}^5 [\sigma_{m,k} \delta_k^m + \sigma_{m+5,k} \dot{\delta}_k^m] \quad (\text{II.D.2})$$

where

$$\sigma_{0,n} = - \sum_{m=1}^5 \sigma_{m+5,k} \dot{\delta}_{k_0}^m$$

where

$\delta_k$  is the distance which a particular body element impinges into a particular surface representing a segment of the vehicle interior

$\dot{\delta}_k$  is the deflection rate

$\dot{\delta}_{k_0}$  is the value of  $\dot{\delta}_k$  when  $\delta_k$  first becomes positive

$\sigma_{0,k}$  is a preload on any given contact surface

$\sigma_{1,k}$  through  $\sigma_{10,k}$  are the material polynomial coefficients

The quantity  $k$  is the general force index. Values of  $k$  greater than four correspond to particular combinations of contact arcs on the body and contact surfaces and are shown in brackets in Table V. Hence, for each value of  $k$  and choice of passenger position, there corresponds a unique contact arc

subscript which appears in parentheses on the left margin of Table V and a unique contact surface subscript which appears in parentheses in the body of Table V. Throughout the remainder of this section "i" is this contact arc subscript and "a" is this contact surface subscript.

The deflections used to compute the force in Eq. (II.D.2) are given in the following equations.

$$\delta_k = r_i - (x_a'' - x_i') \sin \psi_a + (y_a'' - y_i') \cos \psi_a$$

$$\dot{\delta}_k = \dot{x}_i' \sin \psi_a - \dot{y}_i' \cos \psi_a$$

$$v_T = \dot{x}_i' \cos \psi_a + \dot{y}_i' \sin \psi_a + r_i \dot{\theta}_i \quad (\text{II.D.3})$$

$$x_1' = x$$

$$y_1' = y$$

$$x_3' = x + L_1 \cos \theta_1 + L_2 \cos \theta_2 + \rho_3' \cos \theta_3$$

$$y_3' = y + L_1 \sin \theta_1 + L_2 \sin \theta_2 + \rho_3' \sin \theta_3$$

$$x_4' = x + L_1 \cos \theta_1 + L_2 \cos \theta_2 + L_3 \cos \theta_3 + \rho_4' \cos \theta_4$$

$$y_4' = y + L_1 \sin \theta_1 + L_2 \sin \theta_2 + L_3 \sin \theta_3 + \rho_4' \sin \theta_4$$

$$x_5' = x + L_1 \cos \theta_1 + L_2 \cos \theta_2 + L_4 \cos \theta_3 + L_5 \cos \theta_5$$

$$y_5' = y + L_1 \sin \theta_1 + L_2 \sin \theta_2 + L_4 \sin \theta_3 + L_5 \sin \theta_5$$

$$x_7' = x + L_7 \cos \theta_7$$

$$y_7' = y + L_7 \sin \theta_7$$

$$x_8' = x + L_7 \cos \theta_7 + L_8 \cos \theta_8$$

$$y_8' = y + L_7 \sin \theta_7 + L_8 \sin \theta_8 \quad (\text{II.D.4})$$

$x_a''$ ,  $y_a''$ ,  $\psi_a$  are the contact surface reference coordinates and orientation,  $r_i$  is the radius of the contact arc attached to each body segment.

TABLE V. OCCUPANT CONTACTS VERSUS VEHICLE CONTACTS

Contact Arc Subscript	Contacts		
	Driver (1)	Front Passenger (2)	Rear Passenger (3)
Hip (1)	Seat back (1) [5]	Seat back (1) [5]	Seat back (1) [5]
Upper torso (3)	Seat back (1) [6]	Seat back (1) [6]	Seat back (1) [6]
	Upper steering wheel (3) [7]	Upper dash (3) [7]	Back of front seat (3) [7]
	Lower steering wheel (5) [8]		
	Steering column (7) [9]		
Head (4)	Seat back (1) [10]	Seat back (1) [8]	Seat (1) [8]
	Roof or head rest (2) [11]	Roof or head rest (2) [9]	Roof or head rest (2) [9]
	Upper steering wheel (3) [12]	Upper dash (3) [10]	Back of front seat (3) [10]
	Windshield (4) [13]	Windshield (4) [11]	
Lower steering wheel (5) [14]			
Elbow (5)	Seat back (1) [15]	Seat back (1) [12]	Seat back (1) [11]
Knee (7)	Lower panel (6) [16]	Lower panel (6) [13]	Back of front seat (3) [12]
Foot (8)	Floorboard (0) [17]	Floorboard (0) [14]	Floorboard (0) [13]
	Toeboard (8) [18]	Toeboard (8) [15]	Back of front seat (3) [14]

NOTE: Numbers in brackets refer to indices 5-18 used in LODFEC and CONTACT printouts (see flow diagrams and Table XX).

$$\dot{x}'_1 = \dot{x}$$

$$\dot{y}'_1 = \dot{y}$$

$$\dot{x}'_3 = \dot{x} - L_1 \dot{\theta}_1 \sin \theta_1 - L_2 \dot{\theta}_2 \sin \theta_2 - \rho'_3 \dot{\theta}_3 \sin \theta_3$$

$$\dot{y}'_3 = \dot{y} + L_1 \dot{\theta}_1 \cos \theta_1 + L_2 \dot{\theta}_2 \cos \theta_2 + \rho'_3 \dot{\theta}_3 \cos \theta_3$$

$$\dot{x}'_4 = \dot{x} - L_1 \dot{\theta}_1 \sin \theta_1 - L_2 \dot{\theta}_2 \sin \theta_2 - L_3 \dot{\theta}_3 \sin \theta_3 - \rho'_4 \dot{\theta}_4 \sin \theta_4$$

$$\dot{y}'_4 = \dot{y} + L_1 \dot{\theta}_1 \cos \theta_1 + L_2 \dot{\theta}_2 \cos \theta_2 + L_3 \dot{\theta}_3 \cos \theta_3 + \rho'_4 \dot{\theta}_4 \cos \theta_4$$

$$\dot{x}'_5 = \dot{x} - L_1 \dot{\theta}_1 \sin \theta_1 - L_2 \dot{\theta}_2 \sin \theta_2 - L_4 \dot{\theta}_3 \sin \theta_3 - L_5 \dot{\theta}_5 \sin \theta_5$$

$$\dot{y}'_5 = \dot{y} + L_1 \dot{\theta}_1 \cos \theta_1 + L_2 \dot{\theta}_2 \cos \theta_2 + L_4 \dot{\theta}_3 \sin \theta_3 + L_5 \dot{\theta}_5 \cos \theta_5$$

$$\dot{x}'_7 = \dot{x} - L_7 \dot{\theta}_7 \sin \theta_7$$

$$\dot{y}'_7 = \dot{y} + L_7 \dot{\theta}_7 \cos \theta_7$$

$$\dot{x}'_8 = \dot{x} - L_7 \dot{\theta}_7 \sin \theta_7 - L_8 \dot{\theta}_8 \sin \theta_8$$

$$\dot{y}'_8 = \dot{y} + L_7 \dot{\theta}_7 \cos \theta_7 + L_8 \dot{\theta}_8 \cos \theta_8 \quad (\text{II.D.5})$$

and the other quantities are defined in Figures 4-7.

The form of  $P_k$  shown in Eq. (II.D.2) is used only while a load is being applied, i.e., when the deflection is increasing. During loading, the material may absorb energy so that its characteristics while unloading can be different than before.

The resulting permanent deformation is modeled by means of two parameters:

G, the ratio of permanent deformation to maximum deflection, and R, the ratio of conserved to total energy.

These two parameters are not independent but the relationship is complex so both are required by the program. The unloading force is assumed to be parabolic in nature and deflection to decrease from a maximum at  $\delta = \Omega_k$  to zero force at  $\delta = G \Omega_k$ . This latter value ( $G \Omega_k$ ) is taken as the permanent deformation, i.e., the value of deflection which must be exceeded before loading will begin again. The formula used for  $P_k$  for unloading is

$$P_k = \frac{3[F_k \Omega_k (1-G) - 2E_{lk}]}{\Omega_k^3 (1-G)^3} (\delta_k - G \Omega_k) \left\{ \delta_k + \frac{\Omega_k [6E_{lk} - F_k \Omega_k (1-G)(2+G)]}{3[F_k \Omega_k (1-G) - 2E_{lk}]} \right\} \quad (\text{II.D.6})$$

where

$F_k$  is the loading force ( $P_k$ ) at the maximum deflection

$\Omega_k$  is the maximum deflection

$E_{lk}$  is the conserved energy. This quantity is computed as R times the total energy for this load-unload cycle plus the conserved energy from previous cycles if any.

The Eq. (II.D.6) results from an evaluation of the coefficients of a parabola which fits the constraints stated below:

- (1) The unloading curve starts at the point of maximum deflection  $\Omega_k$  with the force  $F_k$ .
- (2) The unloading curve goes to zero at the point where deflection equals the permanent deformation (i.e.,  $G \Omega$  by definition of G).
- (3) The total work done by the unloading curve (the conserved energy in the contact) is  $RE_k$  where  $E_k$  is the total energy and R is the ratio of conserved to total energy as defined above. The total energy is computed by a stepwise approximation through the loading portion of the cycle and



$E_{lk}$  which appears in the formulas above is computed as  $RE_k$ .

Since  $G$  and  $R$  are not really independent, a constraint:

$$2E_{lk} \leq F_k \Omega_k (1-G) \leq 3E_{lk} \quad (\text{II.D.7})$$

is applied to insure that the force goes to zero at  $\delta = G \Omega_k$ . The constraint equation (II.D.7) comes about from evaluation of the roots of the unloading curve. The conditions that  $G \Omega_k$  be the larger root and that the unloading curve increase for increasing deflection at that point yield the two halves of the constraint.

Loading followed by unloading constitutes one cycle. Provision is made for accumulating permanent deformations over several cycles. The effect of this accumulation is used to determine the starting point of succeeding cycles; however, the shape of the loading curve is always the same as the first cycle. The unloading curve is recomputed for each cycle.

The contribution to the equations of motion due to contact forces is a sum of the effects of the many possible interactions. For each passenger position, the number of possible interactions changes. In particular, the total number of interactions is fourteen for the driver (NPASGR = 1), eleven for the front right passenger (NPASGR = 2), and ten for the back seat passenger (NPASGR = 3).  $NS$  is the maximum value of the subscript  $k$  and is the above stated total number of interactions plus four.

$$Q_1 = L_1 \sum_{k=6}^{NS-3} P_k \cos (\theta_1 - \psi_a) \quad (\text{II.D.8})$$

where  $a$  again is the corresponding  $a$  for the  $k$  as explained on page 27.

$$Q_2 = L_2 \sum_{k=6}^{NS-3} P_k \cos (\theta_2 - \psi_a) \quad (\text{II.D.9})$$

$$Q_3 = \rho'_3 \sum_{k=6}^L P_k \cos(\theta_3 - \psi_a) + L_3 \sum_{k=K+1}^L P_k \cos(\theta_3 - \psi_a) + L_4 P_{L+1} \cos(\theta_3 - \psi_1) \quad (\text{II.D.10})$$

$$Q_4 = \rho'_4 \sum_{k=K+1}^K P_k \cos(\theta_4 - \psi_a) \quad (\text{II.D.11})$$

$$Q_5 = L_5 P_{L+1} \cos(\theta_5 - \psi_1) \quad (\text{II.D.12})$$

where K and L are a function of NPASGR as follows:

NPASGR	K	L
1	9	14
2	7	11
3	7	10

$$Q_6 = 0$$

$$Q_7 = L_7 \sum_{k=NS-3}^{NS} P_k \cos(\theta_7 - \psi_a)$$

$$Q_8 = L_8 \sum_{k=NS-1}^{NS} P_k \cos(\theta_8 - \psi_a)$$

$$Q_9 = - \sum_{k=5}^{NS} P_k \sin \psi_a$$

$$Q_{10} = \sum_{k=5}^{NS} P_k \cos \psi_a \quad (\text{II.D.13})$$

The contribution to the generalized force due to friction at the force contact is of the form

$$\vec{\Delta b}_q = P'_k \vec{U}_i \quad (\text{II.D.14})$$

where  $P'_k$  is the computed frictional force explained on page 26 corresponding to the normal force  $P_k$ .

$\vec{U}_i$  is the proper "lever arm" vector defined below for the value of the contact arc subscript corresponding to  $k$ . The quantity  $a$  is the matching contact surface subscript for the  $k$  in what follows.

Where

$$\vec{U}_1 = \begin{bmatrix} -r_1 \\ 0 \\ 0 \\ 0 \\ 0 \\ 0 \\ 0 \\ 0 \\ -\cos \psi_a \\ -\sin \psi_a \end{bmatrix} \quad (\text{II.D.15})$$

$$\vec{U}_2 = 0 \quad (\text{II.D.16})$$

$$\vec{U}_3 = \begin{bmatrix} L_1 \sin (\theta_1 - \psi_a) \\ L_2 \sin (\theta_2 - \psi_a) \\ \rho_3' \sin (\theta_3 - \psi_a) - r_3 \\ 0 \\ 0 \\ 0 \\ 0 \\ 0 \\ -\cos \psi_a \\ -\sin \psi_a \end{bmatrix} \quad (\text{II.D.17})$$

$$\vec{U}_4 = \begin{bmatrix} L_1 \sin (\theta_1 - \psi_a) \\ L_2 \sin (\theta_2 - \psi_a) \\ L_3 \sin (\theta_3 - \psi_a) \\ \rho'_4 \sin (\theta_4 - \psi_a) - r_4 \\ 0 \\ 0 \\ 0 \\ 0 \\ -\cos \psi_a \\ -\sin \psi_a \end{bmatrix} \quad (\text{II.D.18})$$

$$\vec{U}_5 = \begin{bmatrix} L_1 \sin (\theta_1 - \psi_a) \\ L_2 \sin (\theta_2 - \psi_a) \\ L_4 \sin (\theta_3 - \psi_a) \\ 0 \\ L_5 \sin (\theta_5 - \psi_a) - r_5 \\ 0 \\ 0 \\ 0 \\ -\cos \psi_a \\ -\sin \psi_a \end{bmatrix} \quad (\text{II.D.19})$$

$$\vec{U}_6 = 0 \quad (\text{II.D.20})$$

$$\vec{U}_7 = \begin{bmatrix} 0 \\ 0 \\ 0 \\ 0 \\ 0 \\ 0 \\ L_7 \sin (\theta_7 - \psi_a) - r_7 \\ 0 \\ -\cos \psi_a \\ -\sin \psi_a \end{bmatrix} \quad (\text{II.D.21})$$

$$\vec{U}_8 = \begin{bmatrix} 0 \\ 0 \\ 0 \\ 0 \\ 0 \\ 0 \\ L_7 \sin (\theta_7 - \psi_a) \\ L_8 \sin (\theta_7 - \psi_a) - r_8 \\ -\cos \psi_a \\ -\sin \psi_a \end{bmatrix} \quad (\text{II.D.22})$$

#### E. SEAT CUSHION

The seat cushion model contains provision for four separate forces as shown in Figure 8. The first one acts vertically at the hip joint whenever it is above the seat cushion and is modeled by a third order polynomial spring and a linear damper. The second, modeled by a linear spring, acts vertically at the front edge of the seat and affects the upper or lower leg depending on the size of the occupant and his position. This is especially useful in the case of children whose lower legs often are on the seat cushion. The third force, also modeled by a linear spring, acts in a forward direction at the top of the front edge of the seat. This force was included to prevent the lower legs from passing backward through the seat and producing large spurious forces. All three of these forces are continuous. The fourth force models seat friction and is discontinuous as well as dissipative. The force applied at the hip is

$$F_s = W_o - \sum_{m=1}^3 \beta_m y_s^m - C_s \dot{y}_s \quad (\text{II.E.1})$$

where

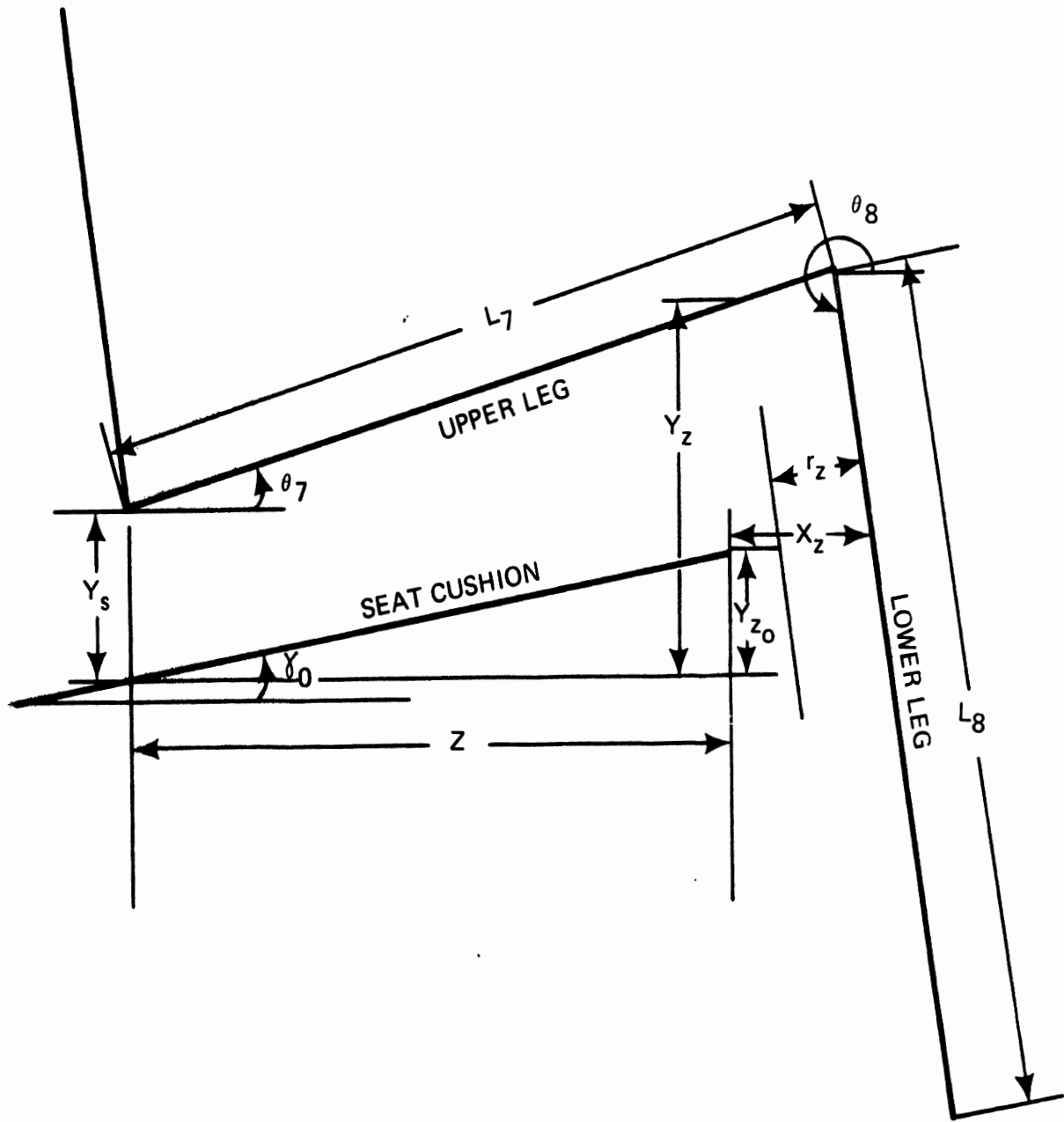


Figure 8. Description of seat bottom.

$$\begin{aligned}
y_s &= y + (X-x) \tan \gamma_0 \\
\dot{y}_s &= \dot{y} + (\dot{X}-\dot{x}) \tan \gamma_0 \\
W_0 &= \text{equilibrium force on seat cushion at hip} \\
\beta_m &= \text{polynomial spring constants} \\
C_s &= \text{damping constant} \\
X &= \text{horizontal position of seat as a function of time} \\
x &= \text{horizontal position of hip as a function of time} \\
y &= \text{vertical position of hip as a function of time} \quad (\text{II.E.2})
\end{aligned}$$

The force acting vertically at the at the front edge of the seat cushion is

$$F'_s = F'_{s0} - s(y_z - y_{z0}) \quad (\text{II.E.3})$$

where

$$y_z = \begin{cases} y + z \tan \theta_7 & \text{for the upper leg} \\ y + L_7 \sin \theta_7 + (z - L_7 \cos \theta_7) \tan \theta_8 & \text{for the lower leg} \end{cases} \quad (\text{II.E.4})$$

and

$$\begin{aligned}
z &= z_0 + X - x \\
F'_{s0} &= \text{initial upward force at front of seat} \\
s &= \text{spring constant} \\
y_{z0} &= \text{vertical distance from seat front edge to level of seat} \\
&\quad \text{cushion directly below hip joint at time zero} \\
z_0 &= \text{initial value of } z
\end{aligned}$$

with all other quantities defined in Figure 8.

The force acting horizontally at the front edge of the seat is

$$F_z = \begin{cases} s_z(r_z - x_z) & \text{for } x_z - r_z < 0 \\ 0 & \text{otherwise} \end{cases} \quad (\text{II.E.5})$$

where

$$x_z = (z_0 \tan \gamma_0 - y - L_7 \sin \theta_7) \frac{\cos \theta_8}{\sin \theta_8} - (z - L_7 \cos \theta_7)$$

$s_z$  = spring constant

$r_z$  = distance from centerline of lower leg to outside of calf

and the other quantities are previously defined.

(II.E.6)

The friction force is

$$f = \begin{cases} -\mu_s (F_s + F'_s) \operatorname{sgn}(\dot{X} - \dot{x}) & \text{for } |\dot{X} - \dot{x}| \geq \dot{x}_s \\ 0 & \text{otherwise} \end{cases} \quad (\text{II.E.7})$$

where

$\mu_s$  = friction coefficient

The contributions from the seat cushion to the generalized force vector,  $\vec{D}$ , are:

$$D_i = 0, \quad i = 1-6$$

$$D_7 = \begin{cases} F'_s z \sec^2 \theta_7 & \text{for } z \leq L_7 \cos \theta_7 \\ F'_s L_7 (\cos \theta_7 + \sin \theta_7 \tan \theta_8) - F_z L_7 \cdot \\ (\sin \theta_7 + \cos \theta_7 \cot \theta_8) & \text{for } z > L_7 \cos \theta_7 \end{cases} \quad (\text{II.E.8})$$

$$D_8 = \begin{cases} 0 & \text{for } z \leq L_7 \cos \theta_7 \\ F'_s (z - L_7 \cos \theta_7) \sec^2 \theta_8 + F_z (y + L_7 \sin \theta_7 - y_{z0}) \csc^2 \theta_8 \\ \text{otherwise} \end{cases}$$

$$D_9 = \begin{cases} -F'_s \tan \theta_7 & \text{for } z \leq L_7 \cos \theta_7 \\ -F'_s \tan \theta_8 + F_z & \text{otherwise} \end{cases}$$

$$D_{10} = F_s + F'_s - F_z \cot \theta_8 \quad (\text{II.E.9})$$



The components of the contribution of seat friction to the generalized force vector,  $\Delta \vec{b}_s$ , are

$$\Delta b_i = \begin{cases} 0 & \text{for } i = 1-8, 10 \\ -f & \text{for } i = 9 \end{cases} \quad (\text{II.E.10})$$

## F. JOINTS

Each joint is considered to have an elastic torque resisting motion away from its initial position, a coulomb-type friction resisting any relative motion above a certain velocity limit (see Figure 9), and a joint stop to prevent substantial motion beyond specified angular limits (see Figure 10 or Figure 11).

The contribution to the system potential energy from torque is defined by

$$J_{ei} = K_i(\theta_m - \theta_i + \theta_{i0} - \theta_{m0}) \text{ for } i = 1-7 \quad (\text{II.F.1})$$

(see Table I for joints associated with each subscript), with each  $i$  defining a unique  $m$  as follows for calculation of proper relative angle.

i	1	2	3	4	5	6	7
m	7	1	2	3	3	5	8

The other two torques are dissipative in nature. The coulomb friction equation is:

$$J_{fi} = \begin{cases} -C_i' \text{sgn}(\dot{\theta}_i - \dot{\theta}_m) & \text{for } |\dot{\theta}_i - \dot{\theta}_m| \geq \xi_i \\ 0 & \text{otherwise} \end{cases} \quad (\text{II.F.2})$$

Also the stop torque is of the same type:

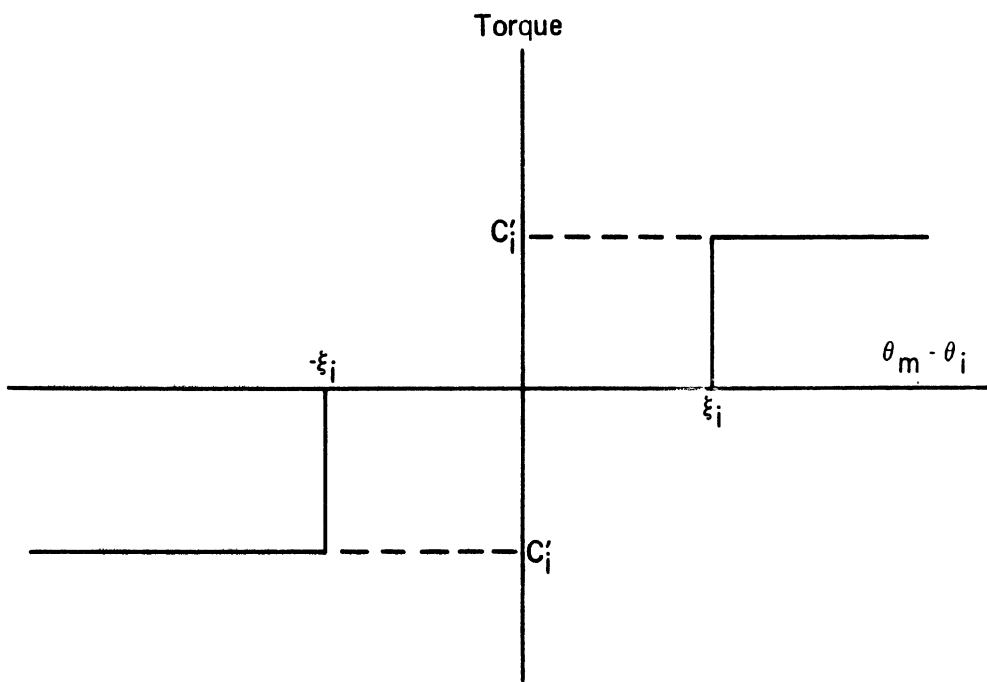


Figure 9. Form of friction in joints.

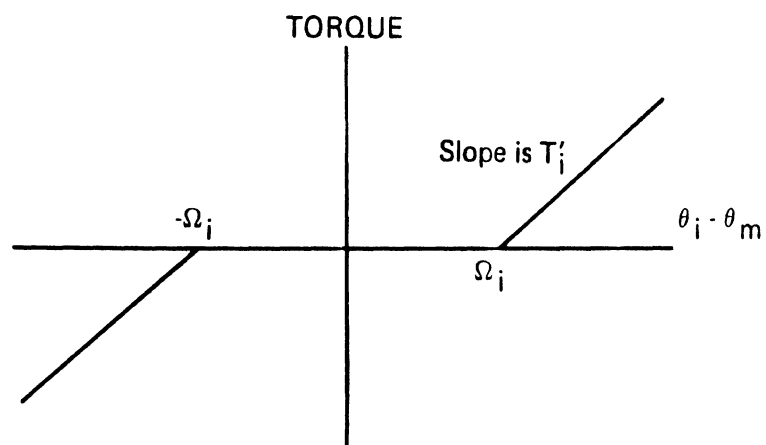


Figure 10. Form of symmetric joint stops for neck and two spinal joints.

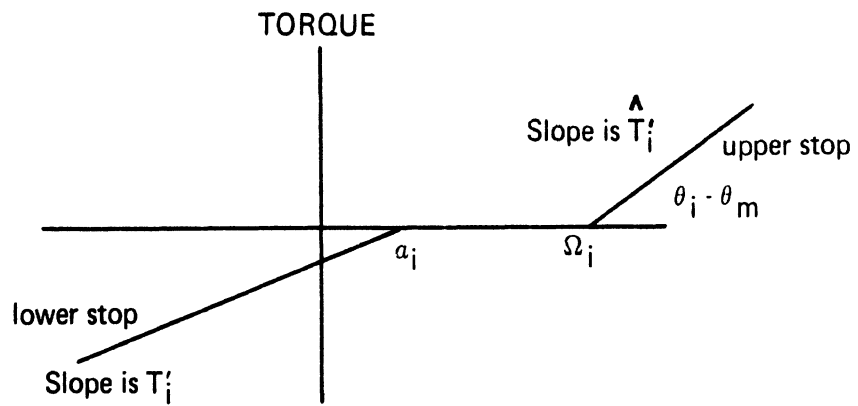


Figure 11. Form of nonsymmetric joint stops of hip, shoulder, elbow, and knee.

$$J_{si} = \begin{cases} T_i & \text{for } |\dot{\theta}_i - \dot{\theta}_m| \geq \xi_i \\ 0 & \text{otherwise} \end{cases} \quad (\text{II.F.3})$$

where the form of  $T_i$  depends on the particular joint.

The elements of the stop torque vector are defined as follows.

$$T_1 = \begin{cases} T_1' (\alpha_1 - \theta_1 + \theta_7) & \text{for } \theta_1 - \theta_7 < \alpha_1 \text{ and } \dot{\theta}_1 - \dot{\theta}_7 < 0 \\ \hat{T}_1' (\Omega_1 - \theta_1 - \theta_7) & \text{for } \theta_1 - \theta_7 > \Omega_1 \text{ and } \dot{\theta}_1 - \dot{\theta}_7 > 0 \\ 0 & \text{otherwise} \end{cases}$$

$$T_2 = \begin{cases} T_2'[\theta_1 - \theta_2 - \Omega_2 \operatorname{sgn}(\theta_1 - \theta_2)] & \text{for } |\theta_1 - \theta_2| > \Omega_2 \\ & \text{and } \operatorname{sgn}(\dot{\theta}_1 - \dot{\theta}_2) = \operatorname{sgn}(\theta_1 - \theta_2) \\ 0 & \text{otherwise} \end{cases}$$

$$T_3 = \begin{cases} T_3'[\theta_2 - \theta_3 - \Omega_3 \operatorname{sgn}(\theta_2 - \theta_3)] & \text{for } |\theta_2 - \theta_3| > \Omega_3 \\ & \text{and } \operatorname{sgn}(\dot{\theta}_2 - \dot{\theta}_3) = \operatorname{sgn}(\theta_2 - \theta_3) \\ 0 & \text{otherwise} \end{cases}$$

$$T_4 = \begin{cases} T_4'[\theta_3 - \theta_4 - \Omega_4 \operatorname{sgn}(\theta_3 - \theta_4)] & \text{for } |\theta_3 - \theta_4| > \Omega_4 \\ & \text{and } \operatorname{sgn}(\dot{\theta}_3 - \dot{\theta}_4) = \operatorname{sgn}(\theta_3 - \theta_4) \\ 0 & \text{otherwise} \end{cases}$$

$$T_5 = \begin{cases} T_5'(\theta_3 - \theta_5 - \alpha_5) & \text{for } \theta_3 - \theta_5 < \alpha_5 \text{ and } \dot{\theta}_3 - \dot{\theta}_5 < 0 \\ \hat{T}_5'(\theta_3 - \theta_5 - \Omega_5) & \text{for } \theta_3 - \theta_5 > \Omega_5 \text{ and } \dot{\theta}_3 - \dot{\theta}_5 > 0 \\ 0 & \text{otherwise} \end{cases}$$

$$T_6 = \begin{cases} T_6'(\theta_5 - \theta_6 + \alpha_6) & \text{for } \theta_6 - \theta_5 < \alpha_6 \text{ and } \dot{\theta}_5 - \dot{\theta}_6 > 0 \\ \hat{T}_6'(\theta_5 - \theta_6 + \Omega_6) & \text{for } \theta_6 - \theta_5 > \Omega_6 \text{ and } \dot{\theta}_5 - \dot{\theta}_6 < 0 \\ 0 & \text{otherwise} \end{cases}$$

$$T_7 = \begin{cases} T_7'(\alpha_7 - \theta_7 + \theta_8) & \text{for } \theta_7 - \theta_8 < \alpha_7 \text{ and } \dot{\theta}_8 - \dot{\theta}_7 > 0 \\ \hat{T}_7'(\Omega_7 - \theta_7 + \theta_8) & \text{for } \theta_7 - \theta_8 > \Omega_7 \text{ and } \dot{\theta}_8 - \dot{\theta}_7 < 0 \\ 0 & \text{otherwise} \end{cases}$$

(II.F.4)

Note that the neck and the two spinal joints are assumed symmetric, while the hip, shoulder, elbow and knee are not.

The joint elasticity generalized force vector is:

$$\begin{aligned}
c_1 &= K_1(\theta_7 - \theta_1 + \theta_{10} - \theta_{70}) - K_2(\theta_1 - \theta_2 + \theta_{20} - \theta_{10}) \\
c_2 &= K_2(\theta_1 - \theta_2 + \theta_{20} - \theta_{10}) - K_3(\theta_2 - \theta_3 + \theta_{30} - \theta_{20}) \\
c_3 &= K_3(\theta_2 - \theta_3 + \theta_{30} - \theta_{20}) - K_4(\theta_3 - \theta_4 + \theta_{40} - \theta_{30}) \\
&\quad - K_5(\theta_3 - \theta_5 + \theta_{50} - \theta_{30}) \\
c_4 &= K_4(\theta_3 - \theta_4 + \theta_{40} - \theta_{30}) \\
c_5 &= K_5(\theta_3 - \theta_5 + \theta_{50} - \theta_{30}) - K_6(\theta_5 - \theta_6 + \theta_{60} - \theta_{50}) \\
c_6 &= K_6(\theta_5 - \theta_6 + \theta_{60} - \theta_{50}) \\
c_7 &= K_7(\theta_8 - \theta_7 + \theta_{70} - \theta_{80}) - K_1(\theta_7 - \theta_1 + \theta_{10} - \theta_{70}) \\
c_8 &= K_7(\theta_7 - \theta_8 + \theta_{80} - \theta_{70}) \\
c_9 &= 0 \\
c_{10} &= 0
\end{aligned} \tag{II.F.5}$$

Joint friction and the joint stops are applied to the generalized force vector by the equation

$$\Delta \vec{b}_j = (J_{fi} + J_{si}) \vec{V}_i \tag{II.F.6}$$

where  $\vec{V}_i$  is a vector whose components are all zero except for the ith and the mth which are plus one and minus one, respectively.

The  $i$  is the joint index and  $m$  is as specified previously on page 39.

#### G. RESTRAINT SYSTEM

The conventional restraint system simulated in this program consists of a set of three belt segments, all of whose forces act independently at fixed points on the body.

The shoulder harness is modeled by two such independent segments (see Figure 12); the upper is assumed to act at the shoulder joint, the lower at a specified distance above the first spinal joint. Both segments have their attachment points fixed in the vehicle and the forces act along the lines connecting the point on the occupant with the belt attachment points in the vehicle.

The lap belt is modeled by one segment, thus assuming that the two sides of the real lap belt have the same fixed attachment point coordinates in the plane of motion. The force produced is twice that of one real segment. The shape of the lap belt segment is more complicated than that of the shoulder harness segments. It has not only a linear portion, but also a circular arc portion centered on the hip joint (see Figure 13). The linear portion is tangent to this circle.

An option in the program allows the user to specify no belts, lap belt only, shoulder harness only, or all three segments. Unconventional restraint systems such as an airbag may be crudely simulated by proper selection of contact surfaces.

For each of the three belt segments, elongation is computed as the current length ( $l_k$ ) minus the zero-time length ( $l_{k0}$ ). Deflection rate ( $\dot{\delta}$ ) is just  $\dot{l}_k$ . The same load-deflection procedure is used to compute force as has been previously used for contact forces. The quantity  $\phi_k$  is the belt angle for the corresponding segment.

For the lap belt, the following equations apply (see Figure 13).



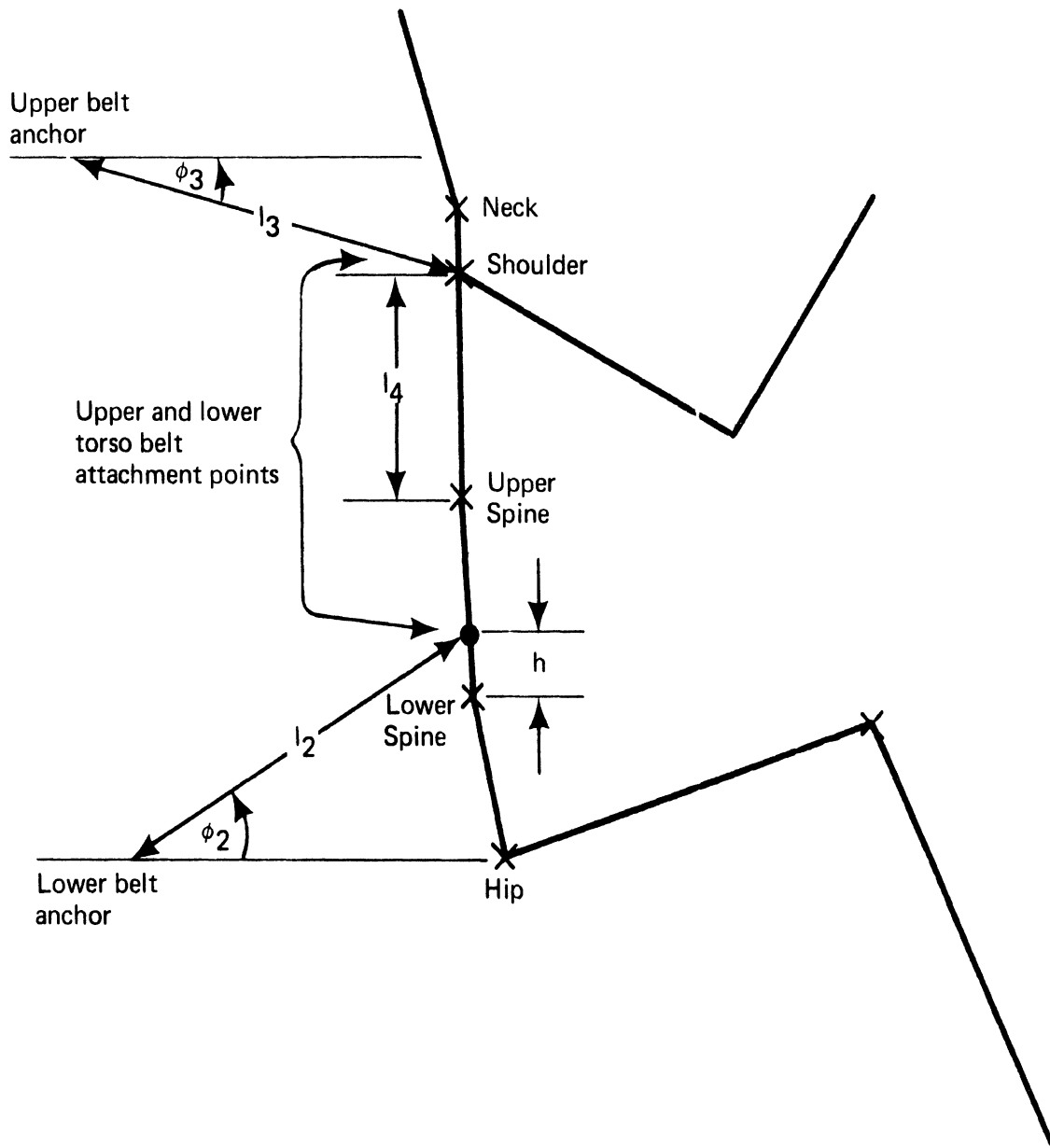


Figure 12. Shoulder belt geometry.

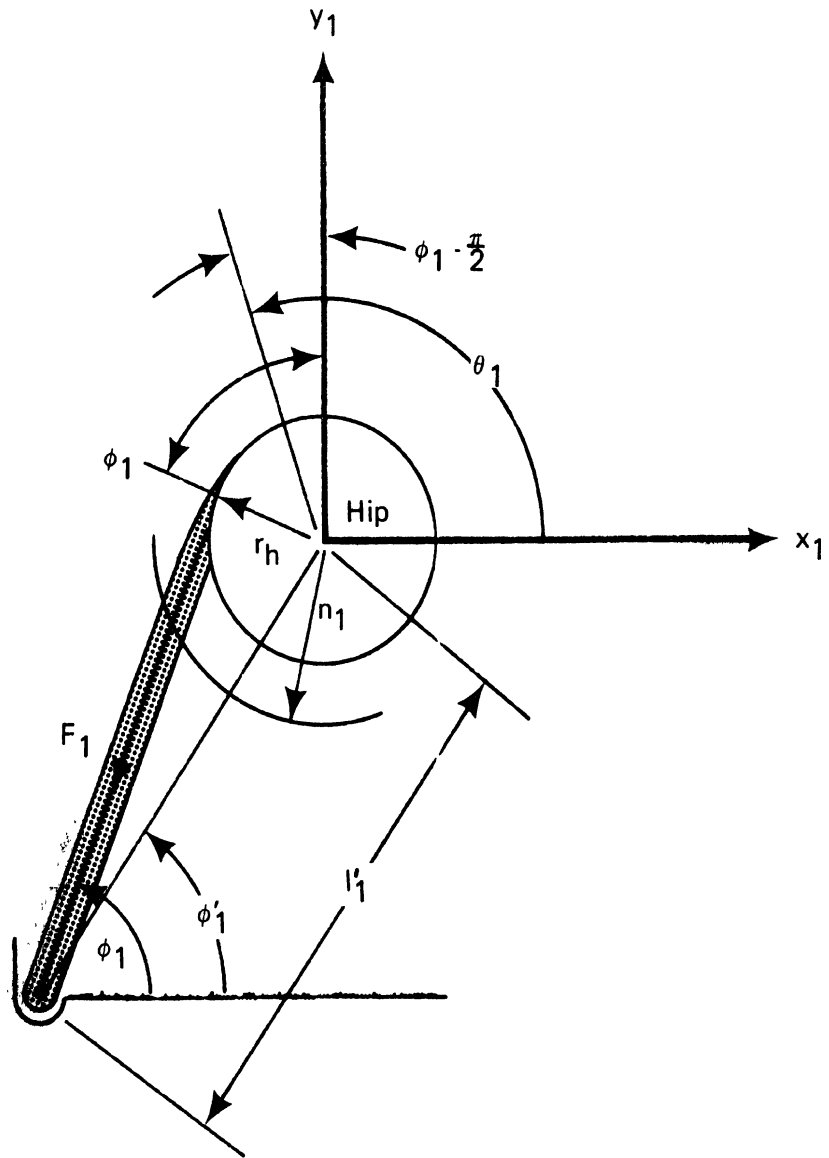


Figure 13. Lap belt geometry.

$$\begin{aligned}
l_1 &= \sqrt{(x + l'_{10} \cos \phi'_{10})^2 + (y + l'_{10} \sin \phi'_{10})^2 - r_h^2} \\
&\quad + r_h (\phi_1 - \phi'_{10} + \pi/2) \\
l_{10} &= \sqrt{(l'_{10})^2 - r_h^2} + r_h (\phi_{10} - \theta_{10} + \pi/2) \\
\phi_1 &= \tan^{-1} \left( \frac{y + l'_{10} \sin \phi'_{10}}{x + l'_{10} \cos \phi'_{10}} \right) \\
&\quad + \tan^{-1} \left( \frac{r_h}{\sqrt{(x + l'_{10} \cos \phi'_{10})^2 + (y + l'_{10} \sin \phi'_{10})^2 - r_h^2}} \right)
\end{aligned}$$

$$\dot{l}_1 = \dot{x} \cos \phi_1 + \dot{y} \sin \phi_1 - r_h \dot{\theta}_1 \quad (\text{II.G.1})$$

For the lower and upper shoulder belt segments ( $k = 2$  and  $3$ , respectively), the equations are: (see Figure 12)

$$\begin{aligned}
l_k &= \sqrt{\Delta x_k^2 + \Delta y_k^2} \quad \text{for } k = 2, 3 \\
\phi_k &= \tan^{-1} \left( \frac{\Delta y_k}{\Delta x_k} \right) \quad (\text{II.G.2})
\end{aligned}$$

A zero appended to the subscripts of a variable denotes the zero time value of that variable.

$$\Delta x_2 = x + L_1 \cos \theta_1 + h \cos \theta_2 - L_1 \cos \theta_{10} - h \cos \theta_{20} + l_{20} \cos \phi_{20}$$

$$\Delta y_2 = y + L_1 \sin \theta_1 + h \sin \theta_2 - L_1 \sin \theta_{10} - h \sin \theta_{20} + l_{20} \sin \phi_{20}$$

$$\dot{i}_2 = \dot{x} \cos \phi_2 + \dot{y} \sin \phi_2 - L_1 \dot{\theta}_1 \sin(\theta_1 - \phi_2) - h \dot{\theta}_2 \sin(\theta_2 - \phi_2)$$

and

$$\begin{aligned} \Delta x_3 = & x + L_1 \cos \theta_1 + L_2 \cos \theta_2 + L_4 \cos \theta_3 - L_1 \cos \theta_{10} \\ & - L_2 \cos \theta_{20} - L_4 \cos \theta_{30} + l_{30} \cos \phi_{30} \end{aligned}$$

$$\begin{aligned} \Delta y_3 = & y + L_1 \sin \theta_1 + L_2 \sin \theta_2 + L_4 \sin \theta_3 - L_1 \sin \theta_{10} \\ & - L_2 \sin \theta_{20} - L_4 \sin \theta_{30} + l_{30} \sin \phi_{30} \end{aligned}$$

$$\begin{aligned} \dot{i}_3 = & \dot{x} \cos \phi_3 + \dot{y} \sin \phi_3 - L_1 \dot{\theta}_1 \sin(\theta_1 - \phi_3) \\ & - L_2 \dot{\theta}_2 \sin(\theta_2 - \phi_3) - L_4 \dot{\theta}_3 \sin(\theta_3 - \phi_3) \end{aligned} \quad (\text{II.G.3})$$

The belt contributions to the generalized force vector are:

$$\begin{aligned}
D_{b1} &= r_h P_1 + L_1 \sum_{m=2}^3 P_m \sin(\theta_1 - \phi_m) \\
D_{b2} &= h P_2 \sin(\theta_2 - \phi_2) + L_2 P_3 \sin(\theta_2 - \phi_3) \\
D_{b3} &= L_4 P_3 \sin(\theta_3 - \phi_3) \\
D_{bi} &= 0, \quad i = 4-8 \\
D_{b9} &= - \sum_{m=1}^3 P_m \cos \phi_m \\
D_{b10} &= - \sum_{m=1}^3 P_m \sin \phi_m \qquad \qquad \qquad (II.G.4)
\end{aligned}$$

where  $P_k$  is the force computed by use of the load-deflection procedure for the kth segment.

### III. EXPERIMENTAL VERIFICATION OF THE MATHEMATICAL MODEL

In this section of the report comparisons are made between the predictions of the mathematical model and an experiment carried out on the HSRI impact sled with an anthropometric dummy. Beginning with an outline of the criteria on which the validation is based, the report continues with a description of the sled test and concludes with a description of the degree to which the model describes the real test situation.

#### A. CHOICE OF A CRITERION OF VERIFICATION

The choice of a criterion of verification of the mathematical model describing human body impact is based on three premises: (a) whether or not the mathematical analysis and computer program are correct; (b) the extraction of appropriate experimental data on which the validation procedures can be based; and (c) the observation that the mathematical model consists of parameters describing the occupant, the force field consisting of belts and contact surfaces which act on the occupant, and the externally applied deceleration forcing function.

The use of a Lagrangian formulation of Newtonian mechanics as a basis for these models follows a long history of successful application to problems in impact, and hence, offers no cause for concern. Thus, sources of problems can arise only in writing down the particular equations and computer program which apply to the present analysis. All equations and the computer program have been derived independently by two or more persons leading to very low incidence of errors in the final computer program.

The second premise, which is concerned with the extraction of appropriate experimental data on which the validation can be based, has been the basis for a major research effort. The acquisition of the necessary transducer and photometric data is straightforward and requires

only the proper usage of the appropriate high speed cameras, data tape recorders, and light beam oscillographs. The processing of the transducer data is also relatively simple. For example, the determination of the magnitude of the linear acceleration of the head of the dummy requires computation of the simple vector sum of the three linear acceleration components.

Analysis and graphing of the test data is only part of the problem because preparation of a well-founded set of input data is necessary for the successful operation of any computer analysis. Therefore, a description of the mass, geometric, and inertial properties of the test subject is required. This must be supplemented by a geometrical profile of the vehicle components with which the test subject is expected to interact. Finally, the force-deformation characteristics of the interactions between the test subject and the vehicle components must be measured in order to specify the proper balance between subject motions and loadings.

In order to define the test subject, the eight basic body elements were weighed and moments of inertia measured using a trifilar pendulum or predicted using formulas similar to those of Hanavan<sup>25</sup> and Patten.<sup>26</sup> After the geometry of the test sled and the initial position of the dummy subject were carefully measured, it was then necessary to develop test procedures defining the force-motion relationships between test subject and vehicle elements. This was carried out for the seat and for a belt restraint system using a combination of photometric and transducer data described later in this report. (The simulation of an airbag restraint system was accomplished using similar techniques and will be discussed in the final report on that phase of the research project.)

The third premise serves to define the mathematical model as a system of parameters describing the occupant, the force field consisting of belts and contact surfaces which acts on the occupant, and the externally applied deceleration forcing function. All these basic parameters must

be included in any test validation.

To properly study the field of forces acting on the subject it is necessary to simulate both contact surfaces (such as a seat cushion and seat back) and belts (such as a lap belt and single diagonal shoulder harness). The use of an occupant unrestrained by belts would not provide a sufficient test of this important section of the analysis.

Based on these three premises, an impact sled test using a 50th percentile male anthropometric dummy was carried out at a speed of approximately 30 mph. This represented the most standard test configuration in use in impact sled test laboratories. The dummy was restrained by a lap belt and a single diagonal shoulder harness. Thus, this test represented a complete and economical test of the basic parameters described in the model—the occupant, the restraint and interior contact forces, and the vehicle deceleration.

## B. THE EXPERIMENT

The validation experiment was carried out on the HSRI impact sled (Figure 14), which is of the acceleration-deceleration type. It can be accelerated over a 12-ft distance up to a top speed of 40 mph using a compressed air-actuated puller arm. The deceleration stroke has a maximum length of 3 ft and a maximum potential of 88 g's. For the purpose of high-speed photography a total of 50 kw of lighting is available. Real time and high-speed movies are taken as well as still photographs before and after each test.

Kistler Piezotron 818's triaxial accelerometer packs were located in the head and chest of the 50th percentile Sierra dummy. A Statham strain-gage accelerometer was used to record the sled deceleration pulse. Four Lebow seat-belt load transducers were mounted on the seat belt and shoulder harness.

The data was recorded simultaneously on a Honeywell 7600 tape recorder and a Honeywell 1612 Visicorder. No filtering was used during



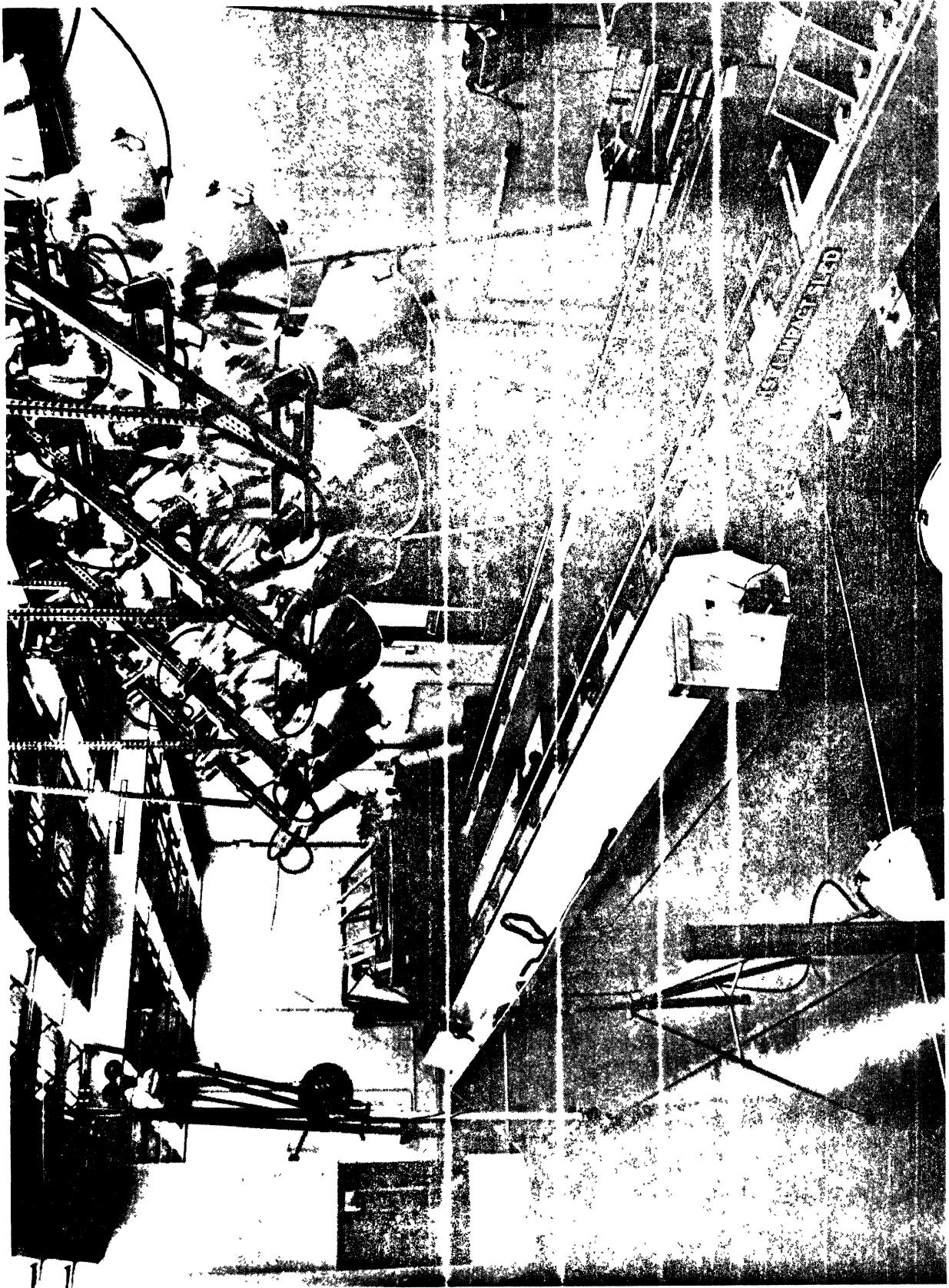


Figure 14. HSRI impact sled.

the initial recording other than the limitation of the light-beam galvanometers to frequencies under 1000 cps. The following transducer data was recorded: (a) lower right shoulder belt force; (b) left lap belt force; (c) upper left shoulder belt force; (d) right lap belt force; (e) sled deceleration; (f) head anterior-posterior G-loading; (g) chest anterior-posterior G-loading; (h) head superior-inferior G-loading; (i) chest superior-inferior G-loading; (j) head left-right G-loading; (k) chest left-right G-loading; (l) impact velocity; and (m) timing signals.

The test setup for the validation of the model is shown in Figure 15. The bucket seat is bolted securely to a framework which is attached to the sled. This framework serves as a mount for attaching belts and other types of restraint systems, and can be rotated to simulate lateral or oblique impact.

The test data presented in Figures 16 through 25 were obtained as a result of either detailed analysis of the high-speed films using a Vanguard Film Analyzer or by measuring points from the oscillographic recording. All acceleration and belt transducer data were determined from the oscillographic records and appropriate sums and resultant values were computed.

In the model, the excursion and forward motion of the head were determined directly by measurement of the motion of a target placed on the head of the dummy. Likewise the angle of head pitch and the upper leg were obtained by direct measurement (and the subsequent scaling and tabulation by means of specially developed computer programs). The motion of the H-point was very difficult to determine as no direct measurements were possible. However, its location was determinable by trigonometry using data from a thigh target, a lower back target, and the angle of the upper leg with a horizontal line. These data, determined on the Vanguard Analyzer, were then processed on the HSRI 1130 digital computer using the appropriate trigonometric data handling subroutines.



Figure 15. Test setup for two-dimensional model validation.

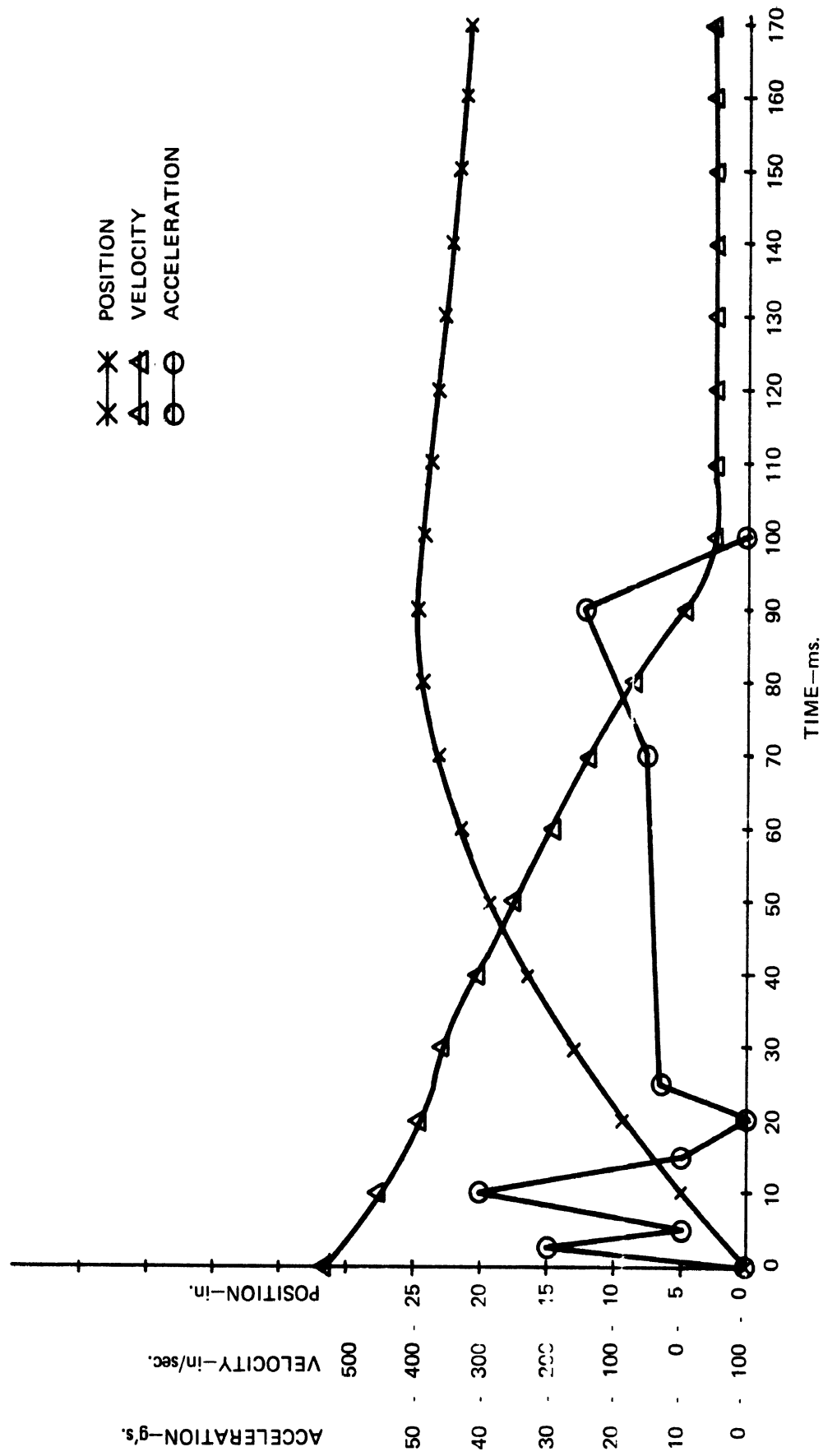


Figure 16. Vehicle kinematics.

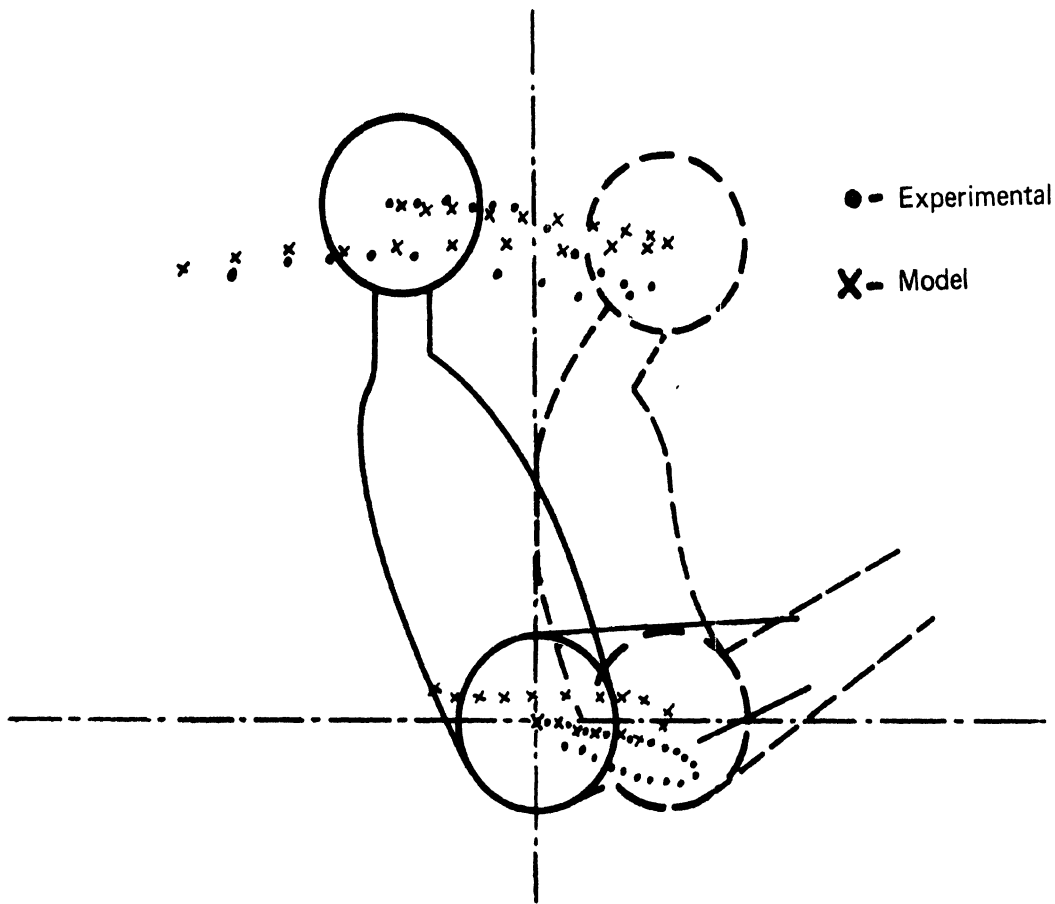


Figure 17. Excursion of head center-of-gravity and H-point as a function of time.

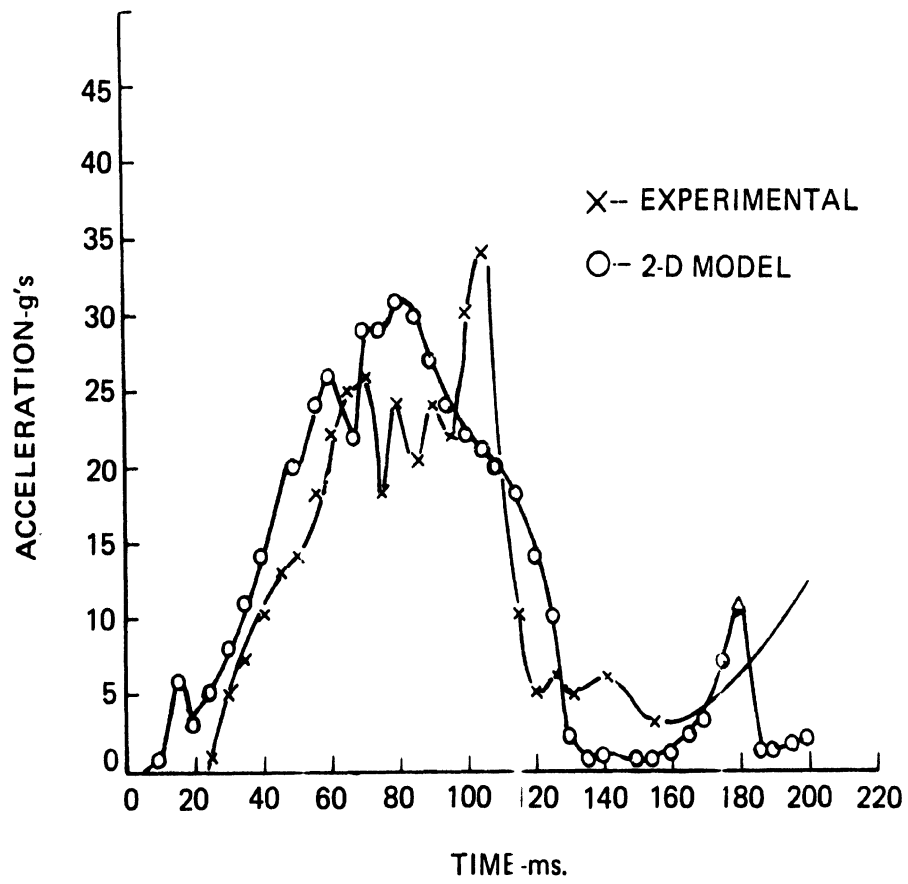


Figure 18. Resultant chest linear acceleration in g's.

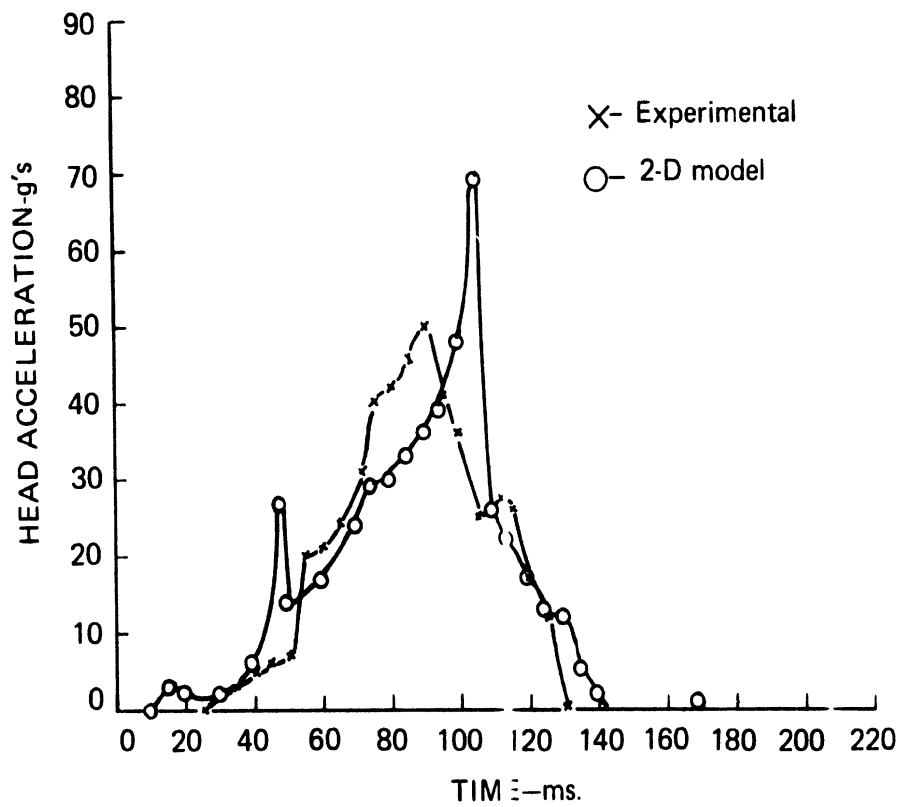


Figure 19. Resultant head linear acceleration in g's.

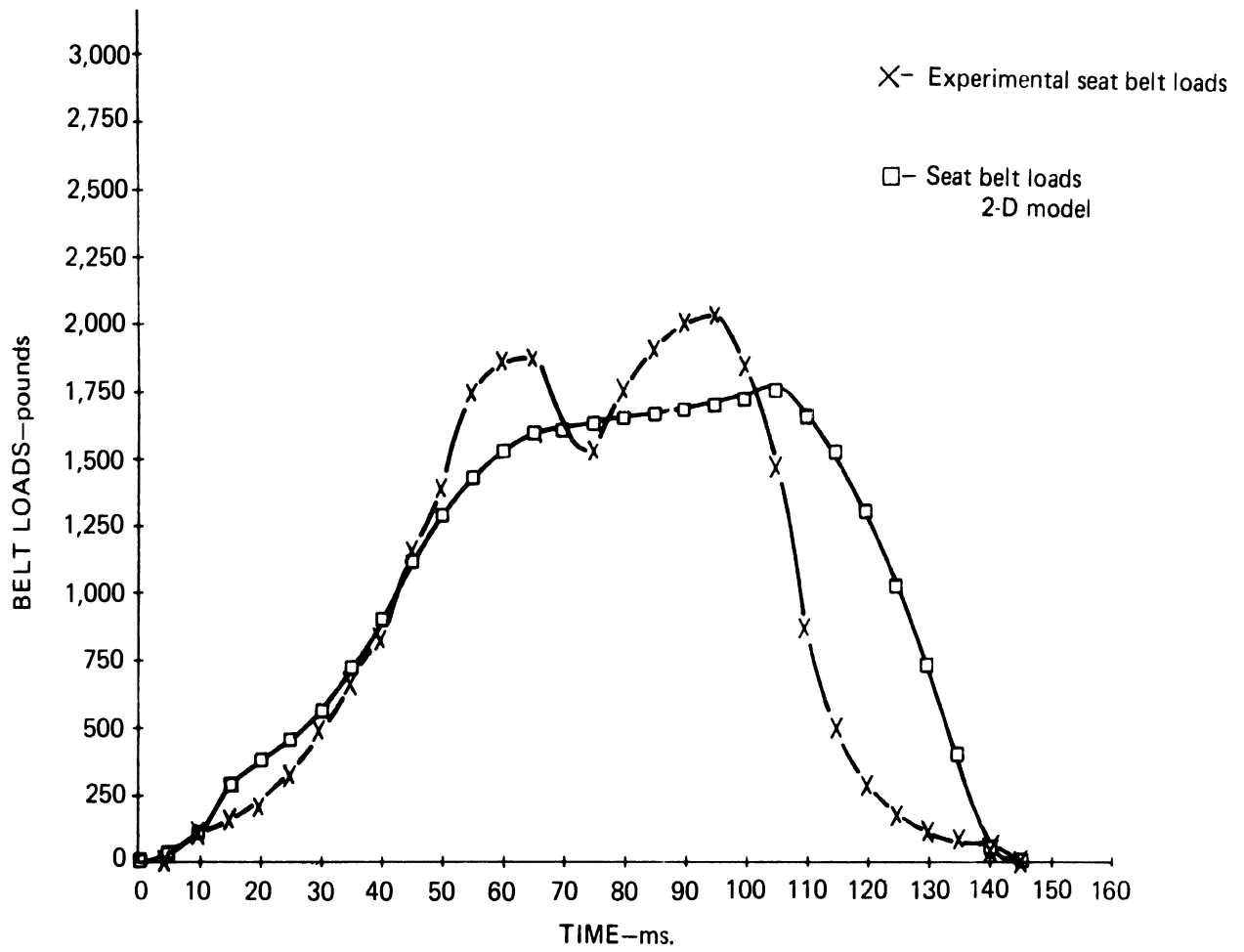


Figure 20. Seat belt loads.



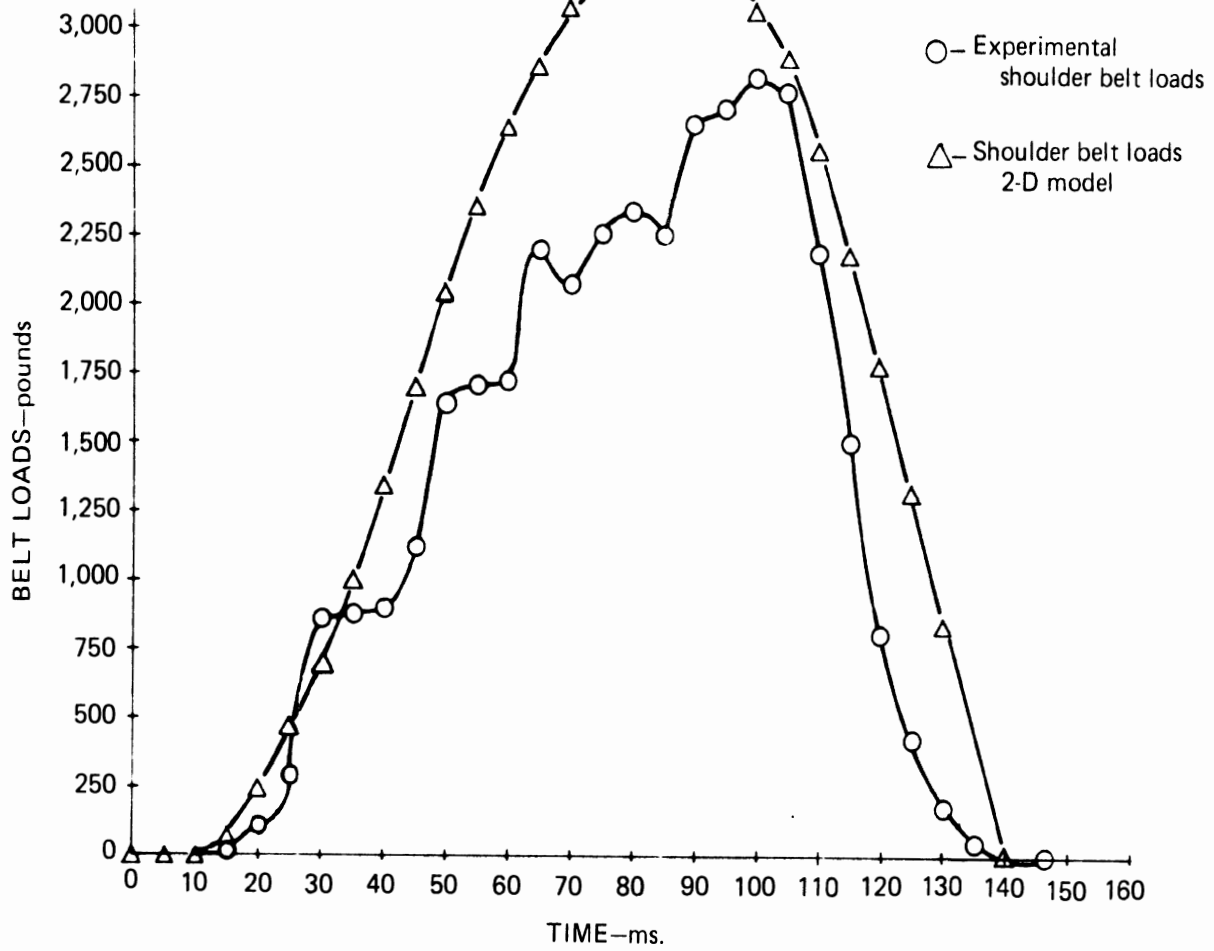


Figure 21. Shoulder harness loads.

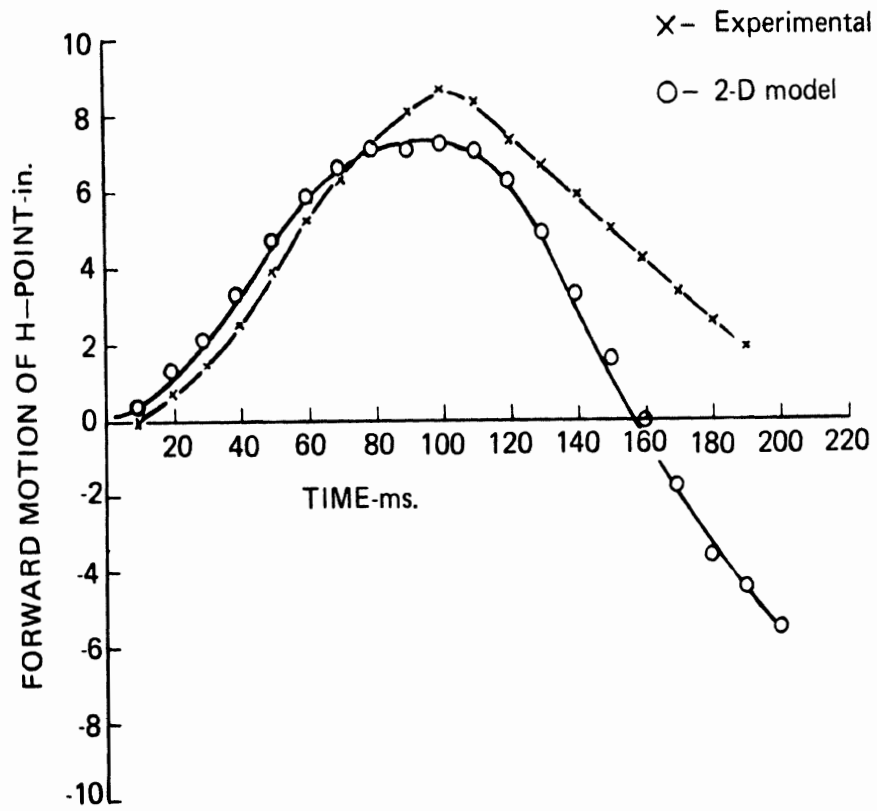


Figure 22. Forward motion of H-point.

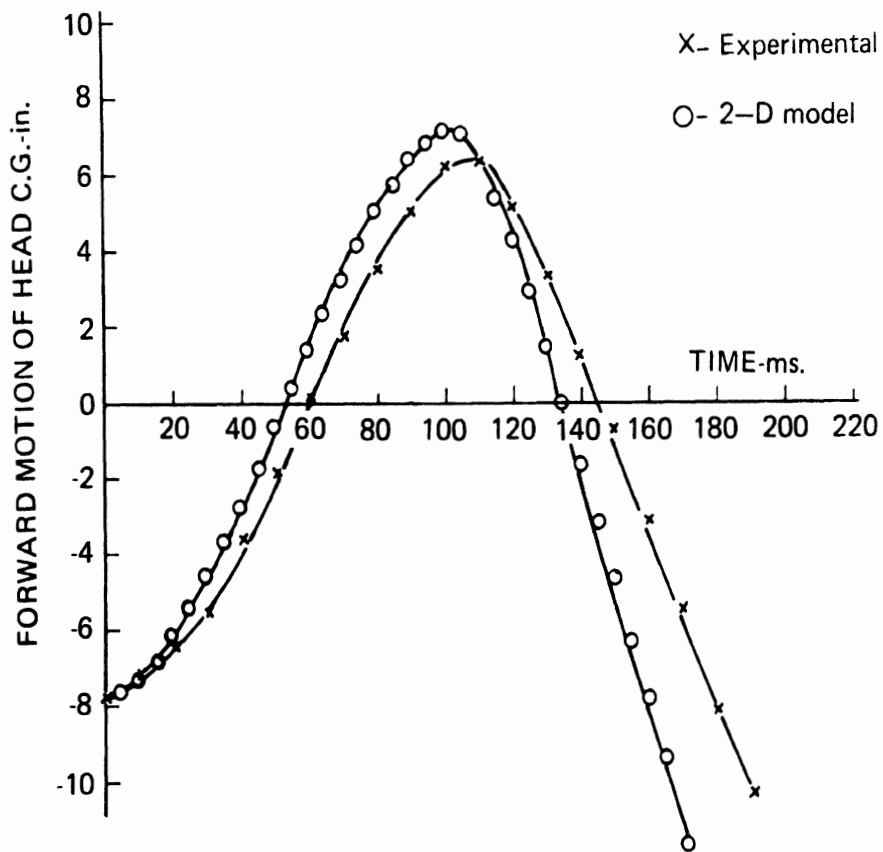


Figure 23. Forward motion of head center-of-gravity.

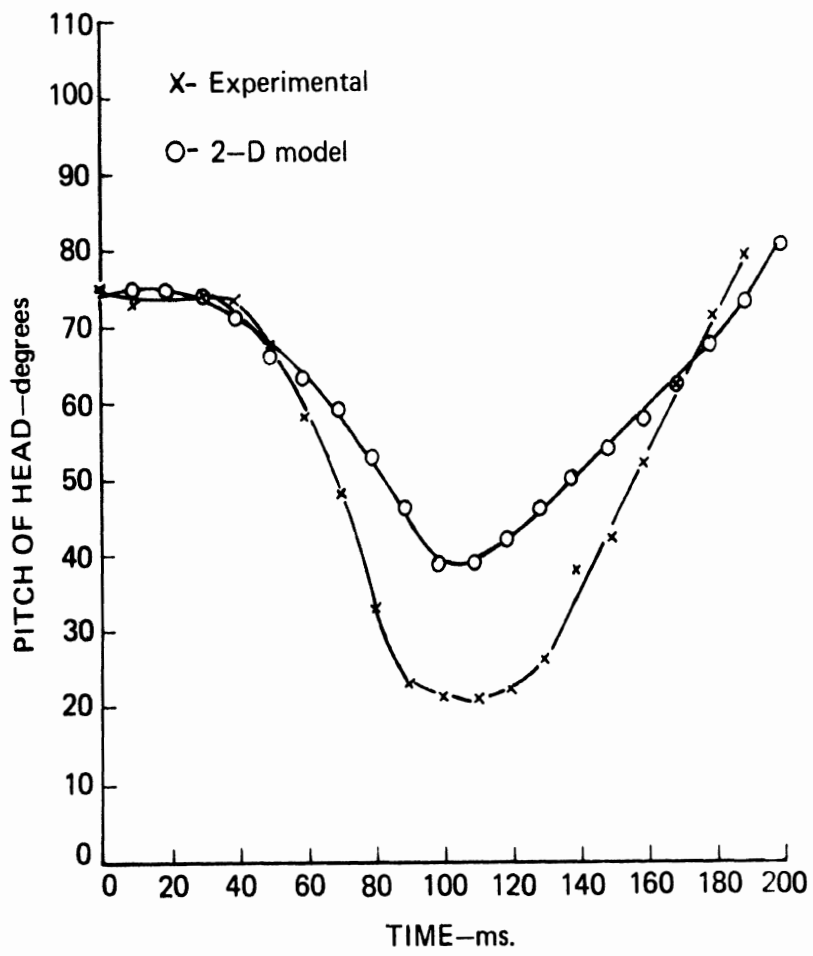


Figure 24. Pitch angle of head.

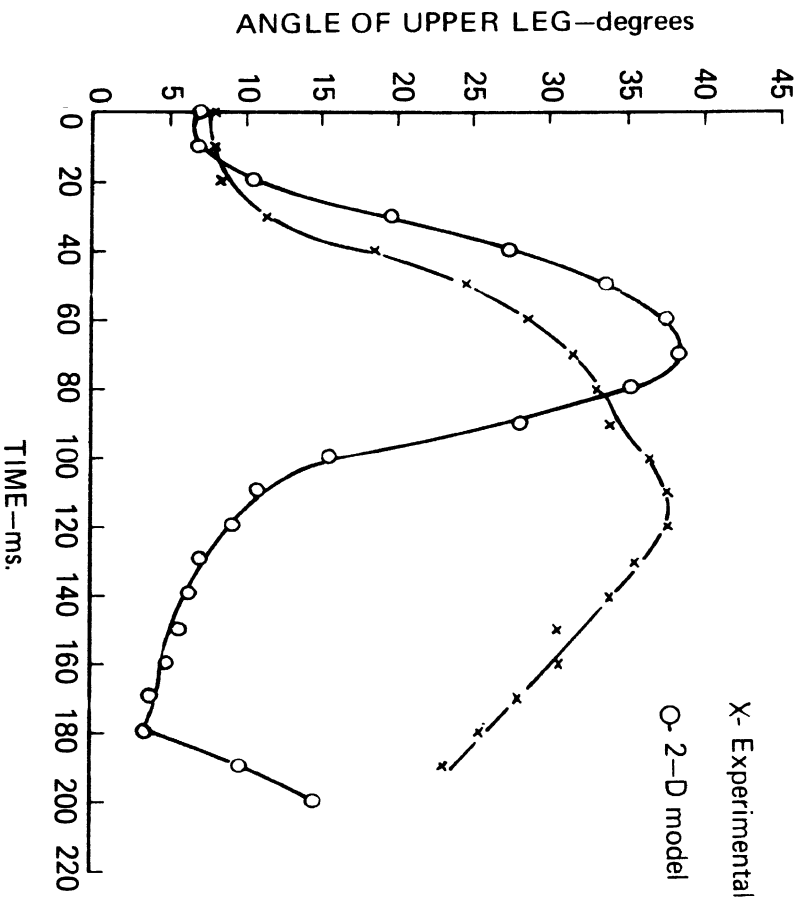
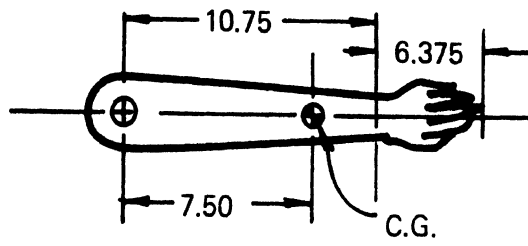
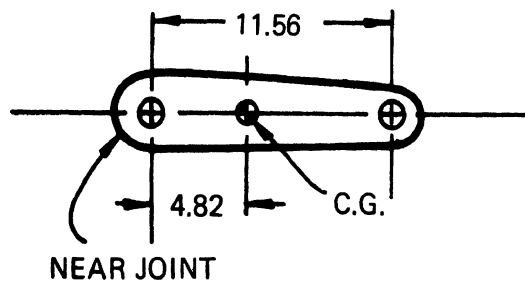


Figure 25. Pitch angle of the upper leg.

Dimensions of Forearms:



Dimensions of Upper Arms



Dimensions of Lower Spine:

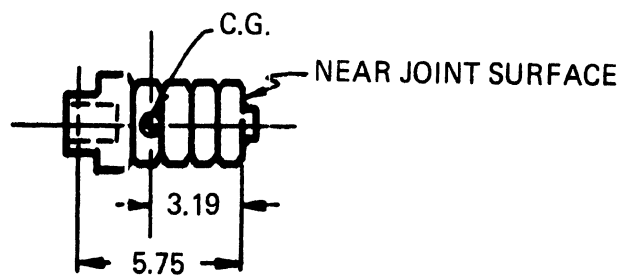
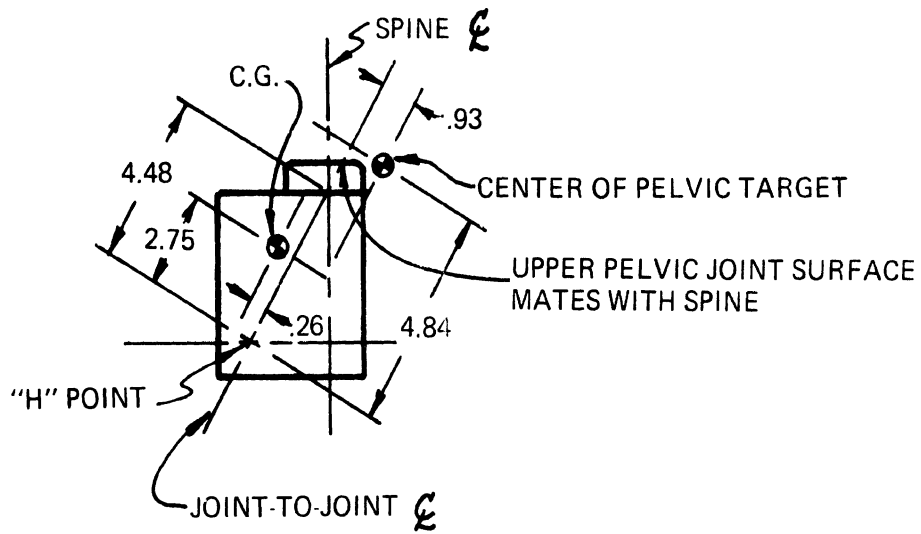
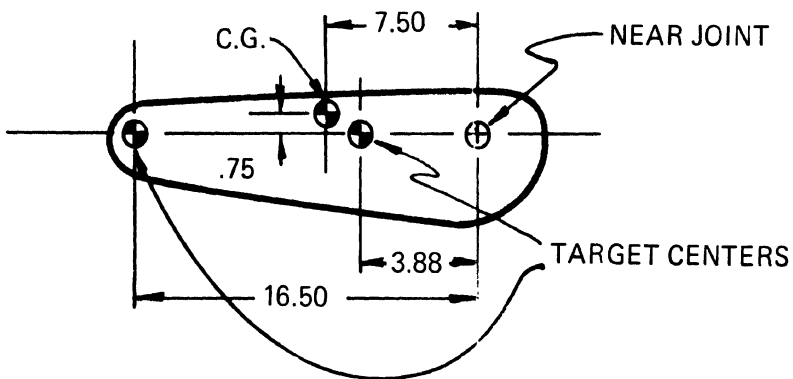


Figure 26. Centers-of-gravity and dimensions of forearms, upper arms, and lower spine.

Dimensions of Lower Torso Pelvic Area:



Dimensions of Upper Leg:



Dimensions of Lower Leg Including Foot:

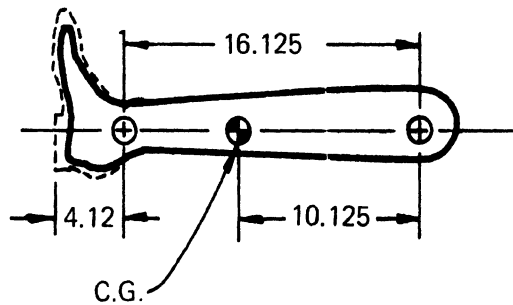
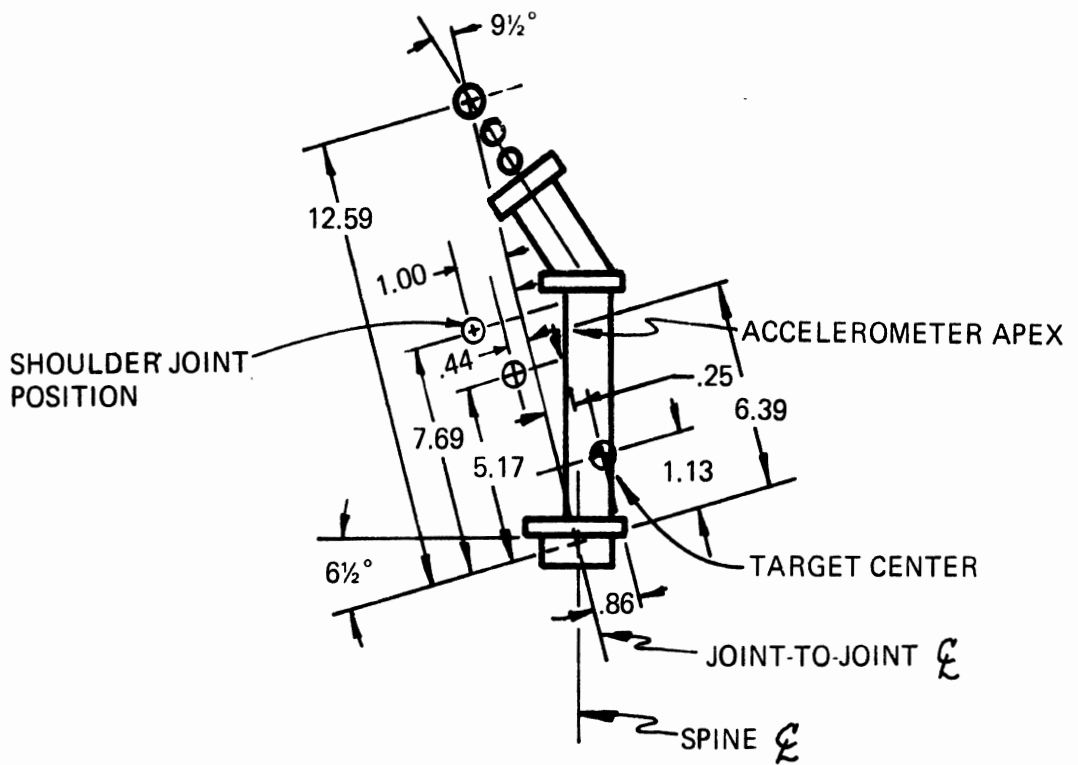


Figure 27. Centers-of-gravity and dimensions of pelvic area, upper legs, and lower legs.

Dimensions of Upper Torso Assembly:



Dimensions of Head Assembly:

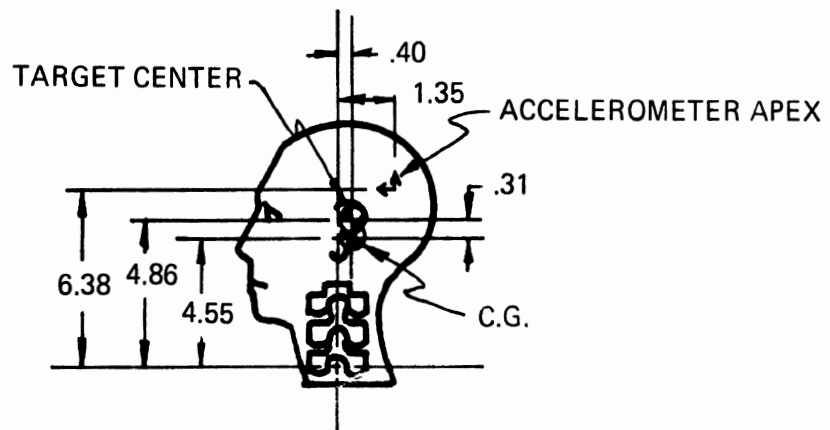


Figure 28. Centers-of-gravity and dimensions of head and upper torso.



### C. PREPARATION OF A DATA SET FOR THE COMPUTER SIMULATION

The preparation of a data set for the validation exercise of the model involved determination of the mass and inertial properties of the HSRI 50th percentile male Sierra dummy as well as the force-deformation interactions between the dummy and his seat and restraint system. Various other quantities such as the initial impact velocity, the sled deceleration profile, and the positioning of the dummy at the beginning of the deceleration event were measured directly from the test movies or transducer data.

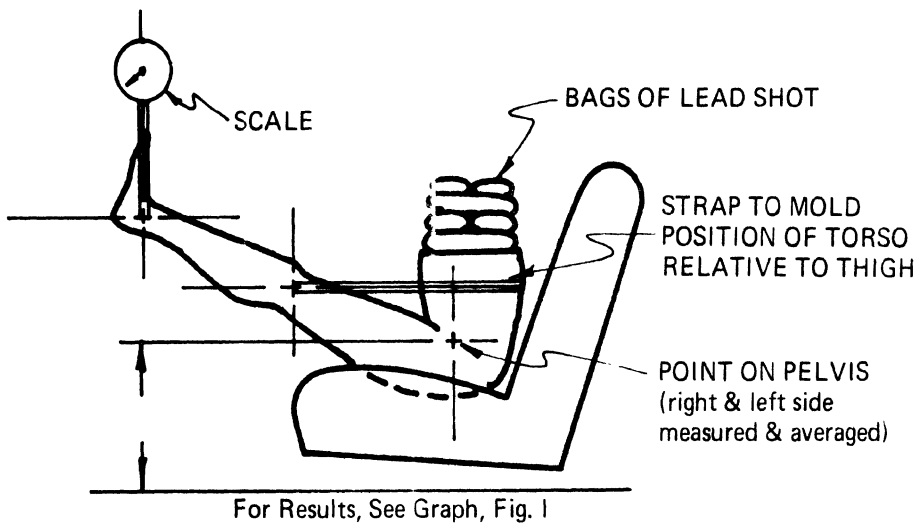
The center of gravity of the various body parts was found by suspending the piece by wires and observing the location of intersecting lines of action. The eight moments of inertia of the body parts for use in the model were found by suspending each piece on a trifilar pendulum. The weights of the body parts were measured on a precision scale. This data, tabulated in Table VI and Figures 26-28, is felt to be accurate within 1% as repeated measurements were taken on the various quantities. A correction to the moments of inertia was made based on the weight and distribution of the body skin element.

Because no impact data is available in a form suitable for use in the computer program, two static tests were carried out. The test configurations are shown in Figure 29 and the results in Figures 30 and 31. In determining the curve for load-deflection under the buttocks, the deflection was measured by taking height readings "h" at points on the pelvis as shown, as weight was added. For determining the load-deflection curve at the front of the seat, the dummy was hung as shown with the legs up, knees locked, and the buttocks just touching the cushion. The hip joint was loose. The legs were lowered gradually, and load scale readings were taken at progressive points until the scale read zero. At this time the seat front is supporting the legs. Weights were then added until the seat front bottomed out of the seat frame. This test has the disadvantages of being static and only applying the load over part of the

TABLE VI. WEIGHTS AND MOMENTS OF INERTIA OF  
HSRI 50th PERCENTILE SIERRA DUMMY

Body Segment	Segment Weight, lb	Segment Moment of Inertia, in. lb sec <sup>2</sup>
Right forearm and hand	5.094	0.300
Left forearm and hand	5.187	0.309
Right upper arm	5.938	0.241
Left upper arm	5.656	0.233
Lower spine	4.531	0.078
Lower torso pelvic area	17.062	1.709
Right upper leg	20.125	1.316
Left upper leg	20.156	1.307
Right lower leg and foot	9.781	1.211
Left lower leg and foot	9.813	1.186
Upper torso (including shoulder and chest mode, plastic "sub-skin" around rib cage and two lower neck vertebrae clamped tight)	37.438	1.344
Head (including two upper neck vertebrae)	15.781	0.436

A) LOAD-DEFLECTION UNDER BUTTOCKS



B) LOAD-DEFLECTION AT FRONT OF SEAT

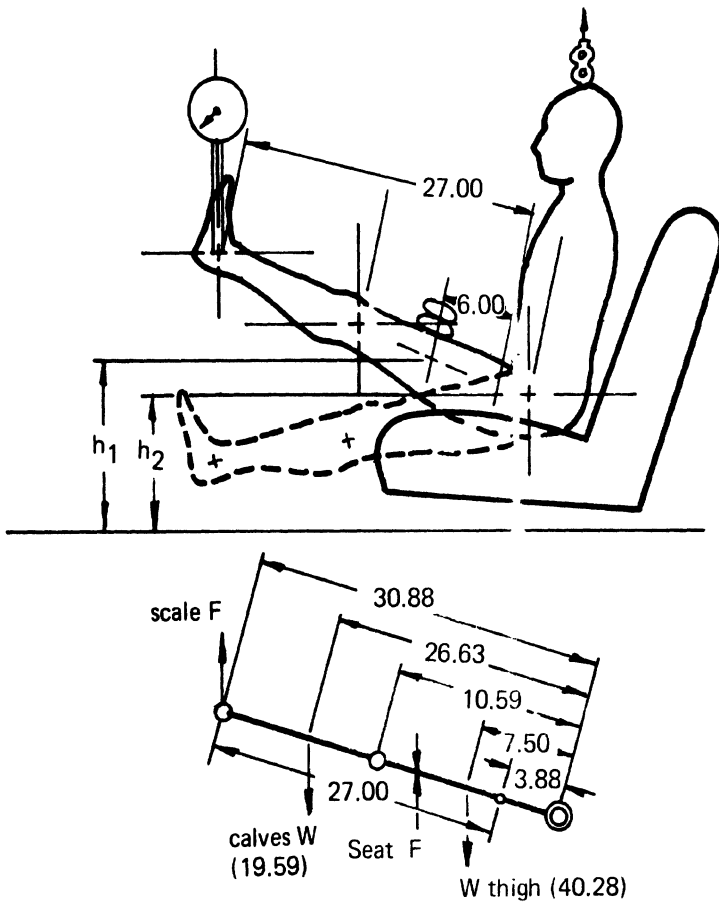


Figure 29. Test configuration for seat property tests.

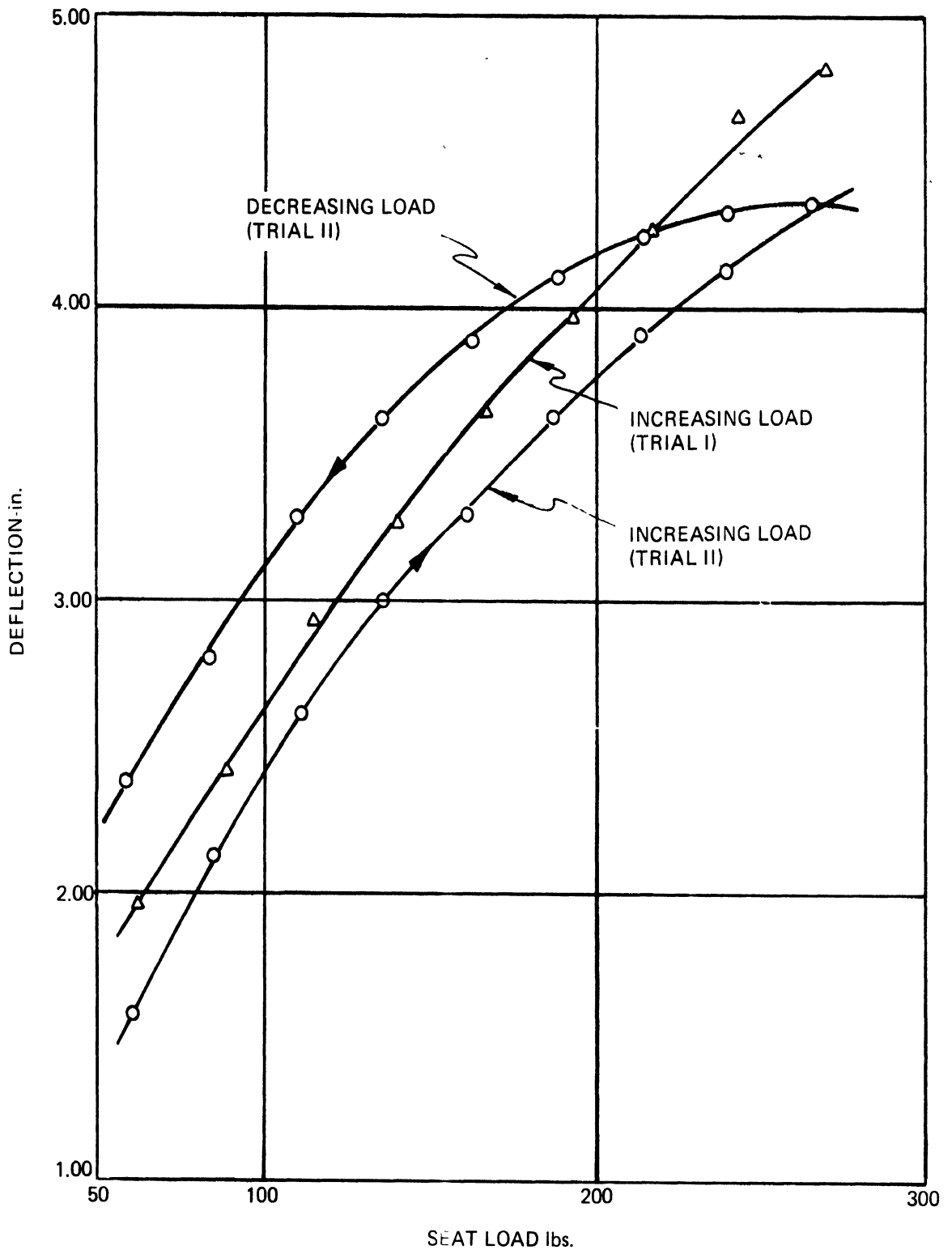


Figure 30. Seat load-deflection characteristics.

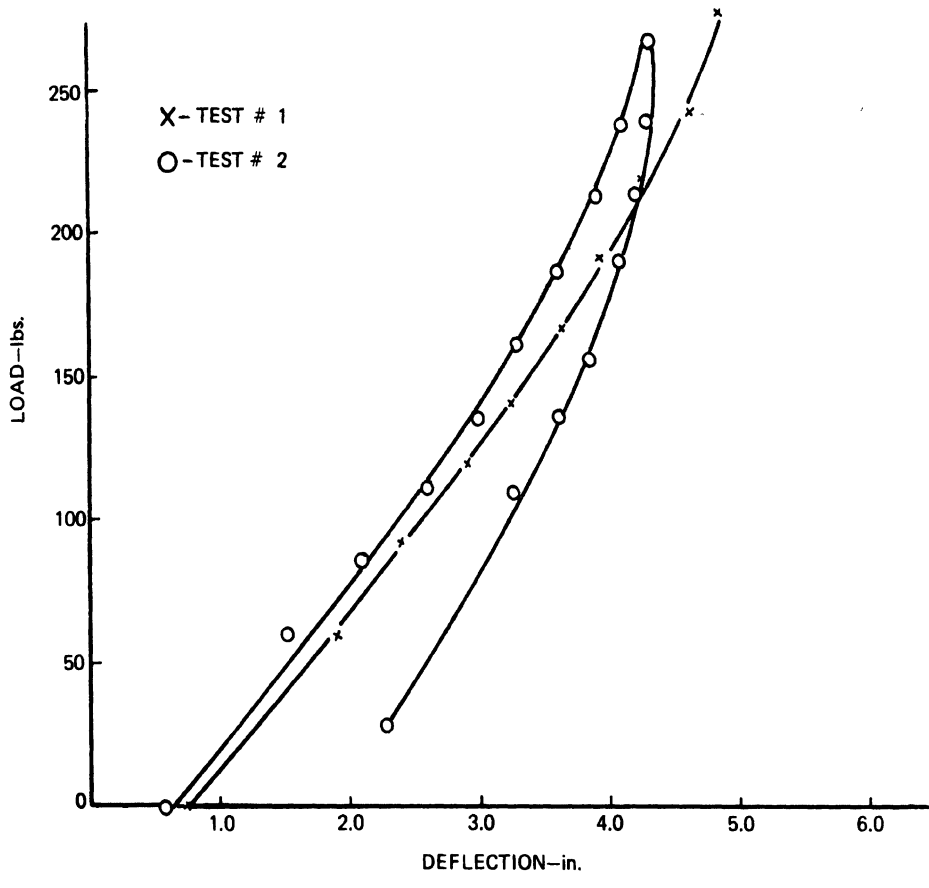


Figure 31. Seat load-deflection characteristics at seat front.

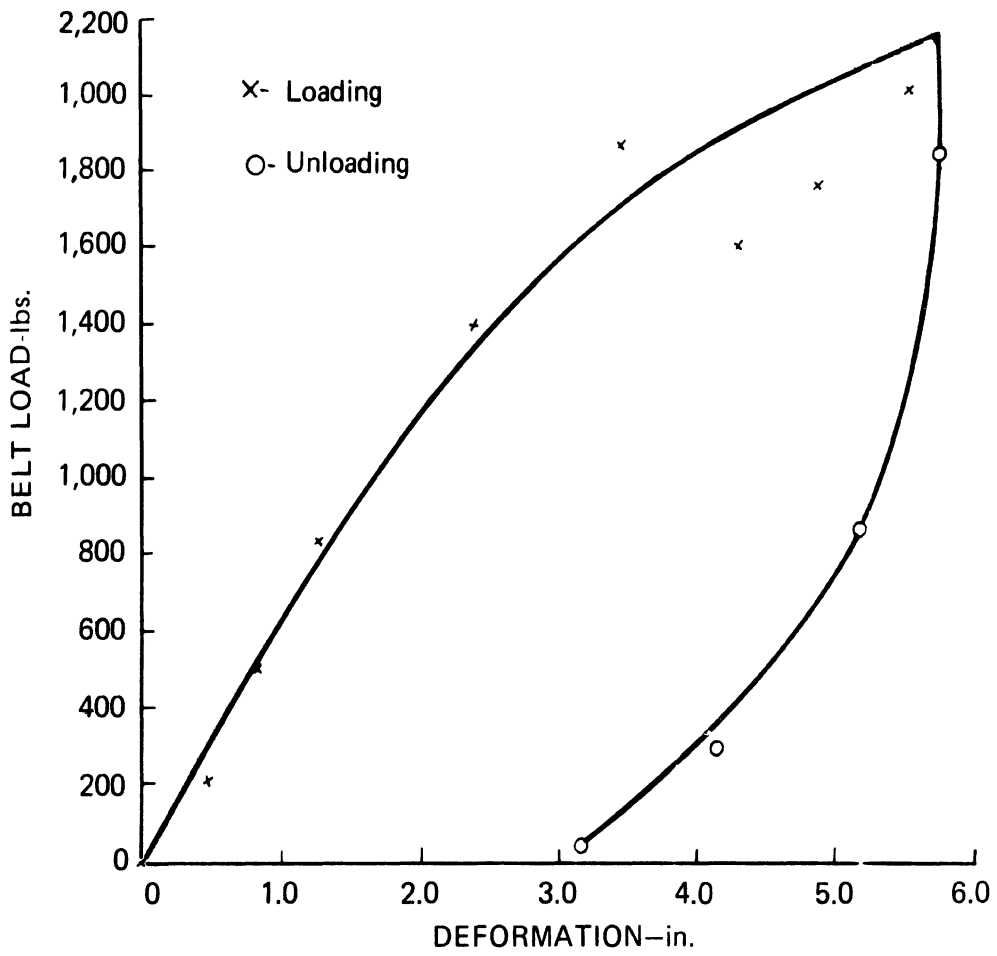


Figure 32. Load-deflection characteristics of seat belts.

seat. However, it does have the advantage of determining a curve which includes deformation properties of both the seat and dummy used in the test.

The seat belt load-deflection characteristic also led to difficulties in measurement. In this case, deformation properties of the belt, buckles, vehicle attachment points, and of the dummy itself must be reflected in the modulus which is used in the model. In addition to this, it is necessary that the deformations be a projection on the two-dimensional plane of events which actually occur in three-space.

Thus, the load-deformation characteristics of the seat belts were measured by making use of data gathered during the test itself. Force transducers were used to record the loads in the belts and high-speed movies recorded a plane view of the action of the belts. Therefore, using the known location of the H-point, the belt angle, and the location of the belt attachment point in the vehicle, it was possible to construct a table of the seat-belt length as a function of time. This, when combined with the data from the load cells, was used to construct Figure 32. Measurement of the deformation characteristics of the shoulder harness elements similarly was carried out using high-speed movies and loads from the force transducers.

#### D. COMPARISON OF THE SLED TEST DATA WITH THE PREDICTION OF THE MODEL

The comparison between the sled test and the mathematical model was accomplished by measuring the parameters necessary for the operation of the model and then exercising the model based on this set of input data. The only parameters which were not determined experimentally were the stiffnesses of the stops in the various joints. These were given arbitrary high values compatible with the definition of a "stop." In most computer simulations the various body segments do not even interact with the stops making precise definition unnecessary. Also, it has been found in other exercises of the model that variation of these quantities over rather wide ranges does not have a large effect on the body kinematics. Thus,

it is felt that the impact data which was measured provides a valid test case.

Two types of comparisons can be made between analysis and experiment. On one hand, the actual dummy body motions are studied; on the other, the forces and accelerations experienced by the body are examined.

The excursion of the head center of gravity and the H-point are shown in Figure 17 as a function of time. It can be noted that both the head and the hip moved down to a greater degree in the test than they did in the simulation. Also, the hip was observed to move further forward in the test. It is felt that this can be explained by an examination of the hip structure of the Sierra dummy in comparison to the model. In the dummy, the seat belt was observed in the test to ride over the pelvic structures into the abdominal area. In the model, the belt was required to stay on a radius which was a fixed distance from the H-point. Thus, in the test submarining was allowed, while in the simulation, it was impossible. The fact that submarining was observed in the test may well explain the substantial nonlinear softening-spring behavior of the seat belt load-deflection curve.

Figures 22 and 23 describe the forward motion of head and hip as a function of time. The prediction of head motion is quite good whereas the motion of the hip differs during rebound possibly as a result of submarining and the fact that the belt is buried in the dummy abdomen after the test.

The pitch angle of the head is plotted in Figure 24. Although the phase is correct, the magnitudes are not. The error in pitch magnitude is about 32%. It is felt at this time that the greater flexibility of the dummy neck (note that this would be even more exaggerated in a living subject) leads to this error. It is possible that this phenomenon can be compensated for by altering the joint stop angle from the values used in this simulation. By increasing their values, greater "flexibility" is introduced to the dummy.



Figure 25 shows the pitch angle for the upper leg. In the model this body element pitched up and down more quickly than in the test. However, the peak values are similar, possibly because the rotation of the pelvic area of the dummy down under the seat belt is in the same direction as the rotation of the upper leg. This seems likely from qualitative observations of the high-speed movies.

Figure 18 shows the resultant chest linear acceleration in G's. Agreement between these curves is remarkably good both with respect to phase and peak G-values. The test data were determined as a combination of the three readings of a triaxial accelerometer pack. The readings for the model were obviously limited to accelerations in the plane. The spike at 180 ms in the model and the rise in the test data reflect rebound into the seat back.

Similarly, in Figure 19 there is fairly good agreement between the predicted and test values of head linear acceleration. The 70 G spike predicted by the model occurred as the head pitched forward sufficiently far to encounter the "stop" briefly. Spikes of this nature are likely to occur in any segmented collection of rigid bodies in which stops are allowed to act. The peaks will be reduced only as flexibility is added to the system.

Figures 20 and 21 show the comparative seat belt and shoulder harness loads. Agreement is quite good both in phase and magnitude in the seat belt loads. The predicted harness loads appear to be low although the peak values are within 15%. The reason for this is unknown at present. It is possible that the error could be experimental in that signal clipping was observed on strain gage channels in several tests conducted near the time of this test. Other reasons could be improper selection of force-deformation curves and slack for the harness system.

The comparisons between theory and experiment which have just been presented represent the beginning of the most important phase of the model development program—the determination of the ability of the model to

describe the physical system. Agreement is good on many important quantities discussed above. The differences noted in other quantities reflect both difficulties in mathematically describing a continuous body by lumped masses and also difficulties in determining the input data with which the model can be exercised.

#### IV. USERS' GUIDE FOR THE TWO-DIMENSIONAL CRASH VICTIM SIMULATOR

This part of the report is intended to serve as a complete Users' Guide for exercising the HSRI Two-Dimensional Crash Victim Simulator. Sections A and B provide information for the preparation of an input data deck or file. Each card (or file line) is defined in Table VII of Section A with references to Figures included in this report describing the physical nature of the various input data and to tabular data included in Section B.

The output from the computer program is discussed in Section C. This material is complete with regard to the detailed printout produced in those cases where debugging information is needed.

Section D is a technical guide to the user familiar with the MTS<sup>27</sup> who wishes to exercise the model from a teletype terminal. The RUN statement for exercising the model is described first, followed by a description of the use of a conversational program which allows the user easy access to desired portions of the output generated in an exercise of the model.

The final four sections of Part IV (E, F, G, and H) describe and document the functioning of the computer program. Section E contains an overall brief description of the program along with a flow diagram; techniques for integrating the equations of motion are described in Section F; and flow diagrams for the individual subroutines are included in Section G.

##### A. DESCRIPTION OF INPUT DATA CARDS

All except the last several input cards have the same format, and are laid out in eight fields of ten columns each. With the exception of the first, each field contains one input datum. The first field contains one input datum in columns two through ten plus an identification letter. This letter, which appears in column one, defines the set of parameters on that card. The order of the data cards is irrelevant up to the "Z" card which precedes the SUMMARY card. If more than one of the same card is included, the last one will be

given priority and its data used.

Starting with "Z" card, the following order must be preserved:

1. "Z" card.
2. SUMMARY card.
3. Relabelling cards (if any).
4. "-2" card.
5. Tolerance level reset cards (if any).
6. "-1" card (if injury potential switch is on).
7. 3 cards containing probability data (if injury potential switch and probability switch are on).
8. First field control card.
9. Second field control card.
10. Cards specifying STYX print times if required.
11. Contact radii print control card.

More than one data deck may be submitted at the same time by simply putting them one after another, each with its own full complement of cards ("A" through "STYX"). When the program is finished with the first data deck, it will look for a second. If it finds more data, it will continue, otherwise it will sign off.

The inclusion of the SUMMARY data card at the end of a deck of input data results in the tabular output included at the end of a computer run. This output is the result of a successfully executed program and allows the user to evaluate the physics of the problem.

At present, the contact surface label is chosen according to Table XV. However, the user may alter the labels using the RELABEL card described in Table VII. This card may be inserted after the SUMMARY card in the data deck with the index of the surface to be relabelled in columns one and/or two and the eighteen BCD characters of the new label in columns eleven through twenty-eight suitably centered; e.g.:

- 2 - - - - - HEAD - REST - - - - -

TABLE VII. INPUT DATA CARDS (page 1)

Cards	Field	Table	Figure	Quantity	Units
A	1-7	VIII	9	joint friction coefficients, $C'_i$	in. lb.
B	1-8	XI	4	body segment moments of inertia, $I_i$	in. lb sec <sup>2</sup>
C	1-7	VIII		joint elasticity coefficients, $K_i$	in. lb/rad
D	1-8	IX	4	body element lengths between joints, $L_i$	in.
E	1-8	IX	4	body segment masses, $m_i$	lb sec <sup>2</sup> /in.
F	1		6	hip contact arc radius, $r_1$	in.
F	2				
F	3		6	upper torso contact arc radius, $r_3$	in.
F	4		6	head contact arc radius, $r_4$	in.
F	5		6	elbow contact arc radius, $r_5$	in.
F	6		6	hand contact arc radius, $r_6$	in.
F	7		6	knee contact arc radius, $r_7$	in.
F	8		6	foot contact arc radius, $r_8$	in.
G	1		11	lower joint stop coefficient, $T_1'\alpha_1$ (See card H, field 1 for $\alpha_1$ . If $\alpha_1 = 0$ , then $T_1'$ should be used in place of $T_1'\alpha_1$ .)	in. lb (or in. lb/rad)

TABLE VII. INPUT DATA CARDS (page 2)

Cards	Field	Table	Figure	Quantity	Units
G	2-4		10	joint stop coefficient, $T'_i$	in. lb/rad
G	5-7		11	lower joint stop coefficient, $T'_i \alpha_i$ (See card H, fields 2-4 for $\alpha_5-7$ . If $\alpha_i = 0$ , then $T'_i$ should be used in place of $T'_i \alpha_i$ .)	in. lb (or in. lb/rad)
H	1	VIII	11	hip joint lower stop location, $\alpha_1$	deg
H	2,3,4	VIII	11	shoulder, elbow, and knee lower stop locations, $\alpha_5, \alpha_6, \alpha_7$	deg
H	5	VIII	11	upper hip stop coefficient, $\hat{T}'_1$	in. lb/rad
H	6-8	VIII	11	shoulder, elbow, and knee upper stop	in. lb/rad
I	1,6-7	VIII	11	upper stop locations $\Omega_1, \Omega_6, \Omega_7$	deg
I	2-5	VIII	10	symmetric stop locations, $\Omega_1$	deg
J	1-7	VIII	9	joint angular velocity limits, $\xi_i$	deg/sec.
K	1-8	IX	6	body segment distance from previous joint to center of gravity, $\rho_i$	in.
L	1-8	IX	5	body initial angular position, $\theta_i(0)$	deg
M	1	IX	8	initial value of front edge seat force $F'_s$ (FSPRMZ)	lb
M	2		13	hip seat belt contact radius, $r_h$	in.

TABLE VII. INPUT DATA CARDS (page 3)

Cards	Field	Table	Figure	Quantity	Units
M	3			(blank field)	
M	4		8	initial seat force at hip, $W_0$	lb
M	5		6	distance to chest center of curvature, $\rho_3'$	in.
M	6		6	distance to head center of curvature, $\rho_4'$	in.
M	7		8	effective angle of seat cushion, $\gamma_0$	deg
M	8	XI		LCONTL	
N	1		8	seat linear damper coefficient, $c_s$	lb sec/in.
N	2		8	seat front linear spring coefficient, $s$	lb/in.
N	3			seat friction velocity limit, $f_s$	in./sec
N	4			seat friction coefficient, $\mu_s$	
N	5-7		8	seat nonlinear spring coefficients, $\beta_1$ ( $\beta_1$ , lb/in.), ( $\beta_2$ , lb/in. <sup>2</sup> ), ( $\beta_3$ , lb/in. <sup>3</sup> )	
N	8		8	initial distance from hip to seat front, $z_0$	in.
0	1		13	lap belt length from hip to attachment, $l_{10}$	in.

TABLE VII. INPUT DATA CARDS (page 4)

Cards	Field	Table	Figure	Quantity	Units
0	2		12	initial length of lower shoulder restraint, $l_{20}$	in.
0	3		12	initial length of upper shoulder restraint, $l_{30}$	in.
0	4		12	distance from lower spinal joint to lower shoulder restraint, h	in.
0	5		13	angle from seat belt attachment to H-point $\phi'_{10}$	deg
0	6			maximum permissible integration time step, $\Delta t_{max}$ (usual value is .0005)	sec
0	7-8		8	$r_z$ and $s_z$ ; parameters of a linear spring at the front edge of the front seat acting forward on the lower leg. $s_z$ is spring constant, $r_z$ is distance from lower leg centerline to skin	in. lb/in.
*P,Q	1	XII		code for belt parameters on card	
P	2			ratio of permanent to maximum elongation, G	
P	3			ratio of conserved to total energy, R	
P	4		13,12	initial belt angle $\phi_{i0}$	deg

\*Cards P, Q, S, T, U, V must be used more than once in specifying several belts, tables, or contact surfaces.



TABLE VII. INPUT DATA CARDS (page 5)

Cards	Field	Table	Figure	Quantity	Units
P	5			belt slack, $\Delta_i$	in.
P	6-8			belt load-deflection coefficients, $\sigma_1, \sigma_2, \sigma_3$	lb/(in.) <sup>n</sup>
Q	2-8			load deflection coefficients, $\sigma_i$ , $i=4, \dots, 10$	lb/(in.) <sup>n</sup> for $n=1-5$ lb(sec/in.) <sup>n-5</sup> for $n=6-10$
R	1	XIV		occupant position option, NPASGR	
R	2			occupant initial velocity $\dot{x}_O$ (XPACZ)	in./sec
R	3			vehicle initial velocity, $\dot{x}_O$ (XVEHZ)	in./sec
R	4			number of belt segments (NBELT = 0, 1, 2, or 3)	
R	5			minimum print-time step, $\Delta t_p$	sec
R	6			duration of simulation, $t_{max}$	sec
R	7			vehicle mass, $M_C$ (not used)	lb sec <sup>2</sup> /in.
R	8			number of $\Delta t_p$ 's in one print-time interval	
S, T, U	1	XV		Cards S, T, U specify contact param- eters for the various contact surfaces. The surface index is in field 1 in each case.	

TABLE VII. INPUT DATA CARDS (page 6)

Cards	Field	Table	Figure	Quantity	Units
S	2		7	contact surface length, D	in.
S	3			ratio of permanent to maximum deflection, G	in.
S	4			ratio of conserved to total energy, R	
S	5		7	reference coordinate, X'', of contact surface relative to initial position of H-point	in.
S	6		7	reference coordinate, Y''	in.
S	7		7	tangential velocity limit for friction, $\xi$	in./sec
S	8		7	reference angle, $\psi$	deg
T	2			friction coefficient, $\mu$	
T	3-8			load deflection coefficients, $\sigma_i$ , $i=1, \dots, 6$	lb/(in.) <sup>n</sup> for $n=1-5$
U	2-5			load deflection coefficients, $\sigma_i$ , $i=7, \dots, 10$	lb(sec/in.) <sup>n-5</sup> for $n=6-10$
U	6-8				
V				cards V constitute the input tables for vehicle deceleration or debug printout control	

TABLE VII. INPUT DATA CARDS (page 7)

Cards	Field	Table	Figure	Quantity	Unit
V	1	XVII		number specifying the input table	
V	2			switch indicating whether table is a constant or not (0=yes, 1=no)	
V	3			time of next break point in piecewise linear curve	sec
V	4			value at the inflection point	in./sec <sup>2</sup>
V	5-8				
W				table element deleting mechanism (not used)	
X,Y				not used	
Z	1	XVIII		debugging switch value (IBUG)	

NOTE: Several additional cards follow the Z-card when the summary table printout, the graphical plot, or the stick drawings are to be produced. These cards are exceptions to the rule governing letters in the first column.

TABLE VII. INPUT DATA CARDS (page 8)

Cards	Field	Table	Figure	Quantity	Unit
SUMMARY*	1			distance along upper spine element centerline from joint specifying accelerometer location (Columns 1-10)	in.
	2			distance along head element centerline from neck joint specifying head accelerom- eter location (Columns 11-20)	in.
	3	XIV		occupant position option, NPSGR (Columns 21-25 form an integer field)	
	4			control for graphical data printout (blank or zero insure execution) (Columns 26-30 form an integer field)	
	5			control for stick figures (Columns 31-35) (integer) (blank or zero execute)	
	6			control for injury potential predictor printout (Columns 36-40) (integer) (blank or zero execute)	
	7			control for injury potential predictor probability page (Columns 41-45) (integer) (blank or zero execute) (See Table XX and reference 28)	

\*NOTE: See text following this table.

TABLE VII. INPUT DATA CARDS (page 9)

Cards	Field	Table	Figure	Quantity	Unit
RELABEL	1,2			Insert contact surface to be relabeled as an integer in Columns 1 and/or 2. (See text following this table.)	
	3-10			Insert eighteen BCD characters of new label suitably centered.	
"GO"	1,2			Inserting -2 in the first two columns of this card indicates to the program that all input data for the production of summary tables has been read.	
INJ	1-10	XIX		Index of tolerance level to be reset.	
	11-20	XIX		New value of tolerance level.	
"GO"	1-10			0 or -1.	
PROBABILITY				These three cards provide input for computation of the probability that the simulated event will happen based on type of collision, position of occupant, and chance of restraint system use. If no cards are entered here, probability will not be computed if the probability switch is off.	

TABLE VII. INPUT DATA CARDS (page 10)

Cards	Field	Table	Figure	Quantity	Unit
(card 1)	1-10	XX		Probability of particular collision type.	
	11-20	XX		Index defining collision type (0,1,2).	
	21-44	XX		New label describing collision type if index is zero.	
(card 2)	1-10	XX		Probability of the chosen occupant position being used.	
	11-20	XX		Index defining position type (0, 1, 2, 3, 4).	
	21-44	XX		New label describing occupant position if index is zero.	
(card 3)	1-10	XX		Probability of restraint system use.	
	11-20	XX		Index defining type of restraint if any (0, 1, 2, 3, 4, 5, 6).	
	21-44	XX		New label describing restraint type if index is zero.	
STYX-1*	1-5			NHL-integer field defining number of horizontal lines.	

\*NOTE: A discussion of the application and use of STYX follows this table.

TABLE VII. INPUT DATA CARDS (page 11)

Cards	Field	Table	Figure	Quantity	Unit
	6-10			NSBH-integer field defining number of spaces between horizontal lines.	
	11-15			NVL-integer field defining number of vertical lines.	
	16-20			NSVB-integer field defining number of spaces between vertical lines.	
	21-25			Switch control for zero coordinate lines (0 specified print).	
	26-30			ISTEP-number of plots to be printed.	
	31-35			METH-If METH=0, the time points for producing plots must be specified by the user, otherwise they are generated automatically.	
STYX-2	1-4			XMIN-maximum value for x on plots.	in.
	5-8			XMAX-maximum value for x on plots.	in.
	9-12			YMIN-minimum value for y on plots.	in.
	13-16			YMAX-maximum value for y on plots.	in.
	17-20			FIRST-first time point for production of drawing.	sec

TABLE VII. INPUT DATA CARDS (page 12)

Cards	Field	Table	Figure	Quantity	Units
	21-25			DELTA-first time point for production of drawing.	sec
METH=0	1-8			If METH=0, a series of cards is entered here. Each one contains a point in time at which a plot is desired. Each time point must be in the first eight columns of its own separate card. ISTEP=the number of cards included if METH=0. If METH≠0, the cards <u>must</u> not be included.	
CONTACT PRINTS	1-5	X	6	NCNTCT (1)	
	6-10			NCNTCT (2)	
	11-15			.	
	16-20			.	A switch in each of these eight integer fields control the printing of contact radii.
	21-25			.	Printing occurs if zero is entered in the field and is omitted if the field contains anything else.
	26-30			.	
	31-35			.	
	36-40			NCNTCT (8)	



A graphical output called STYX which is based on the tabular data output is in use at HSRI. The user of STYX has several options available which are fixed both in the input to the main program in the case of the contact surfaces and in the input directly to STYX. Furthermore, there is the option to use STYX or skip it altogether.

The contact surfaces which are specified in the input for a particular run are represented in the STYX output. To this end, each contact must have its reference point fixed, and its length and angle specified on its own S card in the input to the main program. In addition, the third field of the T card for each contact surface desired must contain a nonzero, floating point number. These set up the vector IGNORE (I) which controls the use of the contact surfaces in both the program and the stick figure representation.

Controlling the use of STYX is a switch, NSTICK, read by SUMMARY. In the input, this switch is on the card immediately following the Z card. There are 2 floating point fields of 10 spaces each and 4 integer fields of 5 spaces; NSTICK is the third integer field. If it is blank or zero, STYX will be executed; if nonzero, it will be skipped.

If STYX is to be used, its input follows the second SUMMARY "go" card. The first card contains seven integer fields, each five columns long. The first field holds the number of horizontal lines, NHL, with restriction:  $2 \leq \text{NHL} \leq 24$ . The second field is used to specify the number of spaces between horizontal lines, NSBH, which must satisfy the inequality:  $(\text{NHL}-1) * \text{NSBH} + \text{NHL} \leq 48$ . The third field has the number of vertical lines, NVL, with restriction:  $2 \leq \text{NVL} \leq 53$ . The fourth field details the number of spaces between vertical lines, NSBV, which must satisfy the inequality:  $(\text{NVL}-1) * \text{NSBV} + \text{NVL} \leq 106$ .

The fifth field is the switch that controls the printing of the zero lines. If this field contains a zero, the zero lines print; otherwise they are omitted. The sixth field specifies ISTEP, the number of plots to be printed, subject to the restriction  $\text{ISTEP} \leq 200$ . The seventh field holds METH, the switch controlling the method of generating input. If  $\text{METH} \neq 0$ , the

time points are generated automatically; if METH = 0, then the time points must be specified by the user.

The next card is divided into six floating point fields, 10.4 wide. The first four of these are the minimum and maximum values of X and Y, respectively, that are to be printed. Care must be exercised so that the entire figure will be contained by these boundaries. For scaling purposes the equation:

$$(XMAX-XMIN) / \left( \frac{NSVB*(NVL-1)}{10.} \right) = (YMAX-YMIN) / \left( \frac{NSBH*(NHL-1) + NHL}{6} \right)$$

must be satisfied. The next two fields are the two parameters necessary when METH  $\neq$  0. FIRST is the first time step to be printed, and DELTA is the increment between the time points. ISTEP, specified above, is the number of time points that are generated automatically.

If METH = 0, the next ISTEP cards contain the desired time points. If METH  $\neq$  0, these cards must not be included. Each time point must be in the first 8 columns of its own separate card, and the number of cards specifying time points must be equal to ISTEP. These time points may be at any regular or irregular intervals, but they must be in chronological order. The requested time points need not match exactly the calculated time points. The nearest available time point to the requested time point will be printed. If any requested time points are larger than the last available time point, the last available one will be printed—but only once. The time that is printed in the label is the actual calculated time, not the requested time.

The last card contains 8 integer fields, 5 wide. These are the switches controlling the printing of the contact radii. Each one prints on 0 and is omitted if the field contains anything else. These switches control respectively: the hip, nothing, the chest, nothing, the elbow, the hand, the knee, the foot.

To avoid congestion, only the man is printed out with connecting dots. All of the contact surfaces have only their end points printed out and must be connected by the user. Similarly, only the end points of the lower shoulder

and seat belts are printed, and the upper shoulder belt should be connected to the fifth joint. The contact radii are indicated as unobtrusively as possible.

## B. INFORMATION TABLES

The following tables describe the subscripting used in the program. In addition, certain print and tabular indices are given as well as quantities used in the injury criteria model. Certain tables listed earlier in the text are repeated in this section for ease and assessability to the user.

TABLE VIII. SUBSCRIPTS OF BODY JOINTS

Subscript	1	2	3	4	5	6	7
Joint	Hip	Lower Spine	Upper Spine	Neck	Shoulder	Elbow	Knee

TABLE IX. SUBSCRIPTS OF BODY SEGMENTS

Subscript	1	2	3	4	5	6	7	8
Body Segment	Lower Torso	Middle Torso	Upper Torso	Head	Upper Arm	Lower Arm	Upper Leg	Lower Leg

TABLE X. SUBSCRIPTS OF CONTACT ARCS

Subscript	1	2	3	4	5	6	7	8
Contact Arc	Hip	-	Upper Torso	Head	Elbow	Hand	Knee	Foot

TABLE XI. LCONTL VALUES

$$LCONTL = \begin{cases} 0 - \text{Prints Summary + Krunch A if IBUG=0} \\ 1 - \text{Prints Summary + Krunch A} \\ 2 - \text{Prints Krunch A} \end{cases}$$

TABLE XII. BELT PARAMETER INDEX

$$\text{Belt parameter index} = \begin{cases} 1, \text{ lap belt} \\ 2, \text{ lower shoulder belt} \\ 3, \text{ upper shoulder belt} \end{cases}$$

TABLE XIII. NBELT VALUES

$$\text{NBELT} = \begin{cases} 0 \text{ no belts} \\ 1 \text{ lap belt} \\ 2 \text{ shoulder belts} \\ 3 \text{ lap belt and shoulder belt} \end{cases}$$

TABLE XIV. OCCUPANT POSITION OPTIONS

$$\text{Occupant position option} = \begin{cases} 1, \text{ driver} \\ 2, \text{ front passenger} \\ 3, \text{ rear passenger} \end{cases}$$

TABLE XV. NORMAL CONTACT SURFACE INDICES

Index*	Normal Contact Surface
0	floor
1	seat back
2	roof or head rest
3	upper steering wheel, upper dash, back of front seat
4	windshield
5	lower steering wheel
6	lower panel
7	steering column
8	toeboard
9	steering wheel

\*It is permissible to use any index for any other contact surface as long as it is compatible with the table of possible contacts in Table XVI. For example, an air bag could be simulated by using the various segments of the steering wheel.

TABLE XVI. OCCUPANT CONTACTS VERSUS VEHICLE CONTACTS (page 1)

Contact Arc Subscript	Front		Front Passenger (3) Contacts
	Driver (1) Contacts	Passenger (2) Contacts	
hip (1)	seat back (1) [5]*	seat back (1) [5]	seat back (1) [5]
upper torso (3)	seat back (1) [6]	seat back (1) [6]	seat back (1) [6]
	upper steering wheel (3) [7]	upper dash (3) [7]	back of front seat (3) [7]
	lower steering wheel (5) [8]		
	steering column (7) [9]		
head (4)	seat back (1) [10]	seat back (1) [8]	seat (1) [8]
	roof or head rest (2) [11]	roof or head rest (2) [9]	roof or head rest (2) [9]
	upper steering wheel (3) [12]	upper dash (3) [10]	back of front seat (3) [10]
	windshield (4) [13]	windshield (4) [11]	
	lower steering wheel (5) [14]		

\*Numbers in brackets refer to indices 5-18 used in LODFEC and CONTACT printouts. (See flow diagrams and Table XX.)

TABLE XVI. OCCUPANT CONTACTS VERSUS VEHICLE CONTACTS (page 2)

Contact Arc Subscript	Driver (1) Contacts	Front Passenger (2) Contacts	Front Passenger (3) Contacts
elbow (5)	seat back (1) [15]	seat back (1) [12]	seat back (1) [11]
knee (7)	lower panel (6) [16]	lower panel (6) [13]	back of front seat (3) [12]
foot (8)	floorboard (0) [17]	floorboard (0) [14]	floorboard (0) [13]
	toeboard (8) [18]	toeboard (8) [18]	back of front seat (3) [14]

TABLE XVII. INPUT TABLE SWITCHES

Input table =  $\left\{ \begin{array}{l} 1 - \text{vehicle deceleration function} \\ 2 - \text{time-varying debugging switches*} \\ 3 - (\text{read but not used}) \end{array} \right.$

\*Use of this switch is controlled by IBUG value in Table XVIII.

TABLE XVIII. IBUG SWITCHER

IBUG =  $\left\{ \begin{array}{ll} \text{negative integer} & - \text{Input table 2 is used} \\ 0 & - \text{no debugging printout} \\ 1-3 & - \text{various levels of debugging} \\ & (\text{See Debug Section}) \end{array} \right.$

TABLE XIX. INDICES FOR THE INJURY CRITERIA QUANTITIES

Index	Quantity
1	Severity Index
2	Head Pitch Acceleration (rad/sec <sup>2</sup> )
3	Chest Load (lb)
4	Shoulder Belt Load (lb)
5	Pelvic Belt Load (lb)
6	Knee Load (each) (lb)
7	Chest A-P G-Load
8	Chest S-I G-Load
9	Hip Angle Flexion (deg)
10	Lower Spine Angle Flexion (deg)
11	Upper Spine Flexion (deg)
12	Neck Angle Flexion (deg)
13	Shoulder Angle Flexion (deg)
14	Elbow Angle Flexion (deg)
15	Knee Angle Flexion (deg)
16	Hip Angle Hyperextension (deg)
17	Lower Spine Angle Hyperextension (deg)
18	Upper Spine Angle Hyperextension (deg)
19	Neck Angle Hyperextension (deg)
20	Shoulder Angle Hyperextension (deg)
21	Elbow Angle Hyperextension (deg)
22	Knee Angle Hyperextension (deg)

Note: See Reference 28 for a discussion of the injury criteria model and a sample output generated by the computer program.



TABLE XX. PROBABILITY LABELS

Index	Card 1	Card 2	Card 3
0	(User option)	(User option)	(User option)
1	Front collision	Driver	No restraint
2	Rear collision	Right front passenger	Lap belt only
3	--	Right rear passenger	Shoulder harness only
4	--	Left rear passenger	Shoulder harness and lap belt
5	--	--	Airbag and lap belt use
6	--	--	Inverted y-yoke and lap belt use

### C. GENERAL PROGRAM OUTPUT

The program printout consists of the following parts: run statement and map, allowable contact specifications, input data, intermediate general printout with various possible debugging options, and tabular summary.

There are four levels of debugging printout provided in the program. The first level of printout (IBUG = 0) is always printed upon program execution. However, not all of it is printed if Fortran Logical Unit Number 6 is set to \*DUMMY\* or equivalent. The other levels (IBUG = 1, 2, 3) are set up using the input data cards labeled "V." Because of the piecewise-linear nature of information inputted to the computer program using "V-cards" it is possible to isolate small time segments within the forward integration period covered by the simulation and produce detailed debugging printout as needed.

Although variable levels of debugging printout are specified only by piecewise linear sections, only integer values of IBUG have meaning, so the best practice is to use a very small time step between integer values of IBUG. A sample of the "V card" input is given in Table XXI and graphed in Figure 34.

If a print time occurs while IBUG is a linear ramp, some intermediate IBUG printout will occur (IBUG = 1, 2) as the values are rounded off approximately to integer values.

The first item printed out after the EXECUTION BEGINS statement is a table of the permissible contacts for the NPASGR option selected. "NS" is the total number of contacts and the next two lines give the indices of the body segment and its corresponding allowed contact surface (see Table XV).

TABLE XXI. SAMPLE V CARD DEBUG INPUT DATA SET

Data Card Column	1	11	21	31
Information on each data card	V2.	1.	0.	0.
	V2.	1.	0.099	0.
	V2.	1.	0.100	3.
	V2.	1.	0.149	3.
	V2.	1.	0.150	0.
	V2.	1.	0.200	0.

It should also be noted that contact forces are labeled by the following scheme in printouts from subroutines LODFEC and CONTAC (see Table XXII). Indices 1, 2, and 3 are belts (lap, lower shoulder harness, upper shoulder harness). Index 4 is vestigial. The index pairs listed under I and A are labeled from 5 through a maximum of 18 (see Table XVI).

The input data follows the listing of the contacts. These variables are described in Part IV, Section A of this paper. The surface index A is printed one greater than the listing in Table VII. For example, A = 1 is the floor index whereas the value in the table is zero.

Intermediate general printout can be described by a table and a list of accompanying comments. Table XXII consists of the debug level, the subroutine generating the output, and the variables included in each output group and Table XXIII lists specific comments which are generated by the program indicating certain error conditions and other aspects of program function.

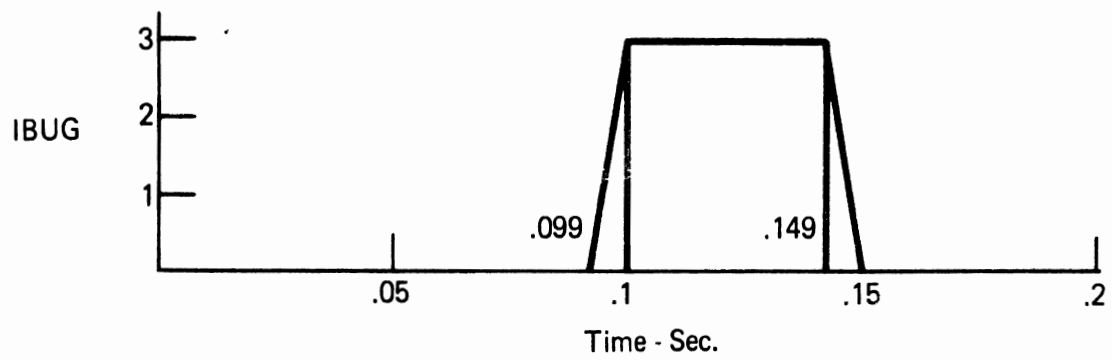


Figure 33. Description of time-varying debug table.

TABLE XXII. INTERMEDIATE GENERAL PRINTOUT (page 1)

Debug Level* (and debug printout number)	Routine	Label	Contents
0 (1)	MAIN	--	Number of contact surfaces (NS), index of contact arcs (I), index of contact surfaces (A) (see note on Table XXIII)
0 (2)	MAIN	--	Output of input (See Part IV. A of report) (see note on Table XXIII)
0 (3)	KRUNCH	IGNORE	Switch indicating status of the contact surfaces (+1 = no contact, -1 = no friction, 0 = friction)
1 (4)	GETY	--	Present time (ARG), time modulo 24 (MOD ARG), table number (TABLE), ordinate (ORD)
3 (5)	ACCEL	STEP	$\sin \theta_i, \cos \theta_i, \theta_i^2, L_i \theta_i^2, a_i \theta_i^2$ in five columns for $i = 1-8$ in eight lines. (L = in.) ( $\theta = \text{rad}$ )*. Quantity "a" is matrix parameter.
2 (6)	SEAT	SEAT	Z (in) (distances from hip to front of seat) FS (Fs) (lb) (hip seat force) FSPRM (F's) (lb) (front edge seat force) FZ (Fz) (lb) (force on front seat) SMALLF (f) (lb) (friction force magnitude) SUMBY ( $\beta_1 y_s + \beta_2 y_s^2 + \beta_3 y_s^3$ ) (lb) (non-linear hip force) ZMLCTS ( $z - L_7 \cos \theta_7$ ) (in.) (distance from knee to front of seat)

\*( $a_i = 1 \text{ lb in. for } i = 1-8, 1 \text{ lb for } i=9, 1 \text{ lb in.}^2 \text{ for } i = 10-17.$ )

\*NOTE: The terms "Debug Level" and "IBUG value" are equivalent throughout this report.

TABLE XXII. INTERMEDIATE GENERAL PRINTOUT (page 2)

Debug Level	Routine	Label	Contents
0 (7)	LODFEC	LODFEC	N (index of force) (See Table XVI and text above) SDL ( $\delta$ ) (in.) (deflection) SDLD ( $\dot{\delta}$ ) (in./sec) (deflection rate) FN (F) (lb) (contact force) ET (E) (in. lb) (energy since last unloaded cycle) EPSLNT ( $\epsilon$ ) (in.) (permanent deformation)
2 (8)	CONTAC	CONTAC	N (index of contact) DELOA ( $\delta$ ) (in.) (deflection) DELIAD ( $\dot{\delta}$ ) (in./sec) (deflection rate) FN (F) (lb) (force) EONE ( $E_1$ ) (in. lb) (total conserved energy) EPSLNY ( $\epsilon$ ) (in.) (permanent deformation)
2 (9)	CONTAC	QUE VECTOR	QUE (Subscript I = 1-10 referring to the body segments (1-8) as defined in Table IX and the x-y coordinates of the hip. Units for subscripts 1-8 are in. lb and for 9-10 are lb) (Contribution to generalized force vector of contact surfaces is defined in Table XV.)
2 (10)	BODY	BODY	I (index for each line defined as QUE subscripts) GEE (gravitational contribution to generalized force vector) DEE (contribution of seat bottom and belts) BEE (contribution of centrifugal forces) SMALLB (total generalized force vector)
2 (11)	ZMAKER	A MATRIX	AA (doubly subscripted matrix of differential equations. Rows possess units defined in QUE)
2 (12)	ZMAKER	A INVERSE	ANVERS (doubly subscripted inverse of AA)
2 (13)	ZMAKER	CHECK OF INVERSE	CK ( $A^{-1}A + AA^{-1}$ ) (check of inversion routine)

TABLE XXII. INTERMEDIATE GENERAL PRINTOUT (page 3)

Debug Level	Routine	Label	Contents
1 (14)	DELZMK	DELZMK	A subscription comment "FOR MODE No. (K), I = (I), A = (A)" K (Index of jittering friction mode. For K = 1-7, index refers to joint. For K = 8, index refers to seat cushion. For K = 9,..., index is k + 4, see page 26. DELZ (J,K) This doubly subscripted vector shows the change in acceleration vector (J = 1-10) due to an instability (K = 1...)
1 (15)	KRUNCH	ZK BASE	ZVECPP (acceleration vector due to continuous forces and unstable friction forces. Subscripts refer to angular coordinates (1-8), linear coordinates (9-10), and vehicle (11). Units are rad/sec <sup>2</sup> and in./sec <sup>2</sup> )
1 (16)	KRUNCH	TIME IMAX	Time since beginning of collision event. MAXI (number of possible instabilities) IBIG (listing of possible unstable modes with subscript I = 1...MAXI)
1 (18)	JITTER	I AK	I (index of averaging pair) AK (weighted averaging coefficient used in eliminating instabilities)
1 (17)	JITTER		Comment: MODE (index) TURNED ON (or OFF) or JITTER FOR MODE (index)
1 (19)	JITTER	ZRV = ZPPP = DELNU = FMM =	Relative acceleration from ZKBASE for mode N Relative acceleration from previous .averagings Relative acceleration from DELZMK (K = 7) Slope of vehicle deceleration (in./sec <sup>3</sup> ) These quantities are largely vestigial

TABLE XXII. INTERMEDIATE GENERAL PRINTOUT (page 4)

Debug Level	Routine	Label	Contents
1 (20)	TAUMAK	TAUMAK	ITAU ( $i_T$ ) (index of jittering friction contact) TAUHAT ( $\hat{\tau}$ ) (selected time interval) TAUI (all predicted time intervals) (I = 1-16, in two lines)
1 (21)	TAUMAK	MODE	MODE (Switch array stating whether each friction mode (1-16) is on (+1), off (-1), or unstably jittering (0).)
3 (22)	LIMIDT	LIMIDT	I (index) AZ (rad or in.) (predicted angular position of body elements, 1-8, x and y hip position 9-10, and cart location 11) AZP (rad/sec or in./sec) (associated velocities) AX (in.) (Horizontal joint coordinates. Note index 8 refers to knee and both 1 and 7 to the hip joint here only) AY (in.) (vertical joint coordinates) AXD (in./sec) (horizontal joint velocity) AYD (in./sec) (vertical joint velocity)
1 (23)	FECLD	FECLD	TIME (sec) (time) INDEX (index of contact force checked) SDEL (in.) (predicted deflection) SDELD (in./sec) (predicted deflection rate) FTT (lb) (predicted contact force)
1 (24) (0 at print times)	NORMUT	AT TIME	TIME (sec)
		THETA	ZVEC (deg) (angular position of body elements 1-8) ZVECP (deg/sec) (angular velocities) ZVECPP (deg/sec <sup>2</sup> ) (angular accelerations)
		XHIP YHIP XCAR	ZVEC, ZVECP, ZVECPP (in., in./sec, in./sec <sup>2</sup> ) (9-12) (position, velocity, and acceleration of hip in x and y directions and of the vehicle)



TABLE XXII. INTERMEDIATE GENERAL PRINTOUT (page 5)

Debug Level	Routine	Label	Constants
		TIME FS FSPRM  SMALLF	TIME (sec) FS (lb) (seat bottom force on hip) FSPRM (lb) (force at front edge of seat bottom) SMALLF (lb) (friction force from seat bottom)
		X  Y  A  GAMMA	XHEAD, XCHEST (in./sec <sup>2</sup> ) (horizontal acceleration of head and chest c. g.) YHEAD, YCHEST (in./sec <sup>2</sup> ) (vertical acceleration of head and chest c. g.) AHEAD, ACHEST (in./sec <sup>2</sup> ) (resultant acceleration of head and chest) GHEAD, GCHEST (deg) (angle of resultant acceleration vector)
		M  DELTA DELTA DOT FM PHI EIM  EPSILON DEM	Index of belt segment: seat belt (1) upper shoulder (2), lower shoulder (3). SDELTA (in.) (elongation of belt) SDELTD (in. sec) (rate of belt elongation) FN (lb) (belt force) PHI (deg) (belt angle) EONE (in./lb) (total energy conserved in belt) EPSLNY (in.) (permanent belt deformation)
1 (25)	KRUNCH	RVEL	MAXR (present number of friction modes being considered) RVEL (rad/sec, in./sec) (relative velocity for the friction modes being considered) RSEL (rad/sec <sup>2</sup> , in./sec <sup>2</sup> ) (relative acceleration for friction modes considered)
0 (26) or 1 if LCONTL > 0	KRUNCH	KRUNCH A	KPRINT (print switch) KINFL (inflection switch) KSTED (maximum time step switch) ITAU (mode selected) TAUHAT (sec) (minimum predicted mode time) TPRINT (sec) (next print time) TINFL (sec) (next inflection time) TSTEP (sec) (last inflection time) DELTAT (sec) (time step selected) TIME (sec) (new time)

TABLE XXIII. PROGRAM COMMENTS (page 1)

Subroutine	Comment	Conditions
GETY	TABLE ____ HAS NO ENTRIES AND CALLED UPON	empty table
GETY	TABLE ____ MINX = ____. EXCEEDED BY ARG ____ Y SET TO ____	off low end of table
GETY	TABLE ____ MAXX = ____ EXCEEDED BY ARG ____. Y SET TO ____	off high end of table
LODFEC	CHANGED R FROM ____ TO ____ FOR INDEX _____	R, G, not compatible
LODFEC	RESET CONSERVED ENERGY TO LOWER LIMIT AT T = __ SEC	R reset lower
LODFEC	RESET CONSERVED ENERGY TO UPPER LIMIT AT T = __ SEC	R reset higher
LODFEC	CHANGED G FROM ____ TO ____ FOR INDEX _____	R, G not compatible
LODFEC	OUTSIDE MONOTOMIC RANGE OF LOADING CURVE FOR INDEX N =	during loading part of cycle $F(t) < F(t - \Delta t)$
ZMAKER	BAD MATRIX. DUMP	determinant of matrix = 0
JITTER	TWO LINEAR JITTER MODES AT T = _____	2 contact friction jitter modes want to jitter at same time (fatal)
LIMIDT	AT TIME = _____ DELTA T = ____ RESET TO ____	some forward contact forces predicted to change by > 1000 lb
NOTE: These comments will be printed out regardless of whether Unit 6 is set to *DUMMY* or not.		
LODFEC	NEGATIVE FORCE SET TO ZERO FOR INDEX N = ____ AT TIME = _____	during loading part of cycle $F(t) < 0$ ; set equal to zero.

TABLE XXIII. PROGRAM COMMENTS (page 2)

Subroutine	Comment	Conditions
TAUMAK	RESET MODE (_____) TO ZERO	Indicates jitter mode selected
KRUNCH	AT TIME = _____, ANGLE _____ EXCEEDS 360 DEGREES	$ \theta_i  > 360^\circ$ (fatal)
KRUNCH	AT TIME = _____, MORE THAN EIGHT ITEMS IN JITTER RUN STOPPED	Space allotted to storage for jitter process would be exceeded (fatal)
FECLD	AT TIME = _____ FORCE COMING ON FFOM BEHIND FOR INDEX _____	fatal

Logical input/output units used are:

6 for statements and most output except first two items  
of Table XII and all of Table XIII

9 for storage for SUMMARY

These must be specified in the run statement.

#### D. TELETYPE USERS' GUIDE

This section is a technical guide for the user of the two-dimensional crash victim simulator who is familiar with MTS<sup>27</sup> and wishes to exercise the model from a teletype terminal remote from The University of Michigan. The RUN statement which causes the model to be exercised is described, followed by a description of the use of a conversational program which allows the user easy access to desired portions of the output generated in an exercise of the model.

The RUN statement for the two-dimensional crash victim simulator is

```
$RUN SP78:2D SCARDS=datafile 9=summary file 6=*DUMMY*
SPRINT=*DUMMY*
```

The terms "data file" and "summary file" refer to file names which must

be supplied by the user. The input data for exercising the program, which has been described in Part IV, Section A of this report is stored in "data file." The output from the program must be stored in a file (referred to here as "summary file") which should be approximately 25 pages in length. The command "6=\*DUMMY\*" deletes printing of 0-level debug output out over the teletype terminal. If it is not desired to produce the output on paper at The University of Michigan Computing Center, then the command "SPRINT=\*DUMMY\*" should be used. If printout is desired, then "\*DUMMY\*" should be replaced by another file, approximately 25 pages in length.

Because the complete output from one exercise of the program could take up to three hours to print out at a teletype terminal, it is necessary to provide a technique for accessing sections of the output quickly and conveniently. Use of the program which accomplishes this is described in the remainder of this section.

The program can also be used to retrieve information from the output of a previous run. In either case, the summary option must have been used in carrying out the exercise. The file in which the summary information is stored ("summary file") becomes the input file to the teletype output access program.

The program has three sections: "initial," "general," and "complex." The "initial" section enables the user to list any of 54 different input values which were used in carrying out the exercise. The "general" section, allows the user to list any of 61 different output variables over any time period. The "complex" section enables the user to make comparisons. When one variable reaches a critical value, the values of other variables can be determined.

The model is designed to be conversational with the user. However, the user is given the option of putting his instructions in a file.

The following command will trigger execution of the program.

```
$RUN SP78:TALK2 1 = summary file
```

or, if no conversation with the program is desired:

\$RUN SP78:TALK2 1 = summary file 7 = \*DUMMY\* 4 = instruction file

The program will begin with

ENTER 6 IF CONVERSATIONAL, 7 IF NOT

If a 7 is entered, the program will proceed to get the rest of its information from the file specified on logical unit 4. If the end of this file is reached and the program has not been terminated, the program will return to conversational mode. If a 6 is entered, the program will proceed to prompt the user for instructions beginning with:

ENTER 1 IF INITIAL, 2 IF GENERAL, 3 IF COMPLEX, 4 IF DONE

Entering a 1, 2, or 3 will cause the program to go to the indicated section—each of which is described below, and a 4 will result in termination of the program.

In using the "initial" section of the teletype output access program, the user is prompted by the following:

- 1 ENTER VARIABLE NUMBER - 0 IF DONE  
( )
- 2 ( )
- 3 ENTER OCCUPANT POSITION NUMBER

Statement 1 indicates that the user should enter a number. The entry of a number from 1 to 54 results in the value of the corresponding input constant (as described in Tables XXIV and XXV) being printed. Then, the user is prompted for another number by a pair of parentheses only. This process can be discontinued at any time by entering a 0.

The first time that 1, 13, or 39 is entered, the user will be prompted with statement 3. A 1, 2 or 3 must be entered, corresponding to driver, front seat passenger or rear seat passenger. (This information is used only to make the titles more descriptive and does not change any of the numerical results.)

In using the "general" section of the teletype output access program,

the user is prompted by the following:

1. HOW MANY VARIABLES
2. ENTER TIME INTERVAL  
FROM (    )(    )(    )
3. ENTER TIME INTERVAL  
FROM (    ) to (    )
4. ENTER OCCUPANT POSITION NUMBER
5. ENTER VALUE OF "PHEAD"
6. ENTER VALUE OF "CHEST"

Statement 1 wants to know how many variables the user is interested in seeing. This number can be from 1 to 4. Statement 2 asks for the appropriate number of variable numbers. These numbers range from 1 to 61 and correspond to the variables as listed in Tables XXVI and XXVII. If a 50 or 55 is entered, statement 4 will ask for the occupant position number. Enter 1 if driver, 2 if front seat passenger, or 3 if rear seat passenger. If a 44 or 45 is entered, statement 5 will ask for a value of "PHEAD." This is the distance from the neck joint to the location of the head accelerometer. If a 46 or 47 is entered for a variable number, statement 6 will ask for the value of "PCHEST." This is the location of the chest accelerometer. After the variable numbers have been recorded, a time interval must be specified. A carriage return will result in initial values being printed. Any other time period must be specified in the appropriate spaces. (NOTE: If a contact that does not occur is asked for, the comment CONTACT NUMBER XX NEVER OCCURRED will be printed and the corresponding heading will be meaningless.)

In using the "complex" section of the teletype output access program, the user is prompted by the following:

1. ENTER DECISION VARIABLE
2. ENTER COMPARISON VALUE
3. ENTER COMPARISON MODE - 1 if GT, 2 if LT
4. HOW MANY VARIABLES?

5. ENTER VARIABLE NUMBERS  
( ) ( ) ( )
6. ENTER TIME INTERVAL  
FROM ( ) to ( )
7. ENTER OCCUPANT POSITION NUMBER
8. ENTER VALUE OF "PHEAD"
9. ENTER VALUE OF "PCHEST"

This section prints the values of variables at the time when another variable reaches a critical value. Any of the variables listed in Tables XXVI and XXVII can be observed in this manner. For example, the user interested in the position of the head when it hits the windshield would make the following entries.

1. 56 (head on windshield is the decision variable)
2. 0 (0 is the critical value—we become interested when the force becomes greater than 0 (hence the 1).)
3. 1
4. 2 (NOTE: maximum is 3)
5. (39) (40)
6. (0.) to (2.0) (Normally the time interval should cover the entire run, although some variables reach the critical point several times during the run and the time interval must be carefully chosen if you are not interested in the first occurrence.)

The user will be prompted by statements 7, 8, and 9 only in certain instances as described in the "general" section, page 116.

The output of this section consists of the time at which the critical value was exceeded, along with the value of the decision variable and the other variables at that time.

TABLE XXIV. INPUT CONSTANTS (NUMERICAL ORDER) (page 1)

Number	Description
1	Floor-X
2	Seat Back-X
3	Roof-X
4	Upper Steering Wheel-X (When NPASGR=1)
	Upper Panel-X (When NPASGR=2)
	Front Seat Back-X (When NPASGR=3)
5	Windshield-X
6	Lower Steering Wheel-X
7	Lower Panel-X
8	Steering Column-X
9	Toeboard-X
10	Floor-Y
11	Seat Back-Y
12	Roof-Y
13	Upper Steering Wheel-Y (When NPASGR=1)
	Upper Panel-Y (When NPASGR=2)
	Front Seat Back-Y (When NPASGR=3)
14	Windshield-Y
15	Lower Steering Wheel-Y
16	Lower Panel-Y
17	Steering Column-Y
18	Toeboard-Y
19	Hip Contact Arc Radius
20	Upper Torso Contact Arc Radius
21	Head Contact Arc Radius
22	Elbow Contact Arc Radius
23	Hand Contact Arc Radius
24	Knee Contact Arc Radius
25	Foot Contact Arc Radius
26	To Chest Center of Curvature



TABLE XXIV. INPUT CONSTANTS (NUMERICAL ORDER) (page 2)

Number	Description
27	To Head Center of Curvature
28	Lower Torso Length
29	Center Torso Length
30	Upper Torso Length
31	Center Torso to Upper Arm
32	Upper Arm Length
33	Lower Arm Length
34	Upper Leg Length
35	Lower Leg Length
36	Floor-Length
37	Seat Back-Length
38	Roof-Length
39	Upper Steering Wheel-Length (When NPASGR=1)
	Upper Panel-Length (When NPASGR=2)
	Front Seat Back-Length (When NPASGR=3)
40	Windshield-Length
41	Lower Steering Wheel-Length
42	Lower Panel-Length
43	Steering Column-Length
44	Toeboard-Length
45	Distance From Hip to Seat Front
46	Number of Belt Segments
47	Lower Torso-Center of Gravity to Lower Joint
48	Center Torso-Center of Gravity to Lower Joint
49	Upper Torso-Center of Gravity to Lower Joint
50	Head-Center of Gravity to Lower Joint
51	Upper Arm-Center of Gravity to Lower Joint
52	Lower Arm-Center of Gravity to Lower Joint
53	Upper Leg-Center of Gravity to Lower Joint
54	Lower Leg-Center of Gravity to Lower Joint

TABLE XXV. INPUT CONSTANTS (ALPHABETICAL ORDER) (page 1)

Number	Description	
39	Back of Front Seat-Length	(When NPASGR=3)
4	Back of Front Seat-X	(When NPASGR=3)
13	Back of Front Seat-Y	(When NPASGR=3)
26	Chest Center of Curvature (Distance to)	
48	Center Torso-Center of Gravity to Lower Joint	
29	Center Torso-Length	
31	Center Torso to Upper Arm (Distance from)	
22	Elbow Contact Arc Radius	
36	Floor-Length	
1	Floor-X	
10	Floor-Y	
25	Foot Contact Arc Radius	
23	Hand Contact Arc Radius	
27	Head Center of Curvature (Distance to)	
50	Head-Center of Gravity to Lower Joint	
21	Head Contact Arc Radius	
19	Hip Contact Arc Radius	
45	Hip to Seat Front (Distance from)	
24	Knee Contact Arc Radius	
52	Lower Arm-Center of Gravity to Lower Joint	
33	Lower Arm Length	
54	Lower Leg-Center of Gravity to Lower Joint	
35	Lower Leg-Length	
42	Lower Panel-Length	
7	Lower Panel-X	
16	Lower Panel-Y	
41	Lower Steering Wheel-Length	
6	Lower Steering Wheel-X	
15	Lower Steering Wheel-Y	

TABLE XXV. INPUT CONSTANTS (ALPHABETICAL ORDER) (page 2)

Number	Description	
47	Lower Torso-Center of Gravity to Lower Joint	
28	Lower Torso-Length	
46	Number of Seat Belt Segments	
38	Roof-Length	
3	Roof-X	
12	Roof-Y	
37	Seat Back-Length	
2	Seat Back-X	
11	Seat Back-Y	
43	Steering Column-Length	
8	Steering Column-X	
17	Steering Column-Y	
44	Toeboard-X	
18	Toeboard-Y	
51	Upper Arm-Center of Gravity to Lower Joint	
32	Upper Arm-Length	
53	Upper Leg-Center of Gravity to Lower Joint	
34	Upper Leg-Length	
39	Upper Panel-Length	(When NPASGR=2)
4	Upper Panel-X	(When NPASGR=2)
13	Upper Panel-Y	(When NPASGR=2)
39	Upper Steering Wheel-Length	(When NPASGR=1)
4	Upper Steering Wheel-X	(When NPASGR=1)
13	Upper Steering Wheel-Y	(When NPASGR=1)
49	Upper Torso-Center of Gravity to Lower Joint	
20	Upper Torso Contact Arc Radius	
30	Upper Torso Length	
40	Windshield-Length	
5	Windshield-X	
14	Windshield-Y	

TABLE XXVI. VARIABLES (IN NUMERICAL ORDER) (page 1)

<u>Number</u>		<u>Description</u>	
1	Body Angles	Lower Torso	Position
2	Body Angles	Center Torso	Position
3	Body Angles	Upper Torso	Position
4	Body Angles	Head	Position
5	Body Angles	Upper Arm	Position
6	Body Angles	Lower Arm	Position
7	Body Angles	Upper Leg	Position
8	Body Angles	Lower Leg	Position
9	Body Angles	Lower Torso	Velocity
10	Body Angles	Center Torso	Velocity
11	Body Angles	Upper Torso	Velocity
12	Body Angles	Head	Velocity
13	Body Angles	Upper Arm	Velocity
14	Body Angles	Lower Arm	Velocity
15	Body Angles	Upper Leg	Velocity
16	Body Angles	Lower Leg	Velocity
17	Body Angles	Lower Torso	Acceleration
18	Body Angles	Center Torso	Acceleration
19	Body Angles	Upper Torso	Acceleration
20	Body Angles	Head	Acceleration
21	Body Angles	Upper Arm	Acceleration
22	Body Angles	Lower Arm	Acceleration
23	Body Angles	Upper Leg	Acceleration
24	Body Angles	Lower Leg	Acceleration
25	Body Motion	Horizontal	Position
26	Body Motion	Horizontal	Velocity
27	Body Motion	Horizontal	Acceleration
28	Body Motion	Vertical	Position
29	Body Motion	Vertical	Velocity

TABLE XXVI. VARIABLES (IN NUMERICAL ORDER) (page 2)

<u>Number</u>	<u>Description</u>		
30	Vehicle	Motion	Velocity
31	Vehicle	Motion	Velocity
32	Vehicle	Motion	Velocity
33	Vehicle	Motion	Acceleration
34	Belt Forces	Lap Belt	Shoulder
35	Belt Forces	Lower	Shoulder
36	Belt Forces	Upper	Shoulder
37	Seat Forces	Hip	
38	Seat Forces	Front Edge	
39	Relative Head	Position	Horizontal
40	Relative Head	Position	Vertical
41	Belt Angles	Lap Belt	
42	Belt Angles	Lower	Shoulder
43	Belt Angles	Upper	Shoulder
44	Accelerometer	Head	Resultant
45	Accelerometer	Head	Angle
46	Accelerometer	Chest	Resultant
47	Accelerometer	Chest	Angle
48	Hip on Seat Back		
49	Upper Torso on Seat Back		
50	Upper Torso on Upper Steering Wheel		(When NPASGR=1)
	Upper Torso on Upper Panel		(When NPASGR=2)
	Upper Torso on Front Seat Back		(When NPASGR=3)
51	Upper Torso on Lower Steering Wheel		
52	Upper Torso on Steering Column		
53	Head on Seat Back		
54	Head on Roof		
55	Head on Upper Steering Wheel		(When NPASGR=1)
	Head on Upper Panel		(When NPASGR=2)
	Head on Front Seat Back		(When NPASGR=3)

TABLE XXVI. VARIABLES (IN NUMERICAL ORDER) (page 3)

<u>Number</u>	<u>Description</u>
56	Head on Windshield
57	Head on Lower Steering Wheel
58	Elbow on Seat Back
59	Knee on Lower Panel
60	Foot on Floor
61	Foot on Toeboard

TABLE XXVII. VARIABLES (IN ALPHABETICAL ORDER) (page 1)

<u>Number</u>		<u>Description</u>	
47	Accelerometer	Chest	Angle
46	Accelerometer	Chest	Resultant
45	Accelerometer	Head	Angle
44	Accelerometer	Head	Resultant
41	Belt Angles	Lap Belt	
42	Belt Angles	Lower	Shoulder
43	Belt Angles	Upper	Shoulder
34	Belt Forces	Lap Belt	
35	Belt Forces	Lower	Shoulder
36	Belt Forces	Upper	Shoulder
18	Body Angles	Center Torso	Acceleration
2	Body Angles	Center Torso	Position
10	Body Angles	Center Torso	Velocity
20	Body Angles	Head	Acceleration
4	Body Angles	Head	Position
12	Body Angles	Head	Velocity
22	Body Angles	Lower Arm	Acceleration
6	Body Angles	Lower Arm	Position
14	Body Angles	Lower Arm	Velocity
24	Body Angles	Lower Leg	Acceleration
8	Body Angles	Lower Leg	Position
16	Body Angles	Lower Leg	Velocity
17	Body Angles	Lower Torso	Acceleration
1	Body Angles	Lower Torso	Position
9	Body Angles	Lower Torso	Velocity
21	Body Angles	Upper Arm	Acceleration
5	Body Angles	Upper Arm	Position
13	Body Angles	Upper Arm	Velocity
23	Body Angles	Upper Leg	Acceleration

TABLE XXVII. VARIABLES (IN ALPHABETICAL ORDER) (page 2)

<u>Number</u>		<u>Description</u>	
7	Body Angles	Upper Leg	Position
15	Body Angles	Upper Leg	Velocity
19	Body Angles	Upper Torso	Acceleration
3	Body Angles	Upper Torso	Position
11	Body Angles	Upper Torso	Velocity
27	Body Motion	Horizontal	Acceleration
25	Body Motion	Horizontal	Position
26	Body Motion	Horizontal	Velocity
30	Body Motion	Vertical	Acceleration
28	Body Motion	Vertical	Position
29	Body Motion	Vertical	Velocity
58	Elbow	On	Seat Back
60	Foot	On	Floor
61	Foot	On	Toeboard
55	Head	On	Front Seat Back (3)
57	Head	On	Lower Steering Wheel
54	Head	On	Roof
53	Head	On	Seat Back
55	Head	On	Upper Panel (2)
55	Head	On	Upper Steering Wheel ( )
56	Head	On	Windshield
48	Hip	On	Seat Back
59	Knee	On	Lower Panel
39	Relative Head	Position	Horizontal
40	Relative Head	Position	Vertical
37	Seat Forces	Hip	
38	Seat Forces	Front Edge	
50	Upper Torso	On	Front Seat Back (3)
51	Upper Torso	On	Lower Steering Wheel



TABLE XXVII. VARIABLES (IN ALPHABETICAL ORDER) (page 3)

<u>Number</u>		<u>Description</u>	
49	Upper Torso	On	Seat Back
52	Upper Torso	On	Steering Column
50	Upper Torso	On	Upper Panel (2)
50	Upper Torso	On	Upper Steering Wheel (1)
33	Vehicle	Motion	Acceleration
31	Vehicle	Motion	Position
32	Vehicle	Motion	Velocity

## E. OVERALL PROGRAM DESCRIPTION AND FLOW DIAGRAM

Figure 34 is a flowchart for the computer program. Initially data is read, constants computed, and the problem initialized to zero where necessary. The cart acceleration and the level of output printing are then ascertained from the data. Acceleration components due to inertia, continuous joint reactions and external forces are computed in subroutine ACCEL. The effective acceleration due to discontinuous forces is then computed and added to the continuous accelerations in subroutines, JITTER and TAUMAK. After the accelerations are finally predicted, standard checking, storing, incrementing and integrating of results are carried out. The program then is run in loop fashion for the required number of print time increments.

Figure 35 shows how the subprograms in the computer implementation fit together in usage. The left margin of the figure contains a numbered list of the subroutines which comprise the program. Across the top is a list of numbers, each representing the subprogram with the same number on the left margin. The figure itself consists of a set of "X"'s at various intersections of rows and columns. An "X" at the mth row and nth columns indicates that subroutine n makes use of subroutine m. The row for a particular subroutine shows all the other subroutines which use it. The column for a particular subroutine also shows all the subroutines which it uses.

Figure 36 is similar to Figure 35 and shows the uses of library routines.

## F. INTEGRATION OF DISCONTINUOUS ACCELERATIONS

In the digital computer simulation, integration is done by mathematical approximation. The usual technique is to base the integration on a polynomial which has been fit through several ordinates of the integrand. This approach will work well only when the integrand is very much like the polynomial obtained by the curve fitting. If the integrand is continuous, it is possible to find a set of intervals over each of which the integrand "looks" like a polynomial. If, however, the integrand is discontinuous, the discontinuity will remain regardless of the length of the interval within which it

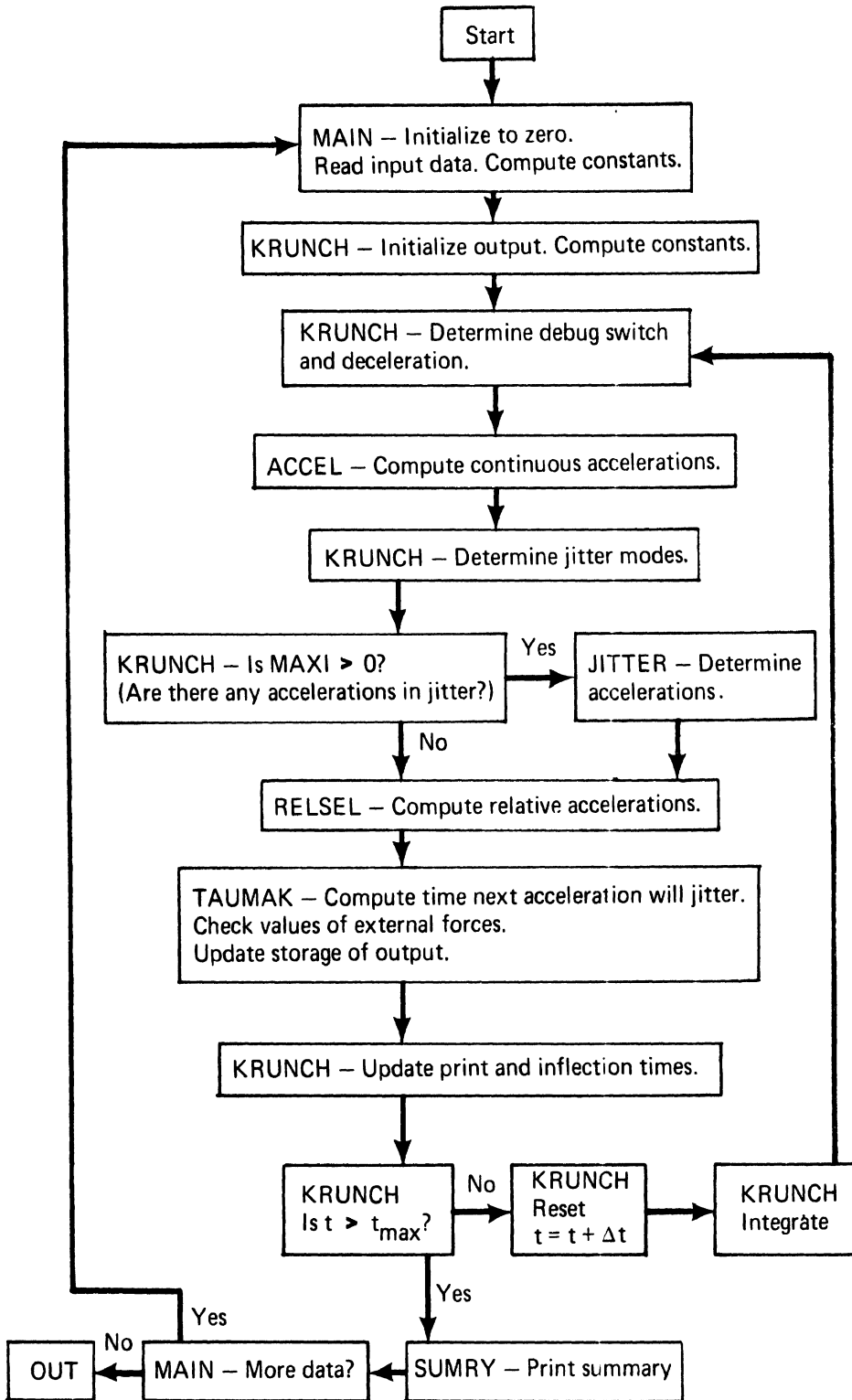


Figure 34. Simplified program flow chart.

Subroutine Number	Called Subroutine	Calling Subroutine																									
		1	2	3	4	5	6	7	8	9	10	11	12	13	14	15	16	17	18	19	20	21	22	23	26		
1	MAIN																										
2	DATE	x																						x		x	
3	PAGE 4																									x	
4	KRUNCH	x																									
5	GETY		x																								
6	ACCEL		x																								
7	SEAT				x																						
8	BELT				y																						
9	LODFEC						x																				
10	MULLER							x																			
11	CONTAC					x																					
12	BODY					x																					
13	ZMAKER																x										
14	HELVEL																x										
15	DELZMK																										
16	JITTER																										
17	ZKMAKR																										
18	RELSEL																										
19	TAUMAK																										
20	LIMIDT																										
21	FECLOD																										
22	NORMUT																										
23	SUMARY	x																									
24	ITOPOW																										
25	ARCSIN	x																									
26	SIPP																										
27	STYX																										

Figure 35. Usage of program subroutines.

Library Routine Called	Calling Subroutine																								
	1	2	3	4	5	6	7	8	9	10	11	12	13	14	15	16	17	18	19	20	21	22	23	24	25
REWIND	x																								
ERROR				x					x			x			x										
MINV												x													
LAND																x									
SIN	x					x		x			x								x						
COS	x					x		x			x								x						
ATAN								x																	
ATAN2																						x	x		
SQRT	x							x			x								x			x	x		x
SIGN																	x								x
AMAX1	x								x																
AMIN1	x																		x						
MAX0																					x				
MIN0	x																								
ABS	x								x													x			x
AMOD																									
TIME																									x

Figure 36. Library routines called by program.

is imbedded, so decreasing the interval length is not effective. In this situation, either the integration must be styled to the discontinuity or the discontinuity removed. For the two-dimensional crash victim simulator, the latter course is adopted.

Discontinuities arise in the model for seat friction force, contact surface friction force, and friction-like forces in the joints. Each of these models has a velocity-dependent component (force, torque, or slope of torque) which assumes a fixed value for all velocities greater than the velocity limit (an input parameter), the negative of the value for all velocities less than the negative of the velocity limit, and zero for the open interval defined by minus and plus values of the velocity limit.

Each instance of these discontinuous models is called a "mode" in the computer program and in the discussion which follows. If a particular mode is in either of the extreme velocity intervals, the mode is said to be "full on." If the mode is in the zero interval, the mode is said to be "full off." When velocity is at the velocity limit or its negative (the points of discontinuity), one of several things can happen, which may be categorized into one of two general possibilities. Either the mode will pass on through the limit point without mishap to full on or full off in the other direction, or the mode will try to do one of these and be thrown back. In the latter case, the mode is said to be "in jitter." Jitter will often take the form of a rapid alternation of the full on and full off states. This occurs when momentum and other forces drive the mode to full on but the force developed by the mode coming on is large enough to throw the mode back to off. The mode going in turn causes the mode force to go to zero which leaves the momentum and other forces free to drive the mode on again and so on, and on.

The jitter type of phenomenon occurs in reality, for example, as chatter due to backlash in gears. The technique employed in the two-dimensional crash victim simulator to compensate for jitter is based on the observation that a rapid alternation of the on-off states would effectively hold the velocity at the velocity limit. Hence, for a time interval during which a

single mode is jittering, the effective body accelerations are computed to be a weighted average of the accelerations computed with the mode turned full off and those computed with the mode turned full on, such that the mode acceleration is made zero, or the mode velocity is the same at the end of the time interval as it was at the beginning.

$$\ddot{\vec{Z}}_{\text{eff}} = \ddot{\vec{Z}}_{\text{off}} - \bar{a} (\ddot{\vec{Z}}_{\text{on}} - \ddot{\vec{Z}}_{\text{off}})$$

where

$$\bar{a} = \frac{\dot{v}_{\text{off}}}{\dot{v}_{\text{on}} - \dot{v}_{\text{off}}} \quad (\text{IV.F.1})$$

$\ddot{\vec{Z}}_{\text{eff}}$  is the effective generalized acceleration vector.

$\ddot{\vec{Z}}_{\text{on}}$  is the generalized acceleration vector with the mode full on.

$\ddot{\vec{Z}}_{\text{off}}$  is the generalized acceleration vector with the mode full off.

$\dot{v}_{\text{off}}$  is the mode acceleration magnitude with the mode full off.

$\dot{v}_{\text{on}}$  is the mode acceleration magnitude with the mode full on.

When the mode is influenced by an outside acceleration (such as vehicle deceleration) applied arbitrarily, the mode acceleration forced to zero may not guarantee that there will be no change in velocity over an interval. Arbitrary accelerations are treated by the two-dimensional crash victim simulator as piecewise linear functions. Those modes which are dependent upon vehicle acceleration, e.g., any interaction of contact surface and contact arc, are termed "coupled" modes and lead to "linear" jitter. Linear jitter requires a different weighted average and also an iteration for resolution.

$$\bar{a} = \frac{\dot{v}_{\text{off}} - 1/2 \dot{v}_{\text{on}}}{\dot{v}_{\text{on}} - \dot{v}_{\text{off}}}$$

$$\hat{\tau}_0 = \frac{\dot{v}_{\text{on}}}{\bar{a} \cos \psi_a} \quad (\text{IV.F.2})$$

where

$\psi_a$  is the orientation angle of the contact surface if a contact surface is involved in the mode.  $\psi_a$  is defined zero if no contact surface is involved in the mode, e.g., seat cushion.

$\hat{\tau}_0$  is a computed time interval in which the mode will reach the velocity limit. It is used in the iteration as shown on page 135.

For several modes in jitter or "multiple jitter," all possible combinations of the jittering modes in the full on state and the full off state are considered and averages developed by reapplications of the single mode averaging procedure so that all the mode velocities are held constant. Only one linear jitter can be handled at one time and must be processed last in combination with other jittering modes.

If no mode changes state during a time interval, then the generalized accelerations are continuous. If the time interval is kept small enough, the generalized accelerations are nearly constant over the interval and a one point integration scheme can be validly employed.

The grand strategy for integration in the two-dimensional crash victim simulator revolves around maintaining the validity of these two requirements and taking advantage of their consequences. At each time throughout the initial value solution of the equations of motion, an integration time interval is computed that will meet the requirements that the generalized accelerations are continuous and approximately constant. The determination of the time interval is carried out by taking the smallest of the predicted time intervals, after the end of which the requirements will no longer be met due to one or another cause. In particular, the computer program predicts the next time at



which any of the modes will change state. If that time is less than the time to which the program would integrate from other considerations (deceleration slope change, print time, etc.), the program integrates to that time and indicates that the mode is jittering. The program always employs the averaging procedure to resolve the questionable accelerations from jittering modes.

The time interval prediction equation (until a change of state) for an uncoupled mode is

$$\tau = \frac{\xi \operatorname{sgn} \eta - v}{\dot{v}}$$

where

$$\eta = \begin{cases} v & \text{for } |v| > \xi \text{ and } \operatorname{sgn} v \neq \operatorname{sgn} \dot{v} \\ \dot{v} & \text{for } |v| < \xi \end{cases}$$

$\xi$  is the mode velocity limit

$v$  is the mode velocity

$\dot{v}$  is the mode acceleration

Note that if  $|\dot{v}| = \xi$ , then  $\tau$  is not used since the mode is already known to be jittering. If  $|v| > \xi$  and  $\operatorname{sgn} v = \operatorname{sgn} \dot{v}$ , then  $\tau$  is infinite since the mode is going away from the velocity limit. The corresponding equation for a coupled mode is

$$\tau = \begin{cases} \frac{\dot{v}}{a_v} \left[ 1 - \sqrt{1 - \frac{2(\xi \operatorname{sgn} \eta - v)}{a_v \cos \psi_a}} \right] \\ \hat{\tau}_0 & \text{for 1. } |v| > \xi \text{ and } \operatorname{sgn} v = \operatorname{sgn} \dot{v} \\ & \text{2. } |v| = \xi \\ & \text{3. arg of radical is negative} \end{cases}$$

where  $a_v$  is the acceleration rate and the other conventions are as previously given. The equation is used in an iterative procedure in which it is alternated with the acceleration averaging procedure and recomputation of  $\hat{\tau}_0$  until

two consecutive values of  $\tau$  are approximately the same.

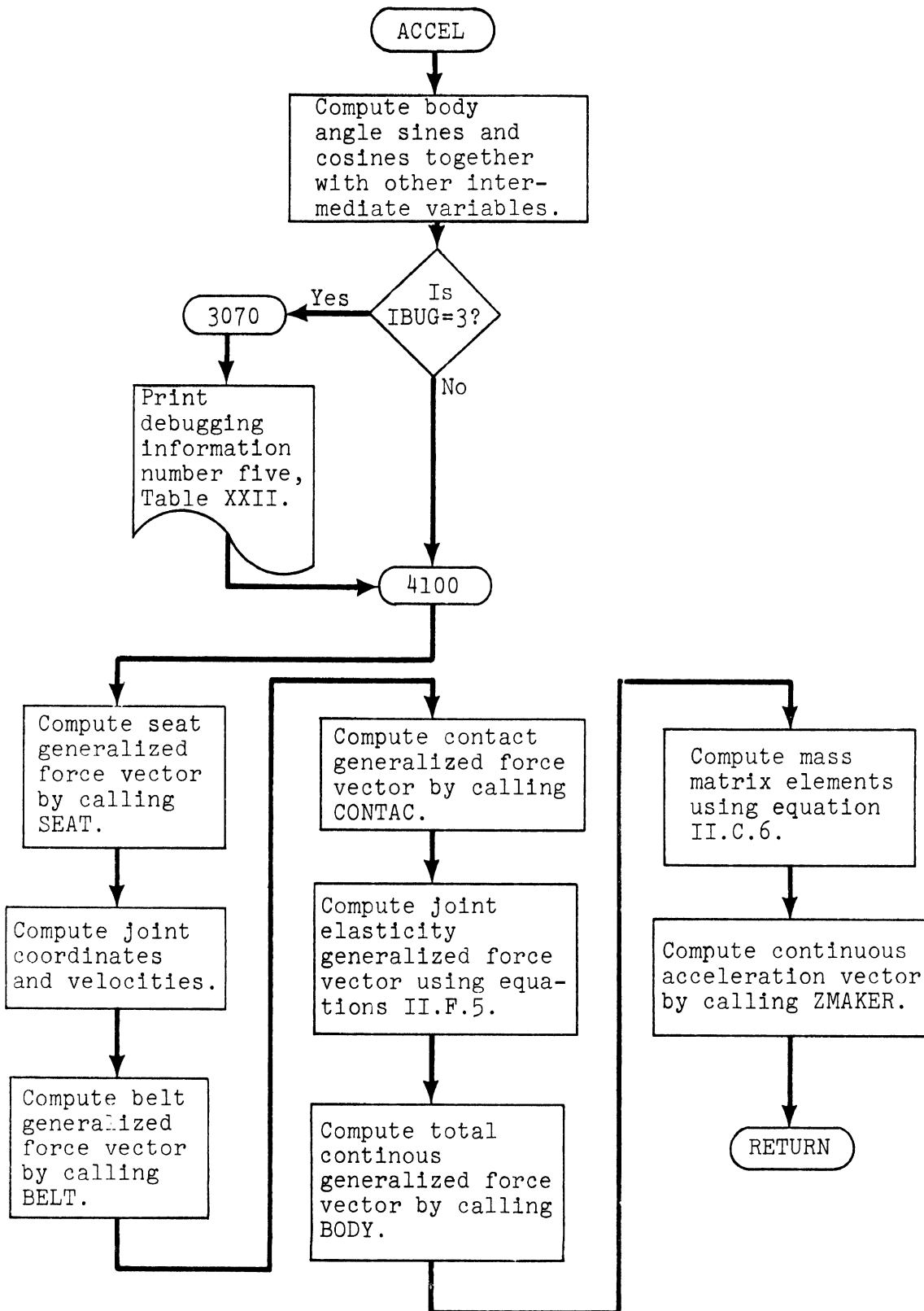
#### G. SUBPROGRAMS DESCRIPTIONS AND FLOW DIAGRAMS

For each of the subprograms which make up the computer implementation of the model a short description together with a flow diagram is presented here. These are in alphabetical order by the subprogram name with the main program ordered as if its name were MAIN. This form is thought to be the most useful reference. The subroutines included are:

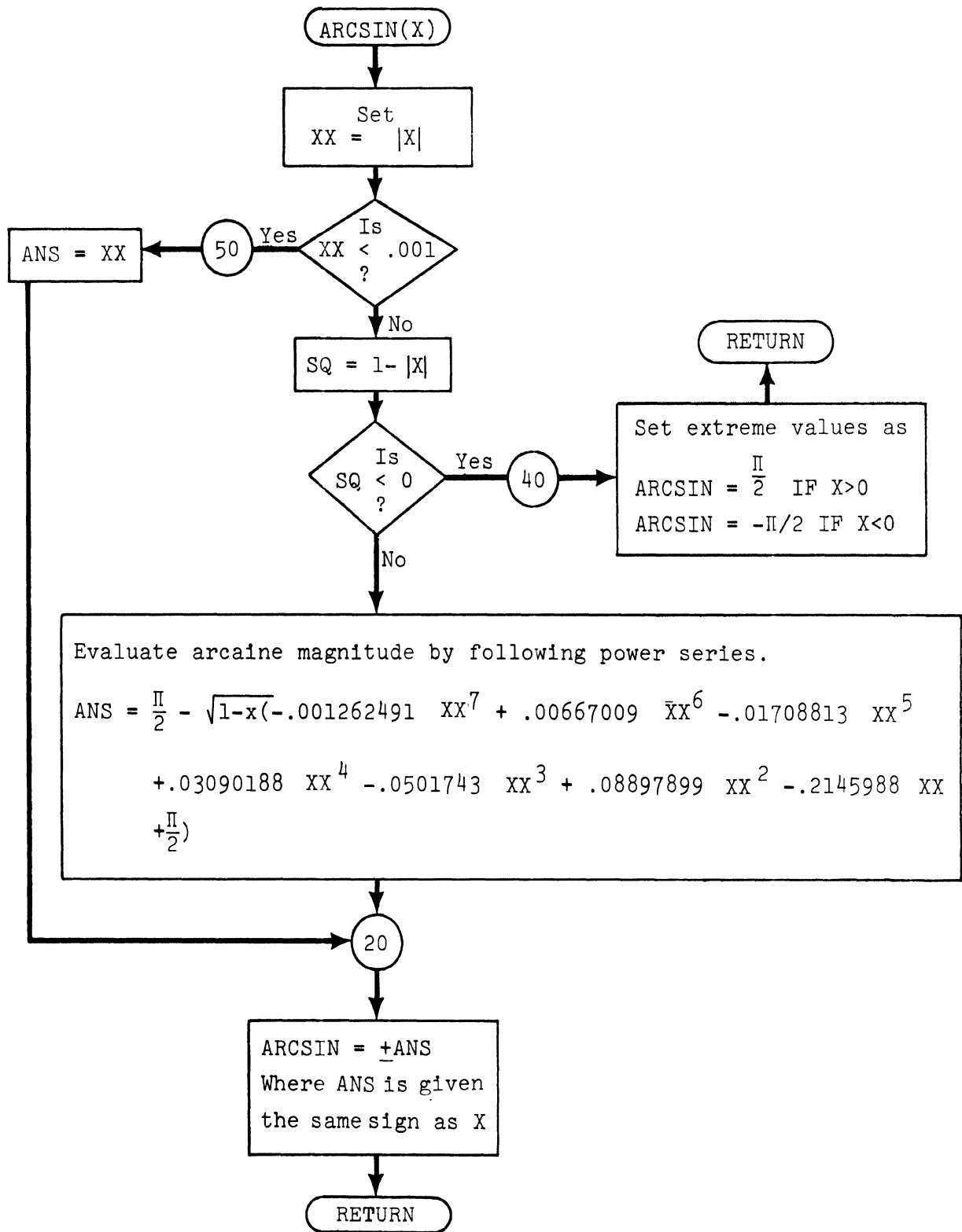
1	ACCEL	15	MAIN
2	ARCSIN	16	MULLER
3	BELT	17	NORMUT
4	BODY	18	PAGE4
5	CONTAC	19	RELSEL
6	DATE	20	RELVEL
7	DELZMK	21	SEAT
8	FECLOD	22	SIPP
9	GETY	23	STYX
10	ITOPW	24	SUMARY
11	JITTER	25	TAUMAK
12	KRUNCH	26	ZKMAKR
13	LIMIDT	27	ZMAKER
14	LODFEC		

Subroutine ACCEL carries out the following steps:

1. Computes sines and cosines of body angles and other needed variables.
2. Gets seat forces and contributions to the generalized force vector via SEAT.
3. Computes all joint coordinate positions and velocities.
4. Gets belt forces and contributions via BELT.
5. Gets contact forces and contributions via CONTAC.
6. Computes joint elasticity torques and contributions.
7. Procures generalized force vector from BODY.
8. Computes variable matrix elements.
9. Procures acceleration vector from ZMAKER.

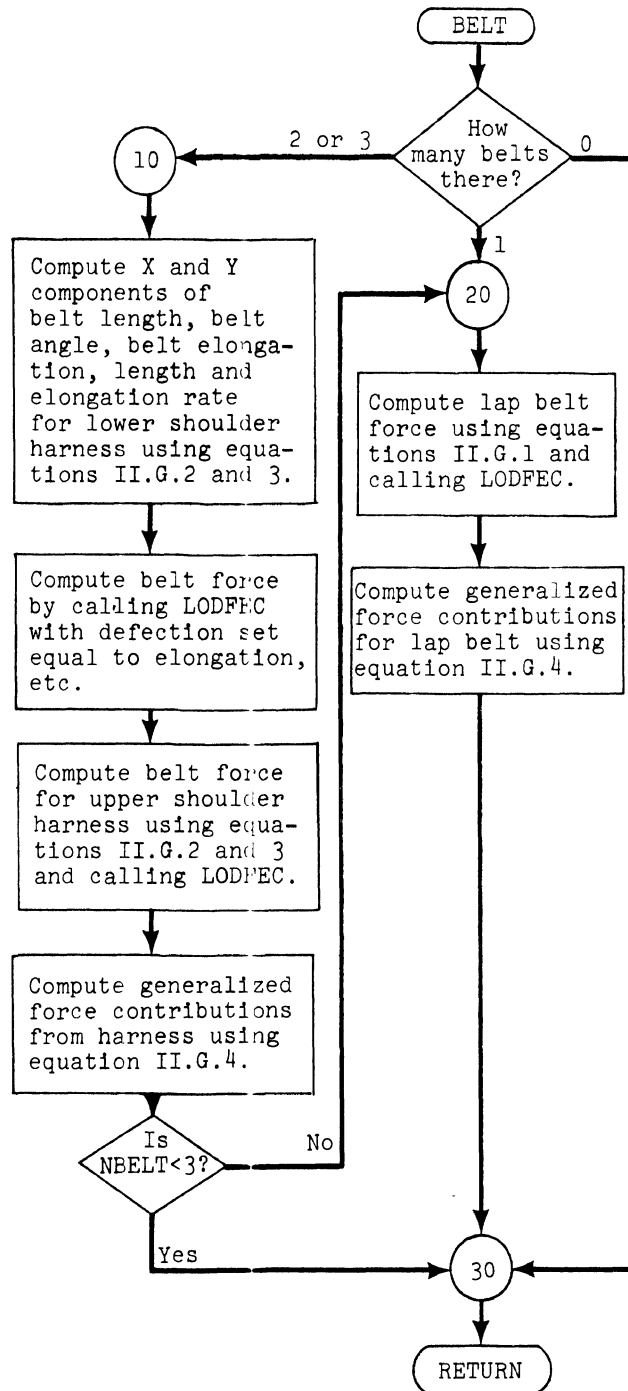


Function ARCSIN finds the angle for a given sine value. The argument X is in the range  $-1 \leq X \leq 1$  and is the sine of the angle to be computed by this routine.



Subroutine BELT carries out the following steps:

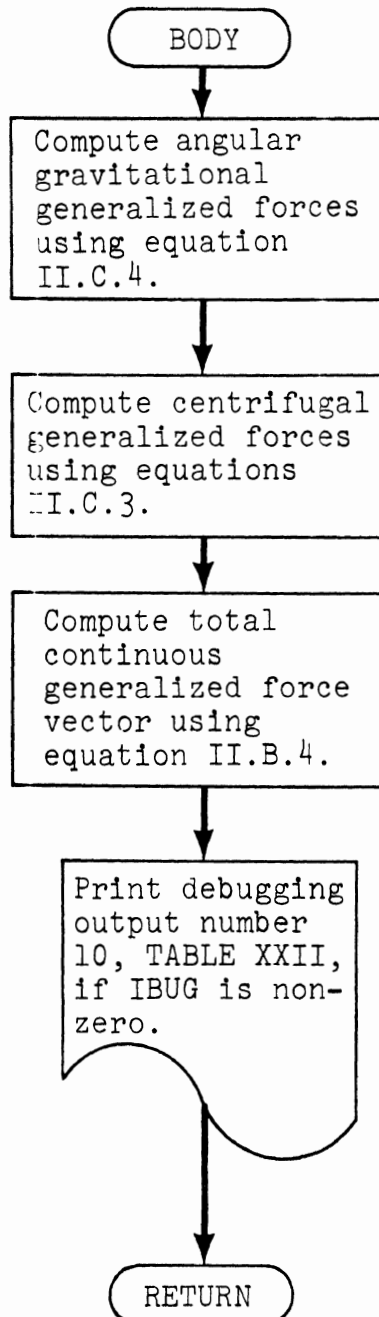
1. Computes angle, elongation, and rate for each belt.
2. Obtains belt force from LODFEC.
3. Computes total belt generalized force vector and adds it to seat total generalized force vector.



Subroutine BODY

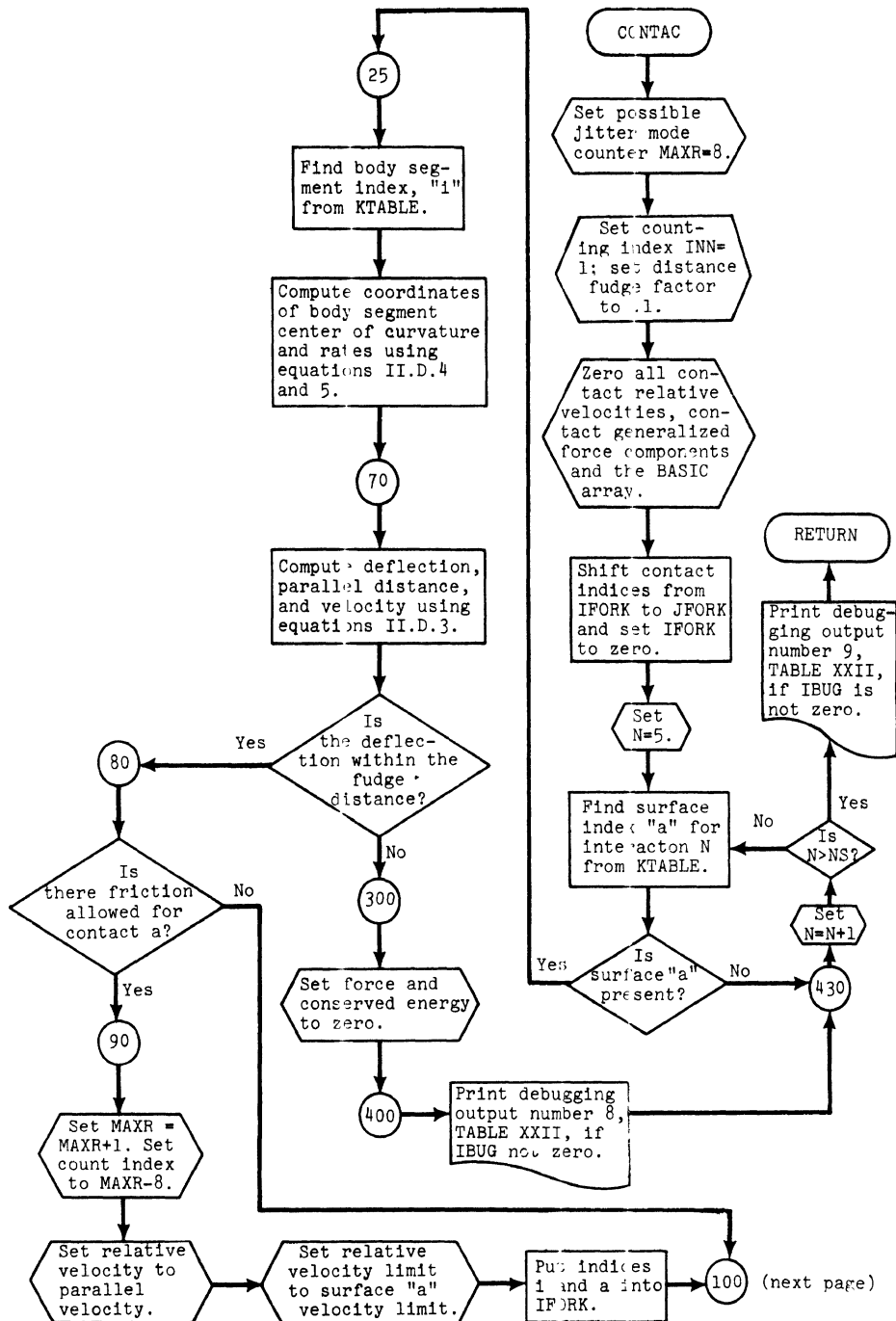
Computes generalized force vectors due to gravity and centrifugal force, and

Combines all five continuous generalized force vectors for total.

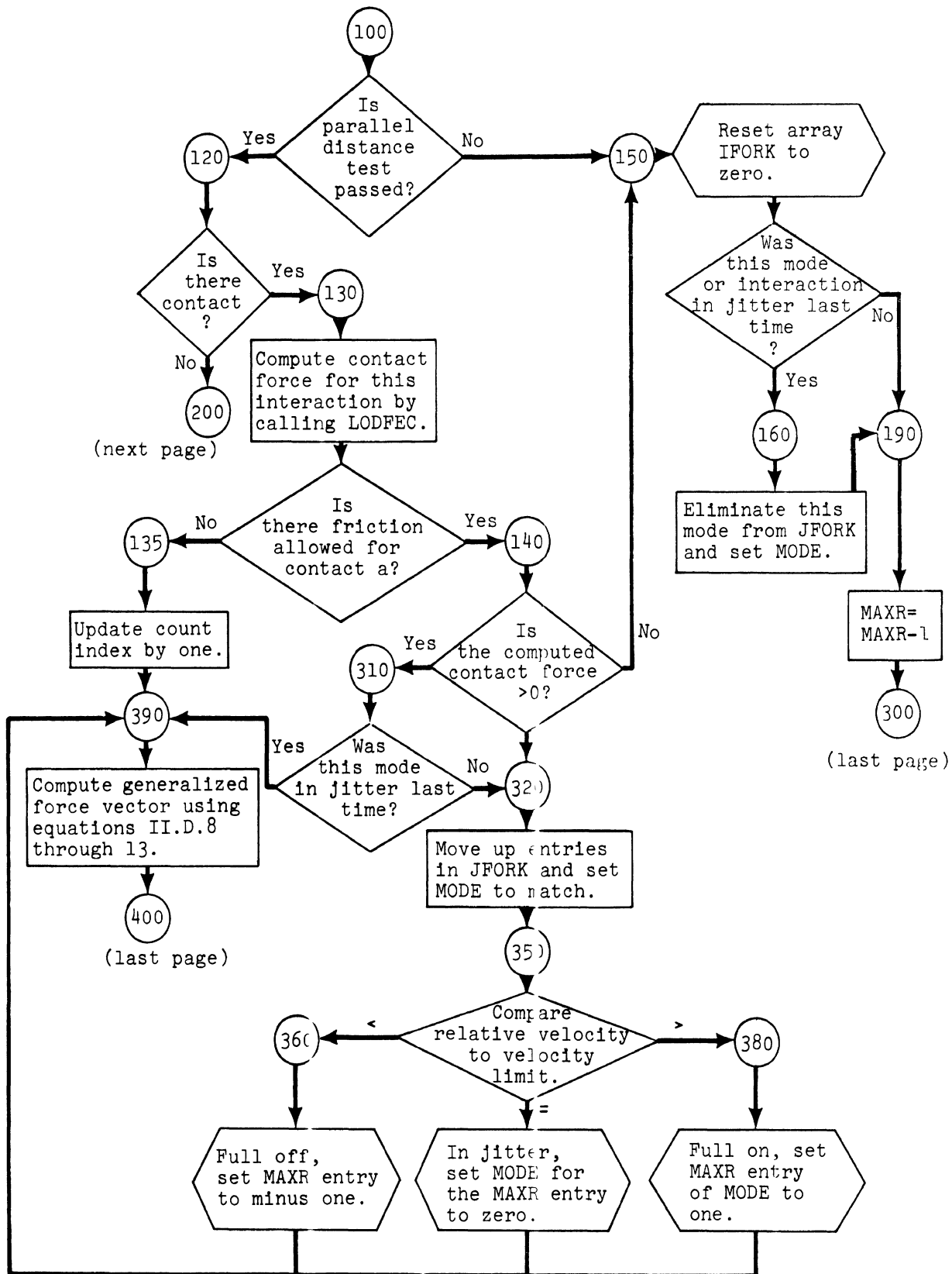


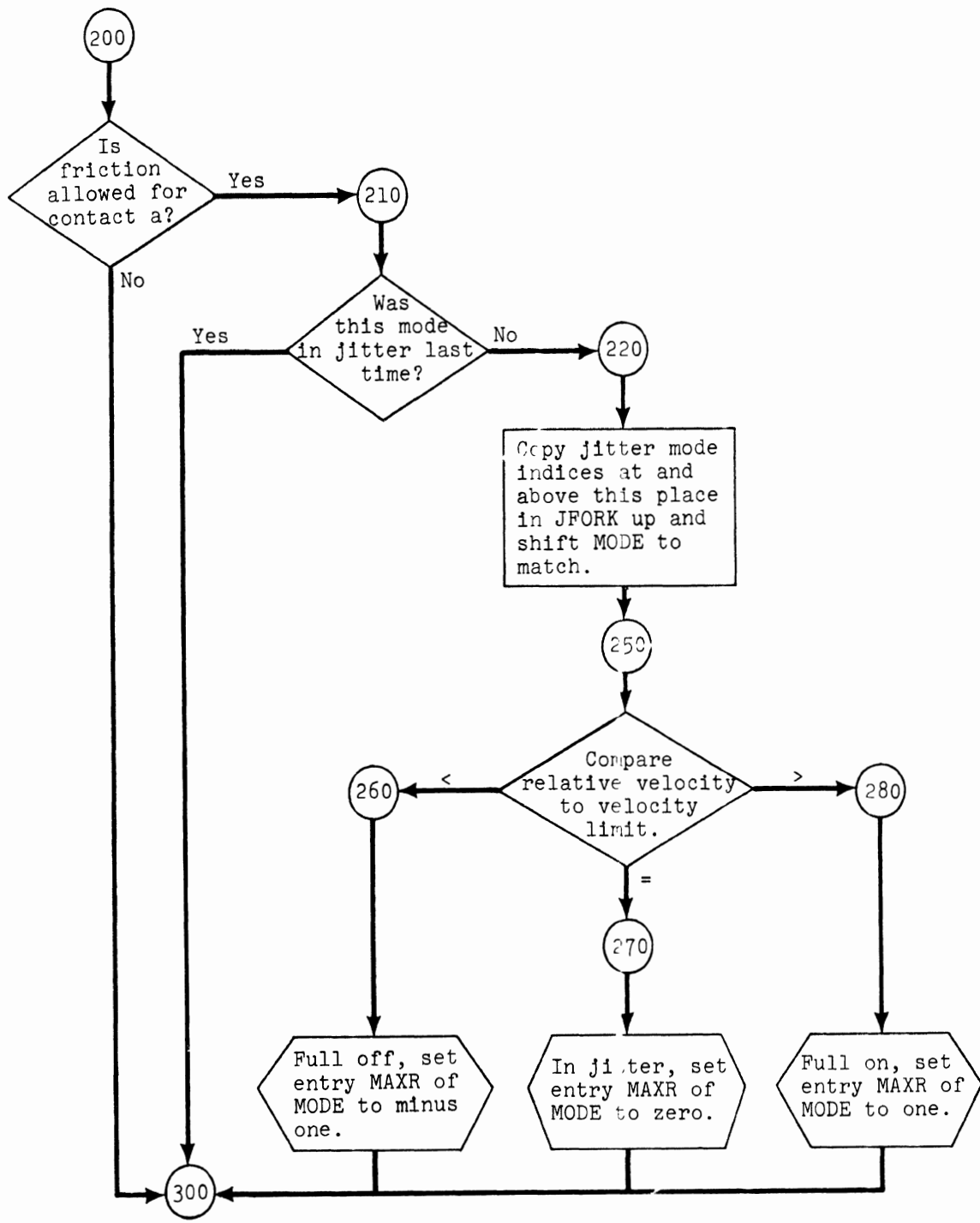
Subroutine CONTACT carries out the following steps

1. Searches table of possible contacts (as set up in MAIN) and determines whether contact exists using coordinates of body segment center of curvature and contact surface reference point.
2. Does bookkeeping for linear jitter modes.
3. Obtains contact forces from LODFEC.
4. Computes contribution of contacts to total generalized force vector.



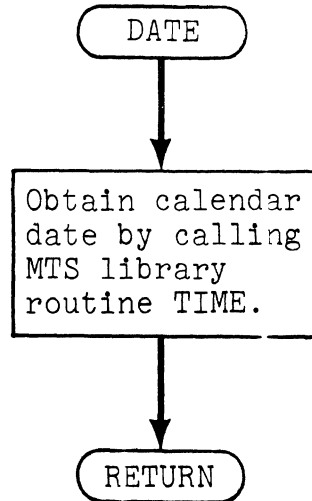






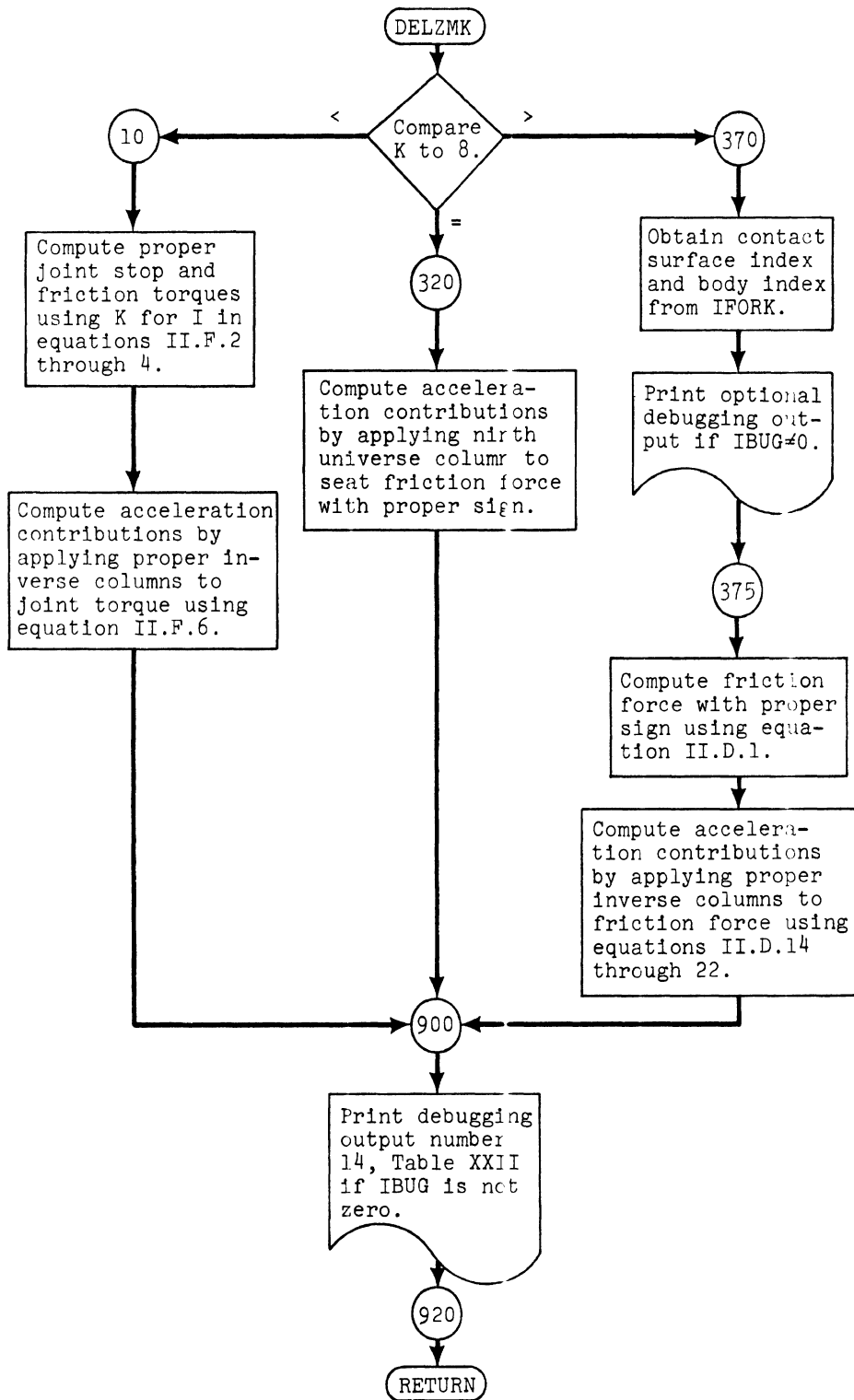
Subroutine DATE

Calls Library routine TIME to get date program is being run for print-out identification.

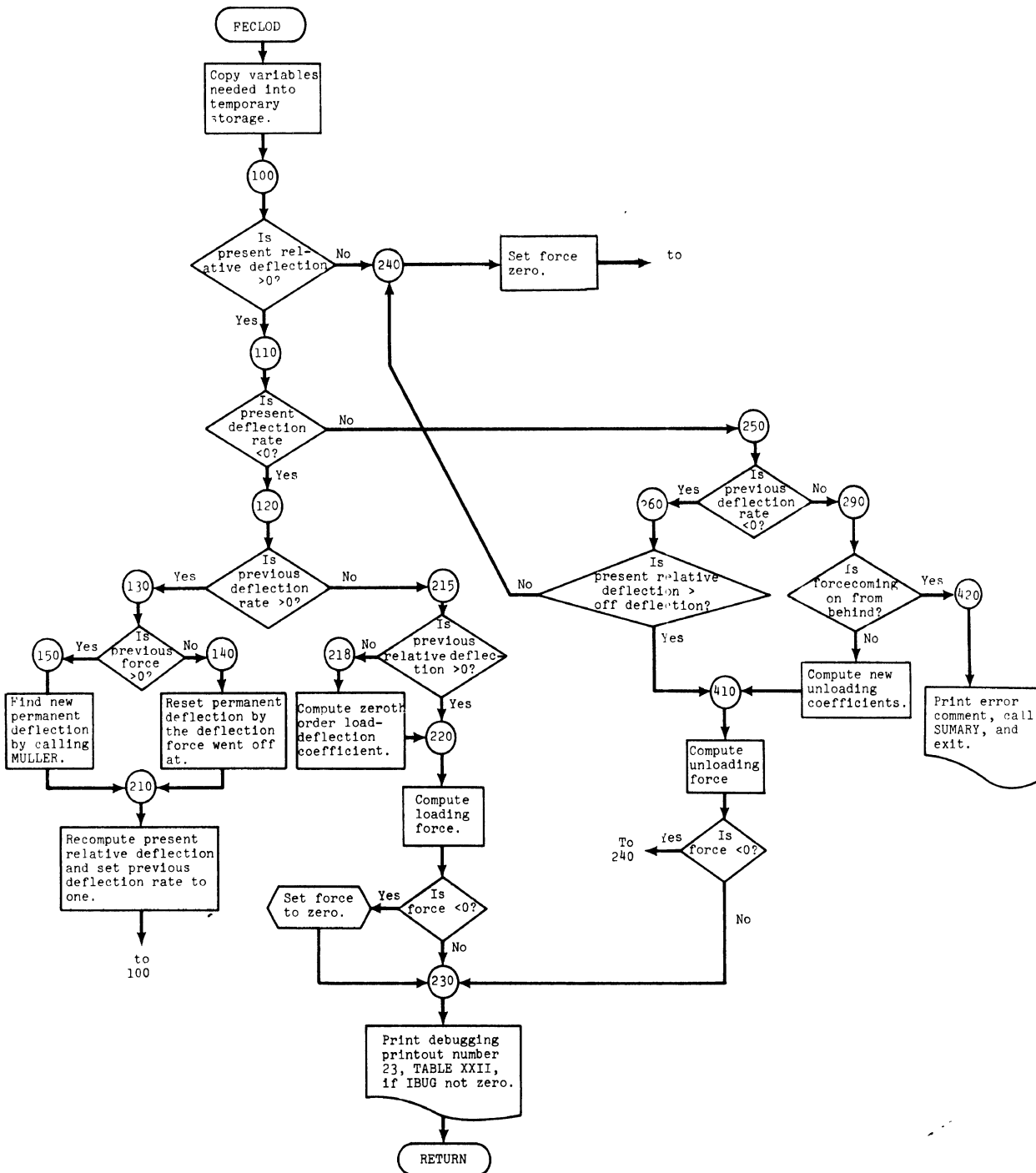


Subroutine DELZMK

Computes contributions to the acceleration vector of joint, seat, and contact friction. The argument K of DELZMK is the mode number for which acceleration contributions are to be computed.



Subroutine FECLOD is used to predict contact and belt forces during the selection a new time step.



Subroutine GETY

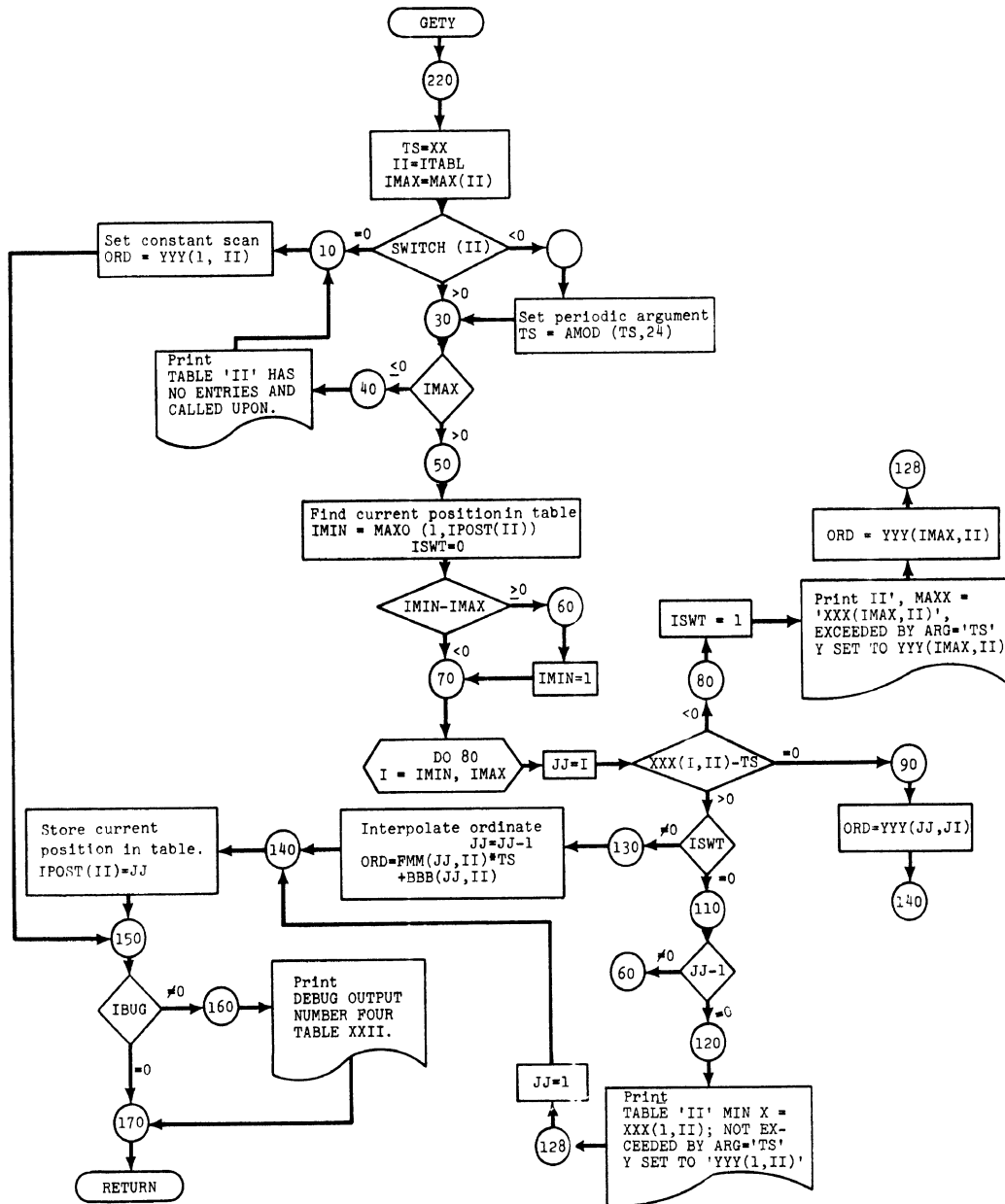
determines the ordinate of piecewise-linear tabular function for a given abscissa.

Arguments are:

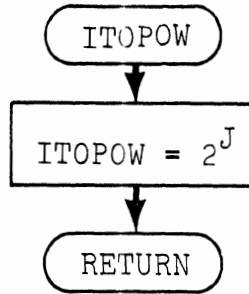
XX = abscissa desired

ITABL = table number, and

ORD = computed ordinate.

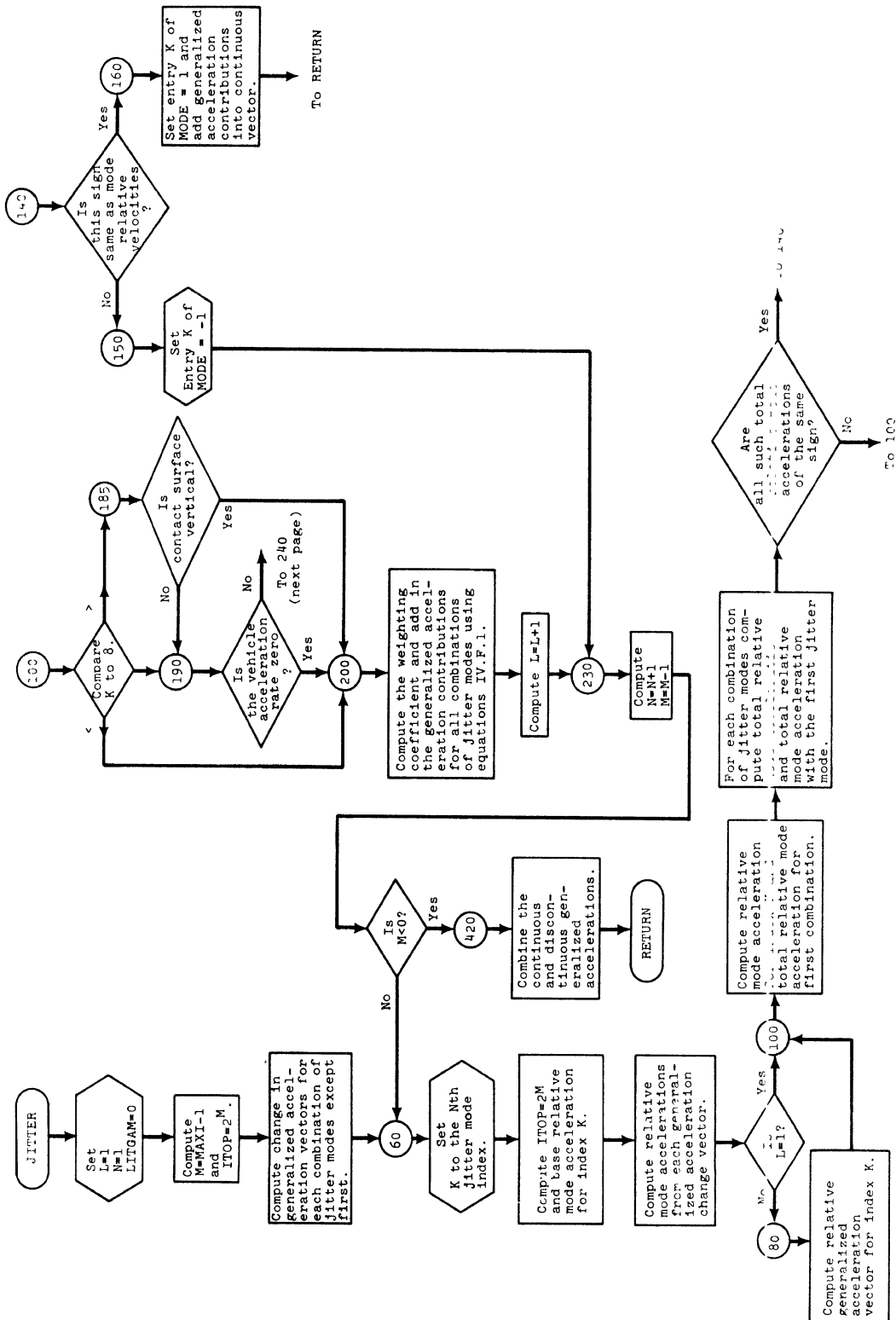


Function ITOPOW raises 2 to an integer power. The argument J is the power of 2 that is desired.

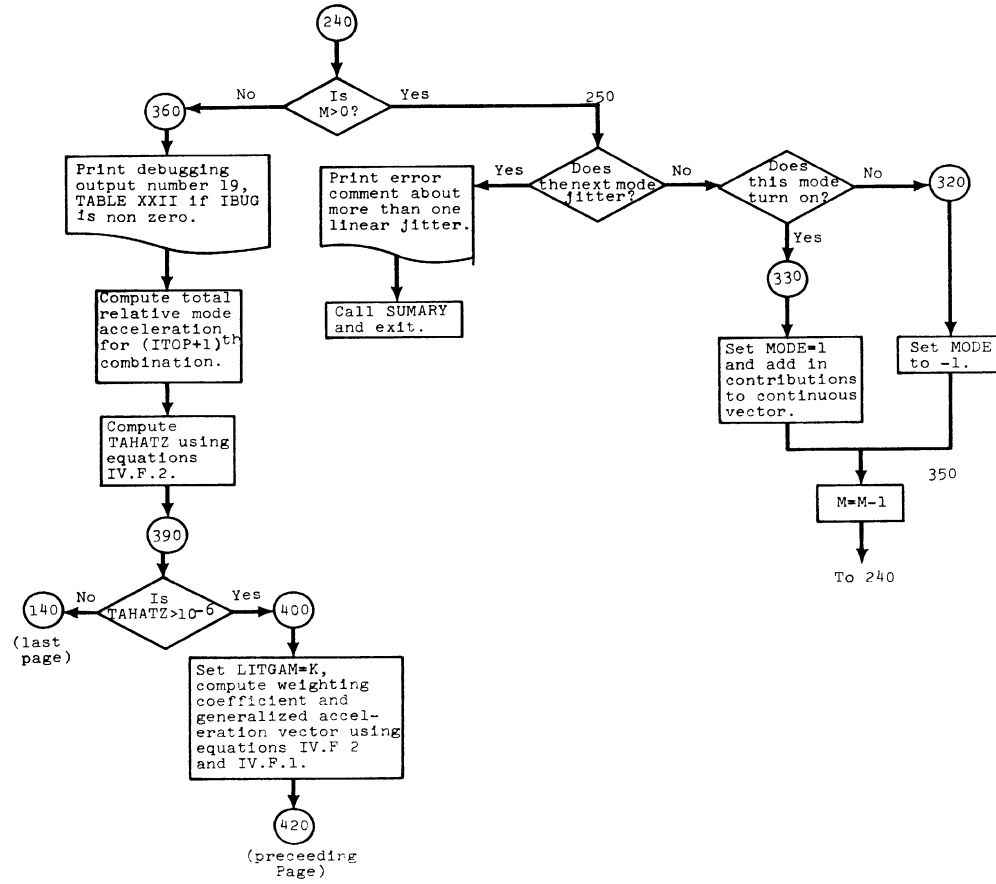


# Subroutine JITTER

Computes the effective acceleration vector by combining the continuous acceleration vector with the contribution of frictional forces in the form of discontinuous accelerations using a weighted averaging technique.

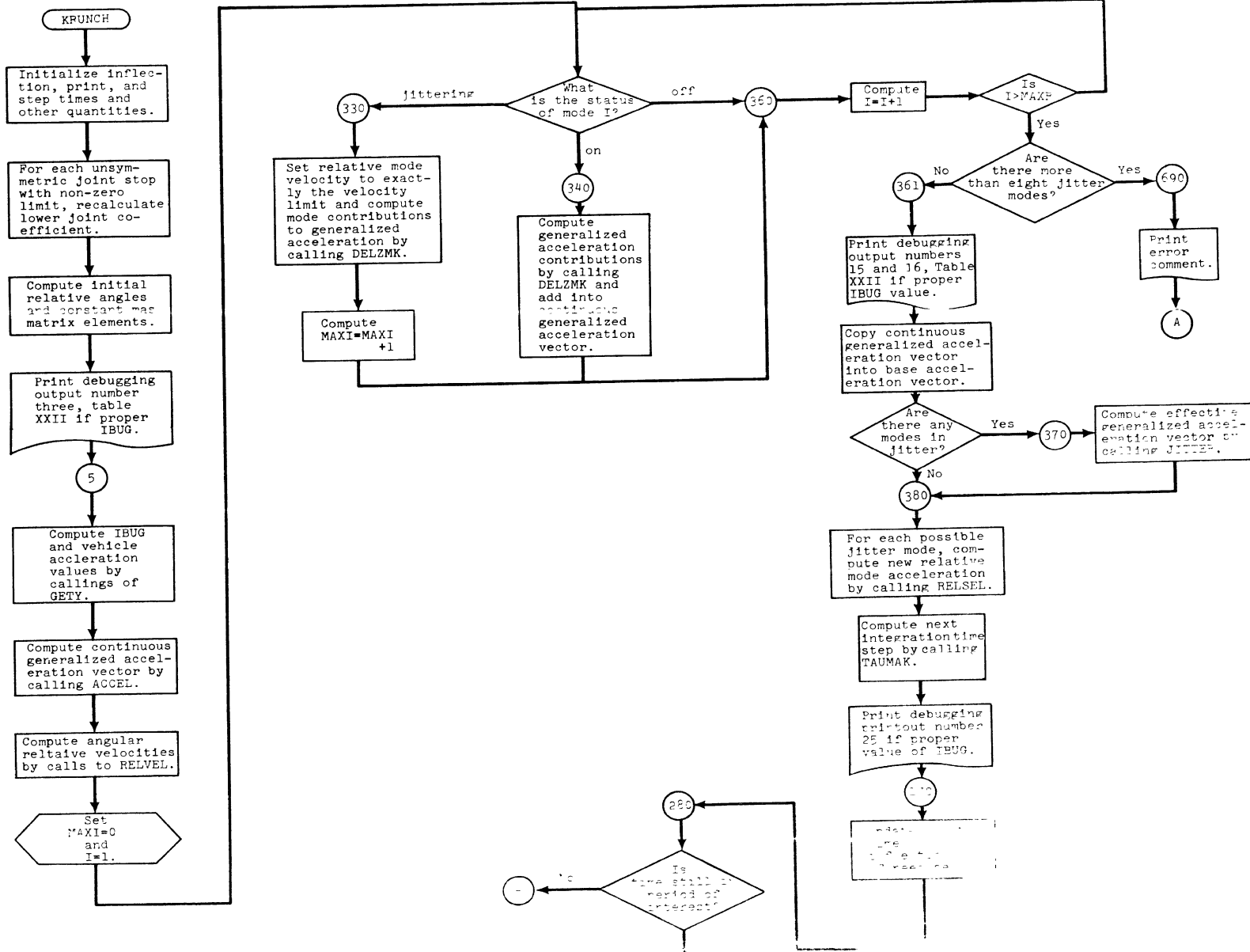


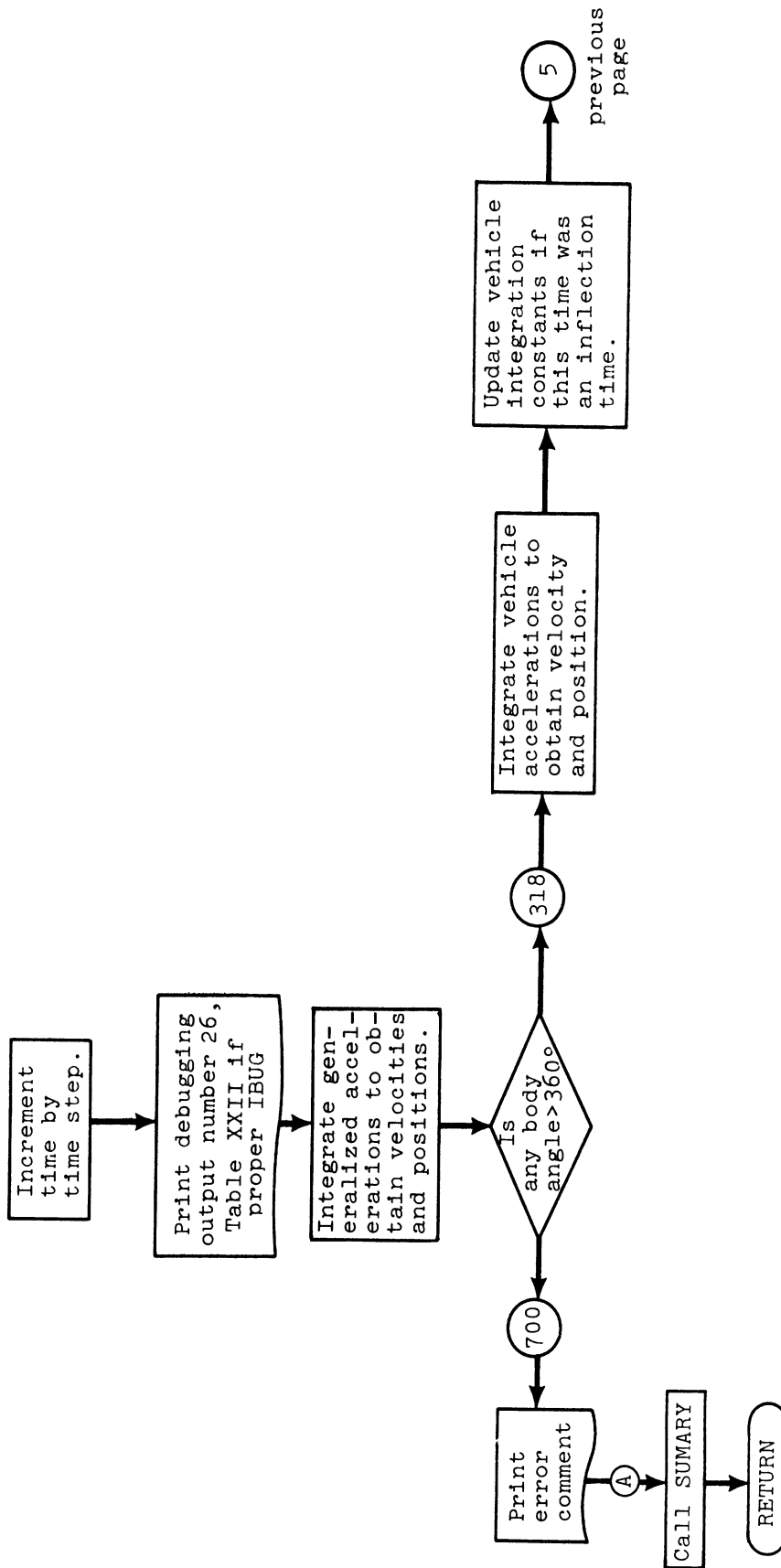




Subroutine KRUNCH carries out the following steps:

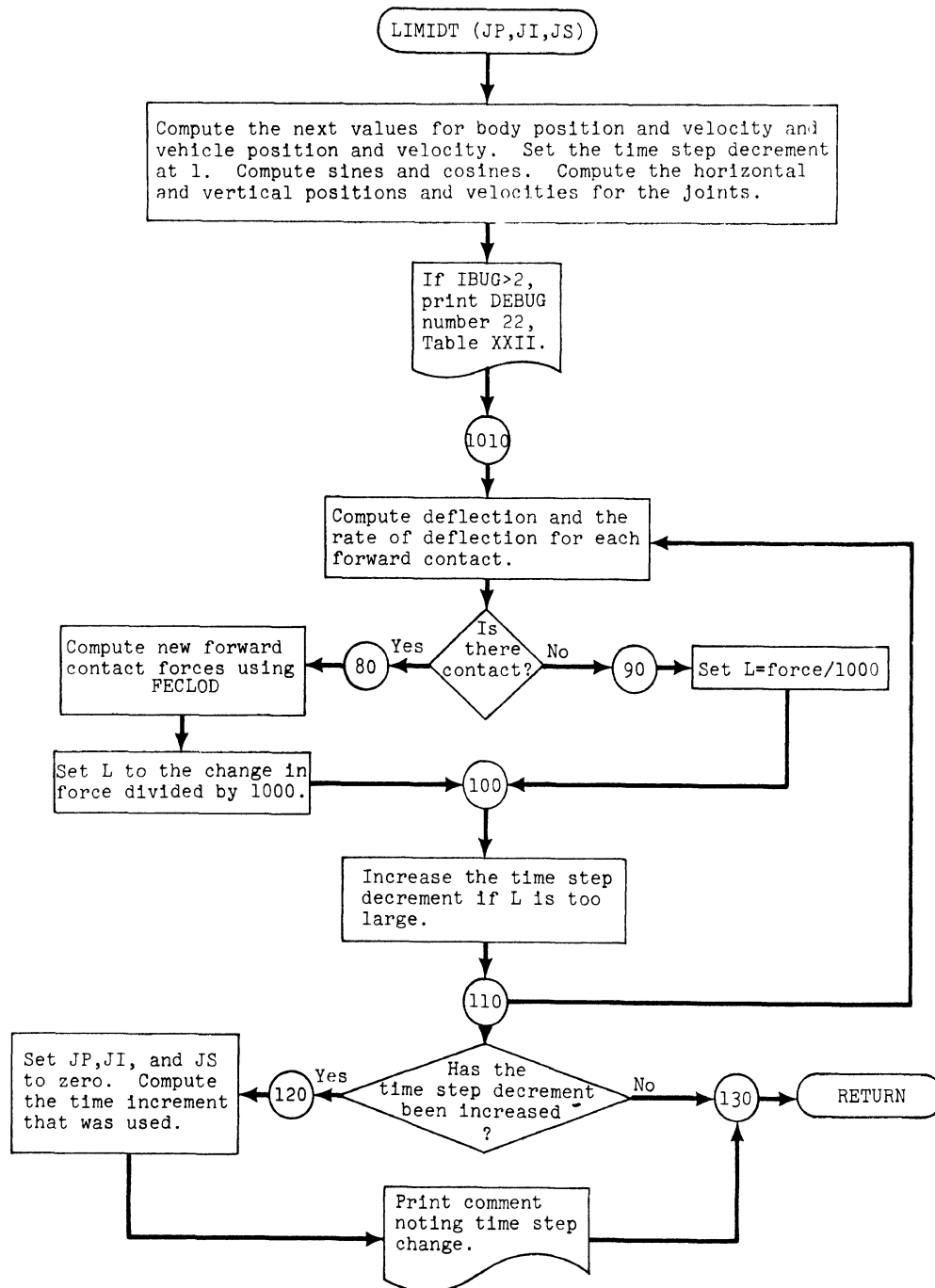
1. Initializes variables and parameters.
2. Recomputes joint stop coefficients as needed.
3. Starts time loop by finding debug variable and vehicle acceleration from tables via GETY.
4. Calls ACCEL for body accelerations due to continuous forces.
5. Computes relative velocities between body segments and between the hip and seat cushion.
6. Predicts unstable computational behavior and sets up the means (jitter vector) for compensating for it.
7. Computes the turned on friction forces contributions to the acceleration vector via DELZMK.
8. Checks number of jitter modes.
9. Computes effective acceleration due to jittering, via JITTER.
10. Computes all relative accelerations via RELSEL.
11. Computes next time interval via TAUMAK.
12. Resets print and inflection times as needed.
13. Checks time for end of program: (1) if done, returns to MAIN, and, (2) if not done, updates time and continues.
14. Integrates body variables.
15. Integrates vehicle deceleration.
16. Returns to 3.





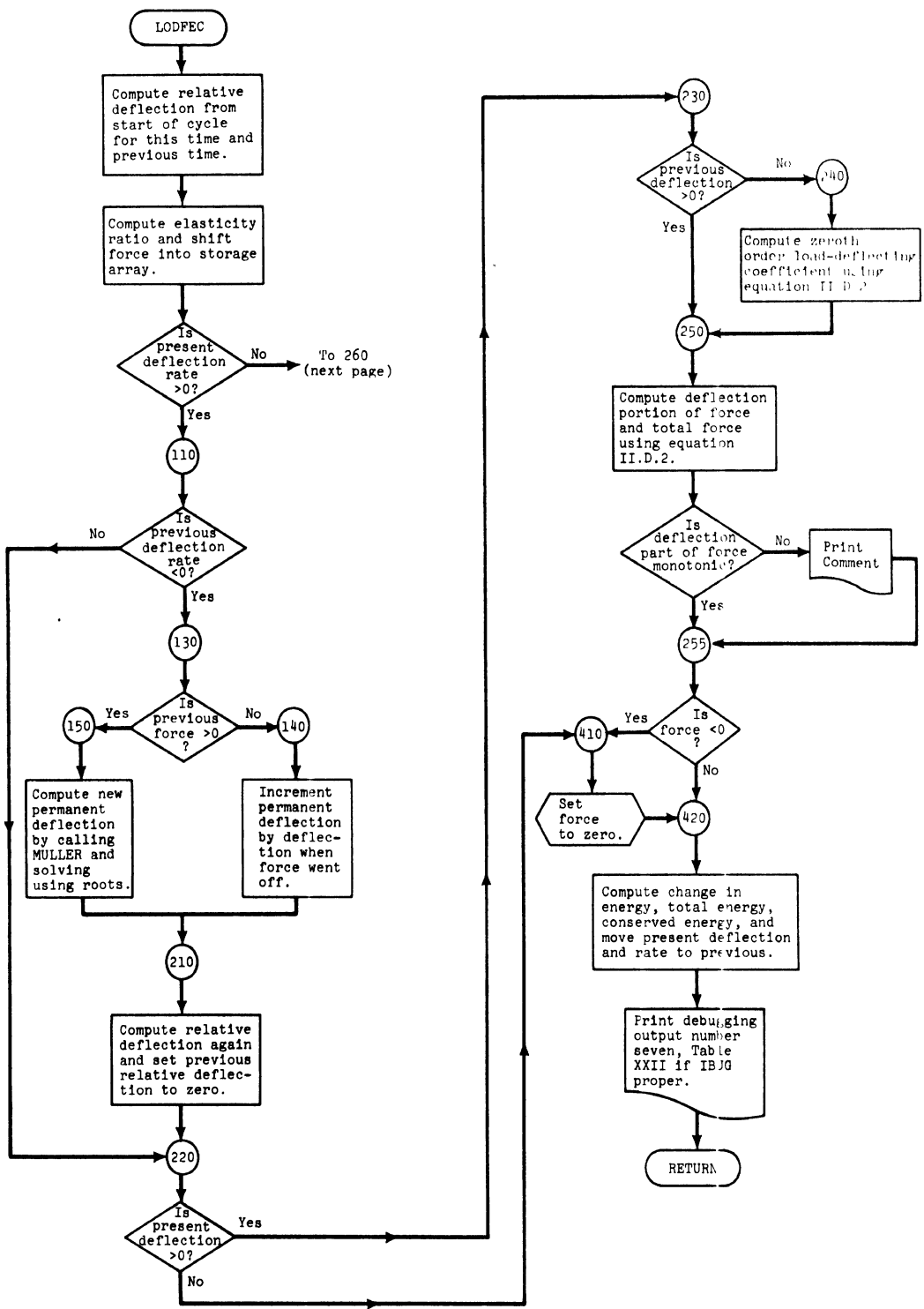
Subroutine LIMIDT carries out the following steps:

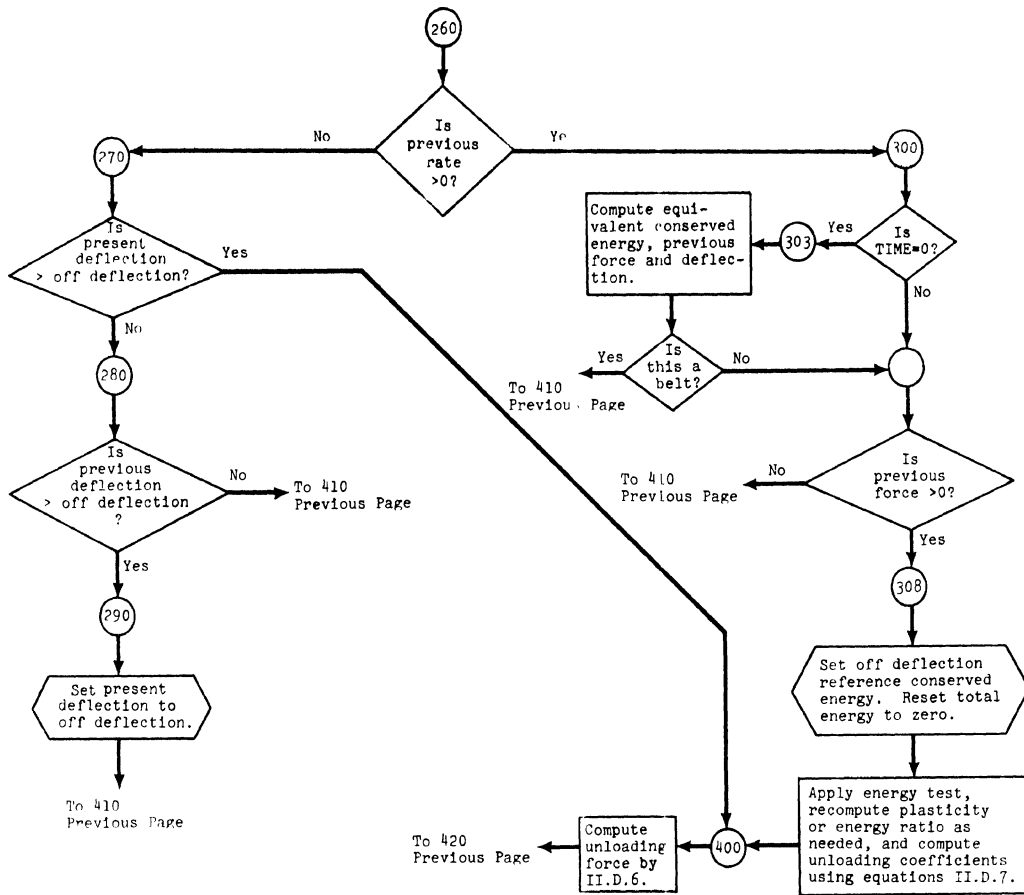
1. Integrates body variables forward to a tentative new time.
2. Computes new forward contact forces via FECLD.
3. Checks to see if changes in forces are more than 1000 lbs. If any one is, the time increment is decreased proportionately.



Subroutine LODFEC carries out the following steps:

1. Determines whether external forces are on loading or unloading portion of force deformation profile.
2. If loading, forces are computed from fifth order polynomial in both deflection and rate.
3. If unloading, forces are computed from second order polynomial.
4. If in transition, the peak value is selected and coefficients for unloading computed.







The main program carries out the following steps:

1. Zeroes some input and variables.
2. Defines some constants and tables.
3. Reads input data for amin program up to and including Z card.
4. Sets up table of contact indices for occupant and prints it out.
5. Sets up input deceleration and debug tables.
6. Prints out input data.
7. Computes constants.
8. Sets time to zero.
9. Rewinds buffer storage unit 9.
10. Calls KRUNCH.
11. Calls SUMMARY.
12. Reads additional data decks if any.

Set up the array IDATE with the EBCD equivalent of the current day's date.

Eject to a new page

Zero the following

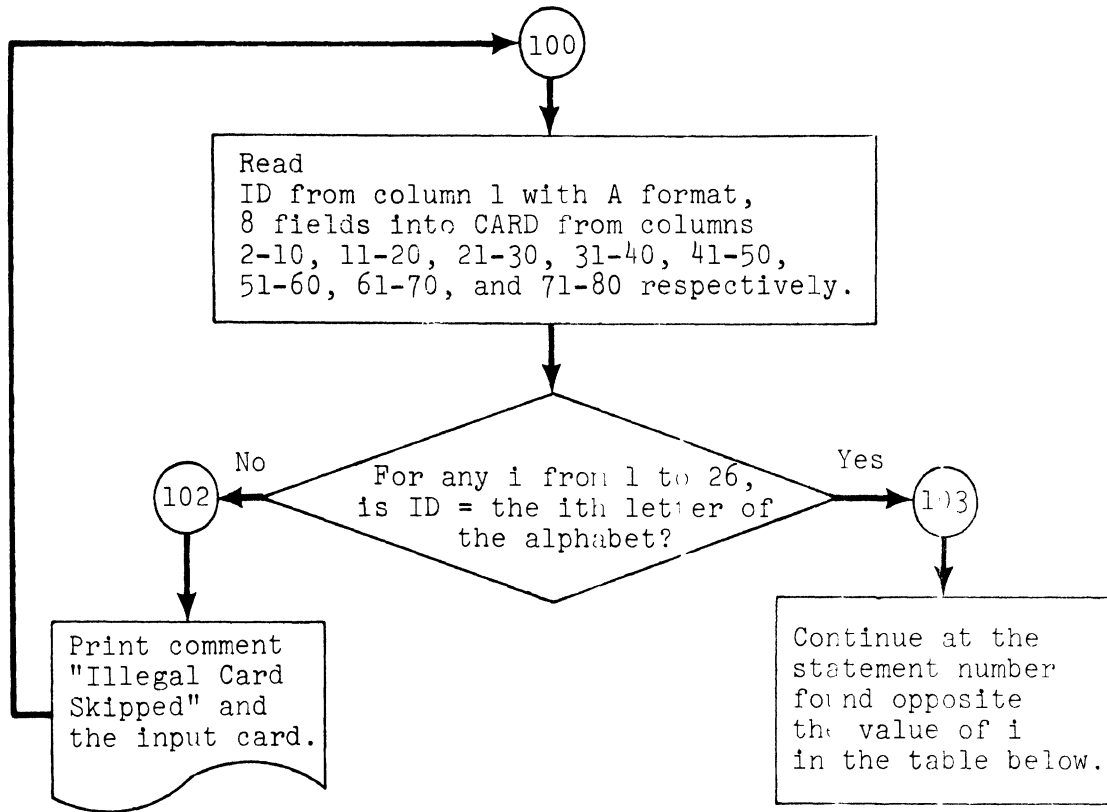
AA	IPOST	SIGMAA
BBB	MAX	SIGMAC
BL	NEW	SPSIA
CPSIA	PHI	SWITCH
	PSIA	XISMLA
DA	RA	XSMALA
FMM	SDELTA	XXX
		YSMALA
FMUA	SDELTD	YYY
GA	SIGMA	ZERO

Set  
MFORI to  
7,1,2,3,3,5,8

Set  
 $OTR = \frac{\pi}{180} = .01745\ 29$   
 $PITWO = \frac{\pi}{2} = 1.5707\ 6$   
GRAVIT=386.4

Set the underflow trap  
monitor

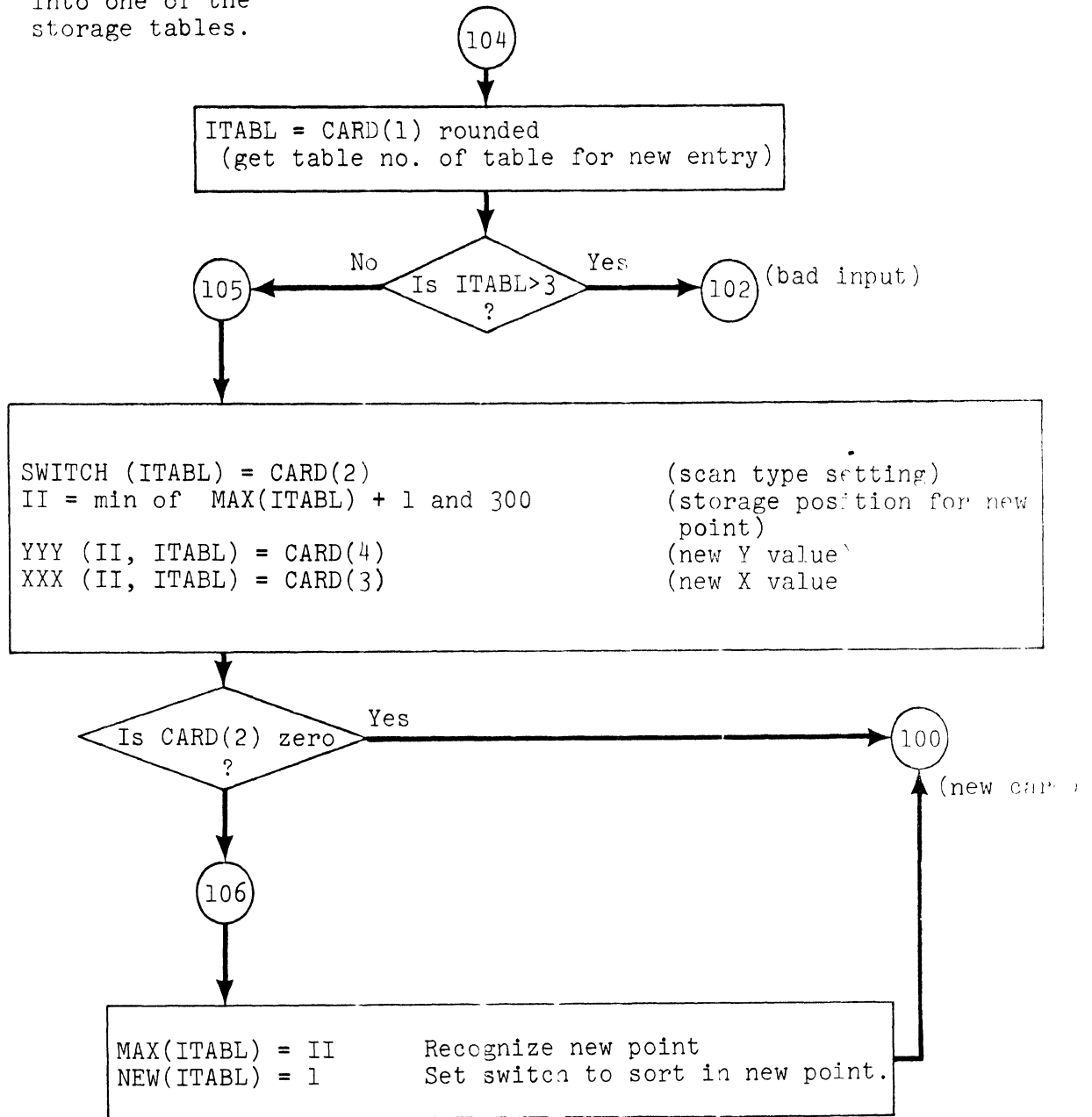
100



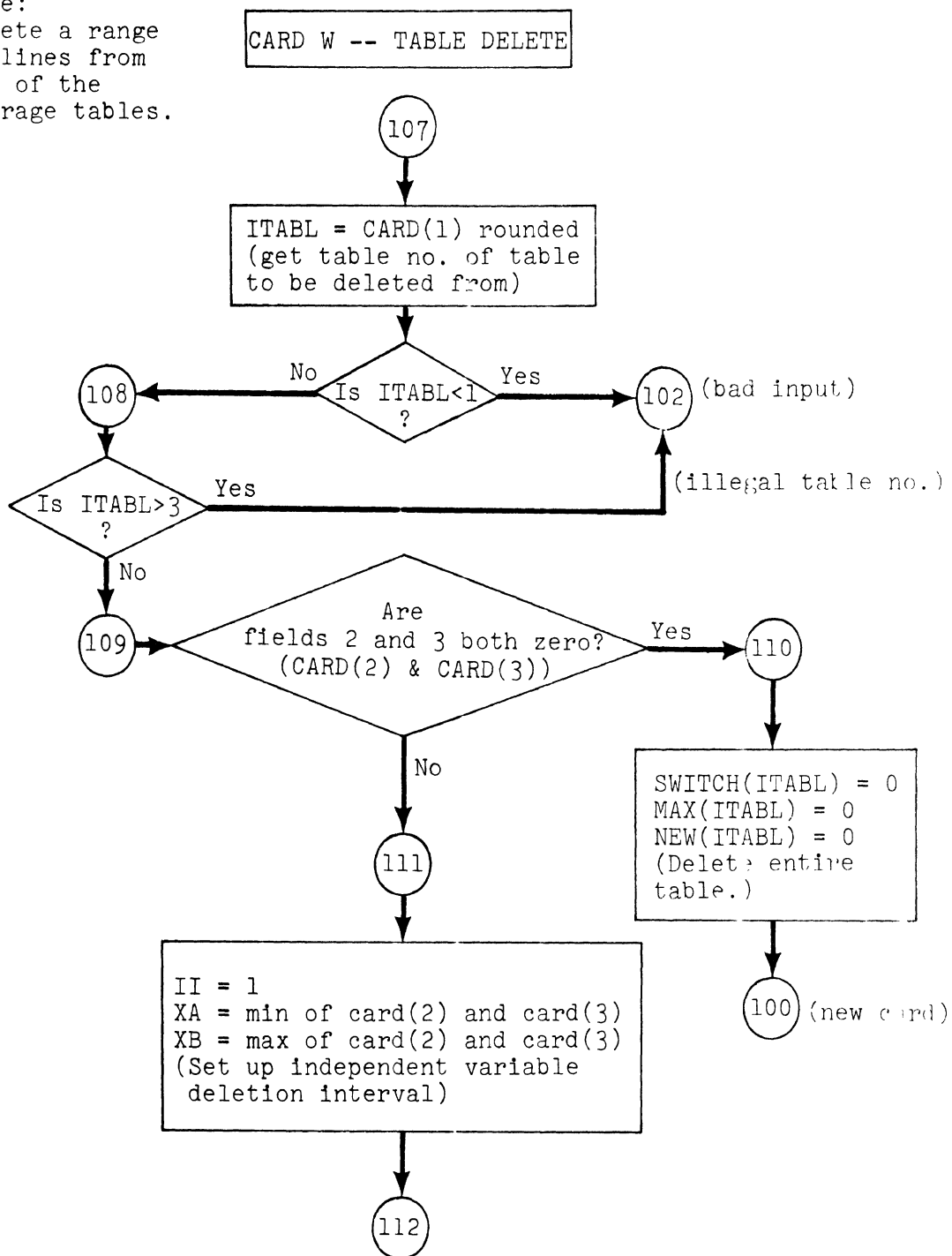
ID letter	i	Statement number	ID letter	i	Statement number
A	1	140	N	14	560
B	2	180	O	15	600
C	3	200	P	16	630
D	4	230	Q	17	660
E	5	260	R	18	700
F	6	300	S	19	730
G	7	330	T	20	760
H	8	360	U	21	800
I	9	400	V	22	104
J	10	430	W	23	107
K	11	460	X	24	850
L	12	500	Y	25	900
M	13	530	Z	26	1000

Note:  
Enter a new point  
into one of the  
storage tables.

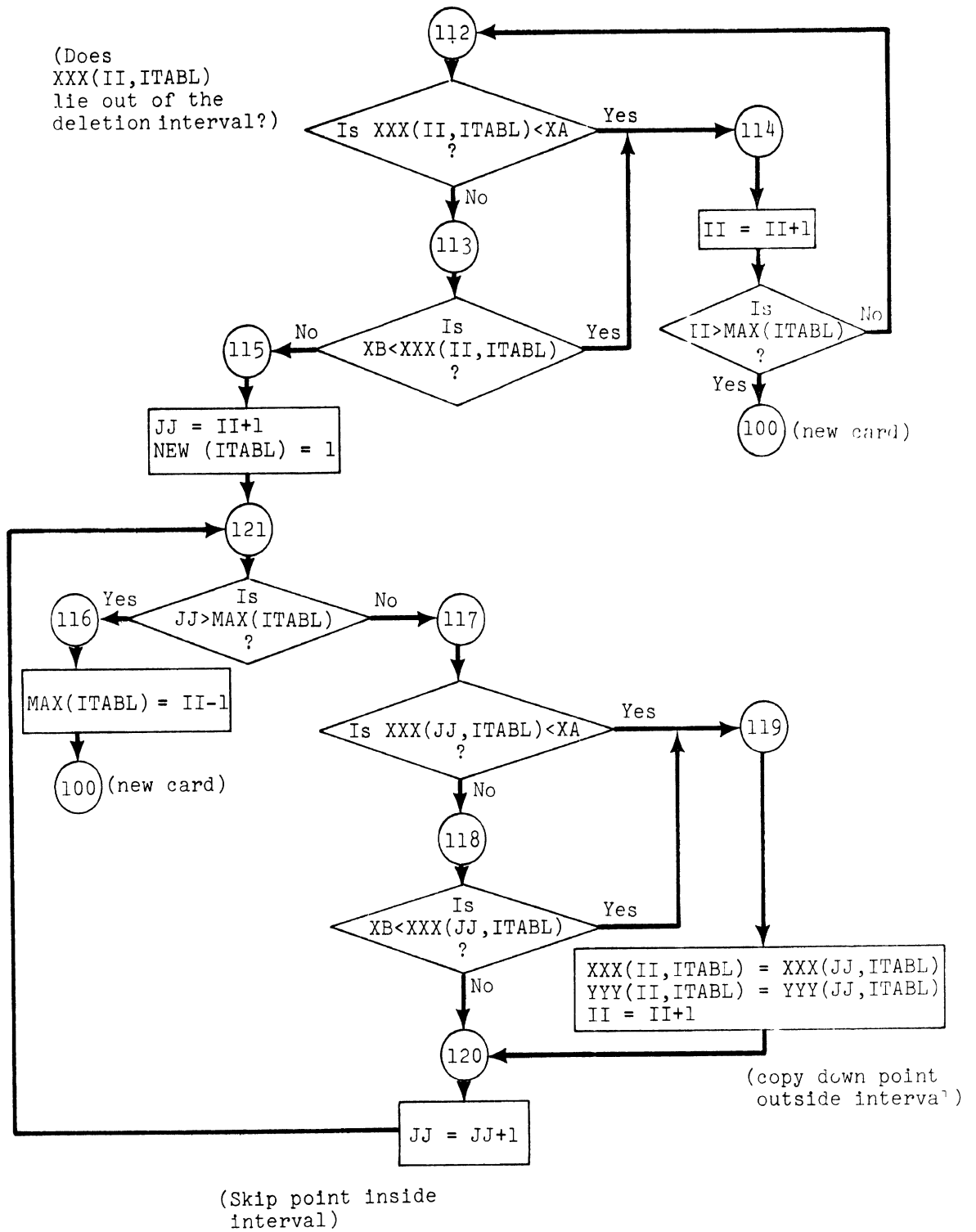
CARD V -- TABLE READ



Note:  
Delete a range  
of lines from  
one of the  
storage tables.



CARD W -- TABLE DELETE (cont)



CARD A

140

Copy CARD elements one through seven into CPRIME on through seven.

100 (new card)

---

CARD B

180

Copy CARD elements one through eight into EYE one through eight.

100 (new card)

---

CARD C

200

Copy CARD elements one through seven into BIGKI one through seven.

100

---

CARD D

230

Copy CARD elements one through eight into EL one through eight.

100

CARD E

260

Copy CARD elements one through eight into EM one through eight.

EMFVSX = EM(5)+EM(6) (sum of 5,6)  
EMTHSX = Sum of 3,4,5,6  
EMTWSX = Sum of 2,3,4,5,6

100

---

CARD F

300

Copy CARD elements one through eight into AR one through eight.

100

---

CARD G

330

Copy CARD elements one through seven into TPRIME one through seven.

100



CARD H

360

Copy CARD elements one through four into ALFAI elements one, five, six, and seven, converting them from degrees to radians.

Copy CARD elements five through eight into THATPW, THATPV, THATPX, and THATPS, respectively.

100

---

CARD I

400

Copy CARD elements one through seven into OMEGA elements one through seven, converting them from degrees to radians.

100

CARD J

430

Copy CARD elements one through seven into RPSI elements one through seven, converting them from degrees to radians.

100

---

CARD K

460

Copy CARD elements one through eight into RHO elements one through eight.

100

---

CARD L

500

Copy CARD elements one through eight into THETAZ elements one through eight, converting them from degrees to radians. Simultaneously compute the sine and cosine for each element of THETAZ and store them in the corresponding elements of STHETAZ and CTHETAZ respectively.

100

CARD M

530

Copy CARD elements one, two, four, five, and six to FSPRMZ, RH, WZERO, RHOPTZ, and RHOPFZ respectively.

Convert CARD(7) from degrees to radians and put it in GAMZER.

Put the rounded absolute value of CARD(8) into LCONTL as an integer.

100

---

CARD N

560

Copy CARD elements one through eight into CS, S, RPSI(8), FMUS, BETA elements one through three, and ZZERO respectively.

100

CARD O

600

Copy CARD elements one through eight into ELPTEN, ELTWTY, ELTHRY, H, FEPTEN converting from degrees to radians, DESTEP, RZ, and SZ respectively.

Set DELTAT = DESTEP

100

CARD P

630

Put the rounded value of CARD(1) into M as an integer.

Is M in the range one to three?

no

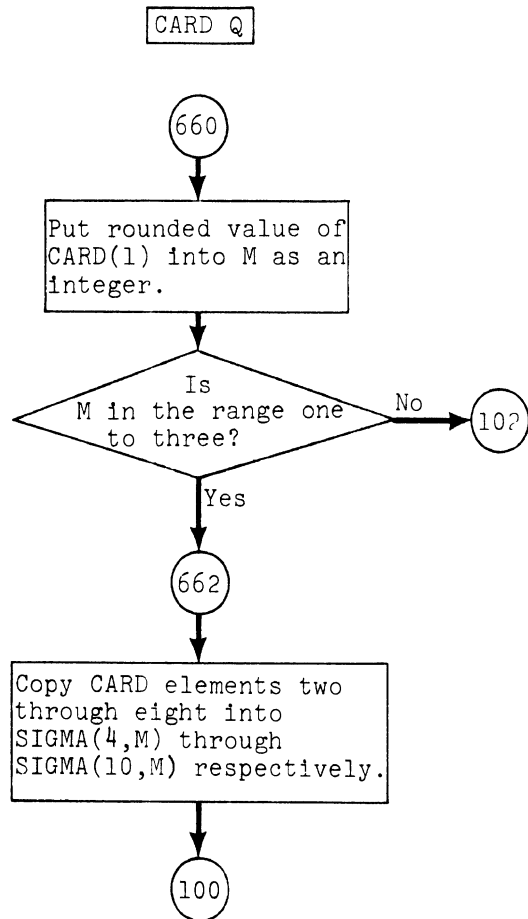
102

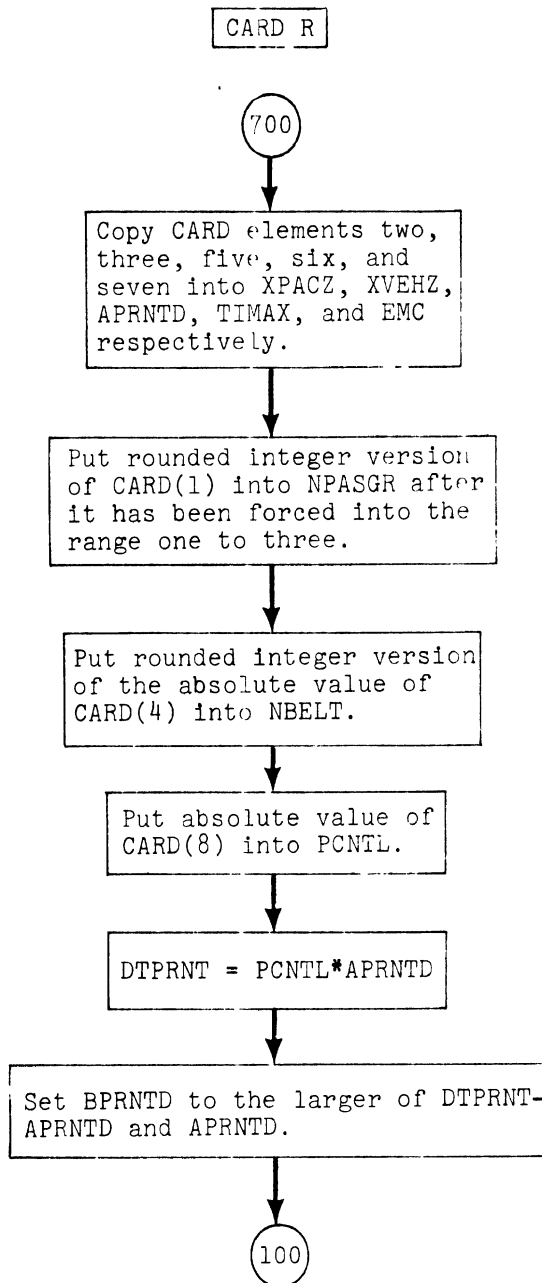
yes

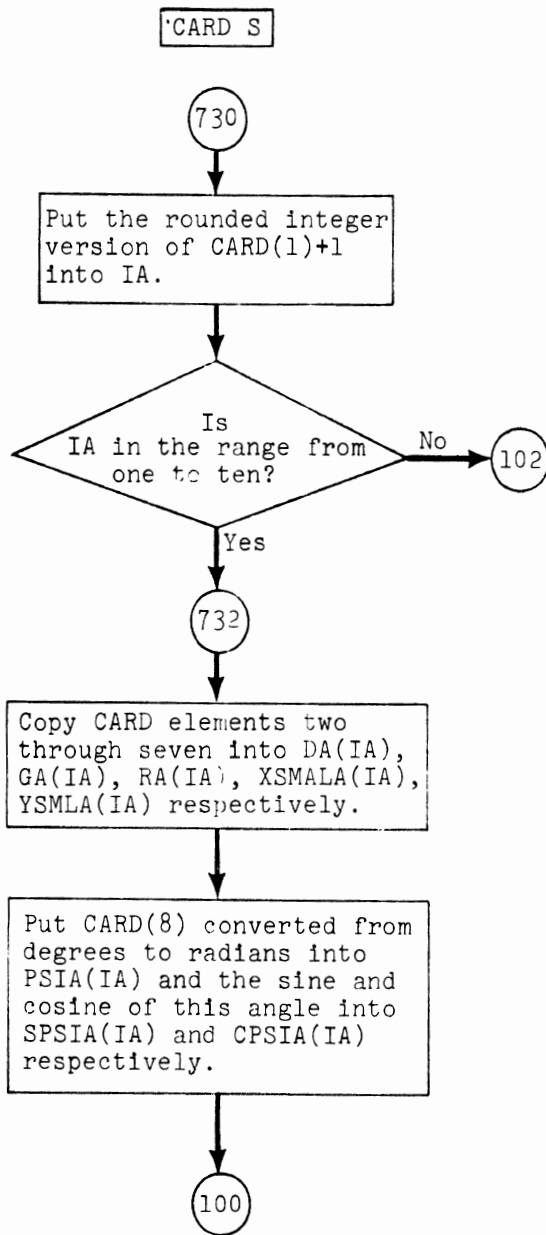
632

Copy CARD elements two through eight into G(M), R(M), PHIZ(M), DELTA(M), SIGMA(1,M), SIGMA(2,M), SIGMA(3,M) respectively, converting CARD(4) from degrees to radians before storing it in PHIZ(M).

100







CARD T

760

Put the rounded integer version of  $CARD(1)+1$  into IA.

Is IA in the range from one to ten?

No

102

Yes

762

Copy CARD elements two through eight into  $FMUA(IA)$  and  $SIGMAA(I,IA)$  through  $SIGMAA(6,IA)$  respectively.

100

CARD U

800

Put the rounded integer version of  $CARD(1)+1$  into IA.

Is IA in the range from one to ten?

No

102

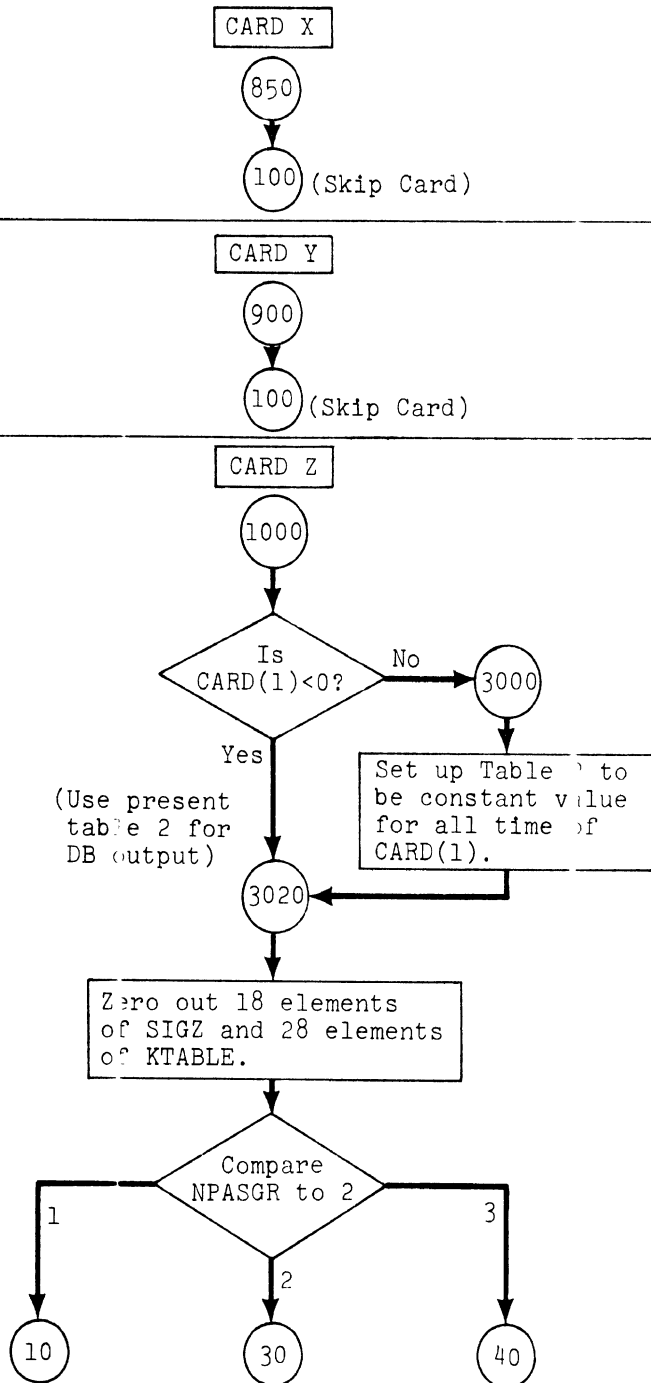
Yes

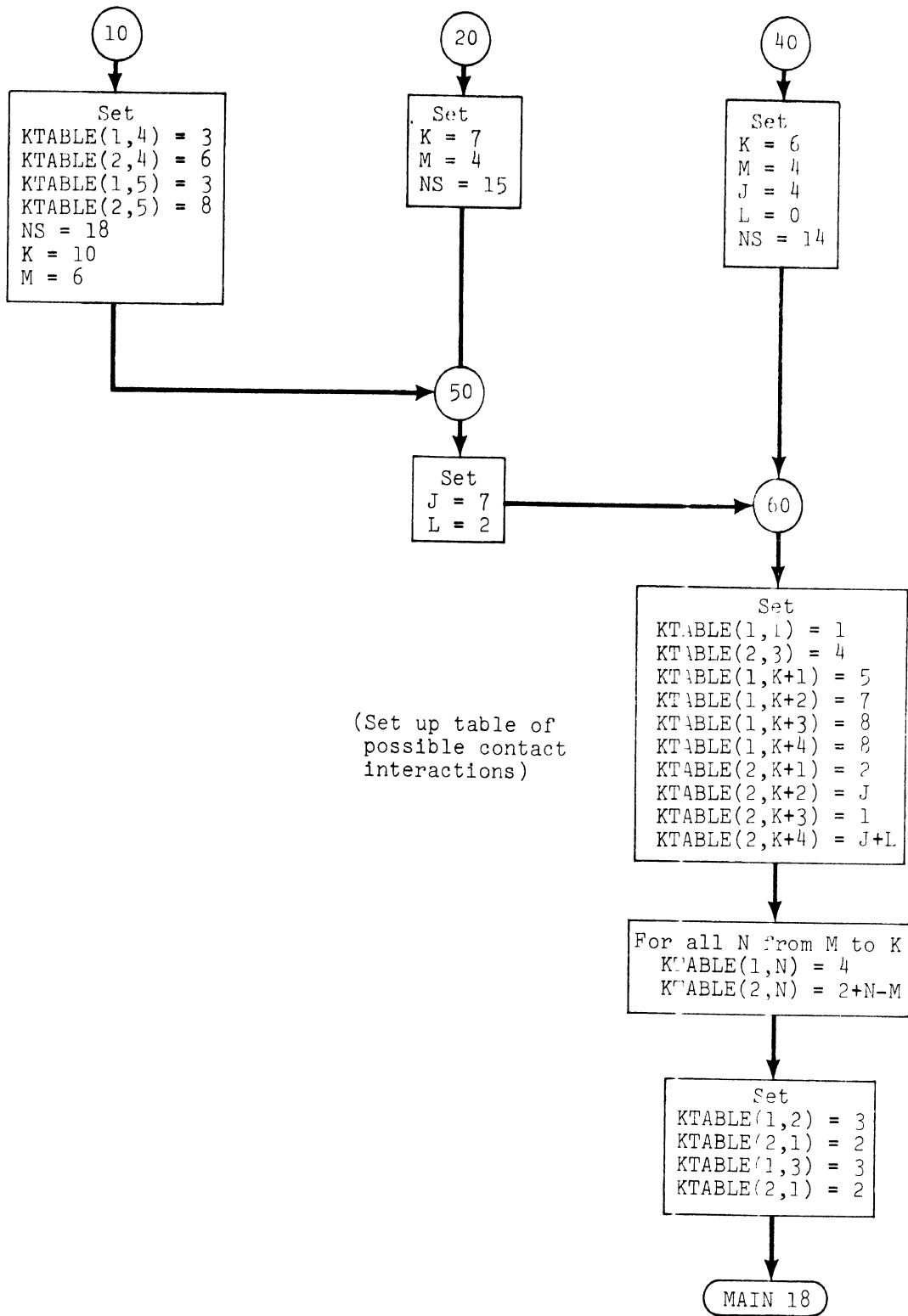
802

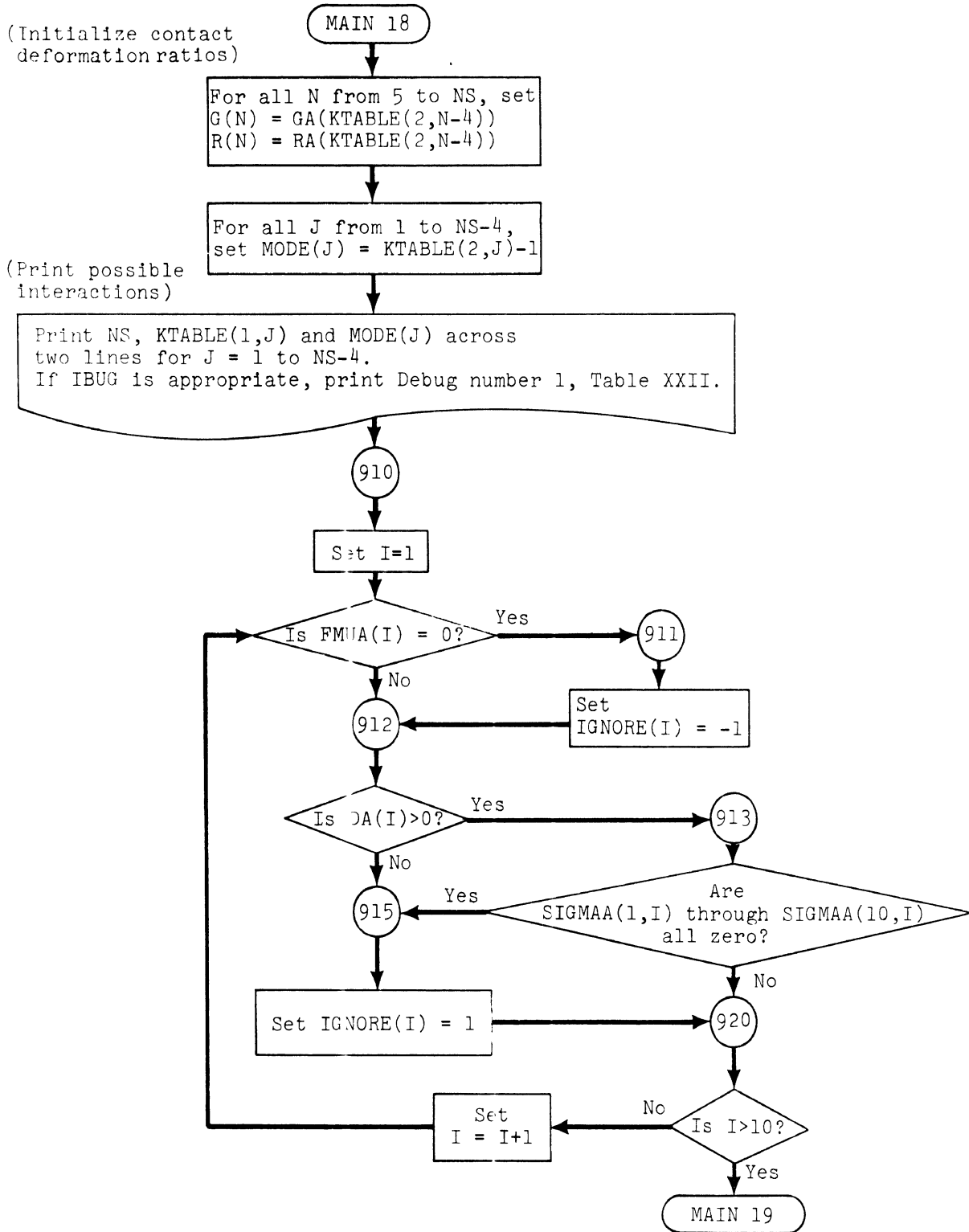
Copy CARD elements two through five into  $SIGMAA(7,IA)$  through  $SIGMAA(10,IA)$  respectively.

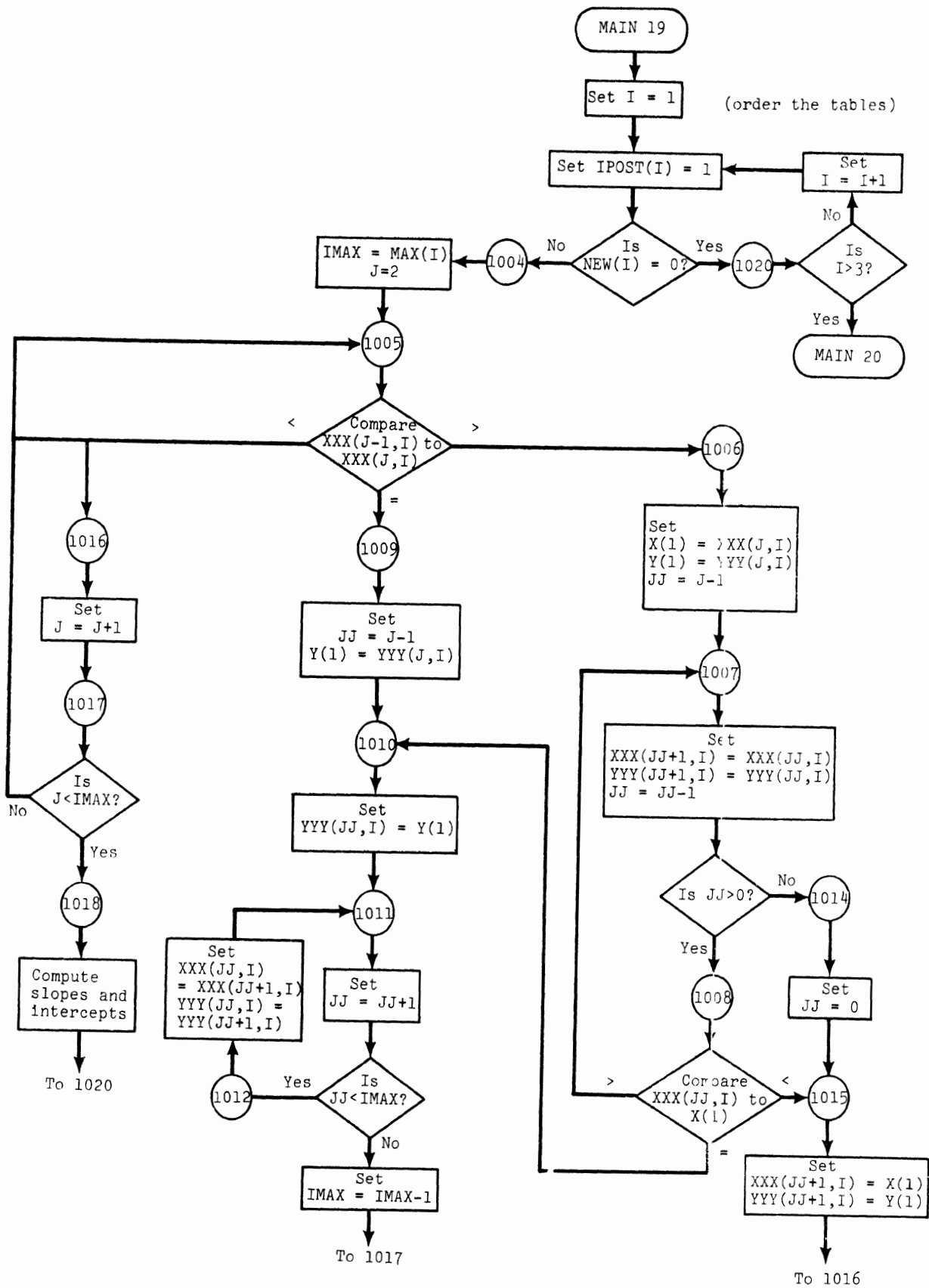
100

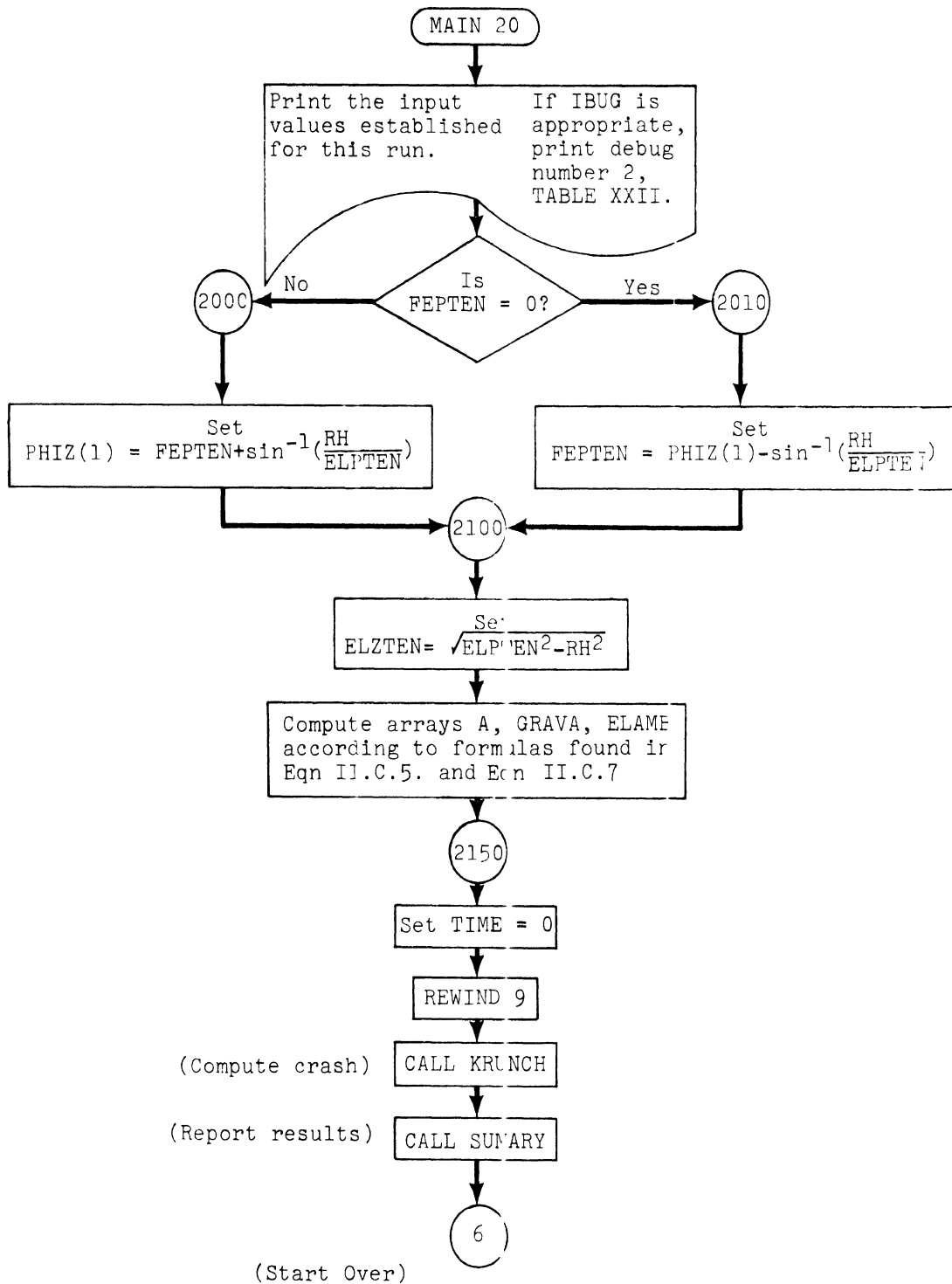






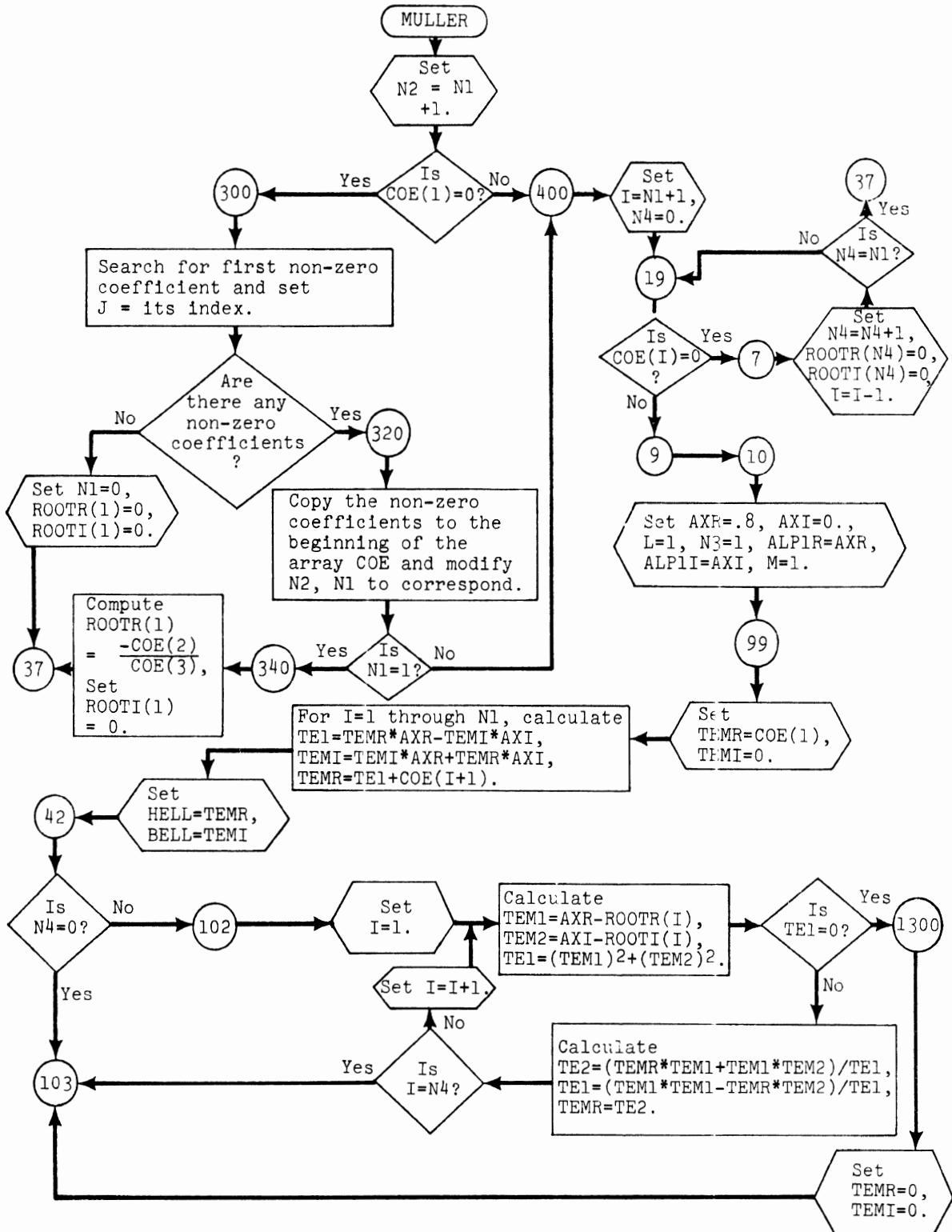


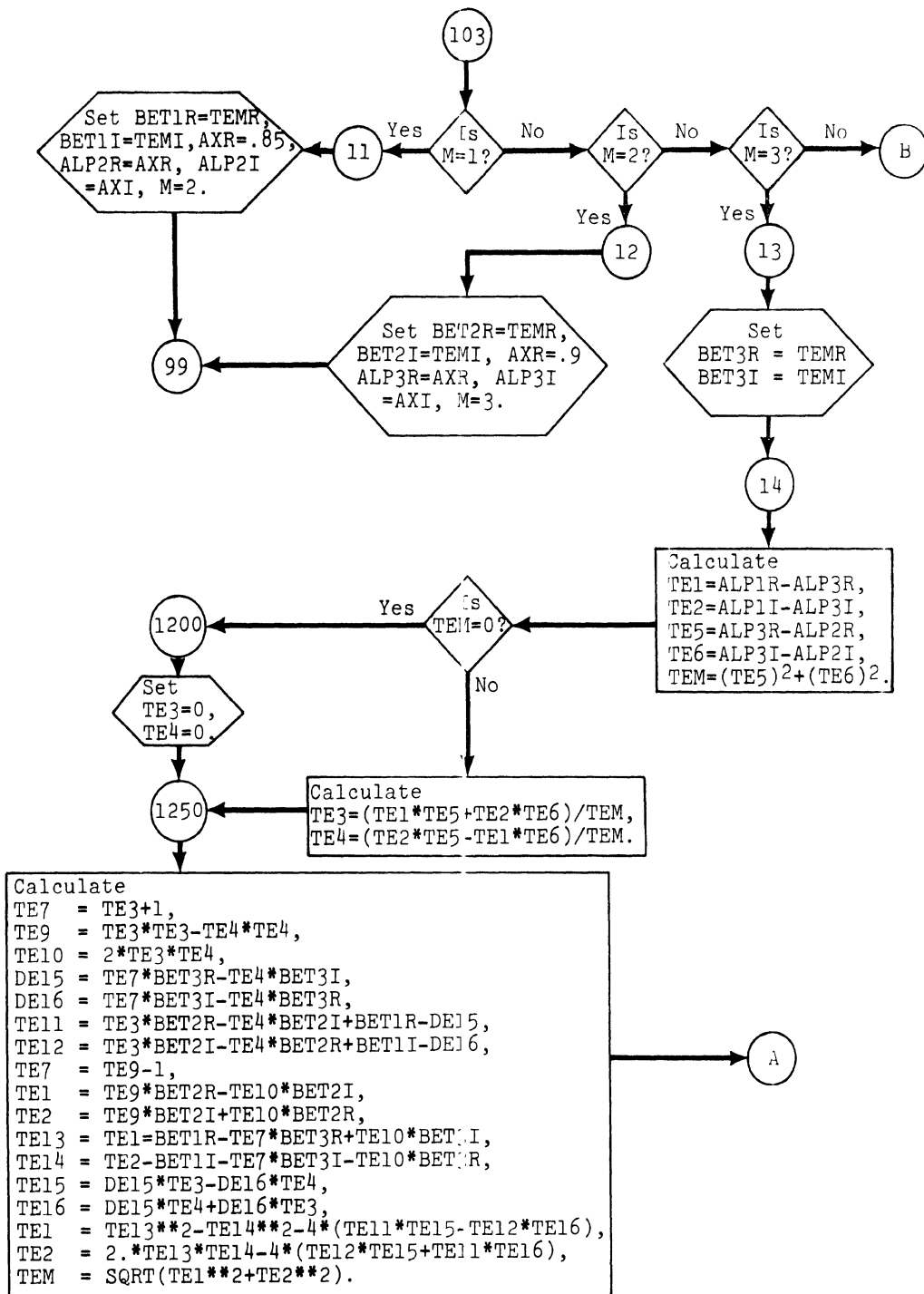


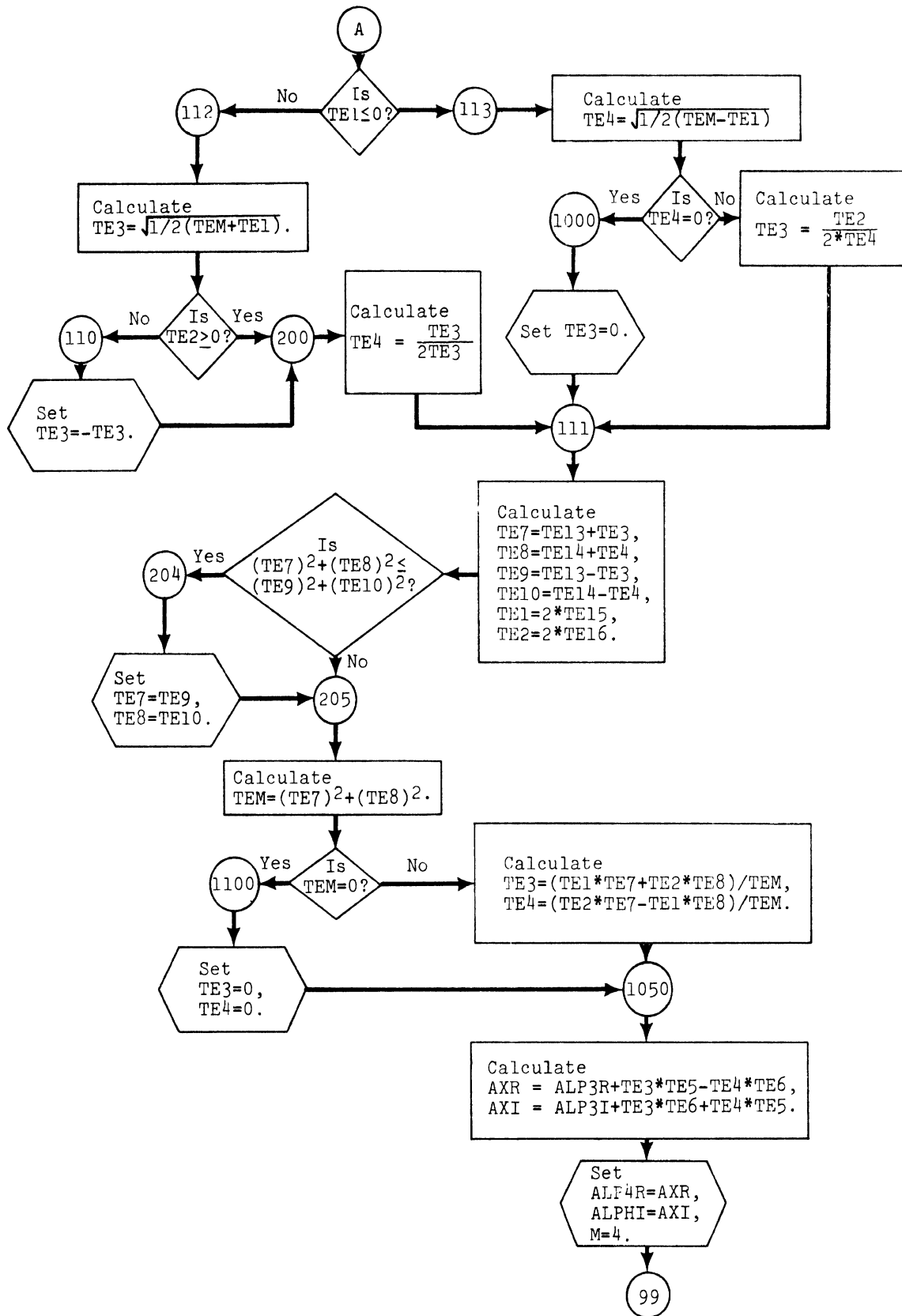


Subroutine MULLER solves a real polynomial for its complex roots.

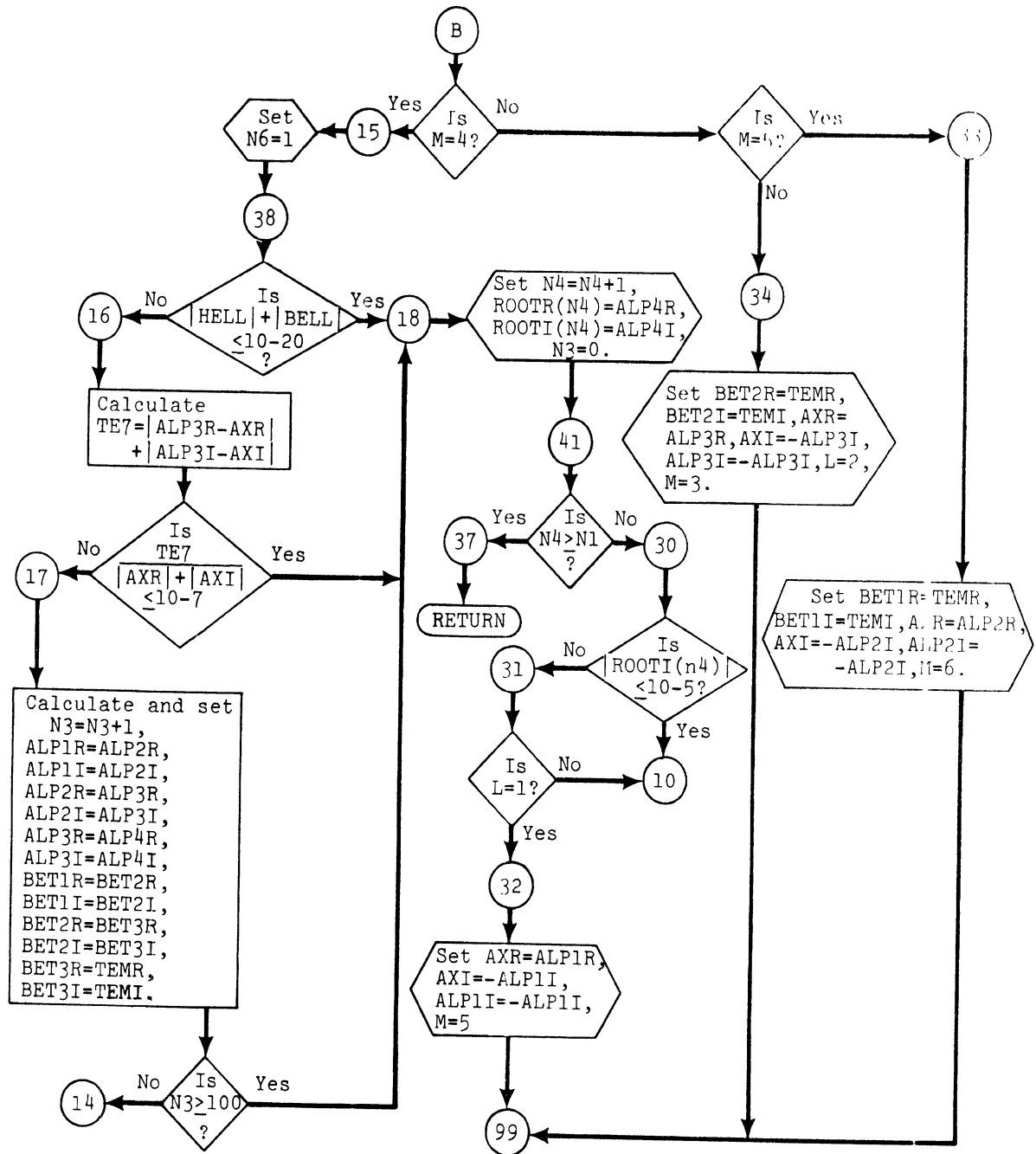
Its arguments are: COE(10), which is the array of coefficients of the polynomial in descending order; N1, which is the order of the polynomial; ROOTR(15) and ROOTI(15), which are respectively the real and imaginary parts of the roots.





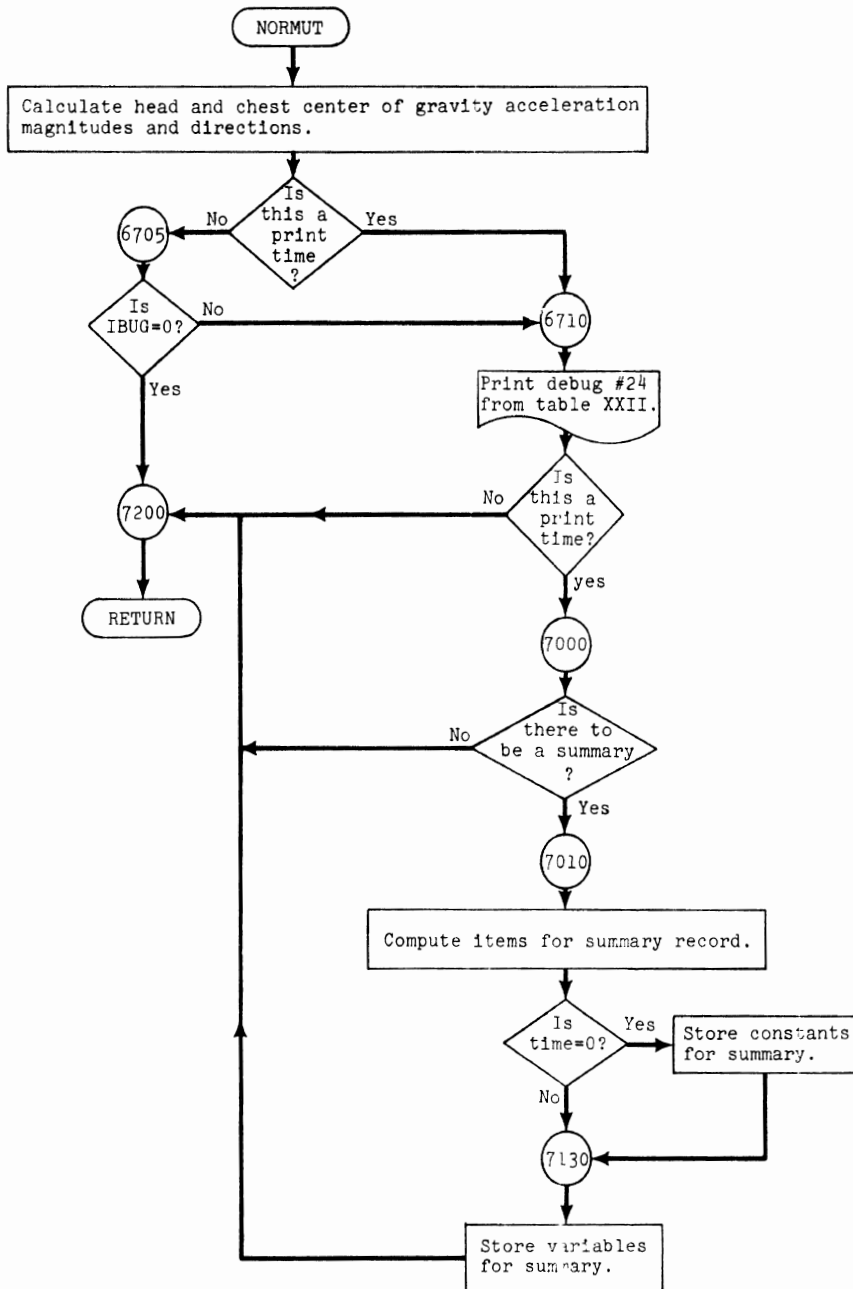




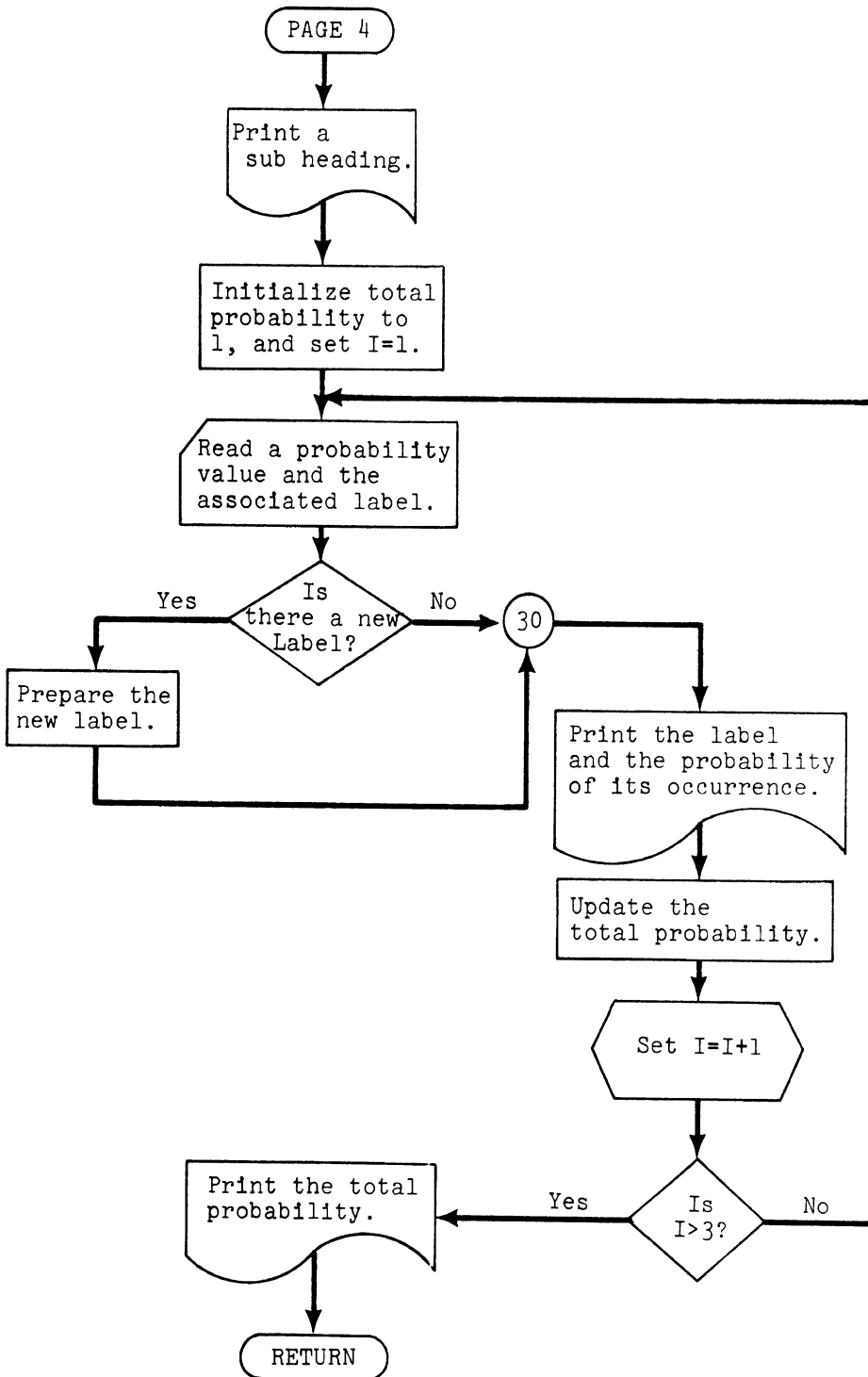


Subroutine NORMUT carries out the following steps:

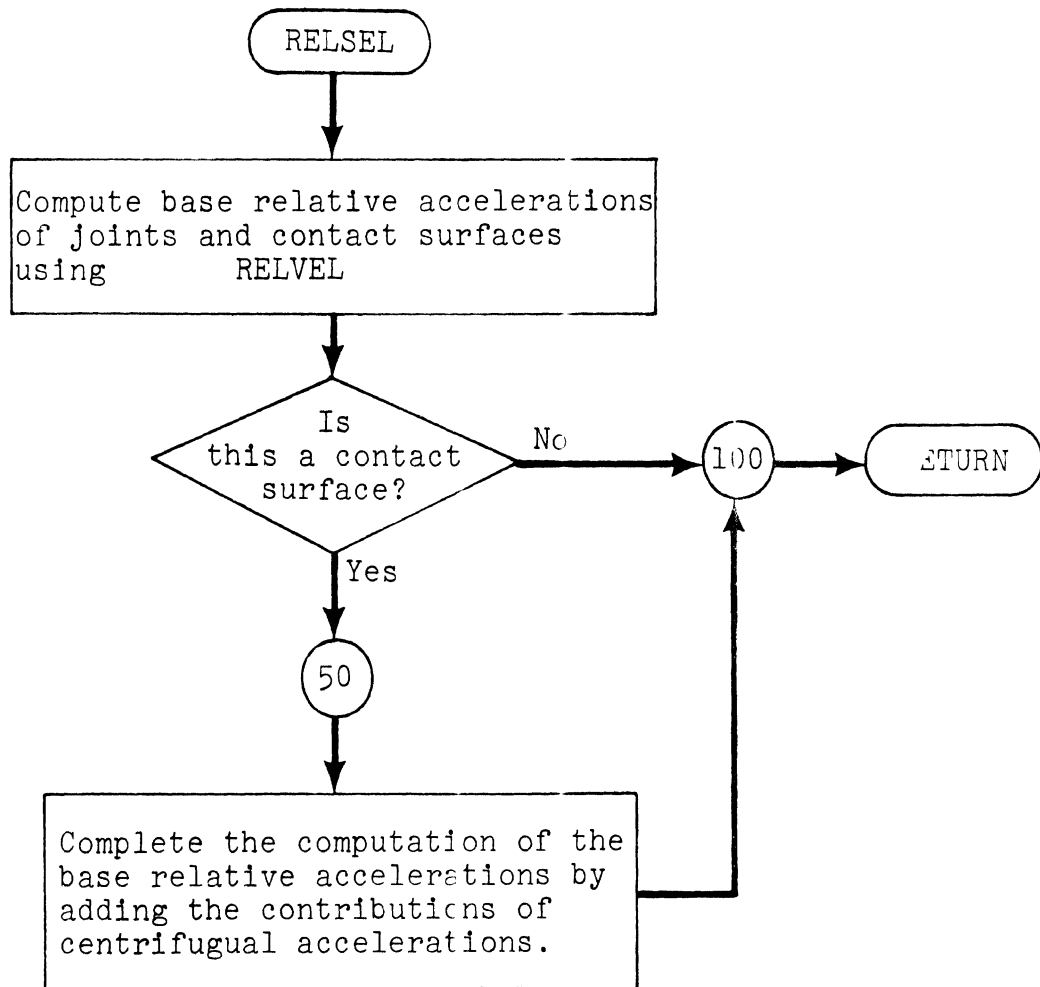
1. Computes head and chest resultant acceleration vectors (magnitudes and angles) at their centers of gravity.
2. Writes normal output on unit 6.
3. Writes data for SUMMARY on unit 9.



Subroutine PAGE 4 computes probability data and prints it out after reading three input cards for the necessary information.

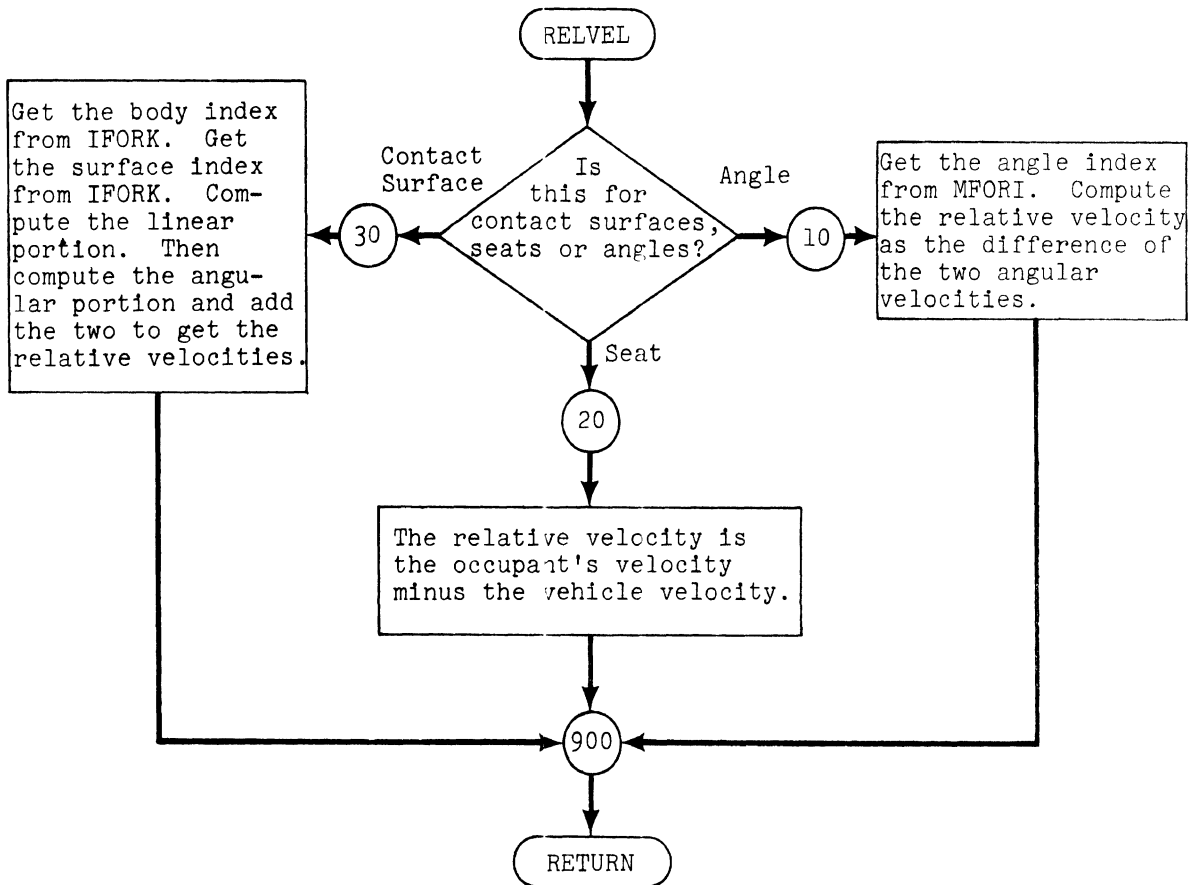


Subroutine RELSEL determines base relative acceleration of joints and contact surfaces subject to jitter via RELVEL and adds contributions of centrifugal accelerations for linear jitter modes.



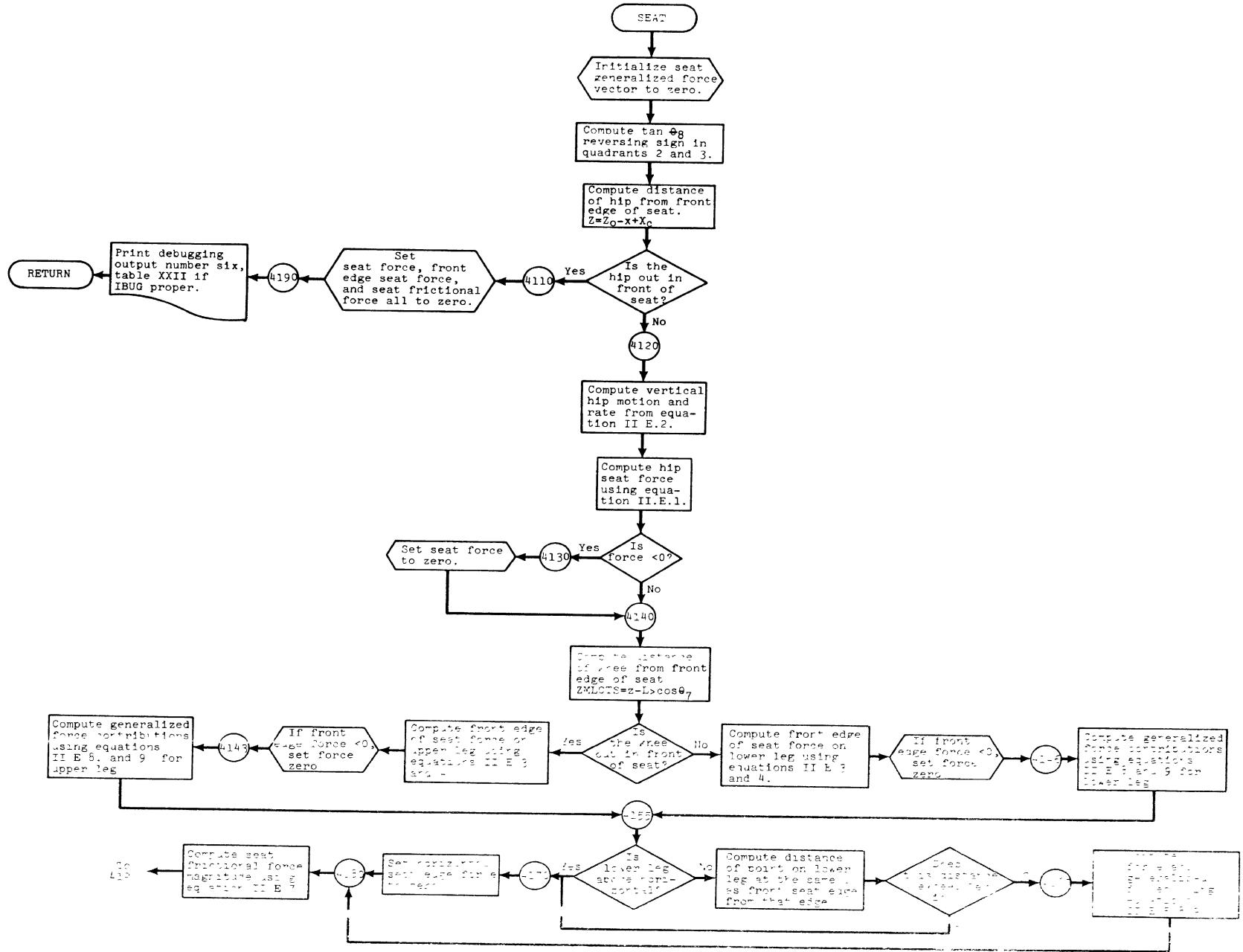
Subroutine RELVEL

Computes relative velocities between joints or contact surfaces and body segments which are subject to jitter.



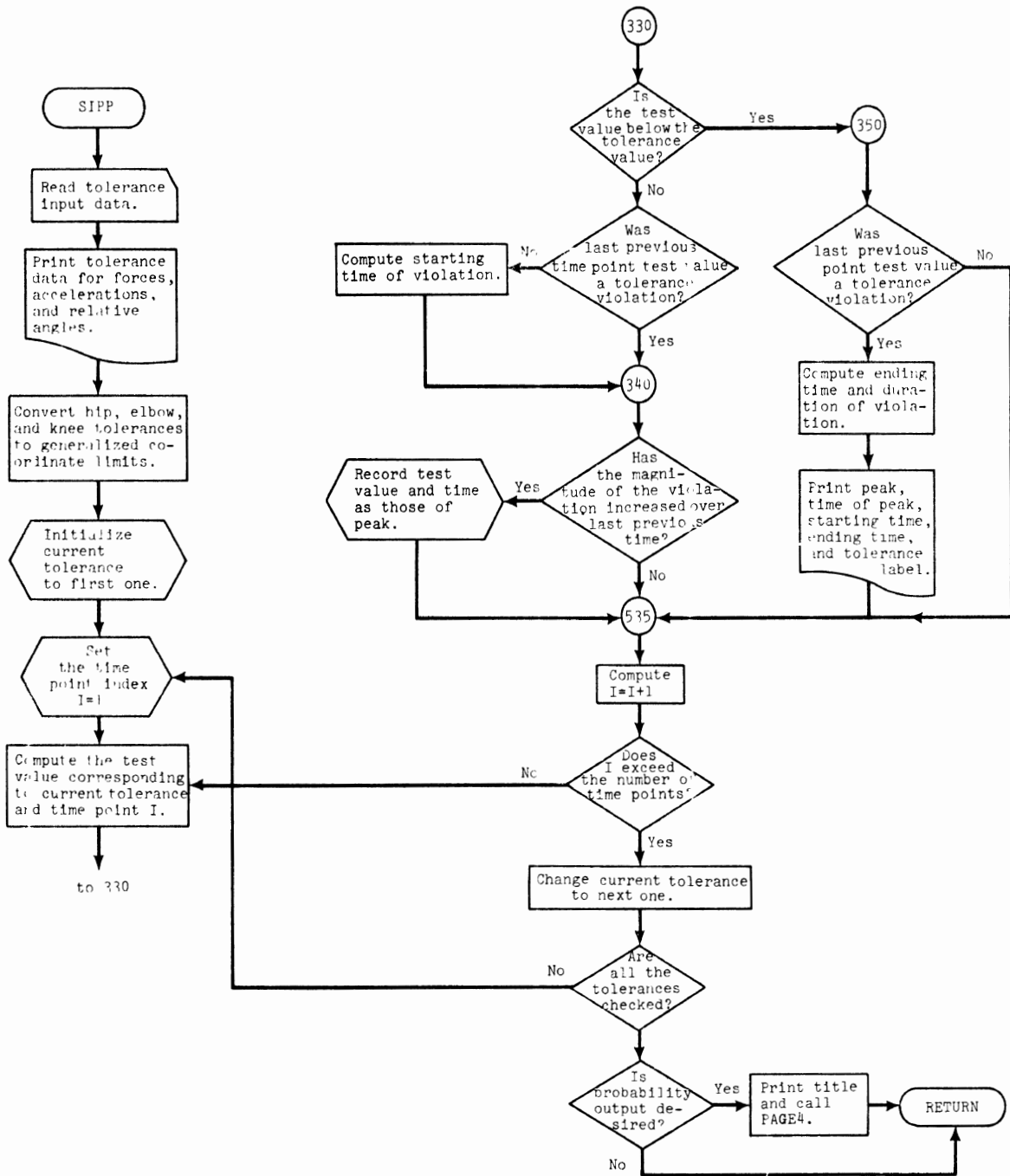
Subroutine SEAT carries out the following steps:

1. Computes vertical hip seat force.
2. Computes vertical seat front force and applies it to proper leg segment.  
Computes horizontal force on lower leg.
3. Computes magnitude of seat friction force.
4. Computes total continuous generalized seat force vector.



Subroutine SIPP carries out the following steps:

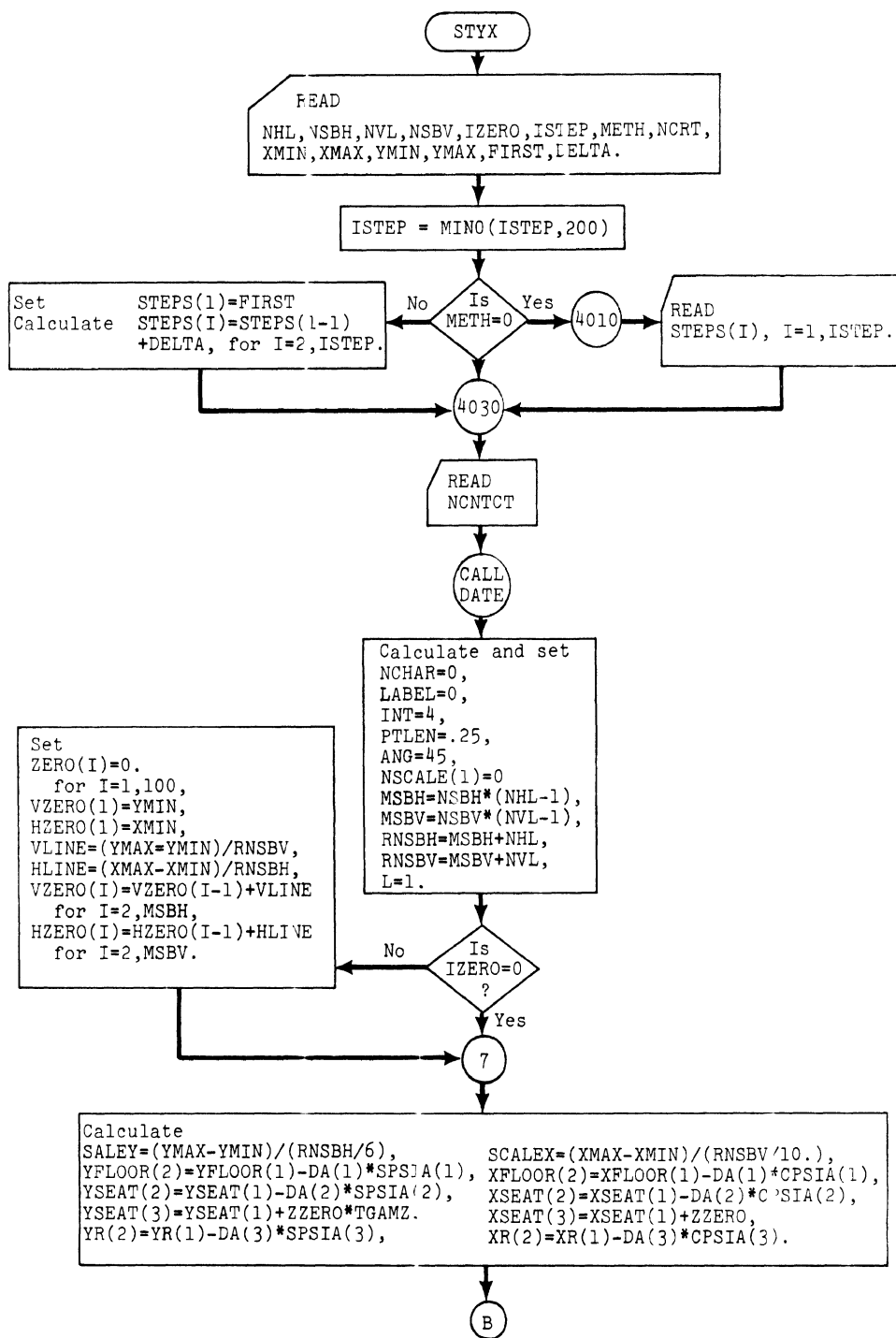
1. Reads cards to reset injury tolerance levels (if any) and prints values, etc.
2. Scans certain variables to see if any exceed their tolerance level and prints out values, times, and durations above tolerance for those that do.
3. Calls PAGE 4 for probability output if desired.

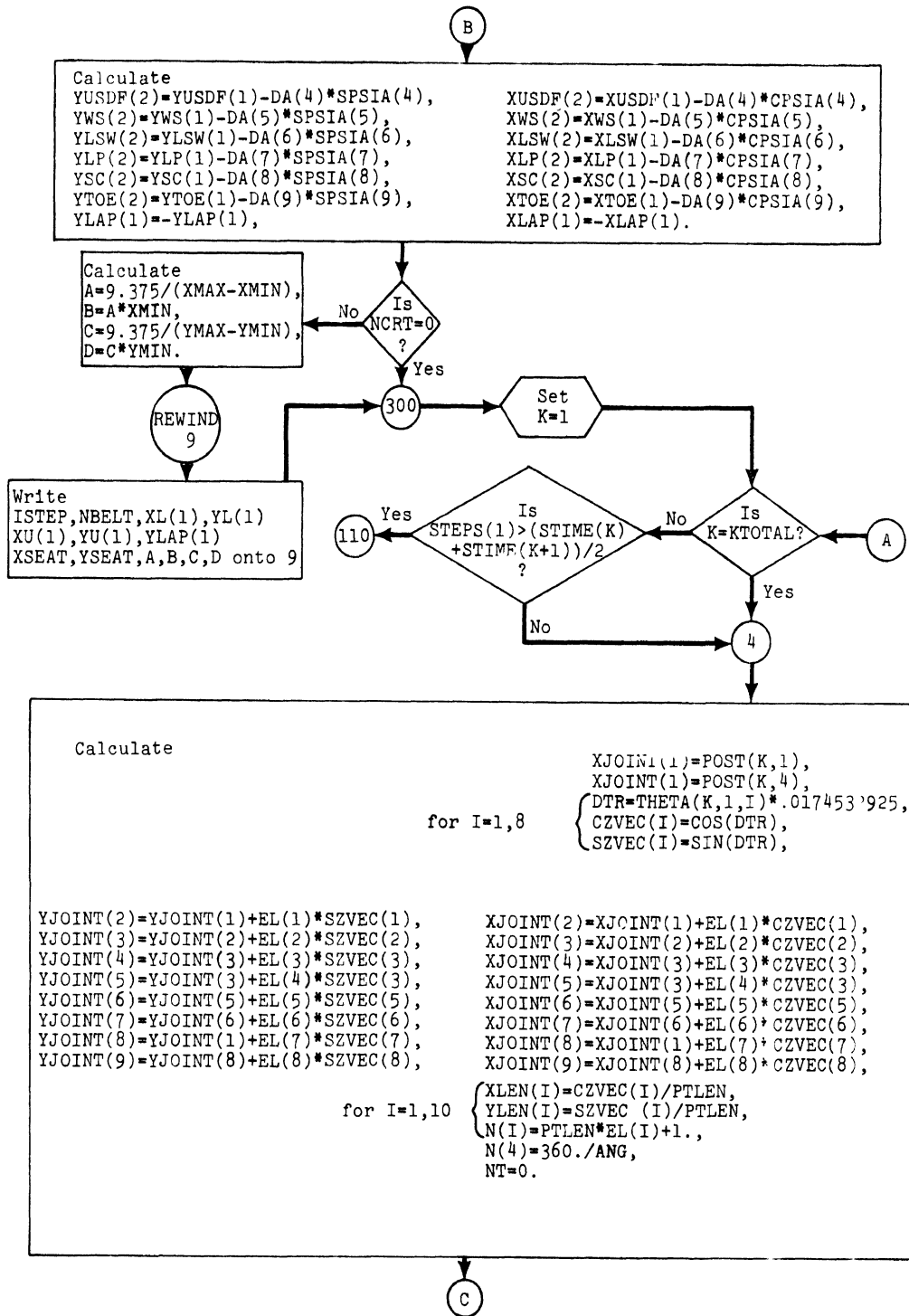


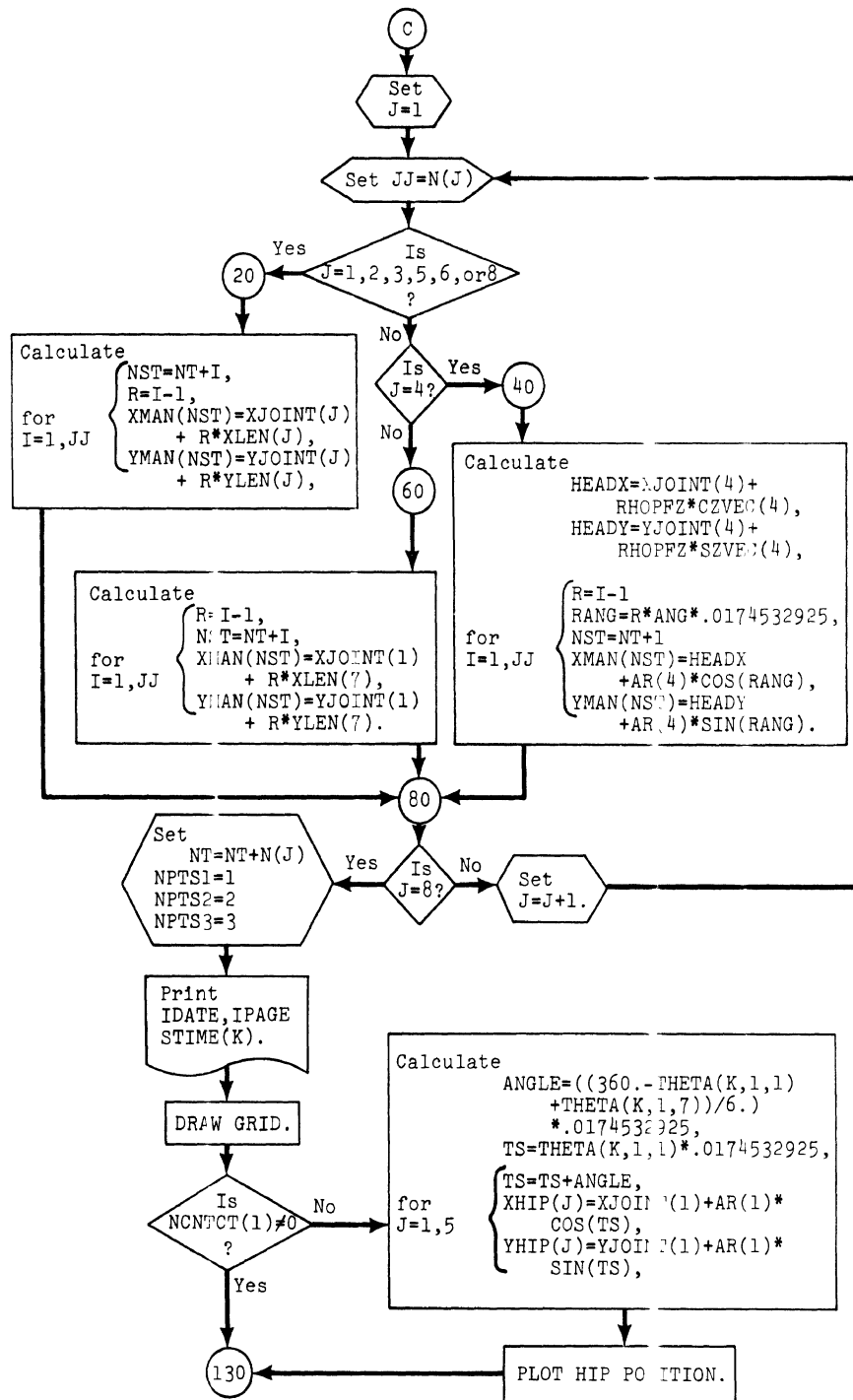


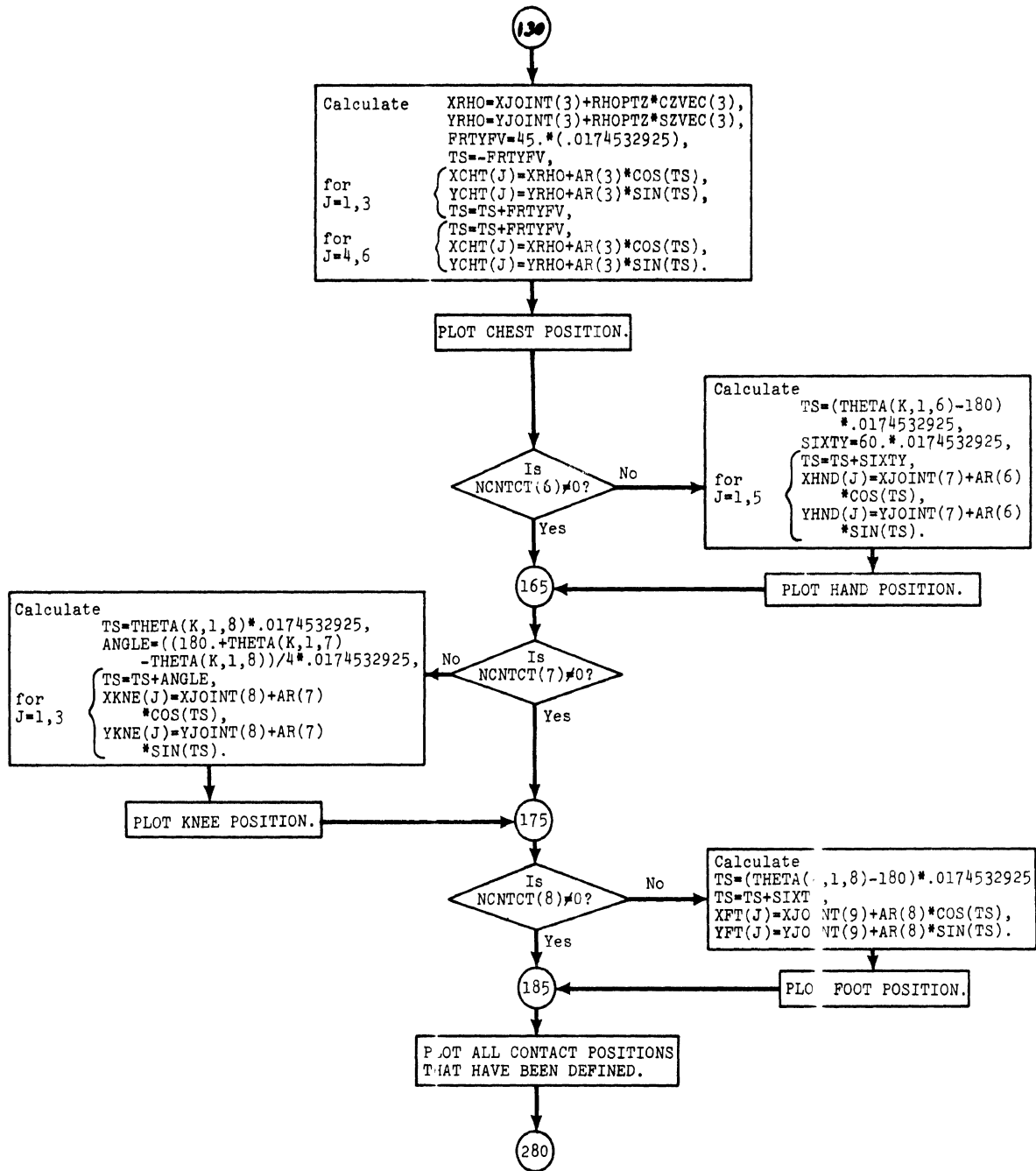
Subroutine STYX carries out the following steps:

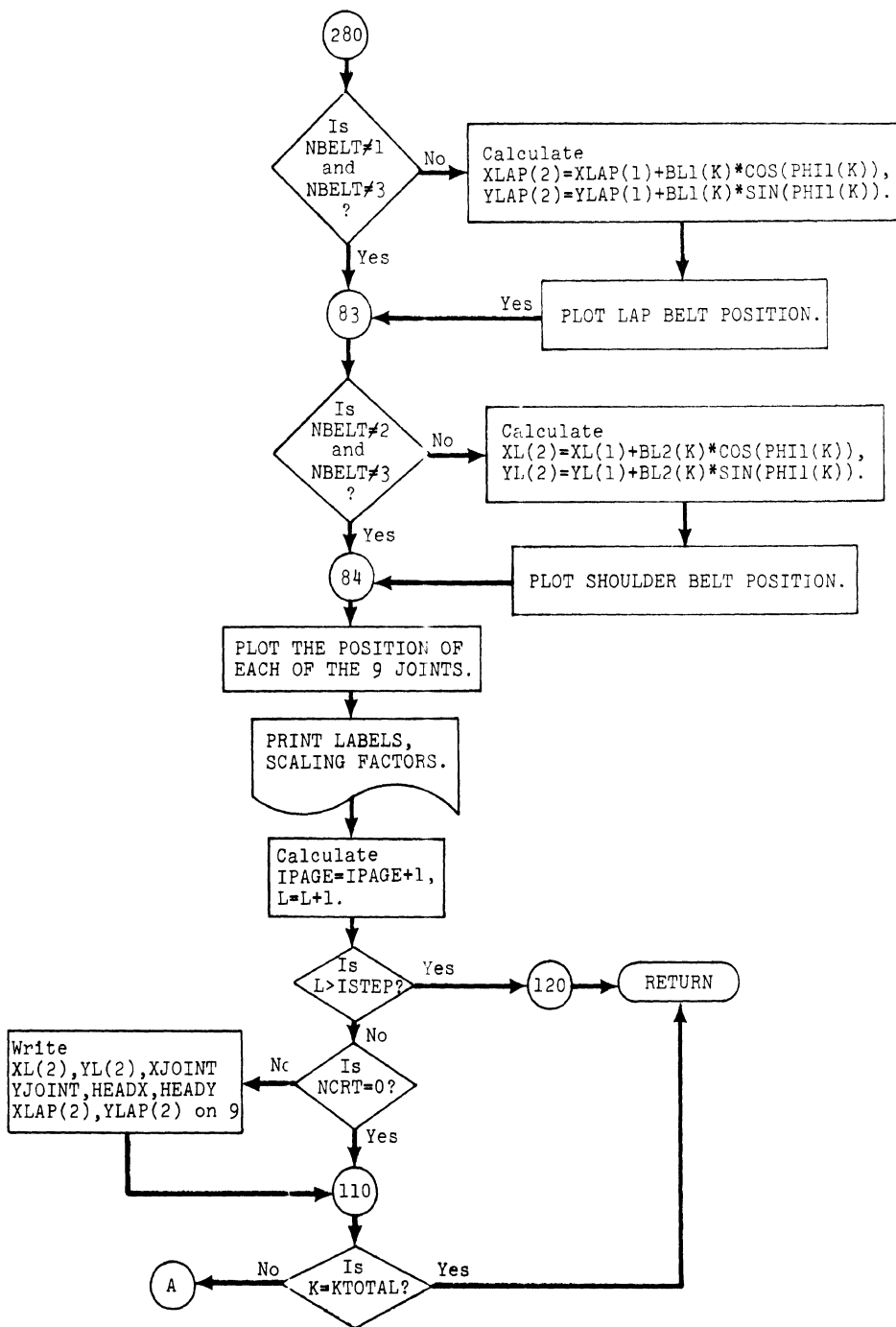
1. Reads its input cards to determine size and content of output stick figures.
2. Computes positions, etc., sets up plot images, and prints.





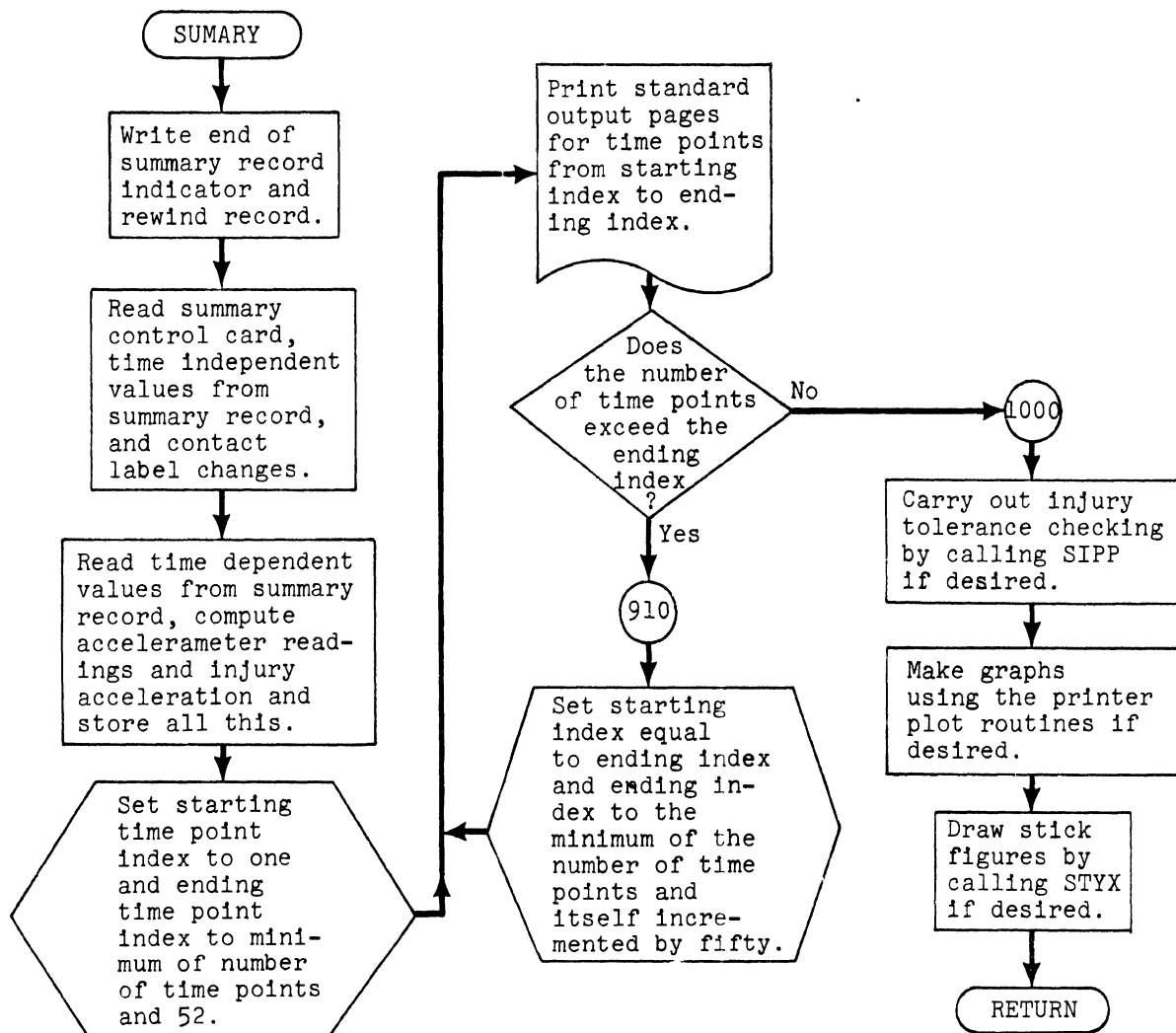






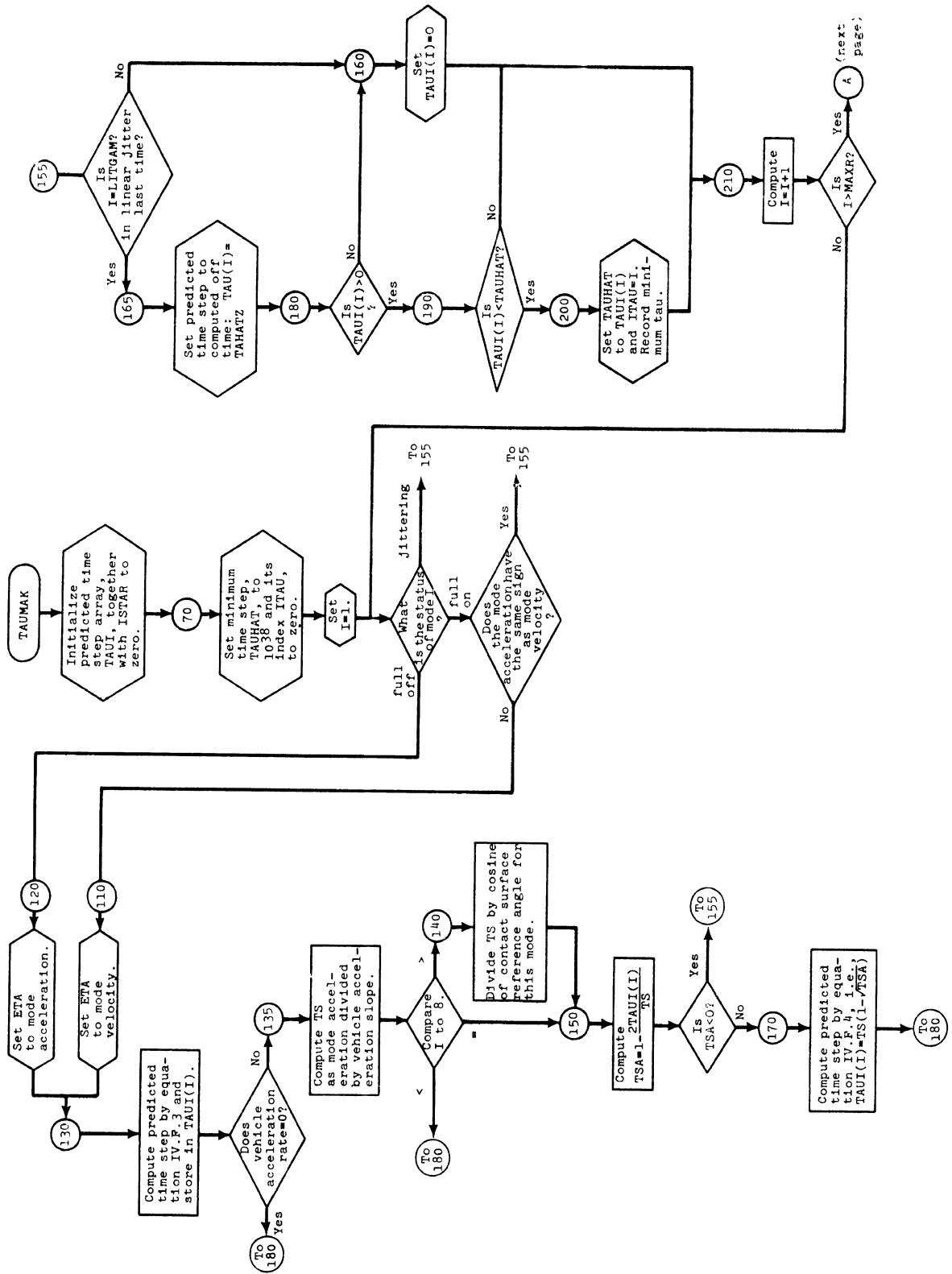
Subroutine SUMMARY carries out the following steps:

1. Writes end-of-run indicator on summary record and rewinds it.
2. Reads one instruction data card.
3. Alters labeling of contact surfaces.
4. Reads storage summary record, sets up page images, and prints.
5. Calls SIPP to produce injury criteria if desired.
6. Uses University of Michigan plot subroutines and produces graphical output if desired.
7. Calls STYX to produce stick figures at selected times if desired.

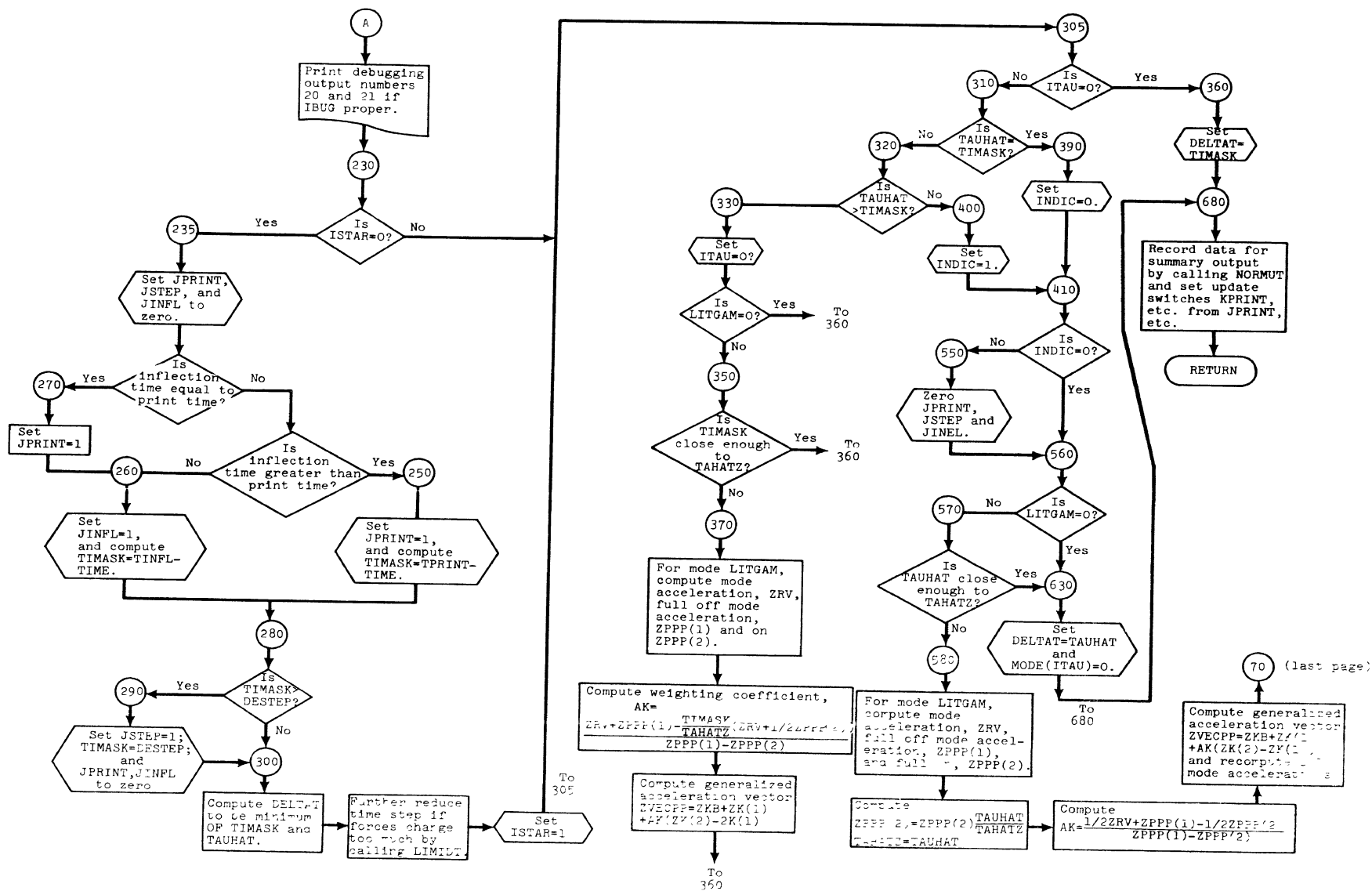


Subroutine TAUMAK carries out the following steps:

1. Computes time intervals in a manner to reduce the probability of instability.
2. Utilizes LIMIDT to check time interval for force change size.
3. Modifies effective acceleration vector to suit time interval.
4. Calls NORMUT for normal printout storage.
5. Updates switches.



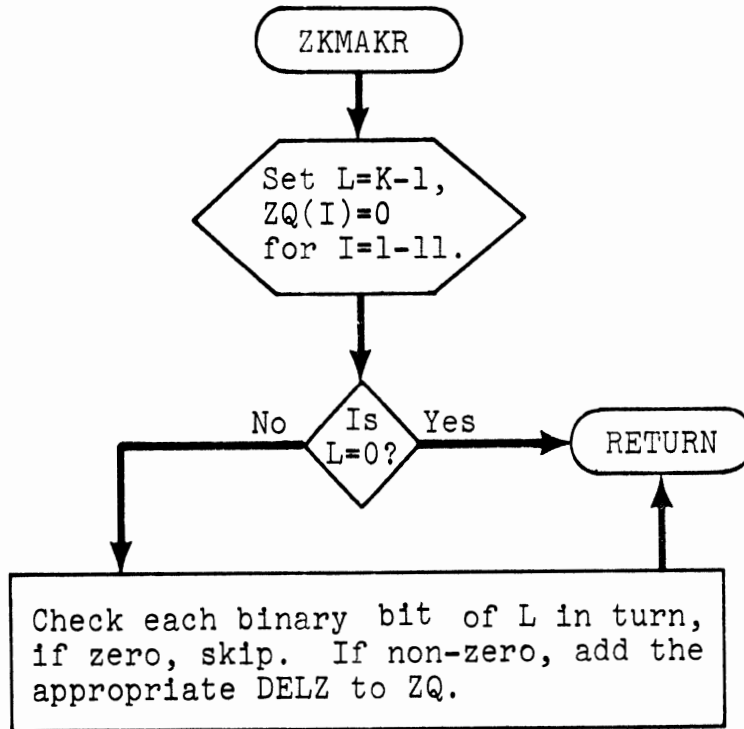




Subroutine ZKMAKR

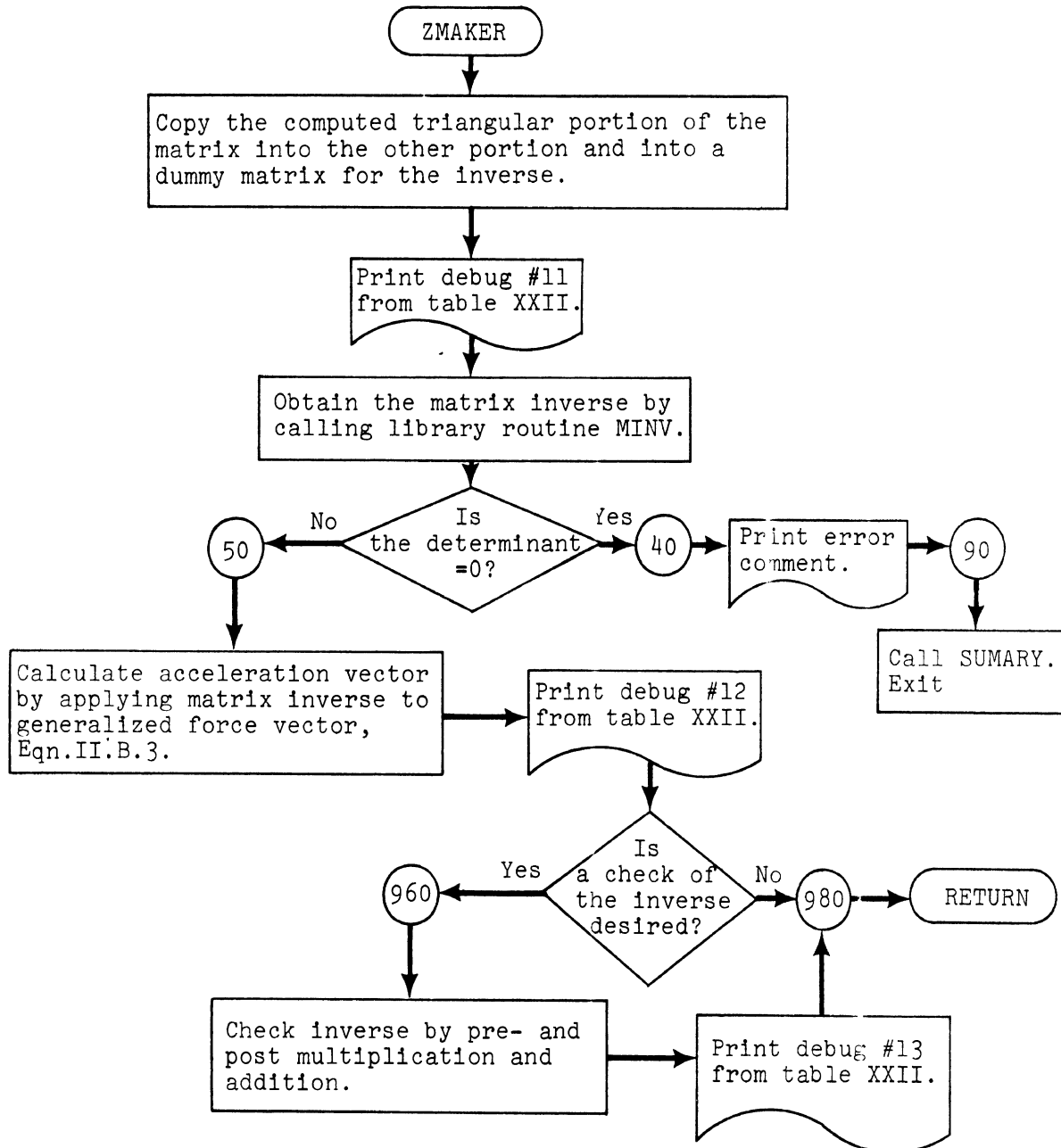
Sets up the components of an array of acceleration vectors needed in JITTER.

Its arguments are: K which is the index of the appropriate combination of jitter modes; ZQ (11) which is the vector containing the resultant accelerations due to this combination.



Subroutine ZMAKER carries out the following steps:

1. Inverts matrix by calling on SSP routine.
2. Computes acceleration vector by applying inverse matrix to generalized force vector.
3. Checks matrix inversion by pre- and post-multiplication if desired.



## H. SYMBOL DICTIONARY

The dictionary which follows is arranged in alphabetical order by the FORTRAN name of each variable or array used in the program. If the same FORTRAN name is used in different subroutines with different meanings, the meanings are listed on separate lines for each of the uses. The second column is the FORTRAN dimension which is specified for arrays. The third column is the analytical symbol which corresponds to this FORTRAN name and is supplied if such a correspondence exists. The fourth column gives the physical units for those quantities which have them. The numbers shown are subscript ranges if units are not the same for all elements of arrays. The last column is a short definition of the quantity.

As an appendix to the symbol dictionary, there is an alphabetical list of analytical symbols together with the corresponding FORTRAN names of each quantity. This list indicates the name which can be used to find the definition.

Symbol Dictionary (page 1)

FORTRAN Name	Dimension	Symbol	Units	Definition
A	-	-	-	horizontal CRT scaling factor (vestigial)
A	17	a <sub>1</sub>	1-8, lb sec <sup>2</sup> 9, lb sec <sup>2</sup> /in. 10-17, lb in. sec <sup>2</sup>	constants used in building matrix, gravity, and centrifugal force vectors
A	36,3	-	-	probability label storage
AA	6	-	-	current probability label
AA	10,10	m	1-8,1-8, lb sec <sup>2</sup> in. 9-10,9-10, lb sec <sup>2</sup> /in. rest, lb sec <sup>2</sup>	the mass matrix
AACCA	-	-	in./sec <sup>3</sup>	third order vehicle position integration coefficient
ACH	-	-	g-units	horizontal acceleration of upper spinal joint
ACHEST	-	-	in./sec <sup>2</sup>	resultant acceleration of chest center of gravity
ACHEST	200	-	in./sec <sup>2</sup>	resultant acceleration of chest accelerometer
ACOM	5,11	-	-	contact surface label storage
AEL	14	-	lb in./sec <sup>2</sup>	constants used in building matrix
AH	-	-	g-units	horizontal acceleration of neck joint
AHEAD	-	-	in./sec <sup>2</sup>	resultant acceleration of head center of gravity

Symbol Dictionary (page 2)

FORTRAN Name	Dimension	Symbol	Units	Definition
AHEAD	200	-	in./sec <sup>2</sup>	resultant acceleration of head accelerometer
AK	-	$\bar{a}_k$	-	weighting coefficient for jitter mode
ALFAI	7	$\alpha_1$	rad	joint stop lower relative angle limit
AIP1I	-	-	-	imaginary part of root, first approximation
AIP1R	-	-	-	real part of root, first approximation
AIP2I	-	-	-	imaginary part of root, second approximation
AIP2R	-	-	-	real part of root, second approximation
AIP3I	-	-	-	imaginary part of root, third approximation
AIP3R	-	-	-	real part of root, third approximation
AIP4I	-	-	-	imaginary part of root, fourth approximation
AIP4R	-	-	-	real part of root, fourth approximation
ANG	-	-	deg	angular spacing of dots in head representation in stickman output
ANGLE	-	-	rad	angular spacing of plus signs in contact arc representation in stickman output
ANS	-	-	rad	absolute value of arcsine

Symbol Dictionary (page 3)

FORTTRAN Name	Dimension	Symbol	Units	Definition
ANVERS	10,10	$m^{-1}$	inverse of AA	inverse of mass matrix
APRNTD	-	-	sec	minimum print time interval
AR	8	$r_i$	in.	body contact arc radii
ARCSIN	-	-	rad	principal value of arcsine
ATDSQ	8	-	lb	intermediate step in centrifugal force vector computation
AVELA	-	-	in./sec <sup>3</sup>	second order vehicle velocity integration coefficient
AX	8	$x_i$	in.	joint x-coordinates
AXD	8	$\dot{x}_i$	in./sec	joint x-velocities
AXI	-	-	-	imaginary part of trial root
AXR	-	-	-	real part of trial root
AY	8	$y_i$	in.	joint y-coordinates
AYD	8	$\dot{y}_i$	in./sec	joint y-velocities
AZ	11	$z_k$	1-8, rad 9-11, in.	generalized coordinate vector
AZP	11	$\dot{z}_k$	1-8, rad/sec 9-11, in./sec	generalized velocity vector

Symbol Dictionary (page 4)

FORTRAN Name	Dimension	Symbol	Units	Definition
B	-	-	in.	horizontal CRT scaling term (vestigial)
B	4,2	-	-	joint direction label storage
BACCB	-	-	in./sec <sup>2</sup>	second order vehicle position integration coefficient
BASIC	11,8	-	1-10, in. 11, in./sec <sup>2</sup>	elements one through five are lever arms for contact frictional forces; elements six through ten are lever arms for contact normal forces; element eleven is centrifugal force term for contact relative accelerations
BBB	300,3	-	1, in./sec <sup>2</sup> 2,3, -	intercept for piecewise linear tables
BCH	-	-	g-units/in.	upper torso horizontal acceleration linear coefficient
BEE	10	B <sub>i</sub>	1-8, in. lb 9-10, lb	centrifugal force vector
BELL	-	-	-	temporary storage for imaginary part of polynomial evaluation
BELTA	200	-	lb	lap belt force storage
BELTB	200	-	lb	lower shoulder belt force storage
BELTC	200	-	lb	upper shoulder belt force storage



Symbol Dictionary (page 5)

FORTRAN Name	Dimension	Symbol	Units	Definition
BETA	3	$\beta_m$	1, lb/in. 2, lb/in. <sup>2</sup> 3, lb/in. <sup>3</sup>	hip seat force spring coefficients
BET1I	-	-	-	imaginary part of first polynomial evaluation
BET1R	-	-	-	real part of first polynomial evaluation
BET2I	-	-	-	imaginary part of second polynomial evaluation
BET2R	-	-	-	real part of second polynomial evaluation
BET3I	-	-	-	imaginary part of third polynomial evaluation
BET3R	-	-	-	real part of third polynomial evaluation
BH	-	-	g-units/in.	head horizontal acceleration linear coefficient
BIGKI	7	$K_i$	in. lb/rad	joint elasticity coefficient for each joint
BIGMI	8	$J_e$	in. lb	joint elasticity torque for each joint
BL	3	$l_k$	in.	belt segment length for each belt segment
BL1	200	-	in.	lap belt length storage
BL2	200	-	in.	lower shoulder belt length storage
BL3	200	-	in.	upper shoulder belt length storage

Symbol Dictionary (page 6)

FORTRAN Name	Dimension	Symbol	Units	Definition
BPRNTD	-	-	sec	first time for summary printing
BVELB	-	-	in./sec <sup>2</sup>	first order vehicle velocity integration coefficient
C	-	-	-	vertical CRT scaling factor (vestigial)
C	3,7	-	-	joint label storage
CACCC	-	-	in./sec	first order vehicle position integration coefficient
CARD	5	-	-	temporary storage for reading input cards
CARD	8	-	-	temporary storage for reading input cards
CAZ	8	-	-	cosines of body angles
CCF	200,4	-	lb	chest contact forces storage
CCH	-	-	g-units	vertical acceleration of upper spinal joint
CEE	10	C <sub>k</sub>	1-8, in. lb 9-10, lb	joint generalized force vector
CFA	200	-	in./sec <sup>2</sup>	chest forward acceleration storage
CH	-	-	g-units	vertical acceleration of neck joint
CI	-	-	-	tolerance index as input data
CK	10,10	-	-	sum of pre- and post-matrix multiplications of matrix and inverse as check

Symbol Dictionary (page 7)

FORTRAN Name	Dimension	Symbol	Units	Definition
CKF	200	-	lb	knee contact force storage
COE	6	-	-	temporary storage for reordering load deflection coefficients
COE	16	-	-	polynomial coefficients in descending order
COMI	3,8	-	-	body contact segment label storage
CONEN	18	C <sub>1</sub>	lb/in.	first order unloading coefficient for each interaction
CONTAC	200,21	-	lb	contact force storage
CPHI	3	-	-	cosines of belt angles
CPRIME	7	C <sub>i</sub>	in. lb	joint coulomb friction coefficients
CPSIA	10	-	-	cosines of contact surface reference angles
CS	-	C <sub>s</sub>	lb sec/in.	hip seat force damping coefficient
CTHETA	8	-	-	cosines of body angles
CTHETZ	8	-	-	cosines of body angles at time zero
CTWON	18	C <sub>2</sub>	lb/in. <sup>2</sup>	second order unloading coefficient for each interaction
CUA	200	-	in./sec <sup>2</sup>	chest upward acceleration storage
CVELA	-	-	in./sec	zeroth order vehicle velocity integration coefficient

Symbol Dictionary (page 8)

FORTRAN Name	Dimension	Symbol	Units	Definition
CZERON	18	C <sub>0</sub>	lb	zeroth order unloading coefficient for each interaction
CZVEC	8	-	-	cosines of body angles for stick figure
C0	-	-	-	coefficient in arcsine evaluation
C1	-	-	-	coefficient in arcsine evaluation
C2	-	-	-	coefficient in arcsine evaluation
C3	-	-	-	coefficient in arcsine evaluation
C4	-	-	-	coefficient in arcsine evaluation
C5	-	-	-	coefficient in arcsine evaluation
C6	-	-	-	coefficient in arcsine evaluation
C7	-	-	-	coefficient in arcsine evaluation
D	-	-	in.	vertical CRT scaling term (vestigial)
DA	10	-	in.	contact surface lengths
DACCD	-	-	in.	zeroth order vehicle position integration coefficient
DCH	-	-	g-units/in.	upper torso vertical acceleration linear coefficient
DEE	10	D <sub>i</sub>	1-8, in. lb 9-10, lb	seat and belt generalized force vector

Symbol Dictionary (page 9)

FORTRAN Name	Dimension	Symbol	Units	Definition
DELDOD	18	$\dot{\delta}_{m-1}$	in./sec	previous deflection rate for each interaction
DELET	-	-	in. lb	change in energy over time interval
DELIA	-	-	in.	contact deflection
DELIAD	-	-	in./sec	contact deflection rate
DELL	-	$\Delta$	in.	slack
DELNN	-	$\Delta v$	accel	change in mode acceleration between two jitter states for a linear mode
DELNU	-	$\Delta v$	accel	change in mode acceleration between two jitter states
DELOLD	18	$\delta_{m-1}$	in.	previous deflection for each interaction
DELTA	3	$\Delta$	in.	belt slack for each belt segment
DELTA	-	-	sec	time interval between stick figures
DELTAT	-	$\Delta t$	sec	integration time interval
DELZ	11,16	$\ddot{\Delta z}_i$	1-8, rad/sec <sup>2</sup> 9-11, in./sec <sup>2</sup>	change in generalized acceleration vector due to each possible jitter mode acting alone
DESPA	3,6	-	-	body contact arc labels
DESPB	6	-	-	vestigial

Symbol Dictionary (page 10)

FORTRAN Name	Dimension	Symbol	Units	Definition
DESPC	5,6	-	-	contact surface labels
DESTEP	-	$\Delta t_{min}$	sec	minimum integration time interval
DETERM	-	-	-	determinant of mass matrix
DEL5	-	-	-	temporary storage in MULLER
DEL6	-	-	-	temporary storage in MULLER
DH	-	-	g-units/in.	head vertical acceleration linear coefficient
DISP	-	x-X	in.	displacement of hip relative to vehicle
DTPRNT	-	-	sec	print time interval for normal summary output
DTR	-	$\pi/180$	rad/deg	degrees to radian conversion factor
DTR	-	-	rad	temporary storage for body angles
DUR	-	-	sec	duration of injury tolerance violation
EHAT	18	$\hat{E}$	in. lb	reference conserved energy per loading cycle for each interaction
EL	8	.L <sub>i</sub>	in.	body segment lengths except element four which is distance from upper spine to shoulder
ELAMB	6	$\lambda_i$	in.	initial condition parameters for belts

Symbol Dictionary (page 11)

FORTRAN Name	Dimension	Symbol	Units	Definition
ELP	5	L'	in.	temporary storage for proper body lengths used in computing lever arms for contacts
ELPTEN	-	$l'_{10}$	in.	initial distance between hip and lap belt anchor point
ELTHRY	-	$l_{30}$	in.	initial upper shoulder belt length
ELTWY	-	$l_{20}$	in.	initial lower shoulder belt length
ELZTEN	-	$l_{10}$	in.	initial lap belt length
EM	8	$m_i$	lb sec <sup>2</sup> /in.	body segment mass for each segment
EMC	-	$m_c$	lb sec <sup>2</sup> /in.	vehicle mass (vestigial)
EMFVSX	-	-	lb sec <sup>2</sup> /in.	total mass of arms
EMTHSX	-	-	lb sec <sup>2</sup> /in.	total mass of upper torso, head, and arms
EMTWSX	-	-	lb sec <sup>2</sup> /in.	total mass of upper half of body (from middle torso and including arms)
EONE	18	$E_L$	in. lb	total conserved energy for each interaction
EONEC	-	$E_c$	in. lb	vehicle conserved energy (vestigial)
EPSLNP	-	$\epsilon'$	in.	residual deformation when loading begins again before unloading is complete
EPSLNY	18	$\epsilon$	in.	cumulative permanent deformation for each interaction

Symbol Dictionary (page 12)

FORTTRAN Name	Dimension	Symbol	Units	Definition
EPSLNZ	-	$\epsilon_0$	sec	linear mode time interval convergence limit
ET	18	$E_t$	in. lb	total energy for current cycle for each interaction
ETA	-	$\eta$	-	determines sign of relative velocity limit used in time prediction of entering jitter
EYE	8	$I_i$	lb sec <sup>2</sup>	body segment moment of inertias at center of gravity
EO	-	$\hat{E}_0$	in. lb	reference conserved energy for prediction
FEPTEN	-	$\phi_{10}^i$	rad	angle of line joining lap belt anchor and hip joint from horizontal at time zero
FFM	3	$F_m$	lb	belt forces for each segment
FIRST	-	-	sec	first time at which a stick figure is desired
FMAX1	-	-	lb	maximum value of all belt forces in crash
FMAX2	-	-	in./sec <sup>2</sup>	maximum value of head and chest accelerations in crash
FMAX3	-	-	in.	maximum value of hip x and y coordinates relative to the vehicle in crash
FMAX4	-	-	in./sec <sup>2</sup>	maximum value of vehicle acceleration in crash
FMAX5	-	-	deg	maximum value of angles of head and chest accelerations in crash



Symbol Dictionary (page 13)

FORTRAN Name	Dimension	Symbol	Units	Definition
FMAX6	-	-	lb	maximum value of seat hip and seat front forces in crash
FMIN1	-	-	lb	minimum value of all belt forces in crash
FMIN2	-	-	in./sec <sup>2</sup>	minimum value of head and chest accelerations in crash
FMIN3	-	-	in.	minimum value of hip x and y coordinates relative to the vehicle in crash
FMIN4	-	-	in./sec <sup>2</sup>	minimum value of vehicle acceleration in crash
FMIN5	-	-	deg	minimum value of angles of head and chest accelerations in crash
FMIN6	-	-	lb	minimum value of seat hip and seat front forces in crash
FMM	300,3	-	1, in./sec <sup>2</sup> 2,3, -	slope of subsequent input table segment
FMUA	10	$\mu_a$	-	contact surface coefficients of friction
FMUS	-	$\mu_s$	-	seat cushion coefficient of friction
FOM	-	$\Omega$	in.	latest maximum deflection
FORCE	-	F	lb	predicted contact force
FRTYFV	-	$\pi/4$	rad	forty-five degrees in radians
FS	-	F <sub>S</sub>	lb	hip seat force

Symbol Dictionary (page 14)

FORTRAN Name	Dimension	Symbol	Units	Definition
FSPRM	-	$F'_s$	lb	front edge seat force
FSPRMZ	-	$F'_{s0}$	lb	front edge seat force at time zero
FSZCNS	-	-	lb	constant used in front edge seat force determination representing force calibration at zero time
FT	-	F	lb	predicted force
FTOLD	18	$F_{m-1}$	lb	previous force for each interaction
FUT	-	F	lb	predicted force
FUDGE	-	-	in.	distance from contact surface used as maximum distance error caused by time prediction error in linear jitter modes
FZ	-	$F_z$	lb	forward seat front edge force
G	18	G	-	material plasticity index, i.e., the ratio of permanent deformation to maximum deflection, for each interaction
GA	10	$G_a$	-	material plasticity index for each contact surface
GAMZER	-	$\gamma_0$	deg	angle of seat cushion surface from horizontal
GCHEST	200	-	deg	angle of chest accelerometer acceleration storage
GEE	10	$G_i$	1-8, in. lb 9,10, lb	negative of gravitational generalized force vector

Symbol Dictionary (page 15)

FORTTRAN Name	Dimension	Symbol	Units	Definition
GHEAD	200	-	deg	angle of head accelerometer acceleration storage
GNEW	-	-	-	plasticity index
GOMG	-	-	in.	required off deflection for unloading curve
GRAVA	10	-	1-8, in. lb 9, lb	parameters used in computation of gravitational generalized force vector; element ten is vestigial
GRAVIT	-	g	in./sec <sup>2</sup>	acceleration of earth standard gravity (32.2)
H	-	h	in.	distance from the point of action of the lower shoulder belt from lower spinal joint along centerline of middle torso
HELL	-	-	-	temporary storage of real part of polynomial evaluation
HEADX	-	x <sub>h</sub>	in.	x-coordinate of head center of gravity
HEADX	-	-	in.	x-coordinate of center of curvature of head
HEADY	-	y <sub>h</sub>	in.	y-coordinate of head center of gravity
HEADY	-	-	in.	y-coordinate of center of curvature of head
HFA	200	.	in./sec <sup>2</sup>	head forward acceleration at center of gravity storage
HLA	200	-	in./sec <sup>2</sup>	vestigial
HLINE	-	-	in.	horizontal distance represented per grid line

Symbol Dictionary (page 16)

FORTTRAN Name	Dimension	Symbol	Units	Definition
HZERO	130	-	in.	horizontal distance represented at plot origin
I	-	i	-	general index but often body segment index
IA	-	a	-	contact surface index
IALPH	26	-	-	contains alphabetic characters for identifying input cards
IBIG	8	$I_k$	-	contains indices of modes in jitter state in order that they came in jitter except for linear jitters which are always last
IBUG	-	-	-	debug printout control level
ID	-	-	-	input card identification field storage
IDATE	3	-	-	contains calendar date of the current run
IFORK	3,8	-	-	element one is body segment index, element two is contact surface index, and element three is the interaction index for each of eight possible linear jitter modes
IGNORE	10	-	-	contains a switch for each of the contacts which tells whether the surface is not used or has no friction
II	-	i	-	body segment index
IMAGE	1392	-	-	temporary storage for prediction of summary plots

Symbol Dictionary (page 17)

FORTRAN Name	Dimension	Symbol	Units	Definition
IMAGE	1500	-	-	temporary storage for prediction of stick figures
IMAX	-	-	-	index of last time point of input table
IMIN	-	-	-	index of latest inflection point of input table
IND	-	-	-	code index for combination of on and off states being tried to resolve jittering modes
INDEX	-	-	-	index of contact interaction
INDIC	-	-	-	switch indicating whether to reset inflection, print and step switches to zero if jitter mode time is selected
INN	-	-	-	index used in contact friction bookkeeping
INT	-	-	-	number of spacer points between plotted points
IPAGE	-	-	-	page number counter
IPOST	3	-	-	pointer for latest input table entry used
ISON	-	-	-	switch indicating whether a tolerance violation is in progress during a scan of values for all time
ISTAR	-	i*	-	switch indicating need for force limiting
ISTART	-	-	-	index of starting time point on printed page
ISTEP	-	-	-	maximum number of stick figure times

Symbol Dictionary (page 18)

FORTRAN Name	Dimension	Symbol	Units	Definition
ISTOP	-	-	-	index of stopping time point on printed page
ISW	-	-	-	extracted mode contribution inclusion switch
ISWT	-	-	-	switch to control new page title printing
ITABLE	-	-	-	input table number
ITAU	-	-	-	index of mode with minimum time to reach jitter
ITOL	-	-	-	temporary storage for tolerance limit data
ITOP	-	-	-	number of possible jitter mode combinations
ITOPOW	-	-	-	two raised to an integer power (vestigial)
ITPH	-	-	-	
IZERO	-	-	-	switch controlling zero line printing
J	-	J	-	general index
JFORK	8	-	-	temporary storage for previous linear jitter mode contact interaction indices
JI	-	-	-	inflection switch for prediction
JINFL	-	-	-	temporary inflection switch
JJ	-	-	-	general index often maximum number of nonzero contact forces at any time

Symbol Dictionary (page 19)

FORTRAN Name	Dimension	Symbol	Units	Definition
JK	-	-	-	general index
JL	-	-	-	general index
JNN	-	-	-	(vestigial)
JOINT	9	-	-	stick figure joint index labels
JP	-	-	-	print switch for prediction
JPRINT	-	-	-	temporary print switch
JS	-	-	-	time step switch for prediction
JSTEP	-	-	-	temporary time step switch
K	-	k	-	general index often maximum number of time points for summary printout or index of present jitter mode
KA	8	a	-	contact surface index for each nonzero force
KI	8	i	-	body contact arc index for each nonzero force
KINFL	-	-	-	inflection switch
KK	-	-	-	general index
KKK	-	-	-	general index
KN	-	-	-	index of second linear jitter mode

Symbol Dictionary (page 20)

FORTRAN Name	Dimension	Symbol	Units	Definition
KPOST	-	-	-	index of current input table entry
KPRINT	-	-	-	print switch
KSTEP	-	-	-	time step switch
KTABLE	2,14	-	-	contains the body arc and contact surface indices for each of the allowable interactions for the current pas-senger position; the interaction index is the second subscript plus four
KTOTAL	-	-	-	total number of time points for printout
KTS	-	-	-	temporary value of KPOST
L	-	l	-	general index
LA	2l	a	-	contact surface indices for contact force printout
LABEL	-	-	-	switch indicating no plot label for stick figure
LCONTL	-	-	-	switch controlling some standard printout options
LI	2l	i	-	body arc indices for contact force printout
LINE	-	-	-	line counter for page length control of printout
LITGAM	-	γ	-	index of linear jitter mode
LL	-	-	-	general index



Symbol Dictionary (page 21)

FORTRAN Name	Dimension	Symbol	Units	Definition
M	-	m	-	general index, often the index of the body segment forming the other side of a joint angle corresponding to the side with the same index as the joint, also used for the number of jitter modes less one left to resolve, or the number of contact forces left to be printed
MASK	8	-	-	masks used to extract individual bit positions
MAX	3	-	-	maximum numbers of time points in input tables
MAXI	-	-	-	number of modes in jitter
MAXR	-	-	-	number of modes for which jitter is possible for an occupant position
METH	-	-	-	switch indicating whether stick figure times are computed or to be inputted
MFORI	7	-	-	table containing the body segment index of the other side of the joint given the joint index
MM	-	-	-	number of nonzero forward chest contact forces
MMAX	-	-	-	maximum number of nonzero contact forces to be printed
MN	-	-	-	number of nonzero knee contact forces
MODE	-	-	-	table containing a status indicator for each possible jitter mode

Symbol Dictionary (page 22)

FORTRAN Name	Dimension	Symbol	Units	Definition
MPRINT	-	-	-	special initial print switch
MSBH	-	-	-	horizontal spaces on stick figure plot without grid
MSBV	-	-	-	vertical spaces on stick figure plot without grid
MSTART	-	-	-	starting index to print contact forces
MSTEP	-	-	-	number of contact forces already printed
MSTOP	-	-	-	stopping index to print contact forces
N	-	n	-	general index
N	8	-	-	number of points to represent each body segment in stick figure plot
NBELT	-	-	-	belt option indicator
NC	-	-	-	switch indicating no captions on graphs
NCHAR	-	-	-	switch indicating no captions on stick figures
NCNTCT	8	-	-	switches indicating whether contact arcs are to appear in stick figure
NCRT	-	-	-	CRT output switch (vestigial)
NEW	3	-	-	input table switches indicating whether changes made

Symbol Dictionary (page 23)

FORTRAN Name	Dimension	Symbol	Units	Definition
NGRAPH	-	-	-	switch indicating whether graphs are desired
NHL	-	-	-	number of horizontal lines in grid
NINJ	-	-	-	switch indicating whether injury tolerance printout is desired
NMAX	-	-	-	maximum ratio of predicted force change to allowed force change
NNK	-	-	-	maximum number of input table entries
NPASGR	-	-	-	occupant position indicator
NPROB	-	-	-	switch indicating whether injury probability printout is desired
NPTS1	-	-	-	number of points plotted on first graph
NPTS2	-	-	-	number of points plotted on second graph
NPTS3	-	-	-	number of points plotted on third graph
NS	-	-	-	maximum value of interaction index for occupant position
NS	5	-	-	plot scaling specification array for graphs
NSBH	-	-	-	number of spaces between horizontal grid lines
NSBV	-	-	-	number of spaces between vertical grid lines

Symbol Dictionary (page 24)

FORTRAN Name	Dimension	Symbol	Units	Definition
NSCALE	5	-	-	plot scaling specification array for stick figures
NST	-	-	-	general index
NSTICK	-	-	-	switch indicating whether stick figures are desired
NSTOP	-	-	-	number of contact forces for a page of printout
NT	-	-	-	general index
NVL	-	-	-	number of vertical grid lines
N1	-	-	-	degree of polynomial
N2	-	-	-	number of polynomial coefficients
N3	-	-	-	iteration counter
N4	-	-	-	general index
N6	-	-	-	general index
OLDELD	-	$\delta_{m-1}$	in./sec	previous deflection rate
OMEGA	18	-	in.	required off deflection for unloading curve for each interaction
OMEGAI	7	$\Omega_i$	rad	upper joint relative angle limits
OMGT	-	$\Omega$	in.	maximum relative deflection

Symbol Dictionary (page 25)

FORTRAN Name	Dimension	Symbol	Units	Definition
OMSGE	-	-	-	elasticity for load-deflection model (1-G)
ON	-	-	-	label used in printing contact forces
ORD	-	-	1, in./sec <sup>2</sup> 2,3, -	ordinate of table point
P	200,9	-	-	storage for hip and vehicle positions, velocities, and accelerations
PCHEST	-	-	in.	distance of chest accelerometer above upper spinal joint along upper torso centerline
PCNTL	-	-	-	number of minimum print times in one print time interval
PEAK	-	-	-	maximum absolute value of injury tolerance violation
PHEAD	-	-	in.	distance of head accelerometer above neck
PHI	3	$\phi_m$	rad	belt angles
PHIZ	3	$\phi_{m0}$	rad	initial belt angles
PHI1	200	-	rad	lap belt angle storage
PHI2	200	-	rad	lower shoulder belt angle storage
PHI3	200	-	rad	upper shoulder belt angle storage
PI	-	$\pi$	rad	180 degrees in radians

Symbol Dictionary (page 26)

FORTRAN Name	Dimension	Symbol	Units	Definition
PI	-	p	-	probability value
PIWO	-	$\pi/2$	rad	ninety degrees in radians
PLC	-	$\ddot{x}$	g-units	vehicle acceleration
PLX	-	$\ddot{x}$	g-units	hip forward acceleration
PLY	-	$\ddot{y}$	g-units	hip vertical acceleration
PN	18	-	lb	elements one through three are belt forces; elements five through eighteen are contact forces stored on the interaction index; element four is vestigial; (this is summarized, "for each interaction")
PNDEL	18	-	lb	spring portion of loading force for each interaction
POMG	-	$\Omega_{m-1}$	in.	previous relative deflection
POST	200,9	-	-	storage for hip and vehicle positions, velocities, and accelerations
POUNDS	-	-	lb	change limit for a forward contact force in one time interval
PP	8	-	lb	current nonzero contact forces storage
PR	-	-	-	total probability
PRMX	-	-	in.	x-coordinate of center of curvature

Symbol Dictionary (page 27)

FORTTRAN Name	Dimension	Symbol	Units	Definition
PRMY	-	-	in.	y-coordinate of center of curvature
PSIA	-	$\psi_a$	deg	contact surface reference angle
PTIM	-	-	sec	time of peak tolerance violation
PTLEN	-	-	in. <sup>-1</sup>	points per inch for plotting stick figure
PVAR	-	-	-	previous value of tolerance violation
QI	-	-	-	combination switch indicating whether a new probability label or which old label by index
QUE	10	$Q_k$	1-8, in. lb 9-10, lb	contact generalized force vector
R	-	-	-	number of points up to current point in stick figure representation of a line used in computation of coordinates
R	18	R	-	material energy absorption index, i.e., ratio of conserved energy to total energy, for each interaction
RA	10	$R_a$	-	material energy absorption index for each contact surface
RANG	-	-	-	temporary storage in stick figure computations
RH	-	$r_h$	in.	radius of arc of action of lap belt force

Symbol Dictionary (page 28)

FORTRAN Name	Dimension	Symbol	Units	Definition
RHO	8	$\rho_i$	in.	distance of body segment centers of gravity above previous joints
RHOPFZ	-	$\rho_4'$	in.	distance of head center of curvature above neck
RHOPRM	8	$\rho_i'$	in.	distance of body segment center of curvature above previous joint
RHOPTZ	-	$\rho_3'$	in.	distance of chest center of curvature above upper spinal joint
RNEW	-	R	-	energy absorption index
RNSBH	-	-	-	number of horizontal spaces in stick figure plot
RNSBV	-	-	-	number of vertical spaces in stick figure plot
ROOTI	5	-	-	imaginary parts of roots of fifth order equation
ROOTI	15	-	-	imaginary parts of roots
ROOTR	5	-	-	real parts of roots of fifth order equation
ROOTR	15	-	-	real parts of roots
RPSI	16	$\xi$	1-7, rad/sec 8-16, in./sec	velocity limits for possible jitter modes
RSEL	16	$\dot{v}$	1-7, rad/sec <sup>2</sup> 8-16, in./sec <sup>2</sup>	relative or mode accelerations for possible jitter modes



Symbol Dictionary (page 29)

FORTRAN Name	Dimension	Symbol	Units	Definition
R7M	-	-	-	temporary storage for root selection
RV	-	-	-	relative or mode velocity
RVEL	16	$v$	1-7, rad/sec 8-16, in./sec	relative or mode velocity for possible jitter modes
RZ	-	$r_z$	in.	distance from lower leg centerline to skin
S	-	$s$	lb/in.	spring constant for front edge of seat
SAGXXX	-	$\sigma_0$	lb	zeroth order loading coefficient
SAZ	8	-	-	sine of body angle
SCALEX	-	-	-	horizontal scale factor for plotting stick figures
SCALEY	-	-	-	vertical scale factor for plotting stick figures
SDEL	-	$\delta_m$	in.	present deflection
SDELA	-	$\delta$	in.	present contact deflection
SDELD	-	$\dot{\delta}$	in./sec	deflection rate
SDELTA	3	$\delta$	in.	belt deflections for each belt segment
SDELTD	3	$\dot{\delta}$	in./sec	belt deflection rates for each belt segment
SDL	-	$\delta_m$	in.	present deflection

Symbol Dictionary (page 30)

FORTTRAN Name	Dimension	Symbol	Units	Definition
SDLD	-	$\dot{\delta}_m$	in./sec	present deflection rate
SETBCK	200	-	lb	hip seat force storage
SETFRT	200	-	lb	seat front vertical force storage
SI	-	-	-	head severity index
SIA	-	-	in.	perpendicular distance of body center of curvature from surface
SIG	10	$\sigma_m$	n=1-5, lb/in. <sup>n</sup> n=6-10, lb/(in./sec) <sup>n-5</sup>	material load-deflection coefficients
SIGMA	10,3	$\sigma_m$	same as SIG	belt load-deflection coefficients
SIGMAA	10,10	$\sigma_{am}$	same as SIG	contact surface load-deflection coefficients for all surfaces
SIGMAC	10	$\sigma_{cm}$	same as SIG	(vestigial)
SIGZ	18	$\sigma_o$	lb	material zeroth order load-deflection coefficients for all interactions
SINTEN	-	-	-	sine of the relative angle between upper torso and upper arm
SIXTY	-	-	rad	angular spacing in foot contact arc representation in stick figure

Symbol Dictionary (page 31)

FORTRAN Name	Dimension	Symbol	Units	Definition
SMALLB	10	$b_i$	1-8, in. lb 9-10, lb	total continuous generalized force vector
SMALLF	-	f	lb	seat cushion friction force
SPHI	3	-	-	sines of belt angles
SPSIA	10	-	-	sines of contact surface angles
SQ	-	-	-	temporary storage
STEPS	200	-	sec	time storage for producing stick figures
STHETA	8	-	-	sines of body angles
STHETZ	8	-	-	initial values of sines of body angles
STIME	200	-	sec	time point storage for summary printout
STIMFJ	6	-	-	sines of belt angles relative to body segments
STIMIJ	13	-	-	sines of angles between body segments
SUMBY	-	-	lb	hip seat spring force
SWITCH	3	-	-	scan type switches for input tables
SZ	-	$s_z$	lb/in.	spring constant for horizontal front edge seat force
SZVEC	8	-	-	sines of body angles

Symbol Dictionary (page 32)

FORTRAN Name	Dimension	Symbol	Units	Definition
T	200	-	sec	time point storage
TA	8	$\ddot{\theta}_i$	deg/sec <sup>2</sup>	body angle accelerations
TAHATZ	-	$\hat{t}_0$	sec	predicted time interval for the linear jitter mode to turn off
TANTEG	-	-	-	tangent of lower leg angle
TANTSV	-	-	-	tangent of upper leg angle
TAUHAT	-	$\hat{t}$	sec	minimum time interval until mode velocity reaches velocity limit
TAUI	16	$\tau_k$	sec	storage of time intervals until mode velocity reaches velocity limit for all modes
TDSQLI	8	$L_i \dot{\theta}_i^2$	in./sec <sup>2</sup>	intermediate step in centrifugal forces
TEM	-	-	-	temporary storage in calculation of zeroes
TEMI	-	-	-	temporary storage in calculation of zeroes
TEMR	-	-	-	temporary storage in calculation of zeroes
TE1	-	-	-	temporary storage in calculation of zeroes
TE2	-	-	-	temporary storage in calculation of zeroes
TE3	-	-	-	temporary storage in calculation of zeroes

Symbol Dictionary (page 33)

FORTRAN Name	Dimension	Symbol	Units	Definition
TE4	-	-	-	temporary storage in calculation of zeroes
TE5	-	-	-	temporary storage in calculation of zeroes
TE6	-	-	-	temporary storage in calculation of zeroes
TE7	-	-	-	temporary storage in calculation of zeroes
TE8	-	-	-	temporary storage in calculation of zeroes
TE9	-	-	-	temporary storage in calculation of zeroes
TE10	-	-	-	temporary storage in calculation of zeroes
TE11	-	-	-	temporary storage in calculation of zeroes
TE12	-	-	-	temporary storage in calculation of zeroes
TE13	-	-	-	temporary storage in calculation of zeroes
TE14	-	-	-	temporary storage in calculation of zeroes
TE15	-	-	-	temporary storage in calculation of zeroes
TE16	-	-	-	temporary storage in calculation of zeroes
TGAMZ	-	-	-	tangent of seat cushion angle
THATPS	-	$\hat{T}_7$	in. lb/rad	upper knee joint stop torque coefficient

Symbol Dictionary (page 34)

FORTRAN Name	Dimension	Symbol	Units	Definition
THATPV	-	$\hat{T}'_5$	in. lb/rad	upper shoulder joint stop torque coefficient
THATPW	-	$\hat{T}'_1$	in. lb/rad	upper hip joint stop torque coefficient
THATPX	-	$\hat{T}'_6$	in. lb/rad	upper elbow joint stop torque coefficient
THEDSQ	8	$\dot{\theta}_i^2$	(rad/sec) <sup>2</sup>	square of body angular velocity
THEFEE	-	-	rad	initial value of relative angle between lower torso centerline and lap belt
THETA	200,3,8	-	deg, etc.	body angular position, velocity, and acceleration storage
THETAZ	8	$\theta_{i0}$	rad	initial values of body angles
TIA	-	$T_{ia}$	in.	length of the line joining the body center of curvature to the contact surface reference point projected on the contact surface
TIMASK	-	$\tau^*$	sec	minimum of print interval, inflection interval, and maximum time step
TIMAX	-	$t_{max}$	sec	duration of simulation
TIME	-	$t$	sec	value of time during simulation
TIMTJ	16	-	rad	body relative angles
TIMTJZ	16	-	rad	initial values of body relative angles

Symbol Dictionary (page 35)

FORTTRAN Name	Dimension	Symbol	Units	Definition
TINFL	-	-	sec	time of next vehicle acceleration table entry (inflection time)
TMATII	8	$T_{ij}$	in. lb	joint stop torque
TOF	-	$t_{off}$	sec	time that the tolerance violation ceases
TOL	22	-	-	tolerance level values
TON	-	$t_{on}$	sec	time that the tolerance violation begins
TPRIME	7	$T'_i$	in. lb/rad	symmetric or lower joint stop torque coefficient
TPRINT	-	-	sec	next print time
TS	-	-	-	temporary storage
TSA	-	-	-	temporary storage
TSB	-	-	-	temporary storage
TSC	-	-	-	temporary storage
TSTEP	-	-	sec	last vehicle acceleration inflection time
TT	8	$\theta_i$	deg	body angles
TV	8	$\dot{\theta}_i$	deg	body angle velocities
VAR	-	-	-	injury tolerance quantity

Symbol Dictionary (page 36)

FORTRAN Name	Dimension	Symbol	Units	Definition
VLINE	-	-	in.	vertical distance represented per grid line
VTIA	-	$V_T$	in./sec	velocity of body segment contact arc along contact surface
VXIA	-	$V_x$	in./sec	forward velocity of body center of curvature
VYIA	-	$V_y$	in./sec	upward velocity of body center of curvature
VZERO	50	-	in.	vertical distances represented at grid line
WORKA	10	-	-	temporary storage for matrix inversion
WORKB	10	-	-	temporary storage for matrix inversion
WZERO	-	$W_0$	lb	initial hip seat force
X	-	-	-	sine of desired angle
X	-	-	in./sec <sup>2</sup>	forward acceleration of chest center of gravity, chest center of curvature, or head center of curvature
X	7	-	-	temporary storage for sorting input tables
X	7	$x_i$	in.	x-coordinates of joints
XA	-	-	sec	one end of deletion interval from input table
XAP	-	$\dot{x}$	in./sec	hip forward velocity



Symbol Dictionary (page 37)

FORTTRAN Name	Dimension	Symbol	Units	Definition
XB	-	-	sec	one end of deletion interval from input table
XC	-	X	in.	vehicle x-coordinate
XCHEST	-	-	in./sec <sup>2</sup>	chest center of gravity forward acceleration
XCHT	5	-	in.	x-coordinates of chest contact arc points
XCP	-	$\dot{X}$	in./sec	vehicle forward velocity
XELB	3	-	in.	x-coordinates of elbow contact arc points
XFLOOR	2	-	in.	x-coordinates of floor end points
XFT	5	-	in.	x-coordinates of foot contact arc points
XHEAD	-	-	in./sec <sup>2</sup>	head center of gravity forward acceleration
XHEAD	200	-	in.	x-coordinate of head center of gravity storage
XHIP	5	-	in.	x-coordinates of hip contact arc points
XHND	5	-	in.	x-coordinates of hand contact arc points
XIDOT	7	-	in./sec	joint forward velocity
XISMLA	10	$f_a$	in./sec	contact surface friction velocity limit
XJOINT	9	-	in.	x-coordinates of joints including wrist and ankle

Symbol Dictionary (page 38)

FORTRAN Name	Dimension	Symbol	Units	Definition
XKNE	3	-	in.	x-coordinates of knee contact arc points
XL	2	-	in.	x-coordinates of lower shoulder belt end points
XLAP	2	-	in.	x-coordinates of lap belt end points
XLEN	8	-	in.	x-coordinates of plot arcs
XLP	2	-	in.	x-coordinates of lower panel end points
XLSW	2	-	in.	x-coordinates of lower steering wheel end points
XMAN	64	-	in.	x-coordinates of stick figure points
XMAX	-	-	in.	maximum x-coordinate of plot area
XMIN	-	-	in.	minimum x-coordinate of plot area
XPACZ	-	-	in./sec	initial value of hip forward velocity
XPRM	8	-	in.	x-coordinates of body centers of curvature
XR	2	-	in.	x-coordinates of roof end points
XRHO	-	-	in.	x-coordinate of chest center of curvature
XSC	2	-	in.	x-coordinates of steering column end points
XSEAT	3	-	in.	x-coordinates of seat end points and intersection

Symbol Dictionary (page 39)

FORTRAN Name	Dimension	Symbol	Units	Definition
XSMALA	10	-	in.	x-coordinates of contact surface reference points
XTOE	2	-	in.	x-coordinate of toeboard end points
XU	-	-	in.	x-coordinate of upper shoulder belt anchor point
XUSDF	2	-	in.	x-coordinates of upper steering wheel end points
XVEHZ	-	-	in./sec	initial value of vehicle forward velocity
XWS	2	-	in.	x-coordinates of windshield end points
XX	-	-	sec	argument of input table
XX	-	-	-	sine of desired angle
XXX	300,3	-	sec	input table time storage
XZ	-	$x_z$	in.	horizontal distance of front edge of seat from lower leg centerline
Y	-	-	in./sec <sup>2</sup>	upward acceleration of chest center of gravity, chest center of curvature, or head center of curvature
Y	7	$y_i$	in.	y-coordinates of joints
YA	-	y	in.	hip y-coordinate
YAP	-	$\dot{y}$	in./sec	hip forward velocity

Symbol Dictionary (page 40)

FORTRAN Name	Dimension	Symbol	Units	Definition
YCHEST	-	-	in./sec <sup>2</sup>	chest center of gravity upward acceleration
YCHT	6	-	in.	y-coordinates of chest contact arc points
YELB	3	-	in.	y-coordinates of elbow contact arc points
YEPSLN	-	-	in.	cumulative permanent deflection
YFLOOR	2	-	in.	y-coordinates of floor end points
YFT	5	-	in.	y-coordinates of foot contact arc points
YHEAD	-	-	in./sec <sup>2</sup>	head center of gravity upward acceleration
YHEAD	200	-	in.	head center of gravity y-coordinate storage
YHIP	5	-	in.	y-coordinates of hip contact arc points
YHND	5	-	in.	y-coordinates of hand contact arc points
YIDOT	7	-	in./sec	joint upward velocity
YJOINT	9	-	in.	y-coordinates of joints including wrist and ankle
YKNE	3	-	in.	y-coordinates of knee contact arc points
YL	2	-	in.	y-coordinates of lower shoulder belt end points
YLAP	2	-	in.	y-coordinates of lap shoulder belt end points

242

FORTRAN Name	Dimension	Symbol	Units	Definition
YLEN	8	-	in.	y-coordinates of plot arcs
YLP	2	-	in.	y-coordinates of lower panel end points
YLSW	2	-	in.	y-coordinates of lower steering wheel end points
YMAN	64	-	in.	y-coordinates of stick figure points
YMAX	-	-	in.	maximum y-coordinate of plot area
YMIN	-	-	in.	minimum y-coordinate of plot area
YPRM	8	-	in.	y-coordinates of body centers of curvature
YR	2	-	in.	y-coordinates of roof end points
YRHO	-	-	in.	y-coordinate of chest center of curvature
YS	-	$y_s$	in.	deflection of hip seat spring
YSC	2	-	in.	y-coordinates of steering column end points
YSEAT	3	-	in.	y-coordinates of seat end points and intersection
YSMALA	10	-	in.	y-coordinates of contact surface reference points
YSP	-	$\dot{y}_s$	in./sec	deflection rate of hip seat spring
YTOE	2	-	in.	y-coordinates of toeboard end points

Symbol Dictionary (page 42)

FORTRAN Name	Dimension	Symbol	Units	Definition
YU	-	-	in.	y-coordinate of upper shoulder belt anchor point
YUSDF	2	-	in.	y-coordinates of steering wheel end points
YWS	2	-	in.	y-coordinates of windshield end points
YYY	300,3	-	1, in./sec <sup>2</sup> 2,3, -	ordinates of input tables
YZZERO	-	$y_{z0}$	in.	vertical distance from the front edge of the seat to the point of seat cushion directly beneath the hip joint
Z	-	z	in.	horizontal distance of the front edge of the seat from the hip joint
ZERO	-	-	-	(vestigial)
ZERO	130	-	-	zero line plot array
ZK	11,128	$\ddot{z}_k$	1-8, rad/sec <sup>2</sup> 9-11, in./sec <sup>2</sup>	generalized acceleration contributions for all combinations of jitter modes on and off
ZKB	11	-	1-8, rad/sec <sup>2</sup> 9-11, in./sec <sup>2</sup>	base acceleration vector including both all continuous and turned on discontinuous
ZKBASE	11	-	1-8, rad/sec <sup>2</sup> 9-11, in./sec <sup>2</sup>	base acceleration vector including both all continuous and turned on discontinuous
XMLCTS	-	-	in.	horizontal distance of knee joint from front edge of seat

44

Symbol Dictionary (page 43)

FORTAN Name	Dimension	Symbol	Units	Definition
ZP	11	-	-	temporary storage for mode velocities or accelerations
ZPAR	-	-	-	(vestigial)
ZPP	-	-	-	mode acceleration
ZPPP	128	-	-	mode acceleration for all combinations of jitter modes on and off for a particular mode
ZQ	11	-	1-8, rad/sec <sup>2</sup> 9-11, in./sec <sup>2</sup>	temporary storage of continuous generalized acceleration vector
ZR	10	-	1-8, rad/sec <sup>2</sup> 9-11, in./sec <sup>2</sup>	temporary storage of continuous generalized acceleration vector
ZRV	-	-	-	mode acceleration from base acceleration vector for jitter mode being considered
ZRVN	-	-	-	mode acceleration from base acceleration vector for second linear jitter mode
ZVEC	11	-	1-8, rad 9-11, in.	generalized coordinate vector including vehicle coordinate
ZVECP	11	-	1-8, rad/sec 9-11, in./sec	generalized velocity vector
ZVECPP	11	-	1-8, rad/sec <sup>2</sup> 9-11, in./sec <sup>2</sup>	generalized acceleration vector

Symbol Dictionary (page 44)

FORTRAN Name	Dimension	Symbol	Units	Definition
ZZERO	-	$z_0$	in.	x-coordinate of front edge of seat



Appendix to Symbol Dictionary (page 1)

<u>Symbol</u>	<u>FORTTRAN Name(s)</u>
a	KA, LA, IA
$a_1$	A
$\bar{a}_k$	AK
$\vec{B}$	BEE
$\vec{b}$	SMALLB
$\vec{C}$	CEE
$C_o$	CZERON
$C_1$	CONEN
$C_2$	CTWON
$C_s$	CS
$C'_1$	CPRIME
$\vec{D}$	DEE
$E_1$	EONE
$E_t$	ET
$\hat{E}$	EHAT
$\hat{E}_o$	EO
F	FORCE, FT, FTT
$F_m$	FFM
$F_{n-1}$	FTOLD
$F_s$	FS
$F_z$	FZ

Appendix to Symbol Dictionary (page 2)

<u>Symbol</u>	<u>FORTTRAN Name(s)</u>
F' <sub>s</sub>	FSPRM
F' <sub>s</sub> <sub>o</sub>	FSPRMZ
f	SMALLF
G	G
G <sup>+</sup>	GEE
G <sub>a</sub>	GA
g	GRAVIT
h	H
I <sub>i</sub>	EYE
i	KI, LI, I, II
i*	ISTAR
K <sub>i</sub>	BIGKI
J <sub>e</sub>	BIGMI
L <sub>i</sub>	EL
L'	ELP
l <sub>k</sub>	BL
l <sub>10</sub>	ELZTEN
l <sub>20</sub>	ELTWTY
l <sub>30</sub>	ELTHRY
l' <sub>10</sub>	ELPTEN
m <sub>i</sub>	EM

Appendix to Symbol Dictionary (page 3)

<u>Symbol</u>	<u>FORTRAN Name(s)</u>
m	AA
$m^{-1}$	ANVERS
p	PI
$\vec{Q}$	QUE
R	R, RNEW
$R_a$	RA
$r_h$	RH
$r_1$	AR
$r_z$	RZ
s	S
$s_z$	SZ
$T_{ia}$	TIA
$T_{ij}$	TMATII
$T'_1$	TPRIME
$\hat{T}'_1$	THATPW
$\hat{T}'_5$	THATPV
$\hat{T}'_6$	THATPX
$\hat{T}'_7$	THATPS
t	TIME
$t_{max}$	TIMAX
$t_{off}$	TOF

Appendix to Symbol Dictionary (page 4)

<u>Symbol</u>	<u>FORTRAN NAME(s)</u>
$T_{on}$	TON
$v_T$	VTIA
$V_x$	VXIA
$V_y$	VYIA
$W_o$	WZERO
X	XC
$\dot{X}$	XCP
$\ddot{X}$	PLC
$\dot{x}$	XAP
$\ddot{x}$	PLX
$x_h$	HEADX
$x_i$	X, AX
$\dot{x}_i$	AXD
$x_z$	XZ
$y_s$	YS
$\dot{y}_s$	YSP
$y_{zo}$	YZZERO
y	YA
$\dot{y}$	YAP
$\ddot{y}$	PLY
$y_h$	HEADY

Appendix to Symbol Dictionary (page 5)

<u>Symbol</u>	<u>FORTRAN Name(s)</u>
$\dot{y}_1$	Y, AY
$z_0$	ZZERO
$\ddot{z}_k$	ZK
$z$	Z
$z_k$	AZ
$\dot{z}_k$	AZP
$\alpha_1$	ALFAI
$\beta_m$	BETA
$\gamma$	LITGAM
$\gamma_0$	GAMZER
$\Delta$	DELL, DELTA
$\Delta$	DELTAT
$\Delta t_{\min}$	DESTEP
$\Delta \vec{z}$	DELZ
$\Delta v$	DELNN, DELNU
$\delta$	SDELTA, SDELA
$\delta_n$	SDL
$\delta_{n-1}$	DELOLD
$\dot{\delta}$	SDELID, SDELD
$\delta$	SDLD
$\dot{\delta}_{n-1}$	OLDELD, DELDOD

Appendix to Symbol Dictionary (page 6)

<u>Symbol</u>	<u>FORTTRAN Name(s)</u>
$\epsilon$	EPSLNY
$\epsilon_0$	EPSLNZ
$\epsilon'$	EPSLNP
$\eta$	ETA
$\theta_1$	TT
$\theta_{1_0}$	THETAZ
$\dot{\theta}_1$	TV
$\dot{\theta}_1^2$	THEDSQ
$\ddot{\theta}_1$	TA
$\lambda_1$	ELAMB
$\mu_a$	FMUA
$\mu_s$	FMUS
$\nu$	RVEL
$\dot{\nu}$	RSEL
$\xi$	RPSI
$\xi_a$	XISMLA
$\pi$	PI
$\rho_1$	RHO
$\rho_1'$	RHOPRM
$\rho_3'$	RHOPTZ
$\rho_4'$	RHOPFZ

Appendix to Symbol Dictionary (page 7)

<u>Symbol</u>	<u>FORTTRAN Name(s)</u>
$\sigma_o$	SIGZ, SAGXX
$\sigma_{am}$	SIGMAA
$\sigma_n$	SIG, SIGMA
$\tau_k$	TAUI
$\tau^*$	TIMASK
$\hat{\tau}$	TAUHAT
$\hat{\tau}_o$	TAHATZ
$\phi'_{10}$	FEPTEN
$\phi_m$	PHI
$\phi_{m_o}$	PHIZ
$\psi_a$	PSIA
$\Omega$	OMGT, FOM
$\Omega_1$	OMEGAI
$\Omega_{n-1}$	POMG

## REFERENCES

1. Roberts, V. L., and Robbins, D. H., "Multidimensional Mathematical Modeling of Occupant Dynamics Under Crash Conditions," SAE Paper No. 690248, January 1969.
2. McHenry, R. R., and Naab, K. N., "Computer Simulation of the Crash Victim—A Validation Study," Proc. of the Tenth Stapp Car Crash Conf., 1966.
3. Haley, J. L., et al., "Crashworthiness Study for Passenger Seat Design," Arizona State University, Engineering Rept. No. 65-01, 1966.
4. Thompson, J. E., "Occupant Response Versus Vehicle Crush: A Total System Approach," Proc. of the Twelfth Stapp Car Crash Conf., 1968.
5. Furusho, H., et al., "Analysis of Occupant Movements in Rear-End Collision. Part I. Simulation of Occupant Movements," SAE of Japan Safety Research Tour Publication, 1969.
6. Robbins, D. H., "Three-Dimensional Simulation of Advanced Automotive Restraint Systems," 1970 International Automobile Safety Conf. Compendium, SAE Publication No. P-30, pp. 1008-1023.
7. Young, R. D., "A Three-Dimensional International Model to Predict the Dynamic Response of an Automobile's Occupant," to be presented at the Annual Meeting of the Highway Research Board, 1971.
8. Segal, D., "Computer Simulation of Body Kinematics Associated with Rapid Deceleration," Dynamic Response of Biomechanical Systems, published by ASME, 1970.
9. Beckett, R., and Chang, K., "An Evaluation of the Kinematics of Gait by Minimum Energy," J. Biomechanics 1(2); 147-159, 1968.
10. Lissner, H. R., and Williams, M., Biomechanics of Human Motion, W. B. Sanders, Philadelphia, Penn., 1962.
11. Weber, W., and Weber, E., "Mechanik der menschlichen Gehwerkzeuge," Gottingen, 1836.
12. Kane, T. R., and Scher, M. P., "Human Self-Rotation by Means of Limb Movements," J. Biomechanics 3(1); 39-50, 1970.



REFERENCES (Continued)

13. Hanavan, E. P., "A Personalized Mathematical Model of the Human Body," AIAA Paper No. 65-498, 1965.
14. Kulwicki, P. V., et al., "Weightless Man: Self-Rotation Technique," AMRL - TDR-62-129, 1962.
15. Chaffin, D. B., "A Computerized Biomechanical Model—Development of and Use in Studying Gross Body Actions," ASME Paper No. 69-BHF-5, 1969.
16. Damon, A., Stodt, H. M., and McFarland, R. A., The Human Body in Equipment Design, Harvard University Press, Cambridge, Mass., 1966.
17. Fischer, O., Theoretische Grundlagen für eine Mechanik der lebenden Körper mit speziellen Anwendungen auf den Menschen, sowie auf einige Bewegungsvorgänge an Maschinen, B. G. Teubner, Berlin, 1905.
18. Weaver, J. R., "A Simple Occupant Dynamics Model," J. Biomechanics 1(3): 185-191, 1968.
19. Aldman, B., and Asberg, A., "Impact Amplification in European Compacts," Proc. of the Twelfth Stapp Car Crash Conf., 1968.
20. Rennecker, D. N., "A Basic Study of Energy-Absorbing Vehicle Structure and Occupant Restraint by Mathematical Model," SAE Automotive Safety Dynamic Modeling Symposium, Anaheim, Calif., 1967.
21. Martinez, J.L., and Garcia, D. J., "A Model for Whiplash," J. Biomechanics 1(1): 23-32, 1968.
22. Mertz, H. J., "Kinematics and Kinetics of Whiplash," Ph.D. Thesis, Wayne State University, 1967.
23. Roberts, S. B., et al., "Head Trauma—A Parametric Dynamic Study," J. Biomechanics 2(4): 397-416, 1969.
24. Hansen, H. M., and Chenea, P. F., Mechanics of Vibration, John Wiley and Sons, Inc., New York, 1952, pp. 128-137.
25. Hanavan, E. P., "A Mathematical Model of the Human Body," AMRL Technical Report No. TR-64-102, 1964.
26. Patten, J. S., and Theiss, C. M., "Auxiliary Program for Generating Occupant Parameter and Profile Data," CAL Report No. VJ-2759, V-1R.

REFERENCES (Concluded)

27. Carnahan, B., and Wilkes, J. O., Digital Computing and FORTRAN IV with MTS Applications, The University of Michigan, Ann Arbor, 1968.
28. Robbins, D. H., Snyder, R. G., and Roberts, V. L., "Injury Criteria Model for Restraint System Effectiveness Evaluation," HSRI Report No. Bio M-70-7, First Draft, Final Report under DOT Contract FH-11-6962, October 1970.